THESIS

For the degree of Doctor of Philosophy of the University of Lille
École Doctorale Biologie Santé de Lille | EDBSL

Team: Pr. Eric BOULANGER (U1167/RID-AGE)
Glycation : de l'inflammation au vieillissement

Effects of Early-Life and Chronic Exposure to Dietary Advanced Glycation End-Products on Chronic Low-Grade Inflammation and Age-Associated Disorders

Publicly presented by
Matheus Thomaz NOGUEIRA SILVA LIMA

Advisor: Frédéric TESSIER (Université de Lille)
Co-advisor: Carine DELAYRE-ORTHEZ (UniLaSalle)

Jury

Pr. **Cristina DELGADO-ANDRADE**	Spanish National Research Council	Rapporteur
Pr. **Michael HELLWIG**	TU Dresden	Rapporteur
Dr. **Hélène EUTAMENE**	École d'Ingénieurs de Purpan	Examiner
Pr. **Frédéric TESSIER**	Université de Lille	Advisor
Dr. **Carine DELAYRE-ORTHEZ**	UniLaSalle	Co-advisor

Lille | 29/09/2023

ACKNOWLEDGMENTS

First, I would like to express my gratitude to all the people involved in the **ExoAGEing project** and their valuable contributions to the completion of this thesis. I extend my thanks to the teams at the **University of Reims** (CNRS/URCA UMR 7369), **UniLaSalle** (ULR 7519), and the **JUNIA** team. Thank you all for the contributions you provide at each project meeting!

I would like to express my special gratitude to the **U1167 team** for their warm welcome and support in fostering my professional growth. I would like to address a special thanks to **Pr. Frederic Tessier** and **Pr. Eric Boulanger** for their commitment and interest in allowing me to be part of the team. I greatly appreciate your professional dedication and willingness to support the development of this thesis and of my professional career. Special thanks to **Pr. Phillipe Gillery**, who leads the ANR ExoAGEing project, for allowing me to participate in the project.

I would also like to address my gratitude to **Pr. Frederic Tessier** and **Dr. Carine Delayre-Orthez** for accepting the responsibility of mentoring me during this thesis. Thank you for your continuous interest and availability to discuss the technical and scientific aspects of this work. I am grateful for your generosity in sharing your knowledge, and I can assure you that I have learned a lot! Je vous remercie énormément !

I would like to express my gratitude to the members of the CSI, **Dr. Helene Eutamene** and **Pr. Sophie Lestavel**, for their evaluation of this work over the past two years. Thank you very much for your contributions to the progress of this research. A special thanks to the jury members, **Pr. Cristina Delgado**, **Prof. Michael Hellwig,** and **Dr. Helene Eutamene** for graciously accepting to evaluate this work, and to the valuable insights that will enhance this work.

My sincere appreciation for the contributions of **Dr. Michael Howsam.** Thank you so much for your advice and extensive academic contributions to the texts presented in this thesis, as well as your work in the experimental aspects. Thanks to **Dr. Chantal Fradin** for her assistance and willingness to answer any questions or doubts I had. I also extend my thanks to **Dr. Steve Lancel** for mediating the

acquisition of the necessary materials for sample collection. Thank you for your availability and support throughout the course of this project.

I would also like to extend my deepest thanks to **Dr. Carine Delayre-Orthez**, **Dr. Pauline M Anton**, and **Dr. Maxime Perot** who actively participated in sample collection. Thanks for the work and dedication in all the long journeys of collections. I would like to express my appreciation for the valuable work carried out by **Dr. Céline Leridon**, **Phillipe Jacolot**, **Dr. Stephane Jaisson**, and **Anaïs Okwieka,** in the acquisition of LC-MS/MS data. Your expertise and dedication have greatly contributed to the success of this project.

Thanks also to the technical staff of the U1167 team, **Gaelle Grolaux**, **Jeremy Lemaire**, and **Fabien Foquet**. The support offered contributed a lot to the development of this project. Thanks for the support offered by the **EOPS2 staff** (Université de Lille). Thank you for your time and work throughout the almost two years of animal experiments.

Finally, I would like to acknowledge the **Doctoral School of Biology and Health of Lille** (EDBSL) for the continuous support throughout these three years of my thesis. I also thank the **Agence Nationale de la Recherche (ANR)** for funding this project and for allowing the progress of science.

In a more personal note, I would like to express my deepest gratitude to people who have played a crucial role in my journey. First and foremost, I am immensely grateful to my parents for their unwavering support and encouragement in pursuing my academic career. **Mazé** and **Márcio**, I cannot thank you enough for your dedication, love, and the effort you have made to provide me with access to education. Your constant support has been invaluable! I would also like to extend my appreciation to **Lucca** and **Iasmin** for their support and encouragement. I am grateful to **Débora and Ricardo** for her encouragement and support along these last years (thanks for answering my calls ^^). Lastly, I would like to express my gratitude to **Maria Luiza**, **Elis and all friends from Lille** for their support and presence during my time in Lille. Your friendship has made this adventure all the more meaningful.

ABSTRACT

Over the past few decades, human life expectancy has increased, and the expanding population of older individuals has been associated with a higher prevalence of age-related diseases. Among various factors, diet plays a significant role in the development of chronic dysfunctions. Consuming an unhealthy diet is thought to contribute to accelerated oxidation, and senescence, and can have an impact on the modulation of the gut-brain axis and microbiota. The long-lasting effect of dietary habits on intergenerational modulation has been a topic of discussion. Advanced Glycation End-Products (AGEs), a class of neoformed compounds found in thermally processed foods, are widely present in the diet. The accumulation of dietary AGEs in various organs is believed to contribute to the initiation of CLGI, the induction of glycoxidative stress, and the modulation of the gut microbiota. Carboxymethyl-lysine (CML) is a well-known AGE used as a gold-standard biomarker of protein glycation. Extensive research has been conducted to explore the interaction between glycation products and the Receptor for Advanced Glycation End-Products (RAGE), in the development diverse pathologies. However, it is still not fully understood whether early and/or lifelong exposure to dietary AGEs contributes to the initiation of CLGI, and whether these effects can be reversed or are permanent. This thesis consisted of three experimental sections: First, we aimed to build up knowledge on the postprandial fate of dietary CML (dCML) both in rodents and humans. In addition, establish the relationship between dCML intake and soluble RAGE (sRAGE) levels in blood in humans. Afterward, we aimed to build up and characterize a model protein (BSA) enriched in CML for future application in animal experiments. The main motivation was to develop an effective method for producing large quantities of CML without the production of toxic hydrogen cyanide (HCN). Further, we aimed to investigate physiological changes in Wild-Type (WT) and RAGE KO mice fed (since the perinatal period) with a standard diet (STD - 20.8 ± 5.1 $\mu g_{dCML}/g_{food}$) or a dCML-enriched diet (255.2 ± 44.5 $\mu g_{dCML}/g_{food}$) during 35 or 70 weeks. We investigated whether an early age (6 weeks old) diet-switch (dCML → STD) would contribute to the reversion of the potentially deleterious effects which included inflammatory, oxidative stress, and senescence parameters. We have shown that an efficient and reproducible synthesis of protein-bound CML can be achieved with the use of glyoxal in a BSA model system. The proposed method reduces potential confounding factors such as vitamin loss. Altogether, although free-CML reaches the bloodstream within 1-2 h and accumulates in excretory and digestive organs, it did not seem to play a strong role in inflammation, senescence, and oxidative stress. Based on our results, we did not observe clear short-term or long-term effects of exposure to dAGEs. The knockout of RAGE was demonstrated to play a protective role in the attenuation of inflammaging. RAGE knockout was suggested to play an epigenetic regulation mediated by *EZH2* downregulation, but it remains to be further elucidated. Furthermore, ongoing research is being conducted to examine biomarkers of immunosenescence and the composition of the intestinal microbiota. This study contributed to the understanding that, despite extensive discussions on the role of dAGEs in inflammaging (at least a diet high in dCML), it does not appear to directly contribute to deleterious health effects. These results go in line with other studies (both in rodents and humans). In addition, we demonstrated for the first time that the exposure of the parental lineage to a CML-rich diet did not appear to influence physiological responses in the offspring. This work opens the perspective for further studies that may focus on the local responses of different inflammaging biomarkers using more sensitive techniques for detecting low-grade stimuli.

Key-words: glycation, carboxymethyl-lysine, lysine, RAGE, inflammaging, senescence, oxidative stress

RESUME

Au cours des dernières décennies, l'espérance de vie humaine a augmenté. Cependant, malgré les progrès médicaux, la population croissante de personnes âgées a été associée à une prévalence plus élevée de maladies liées à l'âge. Parmi les divers facteurs, l'alimentation joue un rôle important dans le développement de maladies chroniques. Il est admis qu'une alimentation déséquilibrée contribue à l'accélération du stress oxydant, de la sénescence cellulaire et peut avoir un impact sur la modulation de l'axe intestin-cerveau et du microbiote. L'effet des habitudes alimentaires à long terme sur la régulation métabolique intergénérationnelle fait l'objet de nombreuses discussions. Les produits terminaux de la glycation avancée (AGE), sont largement présents dans les aliments soumis à un traitement thermique. On estime que l'accumulation d'AGE alimentaires dans divers organes pourrait contribuer à l'initiation d'une inflammation chronique à bas bruit (CLGI). La carboxyméthyl-lysine (CML) est un AGE bien connu. Des recherches approfondies ont été menées pour explorer le rôle potentiel de l'interaction entre les produits de glycation, tels que la CML, et le récepteur des AGE (RAGE). Cependant, la relation causale entre une exposition précoce et/ou chronique aux AGE alimentaires et l'initiation de CLGI favorisant ainsi l'inflammaging reste incertaine, et la réversibilité des effets potentiellement toxiques des AGE encore inconnue. Tout d'abord, nous avons cherché à approfondir nos connaissances sur le devenir postprandial de la CML alimentaire (dCML) à la fois chez la souris et chez l'homme, ainsi qu'à établir la relation entre l'apport en dCML et les niveaux circulants du récepteur soluble des AGE (sRAGE) chez l'homme. Ensuite, nous avons cherché à construire et à caractériser un modèle protéique (albumine) enrichi en CML pour des applications futures en expérimentation animale. Ensuite, nous avons cherché à étudier les changements physiologiques chez les souris de type sauvage (WT) et les souris RAGE KO nourries depuis la période périnatale avec un régime standard (STD - 20,8 ± 5,1 μg_{dCML} /g_{food}) ou un régime enrichi en dCML (255,2 ± 44,5 $\mu g_{dCM}L/g_{aliment}$) pendant 35 et 70 semaines. Nous avons étudié si un changement de régime à un âge précoce (6 semaines) (dCML → STD) contribuerait à inverser les effets potentiellement néfastes. Nous avons montré qu'une synthèse maitrisée et reproductible de la CML liée aux protéines peut être obtenue en utilisant du glyoxal dans un système modèle d'albumine. Dans l'ensemble, bien que la CML libre atteigne la circulation sanguine en 1 à 2 heures et s'accumule dans les reins et le tube digestif, elle ne semble pas jouer un rôle important dans l'inflammation, la sénescence et le stress oxydant. Nous n'avons pas observé d'effets clairs à court ou à long terme de l'exposition aux AGE alimentaires. Par contre, il a été démontré que la suppression de RAGE joue un rôle protecteur dans l'atténuation de l'inflammaging. RAGE pourrait être impliqué dans une régulation épigénétique par la régulation négative d'*EZH2*, mais cela reste à confirmer. De plus, la poursuite des analyses permettra l'élucider les effets d'une exposition à la CML sur l'immunosénescence et sur la composition du microbiote intestinal. Globalement, les résultats de cette étude, bien que non finalisés, semblent indiquer que les AGE alimentaires (tout au moins la CML chez la souris) n'auraient pas d'effet néfaste significatif sur la santé. Ces résultats sont cohérents avec d'autres études pré-cliniques et épidémiologiques récentes. De plus, nous avons démontré pour la première fois que l'exposition de la lignée parentale à un régime riche en CML ne semblait pas influencer les réponses physiologiques chez la progéniture. Ce travail ouvre la voie à d'autres études qui pourraient se concentrer sur les réponses locales de différents biomarqueurs de l'inflammation en utilisant des techniques plus sensibles pour détecter des stimuli de bas bruit.

Mots clés : glycation, carboxyméthyl-lysine, lysine, RAGE (récepteur des produits avancés de glycation), inflammaging, sénescence, stress oxydatif

SUMMARY

LIST OF FIGURES

CHAPTER 1

CHAPTER 2

CHAPTER 3

CHAPTER 4

CHAPTER 5

CHAPTER 6

LIST OF TABLES

CHAPTER 1

CHAPTER 3

CHAPTER 4

CHAPTER 5

CHAPTER 6

LIST OF ABBREVIATIONS

AGE	Advanced Glycation End-Products
AKT	Protein Kinase B
ANR	Agence Nationale de la Recherche
ApoE	Apolipoprotein E
AUC	Area Under the Curve
CD4+	Cluster of Differentiation 4
CEL	Carboxyethyl-lysine
CKD	Chronic Kidneys Disease
CLGI	Chronic Low-grade Inflammation
CMA	Carboxymethyl-arginine
CM-APA	N-Carboxymethylaminopentanoic acid
CM-CAD	N-Carboxymethylcadaverine
CML	Carboxymethyl-lysine
CRP	C-Reactive Protein
D2-CML	Deuterated-CML
DAMPs	Damage-Associated Molecular Patterns
dCML	Dietary Carboxymethyl-lysine
DNA	Deoxyribonucleic Acid
EZH2	Enhancer of Zeste Homolog 2
FL-RAGE	Full-length RAGE
GLO1	Glyoxalase 1
GLO2	Glyoxalase 2
GLβ1	Beta-Galactosidase-1
GSH	Gluthatione
GWB	Grilled Western-inspired Break-fast
HFD	High Fat Diet
ICAM	Intercellular Adhesion Molecule 1
IFN	Interferon
IL	Interleukin
KO	Knockout
LPS	Lipopolysaccharide
MB	Mediterranean-inspired breakfast
MCP-1	Monocyte Chemoattractant Protein-1
MG-H1	Methylglyoxal-Derived Hydroimidazolone 1
MIF	Macrophage Migration Inhibitory Factor
mRNA	Messenger Ribonucleic Acid
MRP	Maillard Reaction Product
mTOR	Mammalian Target of Rapamycin
NAFLD	Non-alcoholic Fatty Liver Disease
NF-κB	Nuclear factor-kappa
P16	Cyclin-Dependent Kinase Inhibitor 2A
p65	NF-kappa-B p65 subunit
PAMPs	Pathogen-Associated Molecular Patterns

PDK1	Pyruvate Dehydrogenase Kinase 1
PGC-1α	Peroxisome Proliferator-Activated Receptor Gamma Coactivator-1α
PMN	Polymorphonuclear Leukocytes
RAGE	Receptor for Advanced Glycation End-products
SIRT1	NAD-Dependent Deacetylase Sirtuin-1
SOD1	Superoxide Dismutase 1 (cytoplasmic)
SOD2	Superoxide Dismutase 2 (mitochondrial)
sRAGE	Soluble RAGE
T2DM	Type 2 diabetes
TLR4	Toll-Like Receptor 4
TNFα	Tumor Necrosis Factor Alpha
UPLC-MS/MS	Ultra Performance Liquid Chromatography in tandem with mass spectrometry
VCAM1	Vascular Cell Adhesion Protein 1
WB	Western-inspired breakfast
WT	Wild-Type

CHAPTER 1

Literature Review

1 Introduction

Aging is an intricate phenomenon that encompasses the deterioration of physiological capacities for repair and the maintenance of homeostasis. It is regarded as a risk factor for several chronic diseases, as it establishes unfavorable circumstances for certain clinical conditions [1]. In particular, unhealthy aging is accompanied by increased immunosenescence and oxidative stress, favoring the rise of a low-grade, pro-inflammatory status called **"Inflammaging"**, which contributes to prevalent age-related pathologies [2]. While recent decades have seen marked increments in human life span, this phenomenon has been accompanied by an increase in the incidence of chronic diseases, and consequently a reduction in the quality of life for many older people [3,4]. Among the multiple factors that may contribute to the aggravation of age-related dysfunctions (*e.g.* cell senescence, insulin resistance) and the worsening of chronic diseases (*e.g.* obesity, hypertension), diet also has an influence [5]. Excessive consumption of ultra-processed foods has recently been implicated in a number of health-related issues. This food category is suspected of contributing to the development of numerous degenerative diseases, not only because of its high, but "empty" calorie content and poor overall nutritional composition, but also because of the presence of high concentrations of additives, pesticides, neoformed compounds and other potentially toxic components [6].

This thesis is part of a larger, ongoing collaborative project, ExoAGEing, financed by the Agence Nationale de la Recherche (ANR). This project focuses on the health effects of chronic consumption of a diet rich in a class of dietary neoformed compounds called dietary Advanced Glycation End-Products (dAGEs), and includes the study of advancing age in a murine model. The following sections will address some historical aspects of human diet, the chemical aspects of thermal processing of foods (in particular molecules associated with the Maillard reaction), the influence of substances in the diet upon different cellular metabolic pathways, and the clinical evidence for possible health effects of these substances.

1.1. General consideration of human dietary habit changes and their implications for human health

Cooking is considered a milestone in human evolutionary history. The use of fire allowed the conservation (*e.g.* prevention of microbiological spoilage), and transformation of foods into more accessible forms of energy (*e.g.* increased starch digestibility) [6]. From the physiological perspective, this remarkable event is believed to have contributed to the human brain expansion and the consequent development of cognitive capacities associated with the greater neuronal number [7]. However, despite the numerous advantages that emerged from mastering fire and the thermal processing of foods, several physiological challenges were created, including human exposure to dietary **neoformed compounds** [6].

More recently in human history, both domestic and industrial heat processing of foods have been extensively used as a way to improve desirable food properties such as appealing color, flavor, and aroma [8]. In addition, the mass production of heated foods containing refined carbohydrates, lipids, and processed proteins made processed and ultra-processed food more easily available. These foods are part of a so-called "**Western diet**", which has been correlated over the last few years with the incidence of chronic diseases such as obesity, neuropathologies, diabetes, and cancer [9–12]. Many factors may be associated with the emergence of diet-related diseases, including the low-nutritional value of such foods, the presence of additives and pesticides, as well as the excessive intake of calories and neoformed compounds [13].

Several reactions may occur during the thermal processing of foods. Neoformed compounds in the food matrix mainly result from the Maillard Reaction between protein amino groups and reactive sugars. It remains controversial whether dietary **Maillard Reaction Products** (MRPs) are potential food contaminants and may be associated with the genesis of chronic pathologies. The ingestion of MRPs has long been implicated in **oxidative stress**, **cellular aging**, and as a trigger of **chronic low-grade inflammation** (CLGI), contributing to the development of non-communicable diseases [14]. In addition, the blockage of essential amino acids such as lysine by the Maillard reaction has been characterized as a loss of protein in foods [15].

The intake of foods high in sugar and protein is suggested to trigger glycoxidative stress, hypothesized to arise from the actions of reactive

intermediates, commonly referred to as **glycotoxins** (*e.g.* glyoxal and methylglyoxal), or non-reactive intermediates such as carboxymethyl-lysine [16]. As a consequence of the aforementioned industrialization processes, individuals are exposed to these neoformed compounds from early life, including the gestational period, and throughout life thereafter. The nutritional status of the mother has significant implications for the development of the newborn, particularly during the initial two years of life [17]. It is during this early period of life that several environmental factors such as diet, and intrinsic genetic and epigenetic factors are thought to influence offspring growth and may have a long-term influence over the intestinal bacterial diversity, the absorption of nutrients, in addition to the regulation of hormones [18]. *In vitro* evidence has demonstrated the potential effect of MRPs on gene expression modulation by mediation epigenetic shifts in podocytes for instance [19,20]. Although MRPs might be considered a risk to human health, no clear association with the long-term effects resulting from chronic exposure to dietary neoformed compounds is currently described. Furthermore, no consensus yet exists on the exact biological mechanisms by which such molecules would exert deleterious effects or participate in the different pathological conditions mentioned above.

The factors described above contextualize the scope of the present thesis, which approached the investigation of the short and long-term effects of the consumption of MRPs in a rodent model. As may be deduced from the various topics covered here, this scientific question is complex and deserves a more accurate description, both from a chemical and biological point of view. In order to fully elucidate the issues addressed in this thesis and contextualize CHAPTERS 3 – 6, a summary of the concerns and current evidence for the health implications of a high dietary MRPs intake will be presented. In the following sections, an introduction to the central aspect of glycation (terminology here interchangeably used in reference to Maillard reaction) will be provided, including a brief historical description of the discovery of the reaction and its chemical aspects. Thereafter, evidence of the involvement of dietary MRPs in health complications will be reviewed, focusing on the different metabolic pathways currently being investigated and described in the literature, in particular in animal models. This section is followed by a description of the effects of MRP-enriched diets across different metabolic pathways in murine models. The corresponding findings both on epidemiological and interventional

studies are also introduced. It is worth remembering that this chapter is followed by a more complete review of the literature (CHAPTER 3) on the effects of dietary AGEs on CLGI in rodents, providing a summary of the currently explored biomarkers in this field.

1.2. Glycation – Discovery, chemistry, and the origin of Advanced Glycation Products

1.2.1. The Maillard reaction and the relevance of glycation research

The Maillard Reaction was first described in 1912 by the French biochemist **Louis Camille Maillard** [21]. Working on a series of reactions between polyalcohols and peptides, Maillard reported the browning phenomenon resulting from the condensation between reactive aldoses/ketones and amino groups (Figure 1). Maillard was able to describe the chemical principles by which the reaction would occur between sugar and amino acids [22]. Despite this important discovery, Maillard did not address the importance of this reaction in food, limiting himself to interpretations about the formation of humic matter [22,23]. In the years following Maillard's main publication, the non-enzymatic browning reaction was described as naturally occurring in food products resulting from brewing, for instance (Figure 1) [24]. In complementary studies, the chemical parameters that could interfere with its kinetics (*e.g.* water activity, pH, temperature) were further characterized [25]. But it was only in 1953, with the description of the complex chemical mechanisms [26] of the reaction previously described by Maillard, that this area of research began to attain a wider relevance (Figure 1).

The discovery of the occurrence of *in vivo* glycation occurred in 1958 when glycated hemoglobin (HbA1c) was first observed in adult and fetal human blood samples [27] (Figure 1). Glycation gained medical relevance from observations of the physicochemical modifications of hemoglobin associated with glucose levels in diabetic patients [28]. The years that followed saw HbA1c become an internationally validated biomarker of the glycemic control in patients with diabetes mellitus [29]. It was also around this time, between 1975-1986, that **carboxymethyl-lysine** (CML) was first described in urine samples [30] and later in cataractous lenses [31] and in milk [32] (Figure 1). CML was discovered to be a stable and abundant glycation biomarker both in food and *in vivo*, becoming the gold standard marker of glycation

status in both domains, originating as it does from glycoxidative processes (the pathways of CML formation are further presented in section 1.2.3.), and with an apparent affinity to the **Receptor for Advanced Glycation End-Products** (RAGE) discovered in bovine and human lung lysates in 1992 [33] (Figure 1). Nowadays, the understanding of RAGE is broad, but it remains a hallmark linking MRPs and their physiological effects. Since the discovery of RAGE, a large body of knowledge has built up elucidating the cellular effects of the activation of the RAGE axis.

Considering the elucidation of the formation process of acrylamide, a potentially carcinogenic compound that emerges from the Maillard reaction in foods, the concerns about the so-called “toxic neoformed compounds” resulting from the Maillard reaction saw renewed attention from the academic community [34]. At the same time, the recent improvement of analytical methods (*e.g.* liquid chromatography with tandem mass spectrometry - LC-MS/MS) has created a fertile environment for the detection of several glycation products in biological samples (both in clinical diagnostics and the food industry).

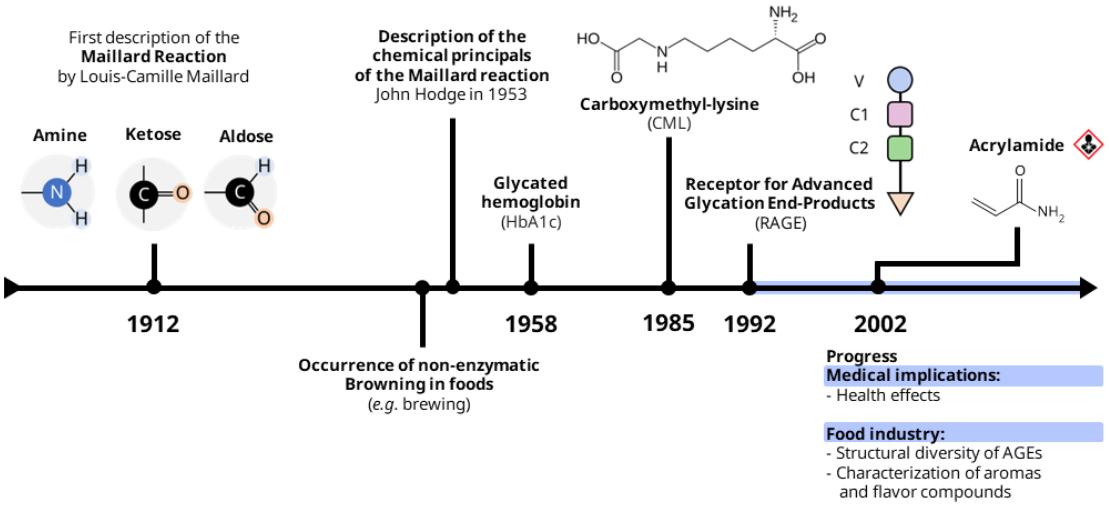

Figure 1 Chronological scheme of the main scientific events associated with the discovery of the Maillard Reaction and its implications both in the medical and food industry fields.

1.2.2. Early and intermediate Maillard reaction

Since Maillard's publication in 1912, great progress has been made over more than 110 years of research in this field. The progression of the Maillard reaction is unique and classically divided into three stages postulated by John Hodge in 1953. Its chemistry is complex and involves several sequential molecular rearrangements. The first phase, also called the "early Maillard reaction", comprises the condensation of aldehyde or ketone groups, present in reducing sugars (aldose or ketose, respectively), and primary or secondary amine groups in proteins. This first phase gives rise to unstable aldimines or cetimines (Schiff bases - *N*-substituted glucosamines) from which Amadori or Heyns products form, respectively, after rearrangements (Figure 2A). At this phase, no color change is observed, but the loss of reactive amino acid residues such as lysine and arginine moieties, contribute to a reduced nutritional value of foods [35].

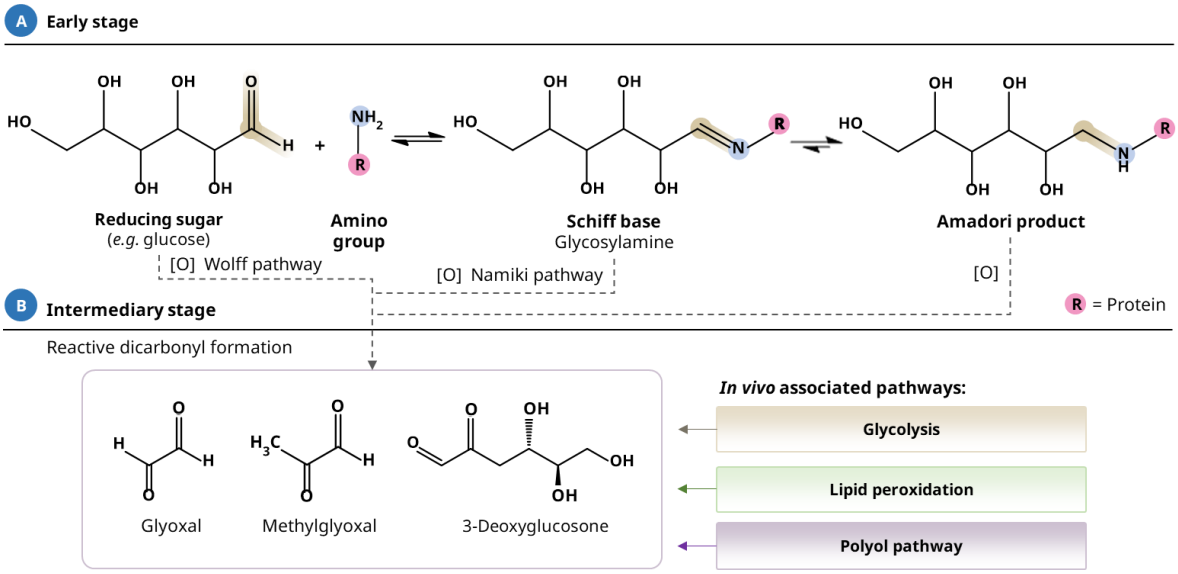

Figure 2 Schematic representation of the early and intermediary phases of the Maillard reaction. **(A)** The initial stages of the Maillard reaction occur from the condensation of a reactive sugar (*e.g.* glucose) and a free amine group. Consecutive chemical rearrangements lead to the formation of the first stable reaction products, Amadori Products which originate from aldoses, or Heyns products, which originate from ketoses. **(B)** From then on, the autoxidation of glucose (Wolff pathway), and glycoxidation of Schiff bases (Namiki pathway), or Amadori products will give rise to reactive dicarbonyls, which contribute to oxidative stress and propagation of the Maillard reaction. The formation of reactive dicarbonyls occurs both in vivo and in food matrices. It is important to point out that different pathways contribute to an increase in dicarbonyl stress in vivo, originating mainly from glycolysis and other accessory pathways such as the polyol pathway (sorbitol > fructose), and lipid peroxidation [36].

The progression of the reaction takes part in the formation of reactive α-oxaldehydes (*e.g.* glyoxal, methylglyoxal) originating from the oxidative breakdown of the Schiff bases (Namiki pathway) and Amadori Products, together with glucose autoxidation (Wolff pathway) [37]. *In vivo*, the formation of reactive dicarbonyls is accompanied by accessory metabolic pathways including the cellular metabolism of glucose, the polyol pathway on the metabolization of sorbitol into fructose, and the peroxidation of lipids [38]. In food systems, the late glycation reaction depends on several conditions (*e.g.* pH, temperature, water activity) and consists of several chemical rearrangements including dehydration, cyclization, isomerization, and condensation leading to the formation of a structurally diverse family of molecules called Advanced Glycation End-Products (AGEs) [35].

Although this thesis is interested in the effects of the consumption of dietary MRPs, here it is important to point out that the pool of AGEs in the human body has its origin in endogenous and exogenous formation of glycation products [39]. Both endogenous and exogenous formation processes of MRPs occur through the same reactions. The difference rests in the fact that the kinetics of the formation of endogenous glycation adducts are slower under physiological conditions (37 °C) and accessory metabolic pathways (Figure 2B) of glycolysis, polyol, and the peroxidation of lipids contribute to *in vivo* glycation [40].

The endogenous protein glycation is described as an extra- and intracellular aging accelerator. The slower kinetic rates of endogenous glycation of proteins under physiological conditions promotes the structural modification of extracellular matrix proteins, and loss of tissue elasticity [41]. The glycation of slow turnover proteins such as collagen, for example, has effects on the connective tissue, reducing its flexibility. Cartilage collagen has been demonstrated to accumulate AGEs including CML, N^{ε}-carboxyethyllysine (CEL), and pentosidine [42] and reduce proteoglycan-collagen interaction, disrupting matrix integrity in cell-adhesion interactions [43].

The endogenous accumulation of dicarbonyl compounds creates a pro-oxidative cellular state, while the peroxidation of cell membrane lipids also contributes to a vicious cycle of formation of dicarbonyl products, leading to the generation of glycation products (*e.g.* albumin glycation) [44]. The glucose metabolism leads to the formation of glycation precursors such as methylglyoxal and 3-deoxyglucosone [45]. In addition, under hyperglycemic conditions, the

production of reactive dicarbonyls is increased by the accumulation of fructose originating from the polyol pathway [46]. Such conditions have been associated with carbonyl stress induced by hyperglycemia or dyslipidemia, resulting from toxic glycolysis by-products such as methylglyoxal, which participate in intermediary-glycation reactions [47]. Natural mechanisms have evolved to counteract the deleterious effects of metabolic pathways related to endogenous glycation. The detoxification of methylglyoxal into D-lactate, for instance, is performed by the cytosolic Glyoxalase System (Figure 3), composed of the glyoxalase 1 (GLO1) and glyoxalase 2 (GLO2) apparatus [48]. GLO1 works on the isomerization of hemithioacetal into S-D-lactoylglutathione, which is in turn hydrolyzed by GLO2, reconstituting the glutathione levels used in the system [49]. However, under pathological conditions, cellular anti-glycation mechanisms such as the GLO system seem to be ineffective in controlling carbonyl stress and hyperglycemia has been shown to suppress *GLO1* expression in human endothelial cells [50].

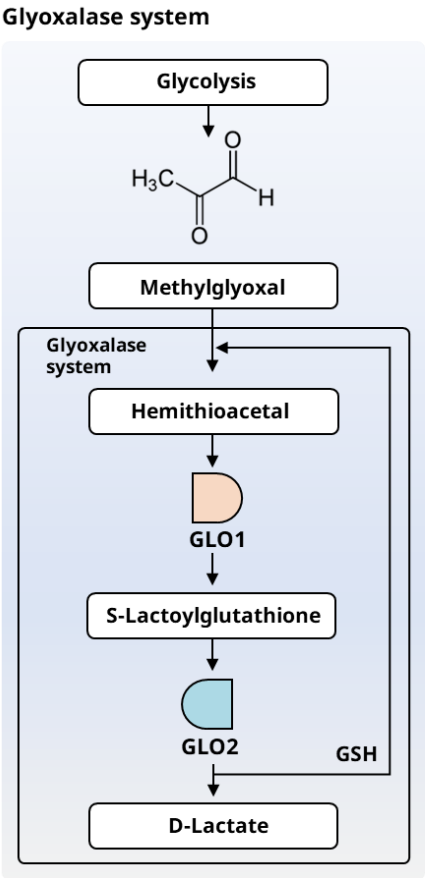

Figure 3 Cellular methylglyoxal detoxification mechanisms related to the glyoxalase system. Methylglyoxal is detoxified in the cytoplasm by two glyoxalases (GLO1 and GLO2) which convert it into D-Lactate, leading to the recovery of glutathione (GSH).

1.2.3. Formation of Advanced Glycation End-Products (AGEs) and other Maillard Reaction Products (MRPs)

The final phase of the Maillard reaction results in the formation of heterogeneous and chemically stable MRPs called Advanced Glycation End-Products (AGEs) (Figure 4). The diversity of known AGEs encompasses single adducts, including non-fluorescent molecules such as carboxymethyl-lysine (CML), carboxymethyl-arginine (CMA), glyoxal-derived hydroimidazolone 1 (GH-1) (Figure 4A). Some other AGEs are fluorescent single adducts such as argpyrimidine, and crosslinks such as pentosidine. Others are non-fluorescent protein crosslinks such as GOLD and GODIC, dimeric lysine-lysine adducts and lysine-arginine crosslinks, respectively (Figure 4B). Some MRPs have long been known to be potentially carcinogenic, such as acrylamide and furan [51,52] (Figure 4C). Others are associated with pleasing sensorial traits of food, such as the volatile products pyrazines, furfural, and thiophene related to roasted, and toasted aromas (Figure 4D) [53]. In addition, a larger class of MRPs called melanoidins - resulting from the polymerization of different compounds (*e.g.* chlorogenic acid) in the final steps of the Maillard reaction (Figure 4E) [54] - are related to the brown color in foods. Although an extensive list of Maillard products is currently known, a significant number of the AGEs and other MRPs remain uncharacterized due to the complex nature of this reaction.

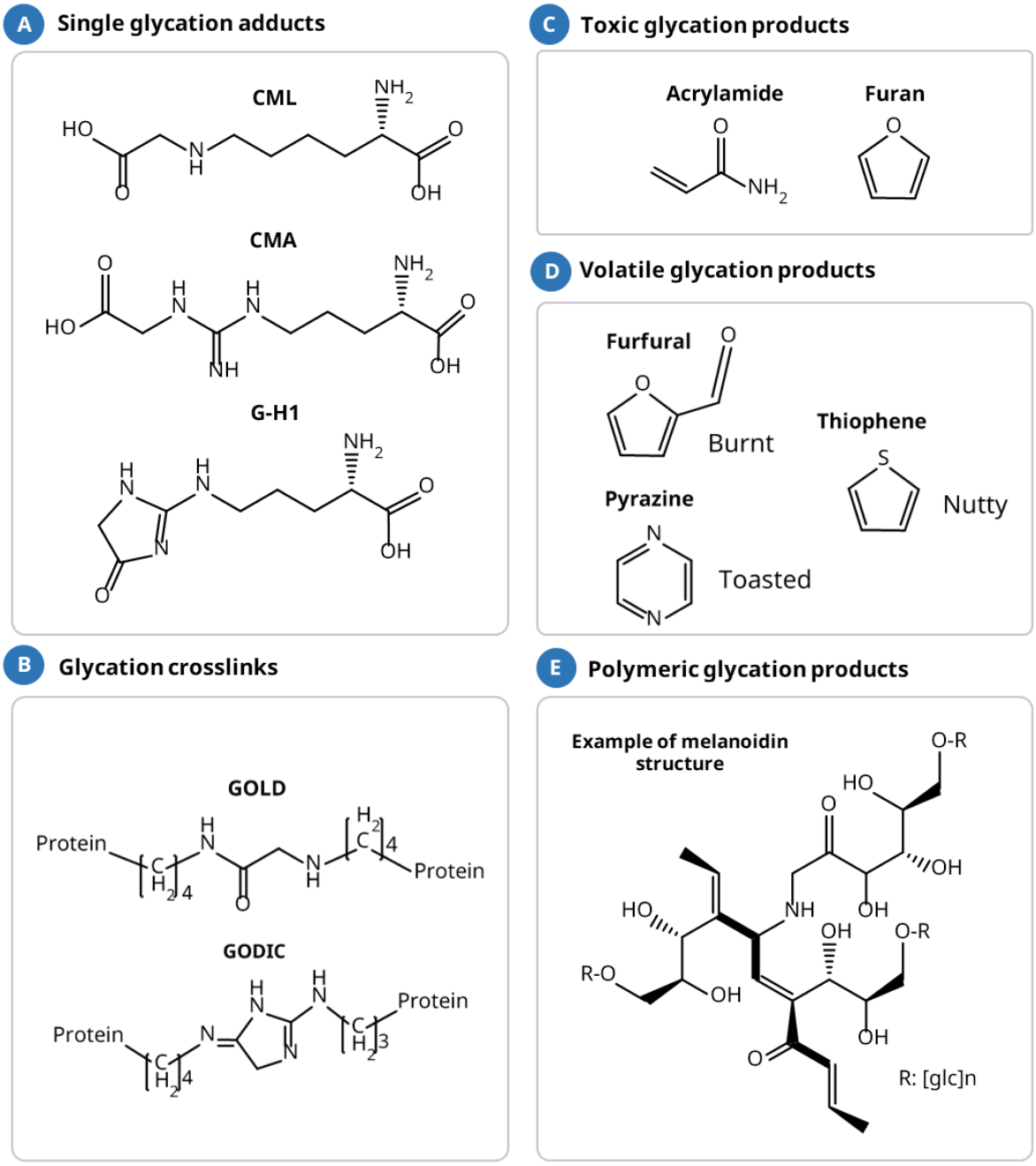

Figure 4 Structural representation of some **(A)** single adduct AGEs, **(B)** crosslinked AGEs, **(C)** potentially toxic MRPs, **(D)** volatile, and **(E)** polymeric MRPs.

CML, on the other hand, is a well-characterized AGE produced under both endogenous and exogenous glycation conditions. It was first described in 1975 as a component present in the urine of both healthy and unhealthy patients [30]. Ten years later, CML was described both in food and *in vivo*. Büser and Erbersdobler (1986) detected this AGE in milk products and defined it as a neoformed compound coming from the heat damage of milk proteins [32]. At the same time, Ahmed and colleagues described for the first time a pathway of CML synthesis originating from

the glycoxidation of fructose-lysine, but also detected CML in human lens proteins, tissue collagens and urine [31]. The formation of CML can occur through multiple pathways, both in vivo and in food matrices, as depicted in Figure 5. CML can be generated through processes such as the autoxidation of glucose (Wolff pathway), oxidation of Schiff bases (Namiki pathway), or from Amadori products. In addition, CML was further discovered to result from different pathways including a Canizzaro reaction involving glyoxal formed from glycation or derived from lipid peroxidation [55] (Figure 5).

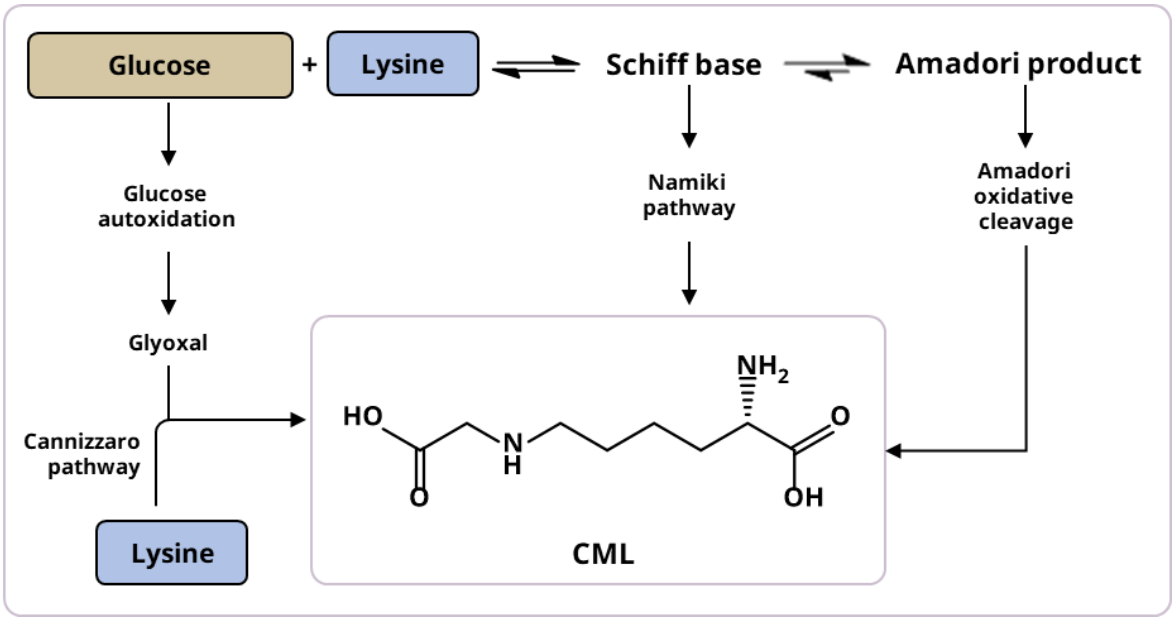

Figure 5 The multiple pathways leading to carboxymethyl-lysine (CML) formation. Glyoxal has also other origins of formation than glucose autoxidation.

In foods, CML (also called dCML when discussing dietary CML) has been described to be an abundant and stable component in different food products, and figures as one of the main biomarkers of glycation in different databases with CEL and N^{δ}-(5-hydro-5-methyl-4-imidazolon-2-yl)-ornithine (MG-H1) [56]. The occurrence of CML in foods is well documented from dairy products to cereal-based products, coffee, and biscuits. Based on ultra-performance liquid-chromatography in tandem with mass spectrometry (UPLC–MS/MS) analysis, Hull et al., (2012) reported that cereal (2.6 $mg_{CML}/100g_{food}$), and meat-based products (2.42 $mg_{CML}/100g_{food}$) presented the higher amounts of CML. On the other hand, minimally processed food such as fruit presented the lowest CML (0.13 $mg_{CML}/100\ g_{food}$) [57].

Humans may also be exposed to high AGE levels at a young age. The CML content in infant formulas has been demonstrated to be 35-70x higher than human breast milk [58]. In a study with 21 neonates who received industrial infant formula o breastfeeding, a 35-fold increase was shown in the circulating CML levels in infants fed with industrial formulas [59]. For adolescent and adult subjects, the daily intake of CML was estimated to be between 83 and 252 μg/kg body weight (bw) for regular European diets, and 34 and 90 μg/kg bw/day in low-MRP diets [60,61].

The protein-bound form of CML is the predominant form in food and has been shown to exhibit a 7-fold higher affinity for RAGE compared with its free, unbound counterpart [62,63]. The metabolism of CML is still not completely elucidated. Once ingested, CML reaches the gastrointestinal tract where proteolysis gives rise to more bioavailable CML forms in peptides or free CML. Results from an *in vitro* CACO-2 monolayer study demonstrated that dipeptides were absorbed by cells via the membrane peptide transporter PEPT1 and hydrolyzed into the intracellular space before bloodstream distribution [64]. Preliminary data on the plasma pharmacokinetics of dCML in Wistar rats showed that the free forms of CML reach the bloodstream after 1h of ingestion, concentrations returning to baseline approximately 10-15 h after exposure [65]. However, a similar approach has not yet been published in human subjects.

Using CML isotopes to discriminate between dietary and endogenously formed CML, Tessier et al (2016) demonstrated that dCML is partially accumulated in target organs as the kidneys, ileum, colon [66]. The cumulative quantification of dCML in urine and feces has demonstrated the elimination of up to 50% of the dCML consumed by humans. Such observations result from the partial accumulation of dCML in these tissues as well as the biotransformation of dCML into other metabolites by colonic microflora [67,68]. CML metabolism by fecal bacteria was shown to be variable among different individuals. However, at least 40% of CML was demonstrated to be degraded by fecal bacteria after 24h of incubation under anaerobic conditions [69]. A recent *in vitro* study on the metabolization of dCML exposed dCML media to fecal bacteria. Under anaerobic conditions, up to 100% of CML was metabolized into carboxymethylated amine derivates and carboxylic acids. By population enrichment assessment, two groups of bacteria were demonstrated to increase in CML-enriched media, *Oscillibacter* and *Cloacibacillus* spp. [67]. Under aerobic conditions, up to 66% of CML was demonstrated to be

degraded and resulting bacterial metabolites were identified as N-carboxymethylcadaverine (CM-CAD), N-carboxymethylaminopentanoic acid (CM-APA), and the N-carboxymethyl-Δ1-piperideinium ion [70].

1.3. Effects of dAGE consumption on cellular processes

The role of dietary advanced glycation end products (dAGEs) as an environmental factor contributing to chronic inflammation and oxidative stress has been extensively debated in the academic community in recent years. Such neoformed compounds may adversely participate in cellular functional decay by different mechanisms including **(1)** tissular accumulation and dysfunction as observed in glomerular cells in chronic kidneys disease (CKD) [71]; **(2)** promotion of oxidative and carbonyl stress, permanently altering the cellular structure and function (*e.g.* β cell failure and modified insulin resistance) [72]; **(3)** or by activation of the AGE-RAGE axis which may participate in oxidative stress and trigger inflammation, but also contributes to the dysregulation of several metabolic pathways described below.

Part of the above-mentioned effects are imputed to the affinity between glycation products and RAGE, which modulates the expression of genes and proteins in response to cell stress [73]. RAGE is a cell membrane receptor that takes part in the immune surveillance of multiple tissues including the lungs, kidneys, and neuronal cells [74]. The baseline expression of RAGE is low, but upregulated in pathological conditions such as in hyperglycemic conditions or within the accumulation of ligands [75]. Currently, RAGE is recognized as a multi-ligand receptor, including Pathogen-Associated Molecular Patterns (PAMPs), Damage-Associated Molecular Patterns (DAMPs), and danger-associated molecules. Such characteristics led to the definition of RAGE as a Pattern Recognition Receptor (PRR), playing an important role in cell survival (Figure 6) [76]. Activation of the RAGE-AGE axis has been related to accelerated cellular aging due to differential and uncontrolled modulation of genes [77].

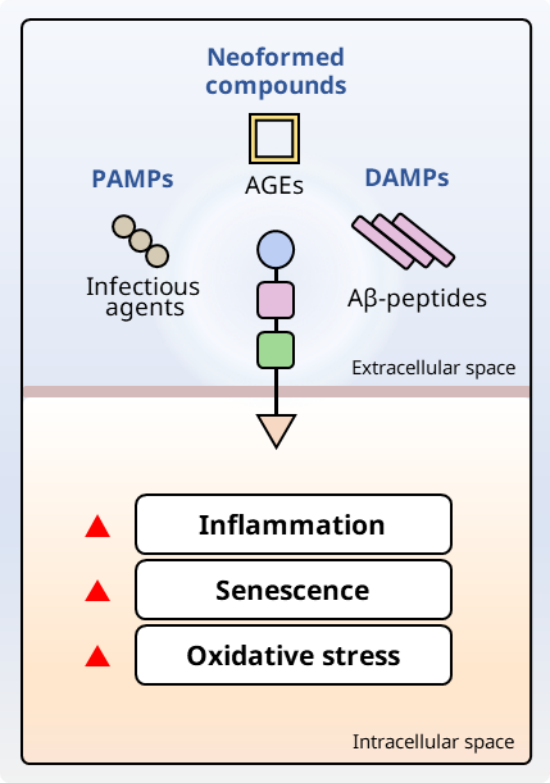

Figure 6 Neoformed compounds (*e.g.* AGEs), PAMPs (*e.g.* bacteria, virus), and DAMPs (*e.g.* Aβ-peptides), are RAGE ligands that can trigger inflammation, senescence, and oxidative stress as a cellular survival response.

Unhealthy aging is related to **immunosenescence**, leading to immune cell profile remodeling and functional decay in the elderly, which are prone to a higher incidence of infections or immune diseases [78]. RAGE is expressed in multiple immune cell types, which may include monocytes, macrophages, and T-lymphocytes such as CD4+ cells [79]. The occurrence of RAGE in immune cells highlights its role in immune surveillance and the mediation of inflammatory response. The $CD4^+$ cells have multiple roles, including the activation of B-lymphocytes as well as other innate immune system cells, and suppressing autoimmune responses [80]. In $CD4^+$ RAGE KO mice, the genetic invalidation of RAGE was demonstrated to have a protective effect against autoimmune disorders such as encephalomyelitis, compared with wild-type littermates [81]. Regarding the importance of $CD4^+$ cells in immunosenescence events, RAGE has been shown to regulate CD4+ T cell differentiation and play a role in the development of diabetic complications [82]. This was suggested by *in vitro* evidence demonstrating that AGEs (increased in diabetic patients) affected neutrophil inflammatory phenotype

and CD4+ differentiation by the RAGE-mediated induction of myeloperoxidase and elastase expression [83].

The intricate RAGE-mediated cellular responses are related to the complex molecular structure of the receptor. RAGE is encoded by a gene of approximately 1400 bp located on human chromosome 6. RAGE is composed of 11 exons and 10 introns, which can undergo alternative splicing, generating different RAGE variants (Figure 7) [84]. Full-length RAGE (FL-RAGE) comprises a 55 kDa protein composed of 404 amino acid residues. Functionally, this protein is divided into three domains including an extracellular domain, a hydrophobic transmembrane, and a cytoplasmic domain [85]. The extracellular domain of RAGE is important in the RAGE-ligand interaction and for triggering cellular response transduction. The extracellular domain is composed of three subdomains nominally identified as V (variable), C1, and C2 (constant domains) [86]. Ligand-RAGE interactions occur mainly at the V-C1 apex, covered by hydrophobic domains, and positively charged amino acids (Arg-Lys). The C2 domain is composed of negatively charged amino acids and is responsible for RAGE homodimerization [87]. Therefore, RAGE variants that do not contain extra or intracellular domains do not promote signal transduction, but they may play a role as AGE as has been reported for the soluble form of RAGE (Figure 7) [88]. In addition, ligands present higher affinity to multimeric RAGE, and it appears that its multimerization (RAGE homodimer – Figure 7) is in fact necessary for ligand binding [89].

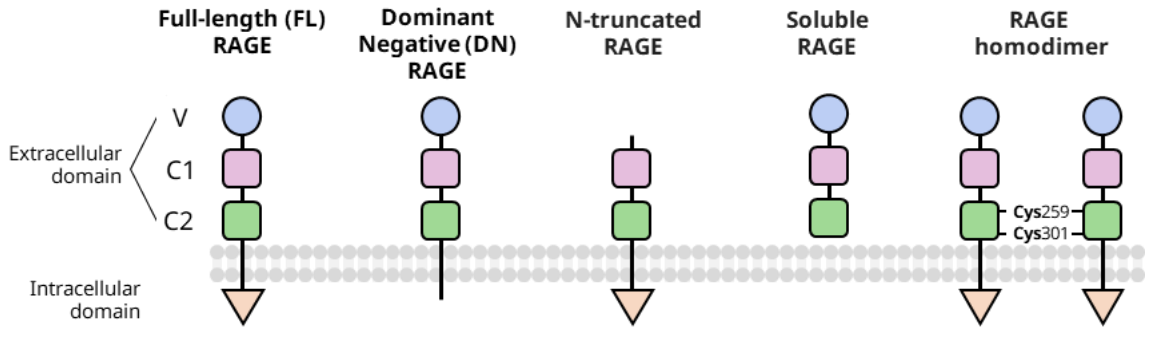

Figure 7 RAGE variants. Diagram of the different RAGE domains including V, C1, and C2 extracellular domains, and the intracellular domain responsible for signal transduction.

RAGE is involved in an intricate network triggering distinct signals for cellular energetic metabolism, the activation of inflammation, oxidative stress control, autophagy, and/or cell senescence [90]. However, despite its putative implication in human health described above, RAGE-mediated signal transduction is not completely understood due to the intrinsic complexity of interactions between the cell receptor and its ligands, and to the many different pathophysiological contexts in which these interactions may arise. Once involved with stress responses, RAGE activation coordinates cell survival and senescence pathways including p13K/AKT/mTOR and AMPK/PGC1α/SIRT1 axis (Figure 8AB) [91,92]. The general role of the target proteins associated with these pathways is summarized in Table 1.

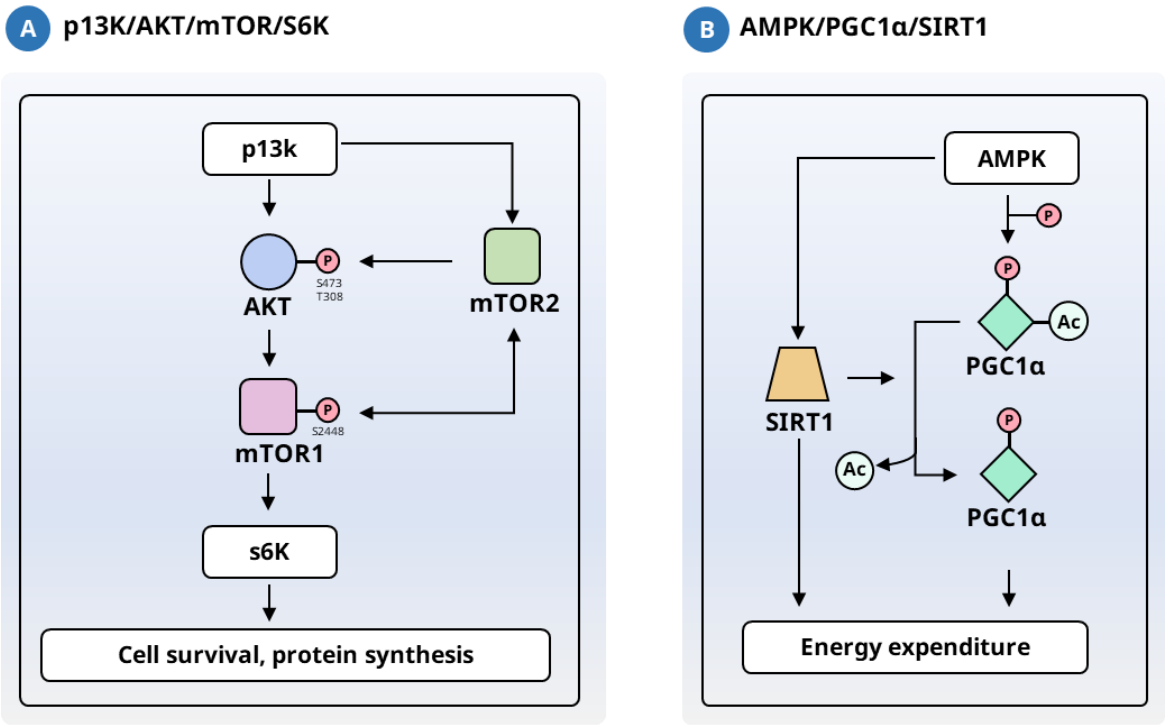

Figure 8 Central signaling pathways take part in the RAGE-initiated cell survival cascade. Both **(A)** p13K/AKT/mTOR and **(B)** AMPK/PGC1α/SIRT1 control cell survival, protein synthesis, and energy usage in different cell types.

Regarding the p13K/AKT/mTOR pathway, AKT is a phosphatidylinositol 3-kinase (p13K) dependent kinase that participates in cell growth, proliferation, and survival [93]. The p13K/AKT/mTOR is a ubiquitous pathway fully activated by the coordinated AKT phosphorylation of serine 473 (S473) and threonine 308 (T308) (Figure 8A) [94]. The activation of AKT is redundant and may occur by several

kinases including p13K, the mammalian target of rapamycin 2 (mTOR2), or by the pyruvate dehydrogenase kinase 1 (PDK1) [93] (Figure 8A). A second key player in cell growth promotion is mTOR, a serine/threonine protein kinase, which in fact consists of two multiprotein complexes: mTOR1 and mTOR2 [95]. mTOR1 includes a Raptor subunit and is an AKT substrate at serine 2448 (S2448), while mTOR2 includes a RIPTOR subunit. mTOR2 is also on a p13K-dependent pathway, performing AKT S473 phosphorylation [95] (Figure 8A). The overall result of the activation of AKT/mTOR is the regulation of cell proliferation, survival, and angiogenesis as evidenced in tumors, and diabetes [96,97].

The metabolic control exerted by the AKT/mTOR axis is pivotal for the energy sensing associated cascade AMPK/SIRT1/PGC1α (Figure 8B). Sirtuin1 (SIRT1), an AMP-activated protein kinase (AMPK)-dependent protein, is a histone deacetylase extensively studied for its role in longevity, DNA damage response, and lifespan regulation [98]. SIRT1 plays a major role in the cell nucleus, working on the deacetylation of peroxisome proliferator-activated receptor Gamma Coactivator-1α (PGC-1α) which acts in mitochondrial biogenesis [99] (Figure 8B). Therefore, the AMPK/SIRT1/PGC1α cascade has implications for energetic metabolism including glucose homeostasis and insulin secretion, fat storage in white adipose tissue, and lipid metabolism, playing a role in different metabolic active organs such as the liver, muscles, and adipose tissue. Further, both AKT/mTOR and SIRT1/PGC1α systems may be interconnected since AKT activation has been shown to downregulate PGC1α expression in insulin-stimulated skeletal muscle [100].

As a deacetylase, SIRT1 performs as an epigenetic regulation agent involved in many biological processes, including maintenance of genomic stability, reprogramming, and cellular aging [101]. Among the well-established epigenomic controllers of gene expression, including acetylation markers, histone methylation is of major importance for the control of gene expression (acting towards a gene silencing). EZH2 is a methyltransferase that plays an important role in the trimethylation of lysine 27 in histone 3 (H3), the main gene expression repressor signal [102]. AKT phosphorylates EZH2 at serine 21 (S21) and suppresses its methyltransferase activity by blocking EZH2 binding to histone H3, which results in a decrease of lysine 27 trimethylation and the repression of silenced genes (Cha et al., 2005).

AKT/mTOR is likely to contribute to cell cycle arrest mediated by cyclin-dependent kinases (CDK) [104]. In this context, P16 (CDKN2a/INK4a), participates in cell cycle control with mTOR as a driver of cellular differentiation, cellular senescence, and death [105]. P16 is a widely accepted senescence biomarker [104]. Evidence from studies on macrophages suggested that the activation of mTOR1 leads to the upregulation of P16 which, together with other CDKs, contributes to cell cycle arrest in the G1 phase. P16 thus engenders a so-called senescence phenotype which is accompanied by elevated lysosomal β-galactosidase (GLβ1) activity, indicative of degenerating cells undergoing programmed cell death. In senescent cells, β-galactosidase takes part in the hydrolysis of β-galactosides into simple monosaccharides [106].

Finally, the major consequence of RAGE signaling is linked to NF-κB gene expression modulation [107]. The different pathways presented in this section are integrated into a transcriptional regulation (also at the epigenetic level) mediated by the translocation of NF-κB into the cell nucleus [85]. NF-κB can activate the expression of cytokines, endothelial markers of cell membrane integrity such as VCAM1, and it regulates the differentiation of different CD4+ subsets, adding to the positive feedback of RAGE expression [85,108].

1.3.1. Evidence of Cellular Mechanisms Affected by AGEs in Rodents

The multiple consequences of RAGE activation here presented show how the RAGE axis contributes to cellular aging by unbalanced energetic use, triggering inflammation, or senescence. It is important to highlight that each mechanism, described here in broad terms, is dependent on different RAGE-ligand interactions, as well as the cell type, and/or organ. Clearly, the molecular mechanisms associated with RAGE activation are intricate, including the phosphorylation of multiple effectors, the translocation of transcriptional agents, and genomic and epigenetic controls. Below, some biomarkers associated with cellular aging, inflammation, and senescence are presented from the perspective of the effects of RAGE-AGE axis activation. Key studies describing the biomarkers proposed in this project are compiled in Table 1.

Table 1 General function and the expression behavior of chronic low-grade inflammation, cell senescence, and oxidative stress biomarkers in the context of dAGEs consumption. Data collected from publications between 2014 to 2021.

Biomarkers	General biological role	Expression Tendance/ Sample
AKT/mTOR	**Protein Kinase B** Regulation of cell survival, metabolism, proliferation, and growth. **Mammalian Target of Rapamycin** Protein kinase regulates growth and survival, nutrients, and energetic metabolism.	AKT: ↔/ Muscles [109] AKT/mTOR: ↓/Cardiomyocytes [91]
EZH2	**Enhancer of zeste homolog 2** Catalytic subunit of the Polycomb Repressive Complex 2 (PRC2), working on the histone-lysine N-methyltransferase activity.	↑/Podocytes [110]
GLO1	**Glyoxalase I** Cytoplasmic enzyme which takes part in methylglyoxal detoxification and is a byproduct of glycolysis.	↓/ Hind Limb Ischemia in Diabetic Mice [111] ↑/GLO1 expression is increased in RAGE KO mice (Heidelberg University lineage) due to a gene doubling [48]
IL-6	**Interleukin 6** Pro-inflammatory cytokine with a wide biological function in immunity and cell metabolism.	↔/ Plasma [62] ↓/ Plasma [112]
P16 (CDKN2a)	**Cyclin-Dependent Kinase Inhibitor 2a** Cell cycle control (arrest in G1 and G2) with an important role as a tumor suppressor.	↑/ Cardiac fibroblasts [113]
PGC1α	**Peroxisome Proliferator-Activated Receptor Gamma Coactivator 1-Alpha** Transcriptional coactivator for steroid receptors. Essential in the control of glucose and fatty acid metabolism.	↓/Human neural stem cells [114]
RAGE	**Receptor for Advanced Glycation End-Products** Cell receptors for AGEs and DAMPs, acts as a mediator of inflammation. AGE/RAGE signaling regulates the expression of cytokines and reactive oxygen species.	↑/aorta [41] ↓/Mononuclear cells [115]
SA-GLβ1	**Beta-Galactosidase 1** Cleaves beta-linked terminal galactosyl residues in senescent cells.	↑/ Cardiac fibroblasts [113]
SIRT1	**Sirtuin 1** NAD-dependent protein deacetylase coordinates intracellular energetics, cell cycle, response to DNA damage, metabolism, and apoptosis.	↑/ Muscles (RAGE KO mice) [116]

Biomarkers	General biological role	Expression Tendance/ Sample
SOD1/2	**Superoxide Dismutase 1 and 2** Oxidative stress control. SOD1 (cytoplasm) and SOD 2 (mitochondria)	↑/ Muscles [116]
TNFα	**Tumor Necrosis Factor Alpha** Pro-inflammatory cytokine is expressed in different cell types including adipocytes, controlling insulin resistance and cell death.	↑/ Plasma [112] ↔/ Plasma [62]
VCAM-1	**Vascular Cell Adhesion Protein 1** Cell-cell adhesion and recognition, signal transduction, and immune cell migration.	↑/aorta [41]

In defining the implications of the RAGE/AGE axis activation, some studies have shed light on the behavior of some of the previously presented signaling pathways. A proper definition of the mechanisms governing the AGE/RAGE/p13K/AKT/mTOR or AGE/RAGE/AMPK/SIRT1/PGC1α pathways is not yet clear and conflicting data are presented in the literature. This may concern the fact that the control of multiple stress stimuli is governed by different pathways. Under hyperglycemic conditions, for instance, AKT/mTOR effectors have been implicated in metabolic dysfunctions such as diabetes and obesity since they are correlated with insulin resistance [117]. AKT/mTOR activation was suppressed in Wistar rat neonatal cardiomyocytes exposed to AGEs, leading to autophagy. This phenomenon was demonstrated to be RAGE dependent as RAGE blockage retained regular AKT phosphorylation levels [91]. Moreover, a similar effect was observed in rats' vascular smooth muscle cells [118].

It is well accepted that SIRT1 expression significantly reduces with age, worsening energy expenditure efficiency and contributing to oxidative stress and inflammation triggers [119]. Gong et al., (2014) demonstrated a 2-fold decrease of SIRT1 in 48-week-old mice compared with younger animals (4 weeks) [119]. SIRT1 has been demonstrated to be upregulated in RAGE-knockout mice, which in turn was suggested to contribute to aging deacceleration due to the maintenance of SIRT1 expression in both renal and muscular tissues [116,120]. The influence of AGEs over SIRT1 results in the acceleration of aging since the AMPK-dependent pathways (including SIRT1 and PGC1α) have been demonstrated to be suppressed, contributing to higher inflammation, mitochondrial dysfunction, and senescence in different pathologies (*e.g.* Alzheimer's disease, diabetes, cirrhosis) [38,114].

While glycation is often the result of an oxidative process in addition to carbonyl stress (also known as glycoxidation), it is implicated in downstream oxidative stress activation [121]. A counterreaction is composed of natural antioxidant barriers as the SOD system. On the definition of the role of the different SOD variants, it has been suggested that SOD2 participates in oxidative stress control initiated by glycated serum albumin in vascular smooth muscle cells during 48 hours of treatment [122]. The role of SOD1 on oxidative stress control was shown to be time-dependent, since SOD1 expression was downregulated over 24h of AGE treatment [123]. AGEs were also reported to upregulate the activity of senescence-associated β-galactosidase activity, as well as P16, in rat cardiac fibroblasts, suggesting it has a role in cardiac aging and fibrosis [113]. Despite a lack of deeper investigations, the initiation of cardiac aging associated with P16 might suggest the origin of arterial stiffness demonstrated by Grossin et al. (2015) on animals submitted to a high-CML diet [41].

Several consequences of the dysregulation of these signaling pathways may occur, with the activation of cell survival pathways as particular targets. These downstream elements include the transcription modulation of inflammation and oxidative stress encoding genes [124]. Cytokines such as IL6 and TNFα, together with endothelial adhesion biomarker, VCAM1, are well explored in dietary studies with animal models and well-established analytical tools are available. Aside from the widespread study of cytokines such as IL6 and TNFα in the literature, the expression patterns described in the literature are not always concordant, making the comparison of results a difficult task, in part due to the different protocols used (*e.g.* different means of diet production or different exposition periods). Data on these inflammaging biomarkers are thus not always in agreement in the literature and they are further reviewed in CHAPTER 3.

The study by Grossin et al. (2015) administered a diet containing 200 $\mu g_{dCML}/g_{food}$ to mice. They observed increased VCAM1 gene expression in aortic tissues under the effects of this high dose of dCML after 35 weeks of dietary exposure. A more complete inflammatory panel including six inflammatory biomarkers (CRP, TNFα, INFγ, KC/GRO, IL6, and IL10) was used by van Dongen et al., 2021 to study the effects of a diet high in AGEs in mice. The authors demonstrated that a baked chow diet only promoted a decrease in plasmatic IL10 (anti-inflammatory) cytokine expression in C57BL/6 female mice plasma. But none

of the other inflammatory biomarkers appeared to be affected by the diet. In another study, the effects of dAGEs were shown to evoke a pro-inflammatory state in C57BL/6 male mice. Animals that received an AGE-enriched diet (casein-methylglyoxal - MG-H1 17.4 g/Kg food) over 22 weeks had increased levels of Il1β, IL17 and TNFα, while anti-inflammatory agents as IL10 and IL6 were downregulated [112].

Furthermore, AGEs have also been demonstrated to modulate gene expression by epigenetic means. Data obtained from murine podocytes exposed to AGEs showed the downregulation of EZH2 and reduced H3K27m3 after 24h of a cell culture treated with 5 mg/mL glycated BSA. This effect suggested that AGEs participate in the aggravation of nephropathy together with metabolic memory in diabetic kidney disease [110].

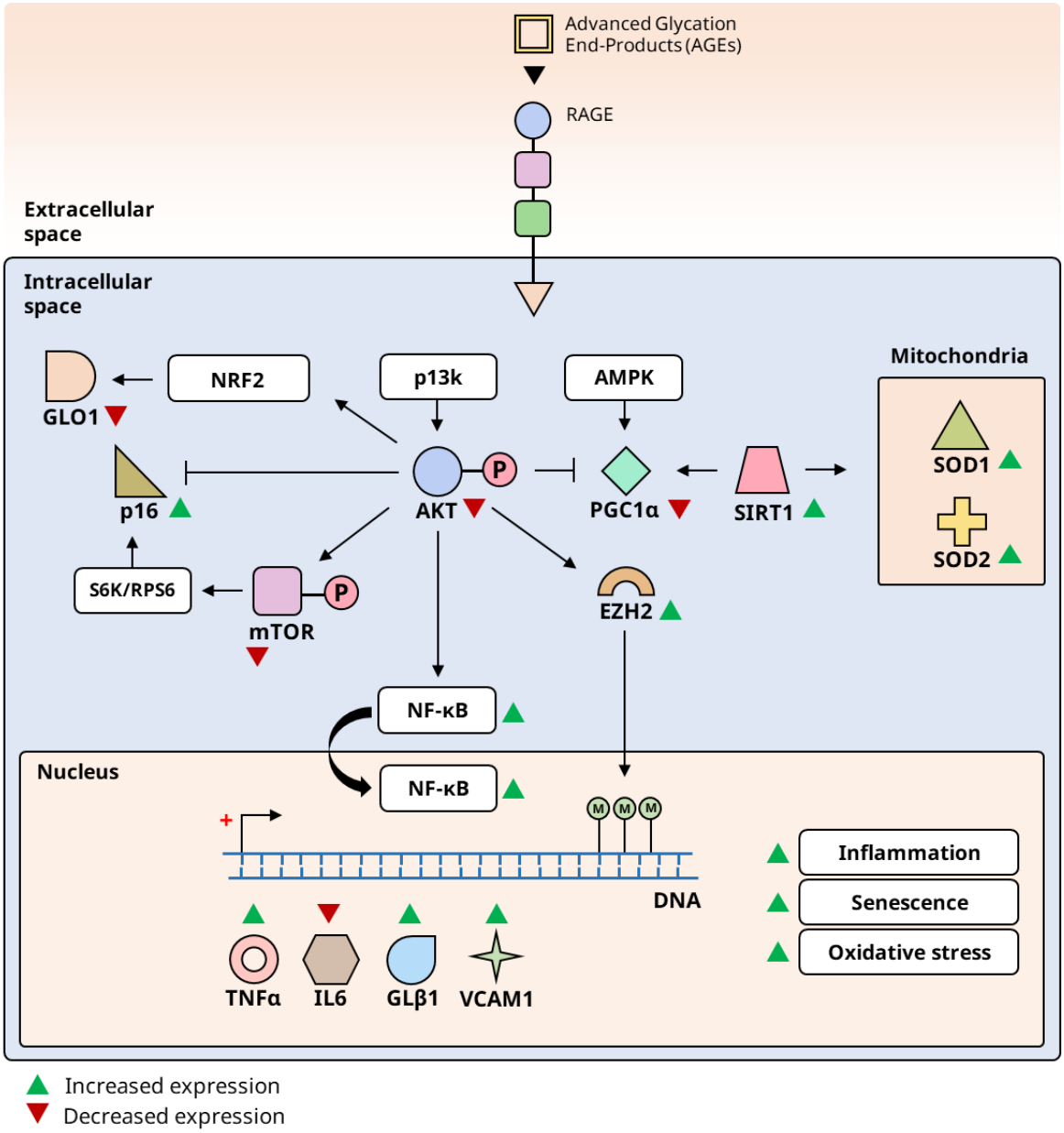

Figure 9 Schematic representation of the intricate molecular pathways affected by the overconsumption of Advanced Glycation End-products (AGEs). Expression patterns are trends presented in the scientific literature from studies in rodents and compiled in Table 1.

It is worth reemphasizing that the nutritional factors cited above as modulating diverse metabolic pathways in the course of life may also be of great importance during early life (including the prenatal period). However, such early-life effects are not yet known, and the influence of maternal nutrition for the health of their offspring, as well as the reversibility of potential effects, remain to be elucidated. To our knowledge, only one study has so far aimed to investigate the possible reversibility of any effects of dAGEs consumption. A study published by van Dongen et al., 2021 included a 10-week exposure to either a regular or a baked

chow diet. Significant increases were observed on the circulating levels of free and protein-bound CML in the group receiving the baked chow, as well as in kidneys and liver. However, a diet switch group had decreased levels of free AGEs, demonstrating the reversibility on the circulating levels of exogenous AGEs. Yet, this study has important limitations associated with the exclusive use of female animals and the lack of information on the influence of perinatal exposure to dAGEs on the resulting offspring. In addition, the AGE production model based on the heat treatment of food given to mice may lead to the genesis of several other neoformed compounds, together with the degradation of micro and macronutrients, which may be confounding factors.

1.3.2. RAGE knockout murine model – a model for the study of the effects of AGE-RAGE axis on mammal health

Different research strategies exist to examine the role of cellular receptors. On the functional prospection of RAGE, the use of immunotherapies (anti-RAGE antibodies), RAGE antagonists (*e.g.* Azeliragon), as well as RAGE-knockout mice have been developed for this purpose. Different RAGE knockout strains exist, but the most widely used is the RAGE-KO HU strain engineered at the University of Heidelberg (Germany), and it is the model currently used by our research group (U1167) in Lille (France). This knockout strain harbors a genetically engineered gene deletion from exons 2 to 7, leading to the synthesis of a non-functional RAGE protein. A comparative gene structure is represented in Figure 10A including both wild type (WT) and the mutated RAGE forms of the mice gene [125,126]. On the protein level, murine RAGE contains 80% of the identity of the human counterpart. Differences are distributed along the extracellular, transmembrane, and intracellular domains (Figure 10B).

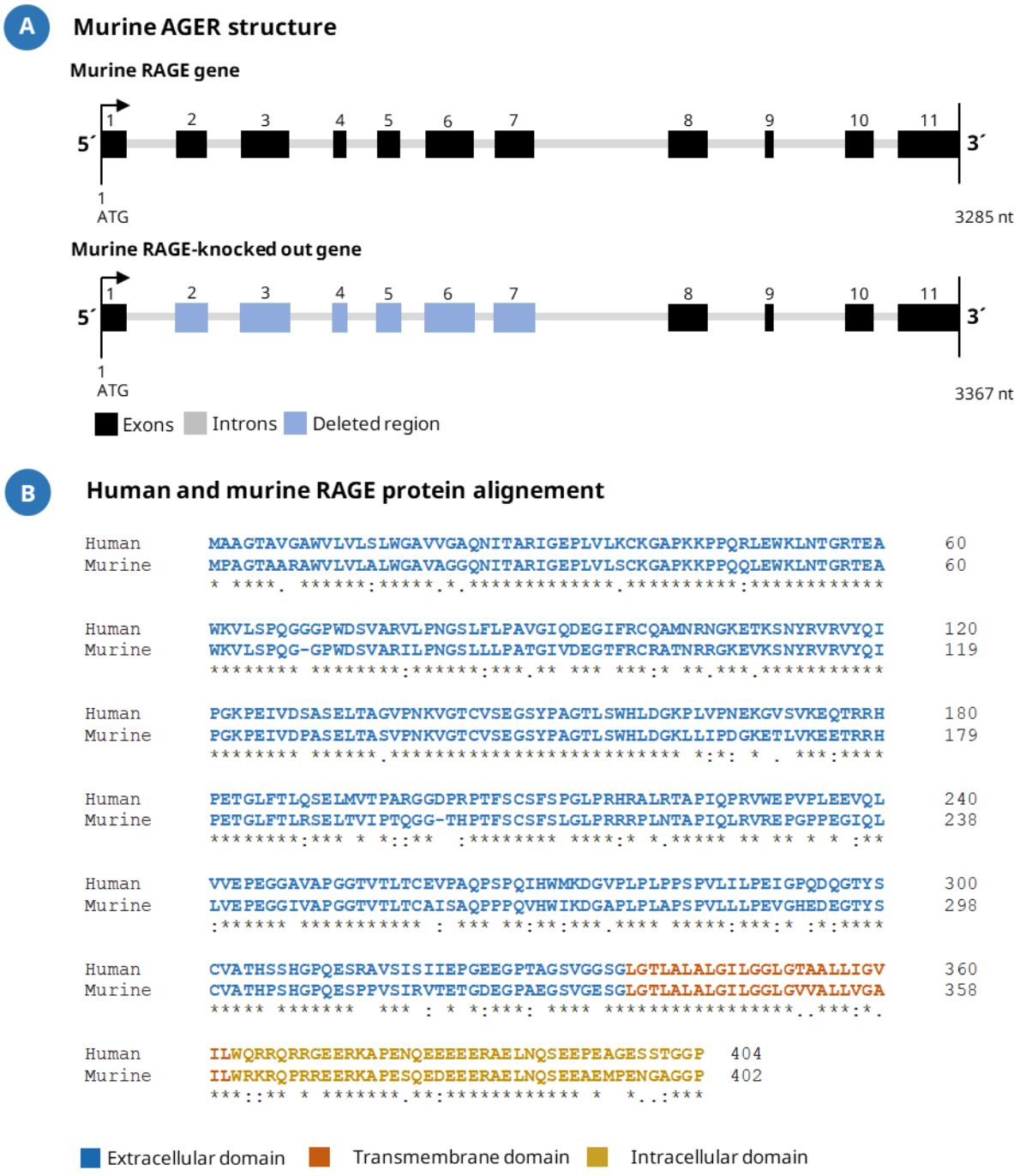

Figure 10 (A) The comparative RAGE gene structure in WT and RAGE-KO mice. The highlight is given to the deleted region from exons 2 to 7, resulting in the codification of an unfunctional receptor. **(B)** Alignment of human and murine RAGE proteins.

RAGE genetic invalidation is compatible with life and no reproduction limitation has been published in the literature [126]. The RAGE KO Kyoto strain, on the other hand, has been reported to have hypersensitivity to auditory stimuli [127] or the impairment of pup care by the mother [128]. Such behavioral features have not been reported for the Heidelberg strain. However, these animals present specific

genetic modifications. Bartling et al. described the doubling of both GLO1/Dnahc8 genes in the RAGE-KO HU genome. The gene doubling was an artifact of the repeated backcrossing used for lineage generation [48]. Two implications may arise from these events. First, both *RAGE* and *GLO1* coding regions are close on chromosome 17, and the chances of avoiding the doubling of GLO1 are low once RAGE has been deleted. Furthermore, given the significance of GLO1 in glycation processes discussed in the introduction, it is crucial for us to explore potential anti-glycation mechanisms that can mitigate the detrimental effects of glycoxidative stress (*e.g.* dicarbonyl stress). The gene duplication was reported to increase GLO1 activity in the lungs, kidneys and liver [48]. In addition, a change in Dnahc8 expression would imply a gender effect since it is expressed in the testis, regulating spermatogenesis. However, it is a ubiquitously expressed gene, and the importance of increased Dnahc8 expression have not been clearly described.

1.4. Physiological effects of dietary glycation end-products in humans

The identification of relevant risk factors in different populations is essential for understanding the negative effects caused by certain human behaviors or habits. Only limited information originating from clinical and epidemiological studies is available on the effects of dietary AGEs on human physiology. Throughout the first decade of the 2000s, much attention was paid to the characterization of MRP content in different food matrices. First, studies relied on the use of ELISA tests for the estimation of AGEs in foods. Tessier & Birlouez-Aragon et al., (2010) reviewed 12 interventional/epidemiological studies published up to 2010, among which 6 estimated AGE levels from ELISA tests. This technique attracted criticism due to its limitations for quantifying AGEs in complex food matrices [60]. Owing to the great discussion over the reliability of ELISA quantification of AGEs, a tendency to prioritize the use of more reliable quantitative methods has driven the use of techniques such as liquid chromatography–mass spectrometry (HPLC-MS/MS). This technique has since been used in the construction of databases and estimation of the consumption of AGEs in different studies as listed in Table 2. Currently, three main databases exist compiling data on the quantification of CML, CEL, MG-H1, and other AGEs by HPLC-MS/MS in different foods [56,57,129]. These databases, in combination with Food Frequency Questionnaire (FFQ) interviews or other food

consumption surveys, have been used as methods for the estimation of the amount of glycation products consumed by different human cohorts.

Interventional and epidemiological studies have examined the relationship between the consumption of dAGEs and potential deleterious effects in human subpopulations. Since the levels of glycation products are affected by the cooking method, a randomized crossover interventional study conducted with 62 healthy volunteers (18-24 years) was designed to compare the effects of two food preparation protocols: steamed and high-temperature treated diets [60]. An association was observed between consumption of a high-heat-treated diet and lower circulating levels of omega-3 and ascorbic acid. In accordance with other studies, reduced insulin sensitivity was observed in the high-temperature diet group compared with the steamed-food group. In addition, an augmentation of plasma levels of cholesterol and triglycerides was observed, both of which may contribute to the development of CVD and diabetes.

Other cohorts have been used to clarify the relationships between dAGEs and deleterious health traits including cardiovascular risk, diabetes, obesity, and several cancer types. A 5-year follow-up study on more than 255 000 adult participants between 25-70 years old, recruited between 1992-2000 by the PANACEA study, reported a marginal contribution of the different dAGEs to an increase in weight: 0.11 kg associated with CEL level, and a lower contribution of CML (0.06 kg) and MH-G1 (0.03 kg) along the 5 years of study [130]. In another study, a short period of high-AGE diet exposure (6 weeks) was shown not to affect plasma levels of CML or inflammatory mediators in 12 patients [131]. The negligible effect of the dietary intake of AGEs in such populations could be masked by a number of confounding environmental and endogenous factors. Furthermore, the measurement of CML concentrations in plasma was conducted using an ELISA test, which is primarily designed to quantify protein-bound CML. As a result, it is not unexpected to observe no direct effect of the diet on protein-bound CML levels. This is because protein-bound CML is believed to originate mainly from endogenous sources, such as the glycation of plasma proteins, rather than from dietary intake.
A recent epidemiological study including 3114 patients evaluated ocular microvascular lesions for assessing the effects of dAGEs on the development of diabetes, in addition to endothelial biomarkers including VCAM1 and E-selectin. However, no strong association between the consumption of dAGEs and general

microvascular function was observed [132]. The same authors demonstrated that even in obese individuals, the supply of a diet high in dAGEs did not have significant effects on inflammatory markers over 4 weeks [133]. Authors recognized the several confounding factors including the short-term diet exposition, the metabolic disparity between the 73 individuals evaluated, and the lack of information on the lifestyle of subjects, as components contributing to increased variability among the experimental groups. A better approach in this case would be a randomized design including controlled trials for each diet intervention [132]. A comparative epidemiological study, including two different age-divergent cohorts (old cohorts *versus* middle-aged cohort), reported an association between plasmatic 3-deoxyglucosone levels and incidence of cardiovascular disease (CVD) in older patients (average age of 74.5 years) but not among the middle-aged subjects (average age of 65.5 years), emphasizing the implication of reactive dicarbonyls in the aggravation of cardiac complications among older people [134].

In addition to the cardiovascular risk, obesity, and diabetes studies mentioned above, the relationship between high-AGE consumption and the incidence of several cancer types has been investigated using epidemiologic studies. To our knowledge, no study has reported a clear association between the ingestion of dAGEs and the incidence of liver cancer [135], or colorectal cancer [136].

Table 2 Intervention/cross-sectional studies published between 2010-2023 on the investigation of the association of the consumption of AGEs and its health effects.

Study design	Populations	Diets	Food survey Methods & Analytical methods	Effects	Reference
4-weeks randomized, crossover, diet-controlled intervention trial	62 healthy subjects between 18-24 years	Isocaloric, steamed and high-temperature treated diets	HPLC, GC-MS/MS	Reduced insulin resistance and circulating omega-3 in the high-heat diet-consuming group	[60]
6-weeks randomized, parallel-arm, controlled dietary intervention	24 healthy subjects between 50-69 years	Isocaloric, food-equivalent diets prepared at either high or mild temperatures	ELISA	No significant changes in CML serum levels, tonometry, or inflammatory biomarkers	[131]
5-years follow up, cross-sectional study	PANACEA Study - 255170 subjects between 25-70 years	-	UPLC-MS/MS	Marginal weight gain associated with CEL levels	[130]
13-years follow up, cross-sectional study	EPIC Study - 450111 subjects between 50-51 years	-	FFQ - UPLC-MS/MS	Inverse association between dietary AGEs and colorectal cancer (CRC) risk	[136]
4-week dietary intervention	82 obese subjects between 51-53 years	Energy- and macronutrient-matched diets low and high in dAGEs	UPLC-MS/MS	Increased circulating AGEs in subjects submitted to a high-AGE diet, but no inflammation, oxidative stress, or insulin metabolism changes	[133]
3-months follow up, cross-sectional study	Maastricht Study 3144 subjects with 60 years old on average	-	FFQ - UPLC-MS/MS	No microvascular deleterious effects	[132]
11-years follow up, cross-sectional study	Cardiovascular Health Study (466 subjects >73 years old) and a case-cohort Multi-Ethnic Study of Atherosclerosis (1631 subjects, 62-69 years)	-	UPLC-MS/MS	Higher circulating dicarbonyls in the older cohort	[134]
13-years follow up, cross-sectional study	Takayama Study - 30722 Japanese subjects of 35 years on average	-	FFQ - UPLC-MS/MS	No increased total cancer risk associated with high-AGE consumption	[135]

2 References

1. Tizazu, A.M.; Mengist, H.M.; Demeke, G. Aging, Inflammaging and Immunosenescence as Risk Factors of Severe COVID-19. *Immun. Ageing* **2022**, *19*, 53, doi:10.1186/s12979-022-00309-5.
2. Franceschi, C.; Garagnani, P.; Parini, P.; Giuliani, C.; Santoro, A. Inflammaging: A New Immune–Metabolic Viewpoint for Age-Related Diseases. *Nat. Rev. Endocrinol.* **2018**, *14*, 576–590, doi:10.1038/s41574-018-0059-4.
3. Carrasco, E.; Gómez de las Heras, M.M.; Gabandé-Rodríguez, E.; Desdín-Micó, G.; Aranda, J.F.; Mittelbrunn, M. The Role of T Cells in Age-Related Diseases. *Nat. Rev. Immunol.* **2022**, *22*, 97–111, doi:10.1038/s41577-021-00557-4.
4. Zamboni, M.; Nori, N.; Brunelli, A.; Zoico, E. How Does Adipose Tissue Contribute to Inflammageing? *Exp. Gerontol.* **2021**, *143*, 111162, doi:10.1016/j.exger.2020.111162.
5. Di Giosia, P.; Stamerra, C.A.; Giorgini, P.; Jamialahamdi, T.; Butler, A.E.; Sahebkar, A. The Role of Nutrition in Inflammaging. *Ageing Res. Rev.* **2022**, *77*, 101596, doi:10.1016/j.arr.2022.101596.
6. Alcock, J.; Carroll-Portillo, A.; Coffman, C.; Lin, H.C. Evolution of Human Diet and Microbiome-Driven Disease. *Curr. Opin. Physiol.* **2021**, *23*, 100455, doi:10.1016/j.cophys.2021.06.009.
7. Armelagos, G.J. Brain Evolution, the Determinates of Food Choice, and the Omnivore's Dilemma. *Crit. Rev. Food Sci. Nutr.* **2014**, *54*, 1330–1341, doi:10.1080/10408398.2011.635817.
8. Somoza, V.; Fogliano, V. 100 Years of the Maillard Reaction: Why Our Food Turns Brown. *J. Agric. Food Chem.* 2013, *61*, 10197–10197.
9. Du, C.; Whiddett, R.O.; Buckle, I.; Chen, C.; Forbes, J.M.; Fotheringham, A.K. Advanced Glycation End Products and Inflammation in Type 1 Diabetes Development. *Cells* **2022**, *11*, 3503, doi:10.3390/cells11213503.
10. Imbroisi Filho, R.; Ochioni, A.C.; Esteves, A.M.; Leandro, J.G.B.; Demaria, T.M.; Sola-Penna, M.; Zancan, P. Western Diet Leads to Aging-Related Tumorigenesis via Activation of the Inflammatory, UPR, and EMT Pathways. *Cell Death Dis.* **2021**, *12*, 1–9, doi:10.1038/s41419-021-03929-9.
11. Kawai, T.; Autieri, M.V.; Scalia, R. Adipose Tissue Inflammation and Metabolic Dysfunction in Obesity. *Am. J. Physiol.-Cell Physiol.* **2021**, *320*, C375–C391.
12. Ma, W.; Nguyen, L.H.; Song, M.; Wang, D.D.; Franzosa, E.A.; Cao, Y.; Joshi, A.; Drew, D.A.; Mehta, R.; Ivey, K.L.; et al. Dietary Fiber Intake, the Gut Microbiome, and Chronic Systemic Inflammation in a Cohort of Adult Men. *Genome Med.* **2021**, *13*, 102, doi:10.1186/s13073-021-00921-y.
13. Calder, P.C.; Ahluwalia, N.; Brouns, F.; Buetler, T.; Clement, K.; Cunningham, K.; Esposito, K.; Jönsson, L.S.; Kolb, H.; Lansink, M.; et al. Dietary Factors and Low-Grade Inflammation in Relation to Overweight and Obesity. *Br. J. Nutr.* **2011**, *106 Suppl 3*, S5-78, doi:10.1017/S0007114511005460.
14. Bastos, D.H.M.; Gugliucci, A. Contemporary and Controversial Aspects of the Maillard Reaction Products. *Curr. Opin. Food Sci.* **2015**, *1*, 13–20, doi:10.1016/j.cofs.2014.08.001.
15. Birlouez-Aragon, I. Assessment of Protein Glycation Markers in Infant Formulas. *Food Chem.* **2004**, *87*, 253–259, doi:10.1016/j.foodchem.2003.11.019.
16. Koschinsky, T.; He, C.-J.; Mitsuhashi, T.; Bucala, R.; Liu, C.; Buenting, C.; Heitmann, K.; Vlassara, H. Orally Absorbed Reactive Glycation Products (Glycotoxins): An Environmental Risk Factor in Diabetic Nephropathy. *Med. Sci.* **1997**, 6.
17. Dattilo, A.M.; Saavedra, J.M. Nutrition Education: Application of Theory and Strategies during the First 1,000 Days for Healthy Growth. **2019**, doi:10.1159/000499544.
18. Likhar, A.; Patil, M.S.; Likhar, A.; Patil, M.S. Importance of Maternal Nutrition in the First 1,000 Days of Life and Its Effects on Child Development: A Narrative Review. *Cureus* **2022**, *14*, doi:10.7759/cureus.30083.
19. Rehman, S.; Aatif, M.; Rafi, Z.; Khan, M.Y.; Shahab, U.; Ahmad, S.; Farhan, M. Effect of Non-Enzymatic Glycosylation in the Epigenetics of Cancer. *Semin. Cancer Biol.* **2022**, *83*, 543–555, doi:10.1016/j.semcancer.2020.11.019.
20. Thieme, K.; Pereira, B.M.V.; da Silva, K.S.; Fabre, N.T.; Catanozi, S.; Passarelli, M.; Correa-Giannella, M.L. Chronic Advanced-Glycation End Products Treatment Induces TXNIP

Expression and Epigenetic Changes in Glomerular Podocytes in Vivo and in Vitro. *Life Sci.* **2021**, *270*, 118997, doi:10.1016/j.lfs.2020.118997.
21. Maillard, L.C. Action Des Acides Amines Sur Les Sucres; Formation Des Melanoidies Par Voie Methodique. *CR Acad Sci* **1912**, *154*, 66–68.
22. Finot, P.-A. Historical Perspective of the Maillard Reaction in Food Science. *Ann. N. Y. Acad. Sci.* **2005**, *1043*, 1–8, doi:10.1196/annals.1333.001.
23. Hellwig, M.; Henle, T. Baking, Ageing, Diabetes: A Short History of the Maillard Reaction. *Angew. Chem. Int. Ed Engl.* **2014**, *53*, 10316–10329, doi:10.1002/anie.201308808.
24. Barnes, H.M.; Kaufman, C.W. Industrial Aspects of Browning Reaction. *Ind. Eng. Chem.* **1947**, *39*, 1167–1170.
25. Doob Jr, H.; Willmann, A.; Sharp, P.F. Influence of Moisture on Browning of Dried Whey and Skim Milk. *Ind. Eng. Chem.* **1942**, *34*, 1460–1468.
26. Hodge, J.E. Dehydrated Foods, Chemistry of Browning Reactions in Model Systems. *J. Agric. Food Chem.* **1953**, *1*, 928–943, doi:10.1021/jf60015a004.
27. Huisman, T.H.J.; Martis, E.A.; Dozy, A. Chromatography of Hemoglobin Types on Carboxymethylcellulose. *J. Lab. Clin. Med.* **1958**, *52*, 312–327, doi:10.5555/uri:pii:0022214358900404.
28. Rahbar, S.; Blumenfeld, O.; Ranney, H.M. Studies of an Unusual Hemoglobin in Patients with Diabetes Mellitus. *Biochem. Biophys. Res. Commun.* **1969**, *36*, 838–843, doi:10.1016/0006-291x(69)90685-8.
29. Gillery, P. A History of HbA1c through Clinical Chemistry and Laboratory Medicine. *Clin. Chem. Lab. Med. CCLM* **2013**, *51*, 65–74, doi:10.1515/cclm-2012-0548.
30. Wadman, S.K.; De Bree, P.K.; Van Sprang, F.J.; Kamerling, J.P.; Haverkamp, J.; Vliegenthart, J.F. N-EPSILON-(CARBOXYMETHYL)LYSINE, A CONSTITUENT OF HUMAN URINE. *Clin. Chim. Acta Int. J. Clin. Chem.* **1975**, *59*, 313–320, doi:10.1016/0009-8981(75)90007-8.
31. Ahmed, M.U.; Thorpe, S.R.; Baynes, J.W. Identification of N Epsilon-Carboxymethyllysine as a Degradation Product of Fructoselysine in Glycated Protein. *J. Biol. Chem.* **1986**, *261*, 4889–4894, doi:10.1016/S0021-9258(19)89188-3.
32. Buser, W.; Erbersdobler, H.F. Carboxymethyllysine, a New Compound of Heat Damage in Milk Products. *Milchwissenschaft* **1986**, *41*, 780–785.
33. Neeper, M.; Schmidt, A.M.; Brett, J.; Yan, S.D.; Wang, F.; Pan, Y.C.; Elliston, K.; Stern, D.; Shaw, A. Cloning and Expression of a Cell Surface Receptor for Advanced Glycosylation End Products of Proteins. *J. Biol. Chem.* **1992**, *267*, 14998–15004.
34. Mottram, D.S.; Wedzicha, B.L.; Dodson, A.T. Acrylamide Is Formed in the Maillard Reaction. *Nature* **2002**, *419*, 448–449, doi:10.1038/419448a.
35. de Oliveira, F.C.; Coimbra, J.S. dos R.; de Oliveira, E.B.; Zuñiga, A.D.G.; Rojas, E.E.G. Food Protein-Polysaccharide Conjugates Obtained via the Maillard Reaction: A Review. *Crit. Rev. Food Sci. Nutr.* **2016**, *56*, 1108–1125, doi:10.1080/10408398.2012.755669.
36. Alhujaily, M.; Abbas, H.; Xue, M.; de la Fuente, A.; Rabbani, N.; Thornalley, P.J. Studies of Glyoxalase 1-Linked Multidrug Resistance Reveal Glycolysis-Derived Reactive Metabolite, Methylglyoxal, Is a Common Contributor in Cancer Chemotherapy Targeting the Spliceosome. *Front. Oncol.* **2021**, *11*, 748698, doi:10.3389/fonc.2021.748698.
37. Twarda-Clapa, A.; Olczak, A.; Białkowska, A.M.; Koziołkiewicz, M. Advanced Glycation End-Products (AGEs): Formation, Chemistry, Classification, Receptors, and Diseases Related to AGEs. *Cells* **2022**, *11*, 1312, doi:10.3390/cells11081312.
38. Rungratanawanich, W.; Qu, Y.; Wang, X.; Essa, M.M.; Song, B.-J. Advanced Glycation End Products (AGEs) and Other Adducts in Aging-Related Diseases and Alcohol-Mediated Tissue Injury. *Exp. Mol. Med.* **2021**, *53*, 168–188, doi:10.1038/s12276-021-00561-7.
39. Mengstie, M.A.; Chekol Abebe, E.; Behaile Teklemariam, A.; Tilahun Mulu, A.; Agidew, M.M.; Teshome Azezew, M.; Zewde, E.A.; Agegnehu Teshome, A. Endogenous Advanced Glycation End Products in the Pathogenesis of Chronic Diabetic Complications. *Front. Mol. Biosci.* **2022**, *9*, 1002710, doi:10.3389/fmolb.2022.1002710.
40. Aragno, M.; Mastrocola, R. Dietary Sugars and Endogenous Formation of Advanced Glycation Endproducts: Emerging Mechanisms of Disease. *Nutrients* **2017**, *9*, 385, doi:10.3390/nu9040385.
41. Grossin, N.; Auger, F.; Niquet-Leridon, C.; Durieux, N.; Montaigne, D.; Schmidt, A.M.; Susen, S.; Jacolot, P.; Beuscart, J.-B.; Tessier, F.J.; et al. Dietary CML-Enriched Protein

Induces Functional Arterial Aging in a RAGE-Dependent Manner in Mice. *Mol. Nutr. Food Res.* **2015**, *59*, 927–938, doi:10.1002/mnfr.201400643.
42. Verzijl, N.; DeGroot, J.; Thorpe, S.R.; Bank, R.A.; Shaw, J.N.; Lyons, T.J.; Bijlsma, J.W.; Lafeber, F.P.; Baynes, J.W.; TeKoppele, J.M. Effect of Collagen Turnover on the Accumulation of Advanced Glycation End Products. *J. Biol. Chem.* **2000**, *275*, 39027–39031, doi:10.1074/jbc.M006700200.
43. Reigle, K.L.; Di Lullo, G.; Turner, K.R.; Last, J.A.; Chervoneva, I.; Birk, D.E.; Funderburgh, J.L.; Elrod, E.; Germann, M.W.; Surber, C.; et al. Non-Enzymatic Glycation of Type I Collagen Diminishes Collagen–Proteoglycan Binding and Weakens Cell Adhesion. *J. Cell. Biochem.* **2008**, *104*, 1684–1698, doi:10.1002/jcb.21735.
44. Rabbani, N.; Xue, M.; Thornalley, P.J. Dicarbonyl Stress, Protein Glycation and the Unfolded Protein Response. *Glycoconj. J.* **2021**, *38*, 331–340, doi:10.1007/s10719-021-09980-0.
45. Thornalley, P.J.; Langborg, A.; Minhas, H.S. Formation of Glyoxal, Methylglyoxal and 3-Deoxyglucosone in the Glycation of Proteins by Glucose. *Biochem. J.* **1999**, *344*, 109–116.
46. Lorenzi, M. The Polyol Pathway as a Mechanism for Diabetic Retinopathy: Attractive, Elusive, and Resilient. *Exp. Diabetes Res.* **2007**, *2007*, 61038, doi:10.1155/2007/61038.
47. Iacobini, C.; Vitale, M.; Haxhi, J.; Pesce, C.; Pugliese, G.; Menini, S. Food-Related Carbonyl Stress in Cardiometabolic and Cancer Risk Linked to Unhealthy Modern Diet. *Nutrients* **2022**, *14*, 1061, doi:10.3390/nu14051061.
48. Bartling, B.; Zunkel, K.; Al-Robaiy, S.; Dehghani, F.; Simm, A. Gene Doubling Increases Glyoxalase 1 Expression in RAGE Knockout Mice. *Biochim. Biophys. Acta BBA - Gen. Subj.* **2020**, *1864*, 129438, doi:10.1016/j.bbagen.2019.129438.
49. He, Y.; Zhou, C.; Huang, M.; Tang, C.; Liu, X.; Yue, Y.; Diao, Q.; Zheng, Z.; Liu, D. Glyoxalase System: A Systematic Review of Its Biological Activity, Related-Diseases, Screening Methods and Small Molecule Regulators. *Biomed. Pharmacother.* **2020**, *131*, 110663, doi:10.1016/j.biopha.2020.110663.
50. Rabbani, N.; Thornalley, P.J. Glyoxalase in Diabetes, Obesity and Related Disorders. *Semin. Cell Dev. Biol.* **2011**, *22*, 309–317, doi:10.1016/j.semcdb.2011.02.015.
51. Bakhiya, N.; Appel, K.E. Toxicity and Carcinogenicity of Furan in Human Diet. *Arch. Toxicol.* **2010**, *84*, 563–578, doi:10.1007/s00204-010-0531-y.
52. Kumar, J.; Das, S.; Teoh, S.L. Dietary Acrylamide and the Risks of Developing Cancer: Facts to Ponder. *Front. Nutr.* **2018**, *5*.
53. Liu, S.; Sun, H.; Ma, G.; Zhang, T.; Wang, L.; Pei, H.; Li, X.; Gao, L. Insights into Flavor and Key Influencing Factors of Maillard Reaction Products: A Recent Update. *Front. Nutr.* **2022**, *9*.
54. Perrone, D.; Farah, A.; Donangelo, C.M. Influence of Coffee Roasting on the Incorporation of Phenolic Compounds into Melanoidins and Their Relationship with Antioxidant Activity of the Brew. *J. Agric. Food Chem.* **2012**, *60*, 4265–4275, doi:10.1021/jf205388x.
55. Hellwig, M.; Nitschke, J.; Henle, T. Glycation of N-ε-Carboxymethyllysine. *Eur. Food Res. Technol.* **2022**, *248*, 825–837, doi:10.1007/s00217-021-03931-7.
56. Scheijen, J.L.; Clevers, E.; Engelen, L.; Dagnelie, P.C.; Brouns, F.; Stehouwer, C.D.; Schalkwijk, C.G. Analysis of Advanced Glycation Endproducts in Selected Food Items by Ultra-Performance Liquid Chromatography Tandem Mass Spectrometry: Presentation of a Dietary AGE Database. *Food Chem.* **2016**, *190*, 1145–1150.
57. Hull, G.L.J.; Woodside, J.V.; Ames, J.M.; Cuskelly, G.J. Nε-(Carboxymethyl)Lysine Content of Foods Commonly Consumed in a Western Style Diet. *Food Chem.* **2012**, *131*, 170–174, doi:10.1016/j.foodchem.2011.08.055.
58. Tessier, F.J.; Birlouez-Aragon, I. Health Effects of Dietary Maillard Reaction Products: The Results of ICARE and Other Studies. *Amino Acids* **2012**, *42*, 1119–1131, doi:10.1007/s00726-010-0776-z.
59. Dittrich, R.; Hoffmann, I.; Stahl, P.; Müller, A.; Beckmann, M.W.; Pischetsrieder, M. Concentrations of Nε-Carboxymethyllysine in Human Breast Milk, Infant Formulas, and Urine of Infants. *J. Agric. Food Chem.* **2006**, *54*, 6924–6928, doi:10.1021/jf060905h.
60. Birlouez-Aragon, I.; Saavedra, G.; Tessier, F.J.; Galinier, A.; Ait-Ameur, L.; Lacoste, F.; Niamba, C.-N.; Alt, N.; Somoza, V.; Lecerf, J.-M. A Diet Based on High-Heat-Treated Foods Promotes Risk Factors for Diabetes Mellitus and Cardiovascular Diseases. *Am. J. Clin. Nutr.* **2010**, *91*, 1220–1226.
61. Seiquer, I.; Díaz-Alguacil, J.; Delgado-Andrade, C.; López-Frías, M.; Muñoz Hoyos, A.; Galdó, G.; Navarro, M.P. Diets Rich in Maillard Reaction Products Affect Protein Digestibility

in Adolescent Males Aged 11-14 y. *Am. J. Clin. Nutr.* **2006**, *83*, 1082–1088, doi:10.1093/ajcn/83.5.1082.
62. van Dongen, K.C.W.; Linkens, A.M.A.; Wetzels, S.M.W.; Wouters, K.; Vanmierlo, T.; van de Waarenburg, M.P.H.; Scheijen, J.L.J.M.; de Vos, W.M.; Belzer, C.; Schalkwijk, C.G. Dietary Advanced Glycation Endproducts (AGEs) Increase Their Concentration in Plasma and Tissues, Result in Inflammation and Modulate Gut Microbial Composition in Mice; Evidence for Reversibility. *Food Res. Int.* **2021**, *147*, 110547, doi:10.1016/j.foodres.2021.110547.
63. Xue, J.; Rai, V.; Frolov, S.; Singer, D.; Chabierski, S.; Xie, J.; Reverdatto, S.; Burz, D.S.; Schmidt, A.M.; Hoffman, R.; et al. Advanced Glycation End Product (AGE) Recognition by the Receptor for AGEs (RAGE). *Struct. Lond. Engl. 1993* **2011**, *19*, 722–732, doi:10.1016/j.str.2011.02.013.
64. Hellwig, M.; Geissler, S.; Matthes, R.; Peto, A.; Silow, C.; Brandsch, M.; Henle, T. Transport of Free and Peptide-Bound Glycated Amino Acids: Synthesis, Transepithelial Flux at Caco-2 Cell Monolayers, and Interaction with Apical Membrane Transport Proteins. *ChemBioChem* **2011**, *12*, 1270–1279, doi:10.1002/cbic.201000759.
65. Alamir, I.; Niquet-Leridon, C.; Jacolot, P.; Rodriguez, C.; Orosco, M.; Anton, P.M.; Tessier, F.J. Digestibility of Extruded Proteins and Metabolic Transit of Nε-Carboxymethyllysine in Rats. *Amino Acids* **2013**, *44*, 1441–1449, doi:10.1007/s00726-012-1427-3.
66. Tessier, F.J.; Niquet-Léridon, C.; Jacolot, P.; Jouquand, C.; Genin, M.; Schmidt, A.-M.; Grossin, N.; Boulanger, E. Quantitative Assessment of Organ Distribution of Dietary Protein-Bound 13C-Labeled Nε-Carboxymethyllysine after a Chronic Oral Exposure in Mice. *Mol. Nutr. Food Res.* **2016**, *60*, 2446–2456.
67. Bui, T.P.N.; Troise, A.D.; Fogliano, V.; de Vos, W.M. Anaerobic Degradation of N-ε-Carboxymethyllysine, a Major Glycation End-Product, by Human Intestinal Bacteria. *J. Agric. Food Chem.* **2019**, *67*, 6594–6602, doi:10.1021/acs.jafc.9b02208.
68. Delgado-Andrade, C.; Tessier, F.J.; Niquet-Leridon, C.; Seiquer, I.; Pilar Navarro, M. Study of the Urinary and Faecal Excretion of Nε-Carboxymethyllysine in Young Human Volunteers. *Amino Acids* **2012**, *43*, 595–602, doi:10.1007/s00726-011-1107-8.
69. Hellwig, M.; Bunzel, D.; Huch, M.; Franz, C.M.A.P.; Kulling, S.E.; Henle, T. Stability of Individual Maillard Reaction Products in the Presence of the Human Colonic Microbiota. *J. Agric. Food Chem.* **2015**, *63*, 6723–6730, doi:10.1021/acs.jafc.5b01391.
70. Hellwig, M.; Auerbach, C.; Müller, N.; Samuel, P.; Kammann, S.; Beer, F.; Gunzer, F.; Henle, T. Metabolization of the Advanced Glycation End Product N-ε-Carboxymethyllysine (CML) by Different Probiotic E. Coli Strains. *J. Agric. Food Chem.* **2019**, *67*, 1963–1972, doi:10.1021/acs.jafc.8b06748.
71. Dozio, E.; Caldiroli, L.; Molinari, P.; Castellano, G.; Delfrate, N.W.; Romanelli, M.M.C.; Vettoretti, S. Accelerated AGEing: The Impact of Advanced Glycation End Products on the Prognosis of Chronic Kidney Disease. *Antioxidants* **2023**, *12*, 584, doi:10.3390/antiox12030584.
72. Nowotny, K.; Jung, T.; Höhn, A.; Weber, D.; Grune, T. Advanced Glycation End Products and Oxidative Stress in Type 2 Diabetes Mellitus. *Biomolecules* **2015**, *5*, 194–222, doi:10.3390/biom5010194.
73. Prasad, K.; Mishra, M. AGE–RAGE Stress, Stressors, and Antistressors in Health and Disease. *Int. J. Angiol.* **2018**, *27*, 1–12, doi:10.1055/s-0037-1613678.
74. Schmidt, A.M. RAGE and Implications for the Pathogenesis and Treatment of Cardiometabolic Disorders – Spotlight on the Macrophage. *Arterioscler. Thromb. Vasc. Biol.* **2017**, *37*, 613–621, doi:10.1161/ATVBAHA.117.307263.
75. Chuah, Y.K.; Basir, R.; Talib, H.; Tie, T.H.; Nordin, N. Receptor for Advanced Glycation End Products and Its Involvement in Inflammatory Diseases. *Int. J. Inflamm.* **2013**, *2013*, 403460, doi:10.1155/2013/403460.
76. Teissier, T.; Boulanger, É. The Receptor for Advanced Glycation End-Products (RAGE) Is an Important Pattern Recognition Receptor (PRR) for Inflammaging. *Biogerontology* **2019**, *20*, 279–301, doi:10.1007/s10522-019-09808-3.
77. Kim, C.-S.; Park, S.; Kim, J. The Role of Glycation in the Pathogenesis of Aging and Its Prevention through Herbal Products and Physical Exercise. *J. Exerc. Nutr. Biochem.* **2017**, *21*, 55–61, doi:10.20463/jenb.2017.0027.
78. Lian, J.; Yue, Y.; Yu, W.; Zhang, Y. Immunosenescence: A Key Player in Cancer Development. *J. Hematol. Oncol.J Hematol Oncol* **2020**, *13*, 151, doi:10.1186/s13045-020-00986-z.

79. Ott, C.; Jacobs, K.; Haucke, E.; Navarrete Santos, A.; Grune, T.; Simm, A. Role of Advanced Glycation End Products in Cellular Signaling. *Redox Biol.* **2014**, *2*, 411–429, doi:10.1016/j.redox.2013.12.016.
80. Luckheeram, R.V.; Zhou, R.; Verma, A.D.; Xia, B. CD4+T Cells: Differentiation and Functions. *Clin. Dev. Immunol.* **2012**, *2012*, 925135, doi:10.1155/2012/925135.
81. Herold, K.; Moser, B.; Chen, Y.; Zeng, S.; Yan, S.F.; Ramasamy, R.; Emond, J.; Clynes, R.; Schmidt, A.M. Receptor for Advanced Glycation End Products (RAGE) in a Dash to the Rescue: Inflammatory Signals Gone Awry in the Primal Response to Stress. *J. Leukoc. Biol.* **2007**, *82*, 204–212, doi:10.1189/jlb.1206751.
82. Chen, Y.; Akirav, E.M.; Chen, W.; Henegariu, O.; Moser, B.; Desai, D.; Shen, J.M.; Webster, J.C.; Andrews, R.C.; Mjalli, A.M.; et al. RAGE Ligation Affects T Cell Activation and Controls T Cell Differentiation. *J. Immunol. Baltim. Md 1950* **2008**, *181*, 4272–4278.
83. Lu, H.; Xu, S.; Liang, X.; Dai, Y.; Huang, Z.; Ren, Y.; Lin, J.; Liu, X. Advanced Glycated End Products Alter Neutrophil Effect on Regulation of CD4+ T Cell Differentiation Through Induction of Myeloperoxidase and Neutrophil Elastase Activities. *Inflammation* **2019**, *42*, 559–571, doi:10.1007/s10753-018-0913-5.
84. Kalea, A.Z.; Reiniger, N.; Yang, H.; Arriero, M.; Schmidt, A.M.; Hudson, B.I. Alternative Splicing of the Murine Receptor for Advanced Glycation End-Products (RAGE) Gene. *FASEB J.* **2009**, *23*, 1766–1774, doi:10.1096/fj.08-117739.
85. Kim, H.J.; Jeong, M.S.; Jang, S.B. Molecular Characteristics of RAGE and Advances in Small-Molecule Inhibitors. *Int. J. Mol. Sci.* **2021**, *22*, 6904, doi:10.3390/ijms22136904.
86. Xue, J.; Manigrasso, M.; Scalabrin, M.; Rai, V.; Reverdatto, S.; Burz, D.S.; Fabris, D.; Schmidt, A.M.; Shekhtman, A. Change in the Molecular Dimension of a RAGE-Ligand Complex Triggers RAGE Signaling. *Structure* **2016**, *24*, 1509–1522.
87. Wei, W.; Lampe, L.; Park, S.; Vangara, B.S.; Waldo, G.S.; Cabantous, S.; Subaran, S.S.; Yang, D.; Lakatta, E.G.; Lin, L. Disulfide Bonds within the C2 Domain of RAGE Play Key Roles in Its Dimerization and Biogenesis. *PloS One* **2012**, *7*, e50736.
88. Taban, Q.; Mumtaz, P.T.; Masoodi, K.Z.; Haq, E.; Ahmad, S.M. Scavenger Receptors in Host Defense: From Functional Aspects to Mode of Action. *Cell Commun. Signal.* **2022**, *20*, 2, doi:10.1186/s12964-021-00812-0.
89. Zong, H.; Madden, A.; Ward, M.; Mooney, M.H.; Elliott, C.T.; Stitt, A.W. Homodimerization Is Essential for the Receptor for Advanced Glycation End Products (RAGE)-Mediated Signal Transduction. *J. Biol. Chem.* **2010**, *285*, 23137–23146, doi:10.1074/jbc.M110.133827.
90. Rouhiainen, A.; Kuja-Panula, J.; Tumova, S.; Rauvala, H. RAGE-Mediated Cell Signaling. In *Calcium-Binding Proteins and RAGE: From Structural Basics to Clinical Applications*; Heizmann, C.W., Ed.; Methods in Molecular Biology; Humana Press: Totowa, NJ, 2013; pp. 239–263 ISBN 978-1-62703-230-8.
91. Hou, X.; Hu, Z.; Xu, H.; Xu, J.; Zhang, S.; Zhong, Y.; He, X.; Wang, N. Advanced Glycation Endproducts Trigger Autophagy in Cadiomyocyte Via RAGE/PI3K/AKT/MTOR Pathway. *Cardiovasc. Diabetol.* **2014**, *13*, 78, doi:10.1186/1475-2840-13-78.
92. Zhong, Y.; Lee, K.; He, J.C. SIRT1 Is a Potential Drug Target for Treatment of Diabetic Kidney Disease. *Front. Endocrinol.* **2018**, *9*, 624, doi:10.3389/fendo.2018.00624.
93. Hassan, B.; Akcakanat, A.; Holder, A.M.; Meric-Bernstam, F. Targeting the PI3-Kinase/Akt/MTOR Signaling Pathway. *Surg. Oncol. Clin.* **2013**, *22*, 641–664, doi:10.1016/j.soc.2013.06.008.
94. Vincent, E.E.; Elder, D.J.E.; Thomas, E.C.; Phillips, L.; Morgan, C.; Pawade, J.; Sohail, M.; May, M.T.; Hetzel, M.R.; Tavaré, J.M. Akt Phosphorylation on Thr308 but Not on Ser473 Correlates with Akt Protein Kinase Activity in Human Non-Small Cell Lung Cancer. *Br. J. Cancer* **2011**, *104*, 1755–1761, doi:10.1038/bjc.2011.132.
95. Laplante, M.; Sabatini, D.M. MTOR Signaling at a Glance. *J. Cell Sci.* **2009**, *122*, 3589–3594, doi:10.1242/jcs.051011.
96. Porta, C.; Paglino, C.; Mosca, A. Targeting PI3K/Akt/MTOR Signaling in Cancer. *Front. Oncol.* **2014**, *4*.
97. Song, M.; Bode, A.M.; Dong, Z.; Lee, M.-H. AKT as a Therapeutic Target for Cancer. *Cancer Res.* **2019**, *79*, 1019–1031, doi:10.1158/0008-5472.CAN-18-2738.
98. Cantó, C.; Auwerx, J. PGC-1alpha, SIRT1 and AMPK, an Energy Sensing Network That Controls Energy Expenditure. *Curr. Opin. Lipidol.* **2009**, *20*, 98–105, doi:10.1097/MOL.0b013e328328d0a4.

99. Tang, B.L. Sirt1 and the Mitochondria. *Mol. Cells* **2016**, *39*, 87–95, doi:10.14348/molcells.2016.2318.
100. Southgate, R.J.; Bruce, C.R.; Carey, A.L.; Steinberg, G.R.; Walder, K.; Monks, R.; Watt, M.J.; Hawley, J.A.; Birnbaum, M.J.; Febbraio, M.A. PGC-1alpha Gene Expression Is down-Regulated by Akt- Mediated Phosphorylation and Nuclear Exclusion of FoxO1 in Insulin-Stimulated Skeletal Muscle. *FASEB J. Off. Publ. Fed. Am. Soc. Exp. Biol.* **2005**, *19*, 2072–2074, doi:10.1096/fj.05-3993fje.
101. Wang, Z.A.; Hsu, W.; Liu, W.R. Role of SIRT1 in Epigenetics. In *Handbook of Nutrition, Diet, and Epigenetics*; Patel, V.B., Preedy, V.R., Eds.; Springer International Publishing: Cham, 2019; pp. 311–329 ISBN 978-3-319-55530-0.
102. Gan, L.; Yang, Y.; Li, Q.; Feng, Y.; Liu, T.; Guo, W. Epigenetic Regulation of Cancer Progression by EZH2: From Biological Insights to Therapeutic Potential. *Biomark. Res.* **2018**, *6*, 10, doi:10.1186/s40364-018-0122-2.
103. Cha, T.-L.; Zhou, B.P.; Xia, W.; Wu, Y.; Yang, C.-C.; Chen, C.-T.; Ping, B.; Otte, A.P.; Hung, M.-C. Akt-Mediated Phosphorylation of EZH2 Suppresses Methylation of Lysine 27 in Histone H3. *Science* **2005**, *310*, 306–310, doi:10.1126/science.1118947.
104. Luan, Y.; Zhang, W.; Xie, J.; Mao, J. CDKN2A Inhibits Cell Proliferation and Invasion in Cervical Cancer through LDHA-Mediated AKT/MTOR Pathway. *Clin. Transl. Oncol. Off. Publ. Fed. Span. Oncol. Soc. Natl. Cancer Inst. Mex.* **2021**, *23*, 222–228, doi:10.1007/s12094-020-02409-4.
105. Khor, E.-S.; Wong, P.-F. The Roles of MTOR and MiRNAs in Endothelial Cell Senescence. *Biogerontology* **2020**, *21*, 517–530, doi:10.1007/s10522-020-09876-w.
106. Hall, B.M.; Balan, V.; Gleiberman, A.S.; Strom, E.; Krasnov, P.; Virtuoso, L.P.; Rydkina, E.; Vujcic, S.; Balan, K.; Gitlin, I.I.; et al. P16(Ink4a) and Senescence-Associated β-Galactosidase Can Be Induced in Macrophages as Part of a Reversible Response to Physiological Stimuli. *Aging* **2017**, *9*, 1867–1884, doi:10.18632/aging.101268.
107. Tóbon-Velasco, J.C.; Cuevas, E.; Torres-Ramos, M.A. Receptor for AGEs (RAGE) as Mediator of NF-KB Pathway Activation in Neuroinflammation and Oxidative Stress. *CNS Neurol. Disord. Drug Targets* **2014**, *13*, 1615–1626, doi:10.2174/1871527313666140806144831.
108. Oh, H.; Ghosh, S. NF-KB: Roles and Regulation in Different CD4(+) T-Cell Subsets. *Immunol. Rev.* **2013**, *252*, 41–51, doi:10.1111/imr.12033.
109. Egawa, T.; Tsuda, S.; Goto, A.; Ohno, Y.; Yokoyama, S.; Goto, K.; Hayashi, T. Potential Involvement of Dietary Advanced Glycation End Products in Impairment of Skeletal Muscle Growth and Muscle Contractile Function in Mice. *Br. J. Nutr.* **2017**, *117*, 21–29, doi:10.1017/S0007114516004591.
110. Liebisch, M.; Wolf, G. AGE-Induced Suppression of EZH2 Mediates Injury of Podocytes by Reducing H3K27me3. *Am. J. Nephrol.* **2020**, *51*, 676–692, doi:10.1159/000510140.
111. Ramasamy, R.; Shekhtman, A.; Schmidt, A.M. The Multiple Faces of RAGE - Opportunities for Therapeutic Intervention in Aging and Chronic Disease. *Expert Opin. Ther. Targets* **2016**, *20*, 431–446, doi:10.1517/14728222.2016.1111873.
112. Mastrocola, R.; Collotta, D.; Gaudioso, G.; Le Berre, M.; Cento, A.S.; Ferreira Alves, G.; Chiazza, F.; Verta, R.; Bertocchi, I.; Manig, F.; et al. Effects of Exogenous Dietary Advanced Glycation End Products on the Cross-Talk Mechanisms Linking Microbiota to Metabolic Inflammation. *Nutrients* **2020**, *12*, 2497, doi:10.3390/nu12092497.
113. Fang, M.; Wang, J.; Li, S.; Guo, Y. Advanced Glycation End-Products Accelerate the Cardiac Aging Process through the Receptor for Advanced Glycation End-Products/Transforming Growth Factor-β-Smad Signaling Pathway in Cardiac Fibroblasts. *Geriatr. Gerontol. Int.* **2016**, *16*, 522–527, doi:10.1111/ggi.12499.
114. Chung, M.-M.; Chen, Y.-L.; Pei, D.; Cheng, Y.-C.; Sun, B.; Nicol, C.J.; Yen, C.-H.; Chen, H.-M.; Liang, Y.-J.; Chiang, M.-C. The Neuroprotective Role of Metformin in Advanced Glycation End Product Treated Human Neural Stem Cells Is AMPK-Dependent. *Biochim. Biophys. Acta BBA - Mol. Basis Dis.* **2015**, *1852*, 720–731, doi:10.1016/j.bbadis.2015.01.006.
115. Chatzigeorgiou, A.; Kandaraki, E.; Piperi, C.; Livadas, S.; Papavassiliou, A.G.; Koutsilieris, M.; Papalois, A.; Diamanti-Kandarakis, E. Dietary Glycotoxins Affect Scavenger Receptor Expression and the Hormonal Profile of Female Rats. *J. Endocrinol.* **2013**, *218*, 331–337, doi:10.1530/JOE-13-0175.

116. Velayoudom-Cephise, F.L.; Cano-Sanchez, M.; Bercion, S.; Tessier, F.; Yu, Y.; Boulanger, E.; Neviere, R. Receptor for Advanced Glycation End Products Modulates Oxidative Stress and Mitochondrial Function in the Soleus Muscle of Mice Fed a High-Fat Diet. *Appl. Physiol. Nutr. Metab.* **2020**, *45*, 1107–1117, doi:10.1139/apnm-2019-0936.
117. Huang, X.; Liu, G.; Guo, J.; Su, Z. The PI3K/AKT Pathway in Obesity and Type 2 Diabetes. *Int. J. Biol. Sci.* **2018**, *14*, 1483–1496, doi:10.7150/ijbs.27173.
118. Hu, P.; Lai, D.; Lu, P.; Gao, J.; He, H. ERK and Akt Signaling Pathways Are Involved in Advanced Glycation End Product-Induced Autophagy in Rat Vascular Smooth Muscle Cells. *Int. J. Mol. Med.* **2012**, *29*, 613–618, doi:10.3892/ijmm.2012.891.
119. Gong, H.; Pang, J.; Han, Y.; Dai, Y.; Dai, D.; Cai, J.; Zhang, T.-M. Age-Dependent Tissue Expression Patterns of Sirt1 in Senescence-Accelerated Mice. *Mol. Med. Rep.* **2014**, *10*, 3296–3302, doi:10.3892/mmr.2014.2648.
120. Teissier, T.; Quersin, V.; Gnemmi, V.; Daroux, M.; Howsam, M.; Delguste, F.; Lemoine, C.; Fradin, C.; Schmidt, A.-M.; Cauffiez, C.; et al. Knockout of Receptor for Advanced Glycation End-Products Attenuates Age-Related Renal Lesions. *Aging Cell* **2019**, *18*, e12850, doi:10.1111/acel.12850.
121. Ahmad, S.; Khan, M.Y.; Rafi, Z.; Khan, H.; Siddiqui, Z.; Rehman, S.; Shahab, U.; Khan, M.S.; Saeed, M.; Alouffi, S.; et al. Oxidation, Glycation and Glycoxidation—The Vicious Cycle and Lung Cancer. *Semin. Cancer Biol.* **2018**, *49*, 29–36, doi:10.1016/j.semcancer.2017.10.005.
122. Lee, B.-W.; Ihm, J.; Kang, J.G.; Choi, M.G.; Yoo, H.J.; Ihm, S.-H. Amadori-Glycated Albumin-Induced Vascular Smooth Muscle Cell Proliferation and Expression of Inhibitor of Apoptosis Protein-1 and Nerve Growth Factor-γ. *BioFactors* **2007**, *31*, 145–153, doi:10.1002/biof.5520310301.
123. Dobi, A.; Bravo, S.B.; Veeren, B.; Paradela-Dobarro, B.; Álvarez, E.; Meilhac, O.; Viranaicken, W.; Baret, P.; Devin, A.; Rondeau, P. Advanced Glycation End-Products Disrupt Human Endothelial Cells Redox Homeostasis: New Insights into Reactive Oxygen Species Production. *Free Radic. Res.* **2019**, *53*, 150–169, doi:10.1080/10715762.2018.1529866.
124. Dong, H.; Zhang, Y.; Huang, Y.; Deng, H. Pathophysiology of RAGE in Inflammatory Diseases. *Front. Immunol.* **2022**, *13*, 931473, doi:10.3389/fimmu.2022.931473.
125. Constien, R.; Forde, A.; Liliensiek, B.; Gröne, H.J.; Nawroth, P.; Hämmerling, G.; Arnold, B. Characterization of a Novel EGFP Reporter Mouse to Monitor Cre Recombination as Demonstrated by a Tie2 Cre Mouse Line. *Genes. N. Y. N 2000* **2001**, *30*, 36–44, doi:10.1002/gene.1030.
126. Liliensiek, B.; Weigand, M.A.; Bierhaus, A.; Nicklas, W.; Kasper, M.; Hofer, S.; Plachky, J.; Gröne, H.-J.; Kurschus, F.C.; Schmidt, A.M.; et al. Receptor for Advanced Glycation End Products (RAGE) Regulates Sepsis but Not the Adaptive Immune Response. *J. Clin. Invest.* **2004**, *113*, 1641–1650, doi:10.1172/JCI18704.
127. Sakatani, S.; Yamada, K.; Homma, C.; Munesue, S.; Yamamoto, Y.; Yamamoto, H.; Hirase, H. Deletion of RAGE Causes Hyperactivity and Increased Sensitivity to Auditory Stimuli in Mice. *PLOS ONE* **2009**, *4*, e8309, doi:10.1371/journal.pone.0008309.
128. Gerasimenko, M.; Lopatina, O.; Munesue, S.; Harashima, A.; Yokoyama, S.; Yamamoto, Y.; Higashida, H. Receptor for Advanced Glycation End-Products (RAGE) Plays a Critical Role in Retrieval Behavior of Mother Mice at Early Postpartum. *Physiol. Behav.* **2021**, *235*, 113395, doi:10.1016/j.physbeh.2021.113395.
129. TUD - AGE Database Available online: https://lemchem.file3.wcms.tu-dresden.de/ (accessed on 14 April 2023).
130. Cordova, R.; Knaze, V.; Viallon, V.; Rust, P.; Schalkwijk, C.G.; Weiderpass, E.; Wagner, K.-H.; Mayen-Chacon, A.-L.; Aglago, E.K.; Dahm, C.C.; et al. Dietary Intake of Advanced Glycation End Products (AGEs) and Changes in Body Weight in European Adults. *Eur. J. Nutr.* **2020**, *59*, 2893–2904, doi:10.1007/s00394-019-02129-8.
131. Semba, R.D.; Gebauer, S.K.; Baer, D.J.; Sun, K.; Turner, R.; Silber, H.A.; Talegawkar, S.; Ferrucci, L.; Novotny, J.A. Dietary Intake of Advanced Glycation End Products Did Not Affect Endothelial Function and Inflammation in Healthy Adults in a Randomized Controlled Trial123. *J. Nutr.* **2014**, *144*, 1037–1042, doi:10.3945/jn.113.189480.
132. Linkens, A.M.A.; Houben, A.J.H.M.; Kroon, A.A.; Schram, M.T.; Berendschot, T.T.J.M.; Webers, C.A.B.; van Greevenbroek, M.; Henry, R.M.A.; de Galan, B.; Stehouwer, C.D.A.; et al. Habitual Intake of Dietary Advanced Glycation End Products Is Not Associated with

Generalized Microvascular Function-the Maastricht Study. *Am. J. Clin. Nutr.* **2022**, *115*, 444–455, doi:10.1093/ajcn/nqab302.
133. Linkens, A.M.; Houben, A.J.; Niessen, P.M.; Wijckmans, N.E.; de Goei, E.E.; Van den Eynde, M.D.; Scheijen, J.L.; van den Waarenburg, M.P.; Mari, A.; Berendschot, T.T.; et al. A 4-Week High-AGE Diet Does Not Impair Glucose Metabolism and Vascular Function in Obese Individuals. *JCI Insight* **2022**, *7*, e156950, doi:10.1172/jci.insight.156950.
134. Lamprea-Montealegre, J.A.; Arnold, A.M.; McCLelland, R.L.; Mukamal, K.J.; Djousse, L.; Biggs, M.L.; Siscovick, D.S.; Tracy, R.P.; Beisswenger, P.J.; Psaty, B.M.; et al. Plasma Levels of Advanced Glycation Endproducts and Risk of Cardiovascular Events: Findings From 2 Prospective Cohorts. *J. Am. Heart Assoc.* **2022**, *11*, e024012, doi:10.1161/JAHA.121.024012.
135. Wada, K.; Nakashima, Y.; Yamakawa, M.; Hori, A.; Seishima, M.; Tanabashi, S.; Matsushita, S.; Tokimitsu, N.; Nagata, C. Dietary Advanced Glycation End Products and Cancer Risk in Japan: From the Takayama Study. *Cancer Sci.* **2022**, *113*, 2839–2848, doi:10.1111/cas.15455.
136. Aglago, E.K.; Mayén, A.-L.; Knaze, V.; Freisling, H.; Fedirko, V.; Hughes, D.J.; Jiao, L.; Eriksen, A.K.; Tjønneland, A.; Boutron-Ruault, M.-C.; et al. Dietary Advanced Glycation End-Products and Colorectal Cancer Risk in the European Prospective Investigation into Cancer and Nutrition (EPIC) Study. *Nutrients* **2021**, *13*, 3132, doi:10.3390/nu13093132.

CHAPTER 2

Main questions, hypothesis, and aims of the thesis

The project of the present thesis has its origins in reports that dietary changes towards higher consumption of dAGEs from heat-processed foods could be involved in physiological disturbances such as inflammation, the dysfunction of certain tissues, alterations in the microbiome and gut permeability. Overall, there is still no conclusive evidence of a causal relationship between chronic exposure to dAGEs and the genesis or aggravation of age-related diseases. As summarized in the introductory section of this thesis (CHAPTER 1), several studies have shed light on the effects of dAGEs, but many questions remain to be answered. The following are some research gaps that still require elucidation and lack solid scientific evidence:

i. What are the kinetics of one of the main dietary glycation biomarker, CML, in rodents and humans? Does the soluble form of RAGE follow the pattern of distribution of this dietary compound?

ii. Are we able to synthetize a glycated protein model exclusively enriched in CML in order to study specifically this major protein-bound AGE? What are the main chemical modifications produced in the glycated protein models commonly used in animal studies?

iii. What are the short- and long-term effects of exposure to dAGEs in rodents?

iv. What are the effects of dAGEs in different organs? Do they present a similar behavior in terms of genetic and protein biomarkers, and/or accumulation of dAGEs? Are there tissue-dependent effects?

v. What is the influence of perinatal exposure to dAGEs on offspring physiology?

vi. Are the physiological effects and the accumulation of dAGEs in different organs reversible?

1 Hypotheses

With the main concepts and the recent scientific discoveries in mind, it was hypothesized that a chronic exposure to dCML (in early life only and/or lifelong) could lead to an accumulation in certain organs and contribute to the installation of chronic low-grade inflammation and inflammaging in a mechanism mediated by the AGE-RAGE axis. In addition, the consumption of dCML was hypothesized to increase oxidative stress and accelerate cell immunosenescence. Meanwhile, we believed that the absence of RAGE in genetically modified knockout mice would play a protective role in this dietary context. On the reversibility of the effects of the exposure to dCML, we hypothesized that an early-life diet switch to a lower level of dCML could contribute to a reduction of its accumulation in organs and to the attenuation or reversibility of the putative long-term deleterious effects.

2 General Aims of the Thesis

The general aim of the research described in this thesis was to contribute to the understanding of the association of AGE intake via the diet with physiological disorders. More precisely, the specific goal of this thesis was to understand the mechanisms by which dCML influences the level of chronic low-grade inflammation, including the evaluation of tissue accumulation of dCML, and biomarkers of inflammation, related pathways of oxidative stress, and immunosenescence. These effects were evaluated by comparing the early and lifelong exposure of mice to dCML using a dCML-enriched diet. In addition, we aimed to understand how RAGE mediates possible effects in such a dietary context. in an attempt to answer these questions, the following sub-objectives were approached:

Sub-objectives

The results obtained from each sub-objective are presented in chapters 3 to 6.

In **CHAPTER 3** a review is provided of the current academic comprehension of Chronic Low-Grade Inflammation and the relationships between such pathological hallmarks and the dietary intake of AGEs and high-caloric diets. The latest findings on the effects of diet-induced CLGI biomarkers in murine models are presented to elucidate the current directions in CLGI research and explore the multiple, concurrent events which shape CLGI in rodent models and the associated physiological events, including findings on gut microbiota remodeling, metabolic endotoxemia, and CLGI initiation. The main research gaps in this field prompted this current thesis within the ExoAGEing ANR project.

In **CHAPTER 4** the goal was to better understand the metabolic fate of dCML in rats and in humans. The postprandial kinetics of dCML in both rodents and humans were studied by measuring changes in plasma CML in rats receiving four different forms of dCML, and in healthy human volunteers receiving three different breakfasts. The circulating levels of soluble RAGE (sRAGE) were also measured in human plasma samples.

In **CHAPTER 5** a methodological study is presented of the best way to produce glycated protein high in CML for use in an animal model system for the fourth and last objective (**CHAPTER 6**). Different bovine serum albumin (BSA) model systems for fortifying this protein in dCML are characterized, comparing alternative synthetic pathways to the classic reductive amination of glyoxylic acid in the presence of $NaBH_3CN$. A novel combination of quantitative and qualitative methods were employed, including isotope dilution, high-performance liquid chromatography with tandem mass spectrometric detection (HPLC-MS/MS), western-blot, fluorescence, and proteomics analyses using matrix-assisted laser desorption ionization with time-of-flight MS (MALDI-TOF) and LC with high-resolution MS (LC-HRMS). These data provide an extensive characterization of the possible modifications of BSA promoted by different carbonyl compounds. The efficiency of the incorporation of protein-

bound dCML into mouse feed pellets, their stability over different storage periods, as well as clearance of dCML in mouse feces was also studied.

In **CHAPTER 6** it was postulated that exposure to dCML during early life and/or throughout life contributes to the development of CLGI and a pro-oxidative state, mediated by the AGE-RAGE axis. Additionally, the potential for the absence of the RAGE receptor in genetically modified knockout mice to confer a protective effect in the context of this dietary exposure was examined. We studied the accumulation of CML in various tissues following consumption of dCML, and whether dCML increased oxidative stress, remodeling of the gut microbiota, or the immune system. In terms of reversibility, we speculated that switching to a lower level of dCML in the diet during early life could potentially mitigate or reverse any long-term detrimental effects. To address these hypotheses, molecular markers related to inflammation, oxidative stress, and the accumulation of free and protein-bound glycation products were investigated in multiple samples obtained from 6, 35, and 70-week-old Wild-Type (WT) and RAGE KO C57BL/6 mice fed either enriched dietary CML or standard diets.

3 Thesis Outline

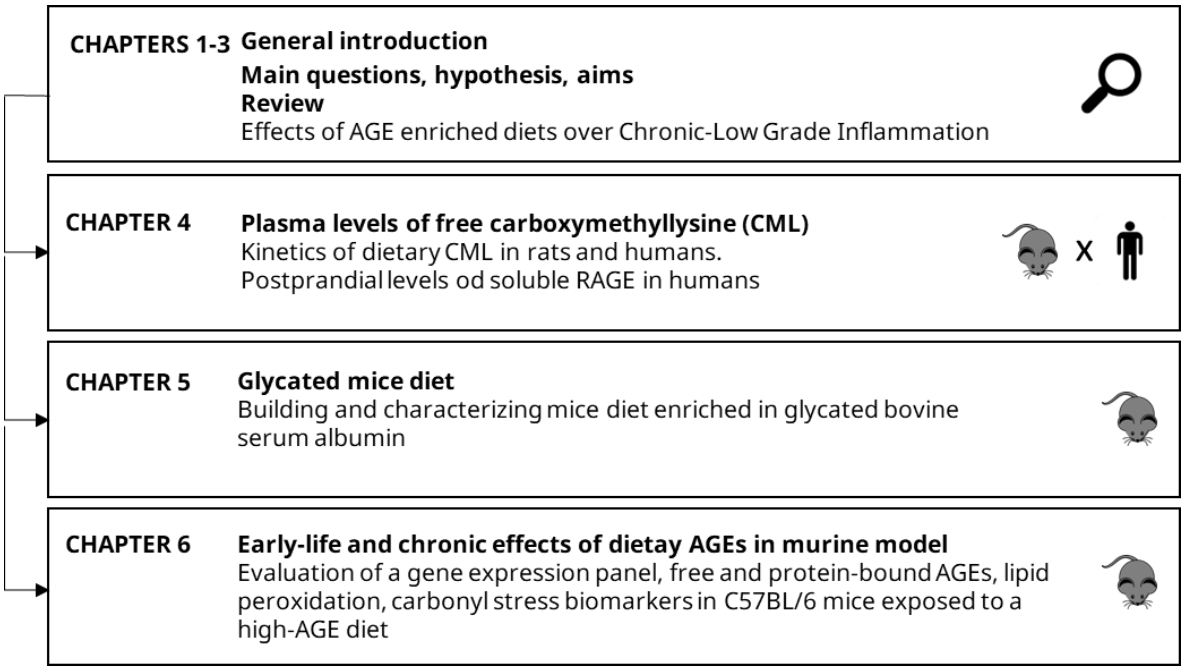

Figure 1 A schematic representation of the different chapters comprising this thesis.

CHAPTER 3

Effect of advanced glycation end-products and excessive calorie intake on diet-induced chronic low-grade inflammation biomarkers in murine models

Matheus Thomaz Nogueira Silva Lima[1], Michael Howsam[1], Pauline M. Anton[2], Carine Delayre-Orthez[2] and Frédéric J. Tessier[1,*]

1 Univ. Lille, Inserm, CHU Lille, Institut Pasteur de Lille, U1167 - RID-AGE – Facteurs de risque et dé-terminants moléculaires des maladies liées au vieillissement, F-59000 Lille, France; matheustho-maz.nogueirasilvalima@univ-lille.fr (M.T.N.S.L.); michael.howsam@univ-lille.fr (M.H.)

2 Institut Polytechnique UniLaSalle, Université d'Artois, ULR 7519, Equipe PETALES, F-60026 Beau-vais, France; pauline.anton@unilasalle.fr (P.M.A.); carine.delayre@unilasalle.fr (C.D.-O.)

* Correspondence: frederic.tessier@univ-lille.fr

This review has been published in Nutrients (MDPI):

Nogueira Silva Lima MT, Howsam M, Anton PM, Delayre-Orthez C, Tessier FJ. Effect of Advanced Glycation End-Products and Excessive Calorie Intake on Diet-Induced Chronic Low-Grade Inflammation Biomarkers in Murine Models. Nutrients. 2021 Sep 2;13(9):3091. doi: 10.3390/nu13093091. PMID: 34578967; PMCID: PMC8468789.

ABSTRACT

Chronic Low-Grade Inflammation (CLGI) is a non-overt inflammatory state characterized by a continuous activation of inflammation mediators associated with metabolic diseases. It has been linked to the overconsumption of Advanced Glycation End-Products (AGEs), and/or macronutrients which lead to an increase of local and systemic pro-inflammatory biomarkers in humans and animal models. This review provides a summary of research into biomarkers of diet-induced CLGI in murine models, with a focus on AGEs and obesogenic diets, and presents the physiological effects described in the literature. Diet-induced CLGI is associated with metabolic endotoxemia, and/or gut microbiota remodeling in rodents. The mechanisms identified so far are centered on pro-inflammatory axes such as the interaction between AGEs and their main receptor AGEs (RAGE) or increased levels of lipopolysaccharide. The use of murine models has helped to elucidate the local and systemic expression of CLGI mediators. These models have enabled significant advances in identification of diet-induced CLGI biomarkers and resultant physiological effects. Some limitations on the translational (murine x humans) use of biomarkers may arise, but murine models have greatly facilitated the testing of specific dietary components. However, there remains a lack of information at the whole-organism level of organization, as well as a lack of consensus on the best biomarker for use in CLGI studies and recommendations as to future research conclude this review.

Keywords: chronic low-grade inflammation; diet; advanced glycation end-products; metabolic diseases; high-fat diet; carboxymethyllysine

1 Introduction

Diet plays a role in the induction and progression of Chronic Low-Grade Inflammation (CLGI) which has been associated with metabolic diseases such as obesity and diabetes [1]. Some food contaminants such as the exogenous Advanced Glycation End-Products (AGEs), produced in thermally processed products, have been shown to contribute to the persistent inflammatory component of diabetes, aging, and heart failure [2]. The same AGEs can also be formed at 37°C, being called endogenous AGES. The deleterious effects of higher circulating levels of AGEs on health may be mediated by their eponymous cell membrane receptor RAGE [3]. Nonetheless, the overconsumption of macronutrients also associated with “western”, processed foods, like lipids and carbohydrates, plays a similar role in triggering the CLGI implicated in obesity and neuroinflammation, both at the local and systemic levels [4]. The consequences of high lipid intake, for instance, range from appetite dysregulation in the hypothalamic core to metabolic endotoxemia [5], with this last being mediated by the Toll-Like Receptor 4 (TLR4) [6].

The clinical differentiation of CLGI is still a matter of significant debate. The main biomarkers currently used in the diagnosis of inflammation, such as C-reactive protein (CRP), are not specific to CLGI. Hence, many studies in recent decades have attempted to define CLGI biomarkers in humans and rodent models, including the proposition that clusters of biomarkers may best define the state [7]. While Calder and colleagues [7–9] have published comprehensive reviews on CLGI in nutritional studies in humans, detailing the biomarkers used to assess inflammation, important discoveries have concomitantly been made in murine models: to our knowledge, however, no review has yet been published on this body of work. Our goal here is to summarize current discoveries on diet-induced CLGI and discuss the factors which influence CLGI biomarker expression in rodent models.

Although centered on diet-induced CLGI in murine models, we begin our review by considering the essential concepts of acute and chronic inflammation in order to clearly define CLGI. Thereafter, those CLGI biomarkers currently explored in the literature are presented so as to demonstrate their use in such studies, their diversity, and their limitations, and to frame the current understanding of diet-induced CLGI. The corresponding literature on diet-induced CLGI is then reviewed, including dietary AGE consumption and obesogenic diets, to elucidate the current directions in CLGI research and explore the multiple, concurrent events which shape

CLGI in rodent models. Firstly, we will explore the effects of immoderate consumption of AGEs on CLGI promotion. In the following sections, the effects of high-calorie diets on CLGI and their implications for adiposity, and the neuroinflammation associated with appetite control will be presented. Findings on gut microbiota remodeling, metabolic endotoxemia, and CLGI initiation will also be discussed. Finally, perspectives on CLGI research gaps that remain to be filled will be addressed.

2 Inflammation and Chronic Low-Grade Inflammation (CLGI)

Inflammation is part of the body's innate and adaptive immune defenses. It comprises a series of cellular and chemical signal barriers which aim to control and conquer endogenous and exogenous stimuli (essentially bacterial or viral infections) and trauma-related damage [10]. Inflammation can be either an acute or chronic process, but both have common aims: namely, to neutralize the source of injury, promote tissue repair, and drive a self-limited return to homeostatic conditions [11]. In contrast to acute inflammation (AI), chronic inflammation (CI) is a process linked to resolution failure and induces continuous recruitment of the cellular immune apparatus, promoting tissue damage [12].

Beyond the difference in duration between AI and CI, the degree of inflammatory response also determines whether inflammation becomes pathological. Under a non-overt inflammation scenario, a chronic, but low-grade inflammatory mechanism comprehends excessive metabolic stress correlated to the rise of circulating levels of inflammation signals [13]. Both CI and CLGI are borderline conditions sharing similar molecular mechanisms, but a distinct involvement of metabolic tissues characterizes CLGI progression. Indeed, CLGI is currently considered to be a possible factor in the pathological aggravation of obesity, type 2 diabetes mellitus (T2DM), atherosclerosis, or cancer [1,14].

Compared to the chronic but severe inflammation present in arthritis or Crohn's disease [15], metabolic disorders (such as obesity) and some age-related conditions (such as frailty) have only a CLGI component [16]. This difference in the intensity of inflammation has orientated research seeking to characterize specific molecular patterns and biomarker clusters in order to develop predictive tools aimed at reducing the health and socioeconomic impacts of these pathologies.

The discovery and elucidation of the CLGI process was an important step in the comprehension of diseases currently considered to be global public health concerns (*e.g.* T2DM). The term “low-grade inflammation” was first used in the 1980s with reference to histologic samples from schizophrenic patients in which increased glial fibrils were observed [17], and to the onset of ocular complications in arthritis patients [18]. However, a more complete body of evidence later emerged with the inclusion of tissues previously considered inactive, which today we understand to play a fundamental role as active metabolic organs (*e.g.* adipose tissue, skeletal muscles, brain) [19]. Hotamisligil and colleagues [20] were the first to report increased expression of TNFα (both mRNA and protein) in the white adipose tissue of obese mice (ranging from 34 to 166 pg/mL), demonstrating that it participated in the aggravation of obesity and diabetes by increasing insulin resistance [20]. Similarly, the expression of adipokines by visceral fat was later confirmed in humans [21,22].

Screening for systemic effects of inflammation has demonstrated that several other organs are implicated in CLGI (Figure 1). In the brain, for instance, the hypothalamus plays a role in the control of appetite, regulating intake of macronutrients and energy [23]. Both hypothalamic macrophage infiltration and TNFα increase were observed in obese mice [24], and increased gliosis in humans was evidenced from retrospective studies of magnetic resonance records of obese patients that had undergone pituitary or epilepsy imaging protocols [25]. In addition, other key molecular events act as a trigger for CLGI. The accumulation of molecular degenerations, mitochondrial dysfunction, DNA damage, and immune dysregulation are all age-related factors implicated in CLGI [26]. T-cell immunosenescence, for instance, has been demonstrated in visceral fat from mice: adiposity led to an increased T-cell population with senescent molecular profiles expressing Programmed Cell Death Protein 1 (PD-1) and Tumor Necrosis Factor Ligand Superfamily Member 8 (TNFSF8) [27,28].

More recently, some evidence appears to suggest that the gut microbiota also plays a critical role in CLGI progression, following remodeling as a result of nutritional imbalances. The consumption of increased quantities of fats and/or carbohydrates has been demonstrated to modify the composition of the microbiota and promote permeability of the gut–mucosal barrier [29,30]. A result of this process is increased circulating levels of endotoxin leading to systemic endotoxemia [29].

Taken together, these data suggest that diet-induced CLGI results from the convergence of several conditions, gut dysbiosis and endotoxemia, adipocyte hypertrophy and death, skeletal muscle oxygen use and hypothalamic macrophage infiltration being key among them (Figure 1). However, the underlying mechanisms of such a complex interaction remain to be fully elucidated.

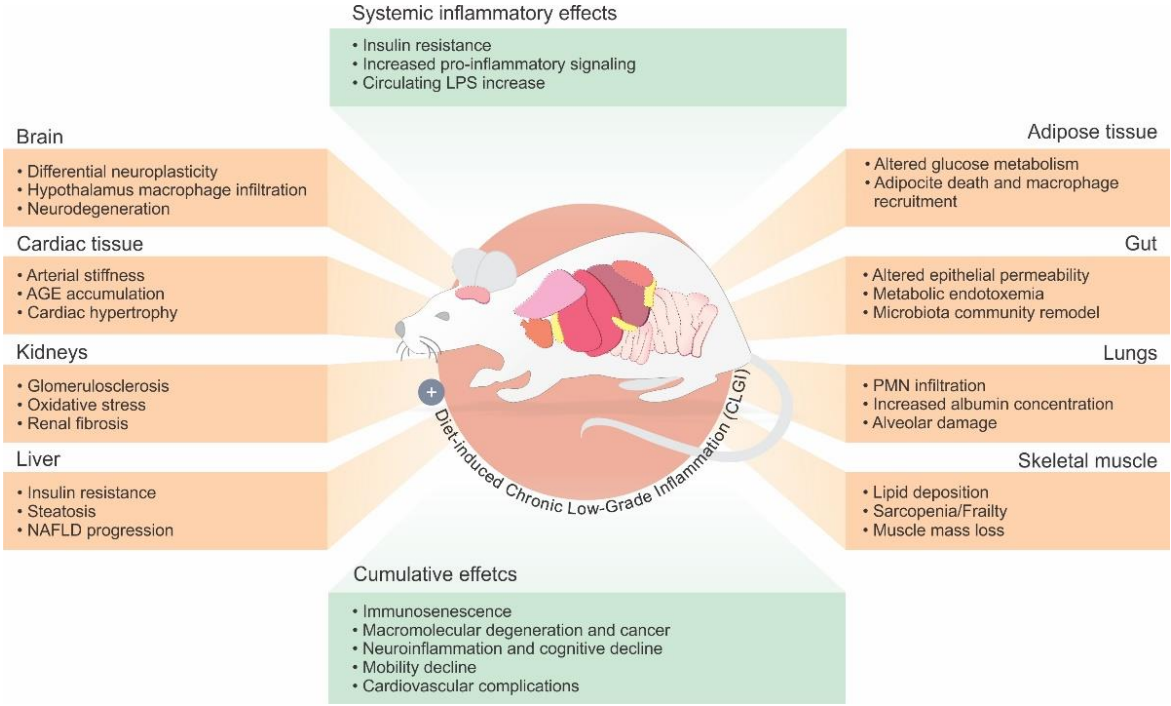

Figure 1 Physiological alterations resulting from diet-induced CLGI in different organs. CLGI is a complex crosstalk among different organs leading to an increase of local (tissue-specific) and circulating levels (Systemic Inflammatory effects) of inflammatory mediators. Organs and respective inflammatory mediators are referenced in Table 1. As a result, lifelong exposure to CLGI is also related to cumulative effects such as, macromolecular degeneration, neuroinflammation, and mobility reduction associate with age-related diseases with LGI components (Alzheimer's disease). Such physiological modifications are related to the activation of inflammation, and tissue dysfunction. NAFLD = non-alcoholic fatty liver disease; PMN = polymorphonuclear leukocytes.

Although the terms "Low-Grade Inflammation" or "Chronic Low-Grade Inflammation" are used interchangeably in the literature, we here take "chronic" to be a compulsory requirement for the low-grade inflammatory stimulus to promote some sort of pathological effect. Thus, based on the extensive literature currently published, CLGI can be formally defined as a pathological state lacking overt inflammation, but characterized by a continuous and unresolved activation of inflammation mediators. It results in increased production of cytokines, reactive oxygen species, macrophage infiltration, adipocyte imbalance or vascular damage;

these effects are associated with metabolically active tissues such as adipose tissue, skeletal muscle and the liver, implicating CLGI in metabolic dis-eases [1,31]. Age-related immunosenescence and the accumulation of cellular debris are also part of CLGI evolution in older people [32,33].

Estimating CLGI via different biomarkers could pave the way for its early detection. But aside from the key discoveries in recent decades describing the expression patterns of some CLGI biomarkers which have cemented its pathophysiological functions, the diagnosis of CLGI remains to be defined from a technical perspective. While biomarkers of CLGI have been identified, their use is hampered by, on the one hand a lack of basal values, and on the other a detailed knowledge of their levels in a pathological context. A cluster or panel of biomarkers could best describe CLGI, and in the following section we present the biomarkers currently under investigation, with a brief description of those from human studies, and a focus on murine models.

3 CLGI Biomarkers

3.1. Human studies

Susceptibility to, and the diagnosis, prognosis, and treatment of several diseases have all benefitted from fundamental and clinical research discoveries of biomarkers. In essence, a biomarker is a physiological, physical, molecular, or elemental indicator of a normal or pathogenic process or response. Biomarkers of CLGI so far investigated are molecules at the local (*e.g.* tissue-specific) or systemic (e.g. blood) levels. However, as we shall see, the commonalities between the different inflammation statuses (*i.e.* AI, CI, CLGI) complicate the use of a single diagnostic biomarker specific to CLGI.

Cytokines, adipokines (*e.g.* leptin), and chemokines are important signals of inflammation but the occurrence of these biomarkers per se cannot distinguish one type of inflammation from another. In humans, along with the numerous CLGI causes, which inevitably lead to modulation of biomarker expression, a considerable interindividual variation exists according to age, body weight, eating habits, smoking, or alcohol consumption [7]. With so many factors producing variability, a consensus on the best biomarkers for the assessment of the physiological role and prediction power of CLGI is far from being reached. Based on the discussions held by the International Life Sciences Institute and the Europe Nutrition and Immunity

Task Force during the first half of the 2010s, Calder et al. [7] suggested that a robust strategy would be to investigate biomarker expression patterns, or the composition of biomarker panels or clusters, from molecules described in human clinical studies. The benefit of this approach is the breadth of its applicability, encompassing nutritional, neurological, and geriatric research. A single biomarker cannot robustly discriminate CLGI from other forms of inflammation, and this approach has a precedent in the various “omics” fields of research.

A recent systematic review of inflammation biomarkers reported that the major inflammation signals currently being explored in human intervention studies are CRP, cytokines (notably IL6 and TNFα), adhesion proteins such as VCAM1 and ICAM1, and the MCP1 chemokine [34]. CRP, for example, is a major AI biomarker, produced in the liver, with a proven record of clinical use and well-established protocols for its analysis and detection. A key feature of CRP is its responsiveness to inflammation stimuli, making it a sensitive biomarker of inflammation [35]. Elevated CRP, for instance, has long been used as a risk indicator of cardiovascular disease (CVD) in humans, and a threshold indicating moderate to high risk to CVD (>1.5 mg/L) is well-defined [35]. However, there are still not widely accepted, conclusive, local, or systemic biomarkers specific to CLGI forth-coming from human studies, nor any definition of the basal expression of potential biomarkers (which deserves particular attention).

3.2. Murine model studies

When it comes to CLGI research in rodents, a similar range of biomarkers to that in human studies is observed. The ensemble of the biomarkers explored in the literature is presented in Table 1, all of them emanating from studies that followed the chronic induction of LGI using AGE-rich diets, obesogenic diets, or the effects of metabolic endotoxemia. These biomarkers were reported in a series of organs including the brain, the adipose tissue, or the kidneys, and non-invasive analysis of feces has been also used to address CLGI in rodents.

Table 1 Diet-induced CLGI biomarkers across publications on murine models.

Role in CLGI	Class	Biomarker	Sample	Biomarker levels between control and experimental conditions (Arrows show expression tendency)	References
Anti-inflammatory	Cytokine	Interleukin 2 (IL-2)	Brain	Control: 10 pg/mg Affected: 120 pg/mg (↑) (Protein)	[36]
			Liver	Control: 100 pg/mg Affected: 150 pg/mg (↑) (Protein)	
		Interleukin 10 (IL-10)	Adipose tissue	No change (→) (mRNA)	[37]
			Liver	No change (→) (mRNA)	[38]
					[37]
			Plasma	Control:10 pg/mL Affected: 20 pg/mL (↑) (Protein)	[37]
				Control: 15 pg/mL Affected: 9 pg /mL (↓) (Protein)	[39]
Pro and anti-inflammatory	Adipokine	Adiponectin	Plasma	Control: 90 µg/mL Affected: 60 µg/mL (↓) (Protein)	[40]
				Control: 30 µg/mL Affected: 45 µg/mL (↑) (Protein)	[41]
				Control: 8 ng/mL (→) (Protein)	[37]
	Cytokine	Interleukin 6 (IL-6)	Adipose Tissue	2-fold change (↑) (mRNA)	[41]
			BAL	No change (→) (Protein)	[42]
			Kidney	15-fold change (↑) (mRNA)	[43]
			Liver	No change (→) (mRNA)	[38]
				8-fold change (↑) (mRNA)	[44]
			Myocardium	Control: 21 ng/µg Affected: 28 ng/µg (↑) (Protein)	[45]
				18-fold change (↑) (mRNA)	
			Plasma	3-fold change (↑) (mRNA)	[46]
				Control: 4 pg/mL Affected: 2 pg/mL (↓) (Protein)	[39]
				No change (→) (mRNA)	[39]
Pro-inflammatory	Adhesion molecule	Intercellular Adhesion Molecule 1 (ICAM-1)	Aorta	1.4-fold change (↑) (mRNA)	[47]
			Myocardium	5.6-fold (↑) (mRNA)	[45]
			Plasma	3.5-fold change (↑) (Protein)	[48]
		Vascular Cell Adhesion Molecule 1 (VCAM-1)	Aorta	2.5-fold change (↑) (Protein)	[49]
				1.4-fold change (↑) (mRNA)	
				2-fold change (↑) (mRNA)	[47]
			Kidney	4-fold change (↑) (mRNA)	[43]

Role in CLGI	Class	Biomarker	Sample	Biomarker levels between control and experimental conditions (Arrows show expression tendency)	References
	Cell receptor	Receptor for Advanced Glycation End-products (RAGE)	Aorta	2-fold change (↑) (Protein)	[49]
				No change (→) (mRNA)	
			Kidney	3-fold change (↑) (mRNA)	[50]
			Liver	3-fold change (↑) (mRNA)	[50]
				1.5-fold change (↑) (mRNA)	[44]
			PBMC	2-fold change (↓) (Protein)	[51]
			Spleen	3-fold change (↑) (mRNA)	[50]
	Chemokine	Keratinocyte chemoattractant (KC ou CXCL1)	BAL	Control: 10 pg/mL Affected: 600 pg/mL (↑) (Protein)	[42]
		Macrophage Inflammatory Protein 2 (MIP-2)	BAL	No change (→) (Protein)	[42]
			Liver	Control: 20 pg/mL Affected: 180 pg/mL (↑) (Protein)	[52]
			Plasma	Control: 900 pg/mL Affected: 1500 pg/mL (↑) (Protein)	[52]
	Cluster of differentiation	CD68 Clone ED1 (ED1)	Colon	4-fold (↑) (Histochemistry)	[53]
			Kidney	2.4-fold (↑) (Histochemistry)	[54]
		Cluster of differentiation 11 (CD11)	Ovary	1.2-fold change (↑) (mRNA)	[55]
		Cluster of differentiation 11 c (CD11c)	Adipose Tissue	No change (→) (mRNA)	[41]
		Cluster of differentiation 14 (CD14)	Plasma	Control: 400 ng/mL Affected: 800 ng/mL (↓) (Protein)	[41]
		Cluster of differentiation 206 (CD206)	Ovary	2.3-fold change (↓) (mRNA)	[55]
		Cluster of differentiation 43 (CD43)	Liver	4-fold change (↑) (mRNA)	[44]
		Cluster of differentiation 68 (CD68)	Adipose Tissue	No change (→) (mRNA)	[41]
			Plasma	4-fold change (↑) (mRNA)	[46]
		Cluster of differentiation 95 (CD95l or FAS Ligand)	Liver	2.5-fold change (↑) (mRNA)	[52]
			Plasma	4-fold change (↑) (mRNA)	[46]
	Complement system	Complement component 5a (c5a)	Plasma	3.5-fold change (↑) (Protein)	[48]
	Cytokine	Interferon Gamma (IFN-γ)	Plasma	No change (→) (Protein)	[39]
		Interleukin 1 Alpha (IL-1α)	Plasma	3.5-fold change (↑) (Protein)	[48]
		Interleukin 1 Beta (IL-1β)	Adipose Tissue	No change (→) (mRNA)	[37]
			BAL	No change (→) (Protein)	[42]
			Colon	2-fold change (↑) (mRNA)	[56]
			Liver	No change (→) (mRNA)	[38]
				2-fold change (↑) (mRNA)	[37]
			Plasma	Control: 1 pg/mL Affected: 5 pg/mL (↑) (Protein)	[39]

Role in CLGI	Class	Biomarker	Sample	Biomarker levels between control and experimental conditions (Arrows show expression tendency)	References
				2-fold change (↑) (mRNA)	[46]
		Interleukin 16 (IL-16)	Plasma	3.5-fold change (↑) (Protein)	[48]
				No change (→) (Protein)	[37]
		Interleukin 17 (IL-17)	Plasma	Control: 11 pg /mL Affected: 18 pg/mL (↑) (Protein)	[39]
		Tumor Necrosis Factor Alpha (TNFα)	Adipose Tissue	3-fold change (↑) (mRNA)	[37]
			BAL	No change (→) (Protein)	[42]
			Brain	Control: 0.2 ng/mg Affected: 0.7 ng/mg (↑) (Protein)	[36]
			Kidney	10-fold change (↑) (mRNA)	[43]
			Liver	3-fold change (↑) (mRNA)	[38]
				No change (→) (mRNA)	[37]
				Control: 0.7 ng/mg Affected: 1 ng/mg (↑) (Protein)	[36]
			Myocardium	2-fold change (↑) (mRNA)	[45]
			Plasma	Control: 4 pg/mL Affected: 10 pg/mL (↑) (Protein)	[39]
				No change (→) (Protein)	[57]
		Tumor Necrosis Factor Soluble Receptor II (TNF-sRII)	BAL	Control: 150 pg/ml Affected: 849.4 pg/ml (↑) (Protein)	[42]
	Histologic hallmark (Dyong adipocytes and macrophages)	Crown-like structures (CLS)	Adipose tissue	Control: 0.4 CLS/mm^2 Affected: 1.8 CLS/mm^2 (↑) (Histochemistry)	[37]
	Inflammatory cell chemoattractant	Monocyte Chemoattractant Protein-1 (MCP-1)	Adipose tissue	2-fold change (↑) (mRNA)	[41]
				4-fold change (↑) (mRNA)	[37]
			Aorta	1.8-fold change (↑) (mRNA)	[47]
			BAL	Control: 10 ng/mL Affected: 90 pg/mL (↑) (Protein)	[42]
			Liver	2-fold change (↑) (mRNA)	[44]
				No change (→) (mRNA)	[37]
			Myocardium	3-fold change (↑) (mRNA)	[45]
			Plasma	4-fold change (↑) (Protein)	[48]
	Intracellular cell-signal	Factor Nuclear kappa B (NF-κβ)	Brain	Control: 15 pg/mL Affected: 50 pg/mL (↑) (Protein)	[36]
			Liver	Control: 10 pg/mL (→) (Protein)	[36]
		IκB kinase (pIKK)	Peritoneum	4-fold change (↑) (mRNA)	[46]

Role in CLGI	Class	Biomarker	Sample	Biomarker levels between control and experimental conditions (Arrows show expression tendency)	References
		Mechanistic Target of Rapamycin (mTOR)	Liver	Control: 3 ng/mg Affected: 6 ng/mg (↑) (Protein)	[52]
		Protein kinase B (AKT)	Adipose tissue	1.5-fold (↓) (mRNA)	[41]
				No change (→) (Protein)	[58]
	LPS presenting protein	Lipopolysaccharide Binding Protein (LBP)	Plasma	Control: 13 ng/mL Affected: 15 ng/mL (↑) (Protein)	[4]
	Macrophage biomarker	Chloroacetate esterase (CAE)	Liver	6-fold change (↑) (Histochemistry)	[38]
		Macrophage glycoprotein (MOMA-2)	Liver	Control: 57 Cells/Area Affected: 70 Cells/Area (↑) (Histochemistry)	[52]
	Macrophage receptor	EGF-like module-containing mucin-like hormone receptor-like 1 (EMR1 or F4/80)	Adipose tissue	4-fold change (↑) (mRNA)	[37]
			Liver	2-fold (↑) (Histochemistry)	[38]
				2-fold change (↑) (mRNA)	[37]
			Ovary	2.3-fold change (↑) (mRNA)	[55]
			Plasma	2.5-fold (↑) mRNA	[46]
	Macrophage scavenger receptor	Scavenger Receptor A (SR-a)	PBMC	2.5-fold change (↓) (Protein)	[51]
	Microglia marker	Ionized Calcium-Binding Adaptor Molecule 1 (IBA1)	Brain	1.25-fold change (↑) (Histochemistry)	[59]
	Mitogen-activated protein kinase	p-p38MAPK	Liver	2.67-fold change (↑) (Protein)	[52]
		c-Jun N-terminal kinase (pJNK)	Brain	2-fold change (↑) (mRNA)	[58]
			Liver	1.84-fold change (↑) (mRNA)	[52]
	Neutrophil gelatinase-associated	Lipocalin-2 (LCN-2)	Colon	95-fold change (↑) (mRNA)	[56]
			Feces	Control: 5 ng/mL Affected: 80 ng/mL (↑) (Protein)	[56]
			Plasma	Control: 100 ng/mL Affected: 300 ng/mL (↑) (Protein)	[56]
	NF-κβ p65 subunit	Transcription factor p65 (p65)	Myocardio	1.5-fold change (↑) (mRNA)	[45]
			Peritone	2-fold change (↑) (mRNA)	[42]
	Oxidative stress biomarker	Myeloperoxidase (MPO)	Colon	No change (→) (Protein)	[56]
	Plasminogen regulation	Plasminogen Activator Inhibitor-1 (PAI-1)	Plasma	Control: 15 pg/mL Affected: 2 pg /mL (↓) (Protein)	[39]
				Control: 2900 pg/mL Affected: 3100 pg/mL (↑) (Protein)	[57]
	RAGE ligand	High–Mobility Group Box 1 (HMGB1)	Plasma	4 ng/mL (↑) (Protein)	[60]
		S100 A8/A10	Myocardio	Control: 0.3 ng/mg Affected: 0.7 ng/mg (↑) (Protein)	[45]

Role in CLGI	Class	Biomarker	Sample	**Biomarker levels between control and experimental conditions** (Arrows show expression tendency)	References
	Secretory serine protease	Serine Protease Inhibitor A3N (Serpina3n)	Brain	Control: 180 IOD Affected: 220 IOD (↑) (In situ hybridization)	[4]
	Signaling adapter	Insulin receptor substrate 1 (IRS-1)	Brain	No change (→) (Protein)	[58]
	Transport protein	Fatty-Acid-Binding Proteins (FABP)	Plasma	2.5-fold change (↑) (mRNA)	[46]

BAL: BronchoAlveolar Lavage; IOD: Integral Optical Density.

Despite the fact that we have not attempted to be exhaustive in this review, significant diversity can be observed among the molecular biomarkers of inflammation listed in Table 1. Cytokines and chemokines are by far the most studied molecules, and IL-6, TNFα, and MCP-1 figure among the most studied biomarkers in dietary studies with animal models. Both IL-6 and TNFα are widely used in CLGI studies and are expressed in sever-al cell types, while TNFα is the most cited CLGI biomarker (Table 1). Both TNFα and IL6 are well-described cytokines with well-established analytical tools available for their analysis in various sample types (*e.g.* validated ELISA tests). It is worth noting that the most studied CLGI biomarker in humans, the CRP protein, is not widely studied in murine models. This is due to the very different behavior of this molecule in rodents compared to humans, where it works as an acute-phase protein – the typical range of rodent expression of CRP, from 5 to 9 mg/L with peaks at only 17 mg/L after AI stimulation with LPS as explored by Huang et al. [61]. Thus, while the transposition of CRP as a CLGI biomarker from rodents to humans is limited, it highlights the need for CLGI biomarkers with similar responsiveness in different taxa.

Among the publications listed in Table 1, several adopted the relative analysis of the expression of several cytokines' genes. Besides the usefulness and importance of such techniques, a more quantitative approach would better address the basal and pathologic levels of certain biomarkers, facilitating the construction of diagnostic biomarker clusters or panels. For example, independent studies on the circulating levels of the anti-inflammatory cytokine IL-10 have described similar basal levels of this cytokine, ranging from 10 to 15 pg/mL [37,39].

A further issue in the research of some CLGI biomarkers is the differences in the expression of certain molecules across publications. For example, the CLGI-induced disruption of adhesion molecules such as ICAM-1 and VCAM-1 is reported to result in their overexpression by different publications investigating high-fat diets (HFD) or AGE consumption [47–49]. Both biomarkers would therefore seem to have a concordant and repeatable expression pattern as a result of inflammation. On the other hand, expression of the RAGE receptor or the transcriptional factor NF-κβ has been reported to be both up- and down-regulated as a result of CLGI, depending on the tissue being studied (Table 1). The following sections summarize current efforts, notably from the last two decades, on the characterization of CLGI, its putative biomarkers, and its proposed physiological roles in murine models.

4 High-AGE Diets and CLGI Initiation in Murine Models

Advanced Glycation End-Products (AGEs) are the result of non-enzymatic, post-translational reactions between reducing carbonyls and protein-amino groups, nucleic acids, or aminophospholipids [62]. The formation of AGEs by the Maillard reaction gained prominence in human health research during the 1950s, after the discovery of glycated hemoglobin under physiological conditions and its reported correlation with glycemic levels in diabetic patients [63]. The glycation of cellular proteins has a negative effect on cell and tissue function, molecular aging, and chronic disease development [64,65]. In addition to their endogenous occurrence, AGEs are also formed during thermal processing of foods, significantly increasing humans' exposure to dietary AGEs (dAGEs). Food-borne AGEs are part of a heterogeneous group of chemically stable molecules resulting from the Maillard reaction, some of which are implicated in benignly improving flavors, aromas, and browning, while others are thought to be involved in adverse health effects (*e.g.* chronic inflammation, degenerative diseases, aging, insulin resistance) [64,65].

AGEs have a close relationship with inflammation and oxidative stress which is mediated by RAGE, their eponymous receptor which is part of the immunoglobulin super-family and participates in immune surveillance in the lungs, liver, vascular endothelium, monocytes, dendritic cells, and neurons, to name only the major locations identified so far [66]. RAGE is a promiscuous receptor for which multiple ligands have been identified (*e.g.* HMGB1, S100, multiple AGEs), making it an important pattern recognition receptor (PRR) and inflammation trigger [3]. Activation of the RAGE-AGE axis has been described as a key mechanism leading to the production of pro-inflammatory cytokines, which leads to the maladaptive tissue remodeling caused by the modulation of genes and proteins implicated in extracellular matrix composition, cellular connectivity, elasticity, and tissue flexibility [67]. In this way, the long-term consumption of dAGEs would expose the immune system to CLGI activation [68].

dAGEs have been proposed as key factors in triggering inflammation in both healthy and diabetic individuals [69]. Among the AGEs already identified and characterized, carboxymethyl-lysine (CML), a glycation product of lysine residues, is the most studied [70,71]. Dietary sources of CML are diverse and include processed meat, dairy products, infant formulas, instant coffee and biscuits [72]. For instance, the average content of dietary CML (dCML) in infant formulas is 70 times

greater compared with maternal milk. For adults, based on the European diet rich in bread and coffee, the minimal daily consumption of dCML is estimated at 5 mg/day (per body weight) [73]. A large body of evidence points to the implication of CML and other AGEs in the inflammatory aggravation of obesity, diabetes, delayed wound healing or ovarian hormone dysregulation in rodent models. Table 2 presents several papers on the investigation of the inflammatory effects of different AGE-enriched diets on health in murine models.

Table 2 Studies (in reverse chronological order) of CLGI induction by Advanced Glycation End-Products in murine models.

Diet	AGE levels in the diets (Technique)	Time of exposure (weeks)	CLGI Biomarkers	Target organ/ Animal Model/ Sex	Reference
High-AGE diet	Control: CML: Free: 3.0 μg/g; Protein-bound: 10.0 μg/g Carboxyethyllysine (CEL): Free: 0.4 μg/g; Protein-bound: 2.1 μg/g MG-H1: Free: 0.4 μg/g; Protein-bound: 89.0 μg/g Baked chow diet: CML: Free: 1.0 μg/g; Protein-bound: 38.0 μg/g CEL: Free: 0.5 μg/g; Protein-bound: 30.5 μg/g MG-H1: Free: 1.6 μg/g; Protein-bound: 137 μg/g (UPLC-MS/MS)	10	CRP, TNFα, IFN-δ, IL6, IL-10	Plasma, fecal microbiota/ C57BL/6/ Females	[74]
High-AGE diet	Control: CML: 2.58 μg/g CEL: 0.89 μg/g MG-H1: 34.51 μg/g Baked chow diet: CML: 4.87 μg/g CEL: 1.38 μg/g MG-H1: 43.49 μg/g (QTRAP LC-MS/MS)	24	MCP1, LPS, C3a, C5a, occludin	Plasma and gut/ Sprague–Dawley and C57BL/6/ Males	[75]
MG-H1-enriched diet	3420 μg/g (HPLC-MS/MS)	22	IL-1β, IL-17, IFN-γ, TNF-α, PAI-1	Plasma, fecal microbiota/ C57BL/6/ Males	[39]
CML-enriched diet	Control: 61.9 μg/g CML diet: 605 μg/g (ELISA)	13	F4/80, CD11c, CD206,	Ovary/ C57BL/6/ Females	[55]
CML-enriched diet	Commercial CML 0.1% w/w	24	C5a, ICAM, IFN-δ, IL-1α, IL-1β, IL-1ra, IL-6, IL-10, IL-12, IL-13, IL-16, IL-17, IL23, TNF-α	Plasma/ Swiss/ Males	[48]
High-AGE diet	Control: CML: 2.79 μg/g	6, 12, 18	Microbiota	Gut/ Sprague–Dawley/ Males	[76]

Diet	AGE levels in the diets (Technique)	Time of exposure (weeks)	CLGI Biomarkers	Target organ/ Animal Model/ Sex	Reference
	Baked chow diet: CML: 14.45 μg/g (HPLC)				
CML-enriched diet	Control: 17.5 μg/g CML diet: 200 μg/g (HPLC-LTQ)	36	VCAM-1, RAGE	Aorta/ RAGE KO/ Males	[49]
High-AGE diet	Control: Furosine: 28.80 μg/g Hydroxymethylfurfural (HMF): 0.44 μg/g CML: 2.20 μg/g Baked chow diet: Furosine: 1787.08 μg/g HMF: 5.15 μg/g CML: 12.46 μg/g (ND)	22	Microbiota	Gut/ Wistar / Males	[77]
High-AGE diet	Control: Furosine: 28.8 μg/g HMF: 0.44 μg/g Bread crust diet: Furosine: 49.5 μg/g HMF: 4.26 μg/g (HPLC)	22	Microbiota	Gut/ Wistar/ Males	[78]
High-AGE methionine choline-deficient diet	Control: 31 nmol/g_{lysine} CML diet: 137 nmol/g_{lysine} (ELISA)	12	Il-6, MCP-1, RAGE, CD43	Liver/ Sprague–Dawley/ Males	[44]
High-AGE diet	Control: CML diet: 13 μg/g Fructoselysine: 104 μg/g Furosine: 268 μg/g H-AGE:	12	RAGE, SR-A	PBMC/ Wistar/ Females	[51]

Diet	AGE levels in the diets (Technique)	Time of exposure (weeks)	CLGI Biomarkers	Target organ/ Animal Model/ Sex	Reference
	CML diet: 760 μg/g Fructoselysine: 205 μg/g Furosine: 526 μg/g (ND)				
High-AGE diet	Control: 23 μg/g AGE diet: 110 μg/g (ELISA)	4	TNFα, TNF sRII, IL-1β, IL-6, IL-10, CXC, KC, MIP-2, CINC-1, MCP-1	Bronchoalveolar lavage/ CD-1/ Mixed	[42]
High-AGE diet	Control: CML: 60649 U/g H-AGE CML: 197305 U/g (ELISA)	39	Neutrophil infiltration	Liver/ C57BL/6NHsd/ Males	[79]
HFD - High-AGE diet	Control: 20.90 nmol CML/mol lysine/g AGE diet: 101.90 nmol CML/mol lysine/g (ND)	16	MCP-1, MIF (Macrophage migration inhibitory factor), RAGE	Kidney/ C57BL/6 (RAGEKO)/ Males	[80]
Market bought High-AGE diet	53- 1473 AU/g	1	HMGB1	Wound healing/ Kunming mice/ Males	[60]
High-AGE diet	Control: 1 μmol CML/lysine/day AGE diet: 4 μmol CML/lysine/day (ELISA)	16	IL-6, TNFα, ICAM-1, MCP-1, p65, RAGE, S1—A8/A9	Myocardio/ RAGE KO/ Males	[45]
High-AGE diet	Control: 112 μg/g CML diet: 785 μg/g (ELISA)	5, 9, and 13	Macrophage infiltration (ED1-positive), MCP-1	Kidney/ Sprague–Dawley/ Males	[54]
High-AGE diet	Control: 119000 μg/g CML diet: 930000 μg/g (ELISA)	11	Macrophage infiltration	Colon/ Sprague–Dawley/ Males	[53]
High-AGE diet	Control CML: 2700 U/mg CML diet: 12500 U/mg Control MG: 0.65 U/mg MG diet: 2.5 U/mg (ELISA)	8	VCAM-1, RAGE, MOMA-2	Aorta/ ApoE KO/ Males	[81]
High-AGE diet	Control CML: 107 U/mg CML diet: 535 U/mg Control MG: 3.6 U/mg	28	Inflammatory cell infiltration	Skin/ db/db/ Females	[82]

Diet	AGE levels in the diets (Technique)	Time of exposure (weeks)	CLGI Biomarkers	Target organ/ Animal Model/ Sex	Reference
	MG diet: 18 U/mg (ELISA)				

ND: not described; MG: methylglyoxal.

Protein-bound CML is a high-affinity RAGE ligand [83,84]. The pro-inflammatory effect of dCML has been demonstrated in a comparison between wild-type and RAGE knockout animals receiving a CML-enriched diet (50, 100, and 200 μg CML/g food). In wild-type animals receiving dCML, a dose-dependent increase in expression of VCAM-1 was observed, both histologically and in mRNA expression, while RAGE expression was in-creased significantly only at the protein level. The RAGE knockout animals were apparently protected from an increase in these inflammation triggers, and no significant VCAM-1 expression increase with dCML dose was reported in this genotype [49]. Such a protective effect over RAGE knockout animals was previously demonstrated in obese male mice that received both fat and AGE enriched diet. Harcourt et al. [80] reported that MCP-1 levels, both in plasma and kidneys of RAGE knockout mice, were reduced followed by improved MIP (macrophage migration inhibitory factor) level in the same samples. Further, the influence of the RAGE-AGE axis upon the promotion of inflammation was highlight-ed by the application of alagebrium, an AGE cross-link breaker currently investigated as an anti-AGE compound [85]. In animals receiving alagebrium, MCP-1 and MIP levels behaved in the same way as in RAGE knockout in addition to improved glycemic control [80]. The potential deleterious effect of dCML can also be inferred from the endocrine perspective, as reported in experiments on mice with ovarian hormone dysfunction. Thornton et al. [55] compared the effect of a CML-enriched and low-AGE (L-AGE) diet on ovary dysfunctions in C57BL/6 mice. The results, after 13 weeks, from mice receiving the high-AGE (H-AGE) diet showed a dysregulation of the estrous cycle and superovulation followed by an upregulation of macrophage marker F4/80 mRNA expression. The local expression of macrophage biomarkers was significantly lower in animals in receipt of a low-AGE (L-AGE) diet. Other CLGI biomarkers were examined in the ovarian tissues, with expression of pro-inflammatory Cluster of differentiation 11(CD11) increasing and anti-inflammatory CD206 decreasing among the H-AGE mice. This may be explained by the different RAGE expression among the follicular cell-types in response to gonadotrophins, since dAGEs can interfere in the gonadal cycle [86]. Chatzigeorgiou et al. [51] reported that peripheral blood mononuclear cells (PBMCs) isolated from female mice receiving a H-AGE diet had both RAGE and scavenger receptor type A (SR-A) downregulation which could be involved in dAGEs accumulation in endocrine tissues as the ovaries.

Similar to observations in animals fed HFD, dAGEs may also play a role in remodeling of gut microbiota. Evidence from experiments on rats and C57BL/6 mice demonstrated that dietary MG-H1 had a pro-inflammatory effect as well as remodeling gut microbiota [39,75]. Diet-induced gut permeability was demonstrated to result from increased CML, CEL, and MG-H1 consumption on Sprague–Dawley male rats exposed to a baked chow diet for 24 weeks. The prolonged exposure to AGEs led to kidney injuries associated with chronic kidney disease (CKD), increased MCP-1 levels in plasma, and the activation of the complement system as measured via C3a and C5a biomarkers. Such inflammatory status was associated with the dysregulation of intestinal permeability. On the high-AGE-diet group, occludin and claudin-1 gene expression were downregulated and increased circulating levels of LPS were evidenced compared to healthy animals. However, the deleterious effect of the overconsumption of AGEs was reversed with alagebrium administration or high fiber ingestion, being this last one associated to C5a proinflammatory effector decrease in db/db mice (more insights on the dietary modulation of gut microbiota and permeability are discussed ahead) [75]. MG-H1 is a methylglyoxal glycation product of arginine residues [39]. Regular animal food pellets supplemented with 15 μmol MG-H1/g food produced a significant change in glucose metabolism, followed by increased expression of pro-inflammatory cytokines IL1β, IL17, TNFα, and a decrease in anti-inflammatory cytokines IL10 and IL6 over 22 weeks treatment. The influence of dietary MG-H1 on gut microbiota was evidenced in reduced butyrate-producing species such as *Candidatus Ar-thromitus* and *Anaerostipes* sp. in animals receiving higher levels of MG-H1 [39]. From the experimental point of view, studies such as these have the benefit of using more accurate technologies (*e.g.* HPLC-MS/MS) for the identification and measurement of protein modification in laboratory-made diets [39,49]. Previously, the AGE enrichment of diets by autoclave, for instance, would result in the formation of several glycation products, making it difficult to attribute the effects of a single target molecule.

An analytical approach employing CML isotopes has demonstrated that dCML accumulates primarily in the kidneys, but also in the ileum, colon, and lungs in a RAGE-independent manner [87]. RAGE is important in triggering respiratory allergies, being involved in complications of lung cancer, asthma, and bronchoalveolar inflammation [88]. To investigate the involvement of the AGE-

RAGE axis in respiratory inflammation, mice were exposed to an H-AGE diet over 4 weeks and the bronchoalveolar lavage analyzed. This presented higher polymorphonuclear (PMN) cells, cytokines (IL1B, IL-6, and MM1, MMP-2) and TNFsRII, all of which may contribute to aggravation of lung injury, and which were associated with the triggering of inflammation by circulating dAGEs. Here, then, the responsiveness of the lungs to dAGEs is likely to be associated with pulmonary RAGE expression [89].

A striking characteristic of dAGEs is their interference in the physiology of multiple organs and tissues. In addition to their influence on the lungs, wound healing has also been shown to be disrupted by dAGEs, especially when associated with diabetes [90]. Diabetic mice with a skin injury receiving an H-AGE diet had slower vascularization, epithelialization, and local inflammatory cell infiltration than controls receiving a L-AGE diet [82]. These wound healing rates were further correlated with increased plasma HMGB1 expression in another study on Kunming mice, a model of age-related decline [60].

However, a question that remains to be answered concerns the reversibility of the several physiological effects of AGE consumption as previously presented in this topic. A recent study published by Dongen et al. (2021) [74] demonstrated that the effects of a high- AGE diet (baked chow diet) were able to shift the gut microbiota composition and promote a pro-inflammatory status in C57BL/6 female mice. These animals presented a significant increase in the circulating levels of free CML, MG-H1, and carboxyethyl-lysine (CEL) after a 10-week exposure to a modified diet compared to control animals in a regular diet. However, both components (including the inflammatory biomarkers and gut microbiota structure) were reversed when a non-baked diet was introduced in week 5, replacing the high-AGE diet. Withal, some light still remains to be shed over longer-exposure protocols where a chronic induction of the inflammatory factors could be distinguished.

5 Other diet-induced CLGI in murine models

5.1. Obesogenic diet-induced CLGI

The underlying role of inflammation in obesity has been discussed for over 20 years [20]. Table 3 summarizes the recent evolution of CLGI studies of high-calorie diets, including HFDs and high-carbohydrate diets (HCDs) To date, as a multifactorial disease, obesity is recognized as a metabolic dysfunction with a strong CLGI factor related to an increase in adipose tissue and hypothalamic dysfunction [91,92]. The relationship between excessive macronutrient intake and inflammation relies upon the promotion of immune cell infiltration in the adipose tissue, in the hypothalamus (the core site on appetite control), as well as the liver [93,94]. Macrophages are central to the development of obesity-induced CLGI, in addition to several other mechanisms which promote inflammation in this context (e.g. hypoxia, inflammasome activation) [13]. White adipose tissue (WAT) is no longer considered to be an inert tissue, and has been shown to participate in metabolic dysfunction linked to inconspicuous inflammation with a low-grade release of inflammatory mediators, as witnessed by the increased expression of inflammation biomarkers in obese animals (*e.g.* TNFα, MCP1, IL6) [19]. In corroboration, the promotion of the pro-inflammatory state in an obese individual is related to their increase in adipose tissue, made manifest when adipokine (*e.g.* adiponectin, leptin) levels were demonstrated to vary with weight gain [95].

Table 3 Studies of CLGI (in reverse chronological order) resulting from high-calorie intake interventions in murine models.

CLGI Trigger	Target organ	Time of exposure (weeks)	CLGI Biomarkers	Animal/ Sex	Reference
HFD	Liver	24	TNF-α, IL-1β, IL-6, IL-10, CAE^+, $F4/80^+$	C57BL/6J/ Females	[38]
	Adipose tissue, liver	24, 40, and 52	TNF-α, IL-1β, MCP-1, $F4/80^{+,}$ crown-like structures	C57BL/6/ Males	[37]
	Adipose tissue	11	CD14, AKT, CD68, C11c, MCP-1, IL-6	C57BL/6/ Males	[41]
	Hypothalamus	8	Serpina3n	C57BL/6J, TLR4 KO, CD14 KO/ Males	[4]
	Gut microbiota	12	NF-kB, mTOR, AKT	C57BL/6/ Males	[57]
	Gut microbiota	8	PPARγ, C/EBPa, FAZ, aFABP, CD68, F4/80, p-IKK β, p65, TNF-α, IL 1β, IL-6	C57BL/6J, TLR4 KO C57BL/10ScNJ/ Males	[46]
High-calorie diet (30% fructose)	Liver, Brain	8	TNF-α, IL-2, NF-κB, HVA	Sprague-Dawley/ Males	[36]
Intragastric fructose injection	Serum, liver, pancreas	20	IL-6, TNF-α, MIP-2, IL-10	Sprague-Dawley/ Males	[96]

Obesogenic diets have been shown to increase CVD risk in humans as well as comorbidities classically associated with being overweight [97]. A closer look at diet-induced obesity (DIO) studies in murine models suggests its involvement in the aggravation of CLGI. DIO promotes alterations in metabolic tissues such as macrophage infiltration, adipocyte hypertrophy and death, as well as the activation of proinflammatory pathways within the WAT and the hypothalamus. Macrophages and lymphocytes are part of the heterogeneous composition of adipose tissues [98]. Adipocyte hypertrophy is followed by early-stage adipocyte cell death, accelerating the abnormal recruitment of bone-marrow macrophages and amplification of immune cell responses [99]. In the light of important histopathologic evidence derived from obese mice, a greater density of macrophages was shown to surround dead adipocytes [100]. A 4-fold incidence of macrophages was demonstrated to occur in the adipose tissue followed by an increase in MCP-1 (a macrophage chemoattractant) in obese mice compared with lean animals [101,102]. Special

attention was paid to the *in situ* expression of cytokines and demonstrated that macrophages and adipocytes participates in augmented expression of adipokines, especially IL-6, leptin and adiponectin, in addition to a reduced blood supply and increased hypoxia and oxidative stress in WAT, all of which contribute to systemic inflammation and insulin resistance [103].

It appears that under a chronic consumption of an HFD, adipose tissue promotes an increase of systemic cytokine production. Heijden et al. [37] observed that after 24 weeks, mice receiving an HFD showed noticeable adipose tissue inflammation, but hepatic inflammation signals were only detectable after 40 weeks. The temporal expression of TNFα, MCP1, and macrophage F4/80+ receptors described in mice suggests that adipose tissue inflammation precedes hepatic inflammatory response to HFDs. At least one other study demonstrated the effect of an HFD on CLGI in the liver. A recent publication by Guerra and colleagues [38] demonstrated that, as described for adipose tissue and the brain, the consumption of an HFD (60% fat) by C57L/6 female mice for 24 weeks promoted the infiltration of macrophages and mononuclear cells into hepatic tissue. The latter finding demonstrates that the hepatocyte expression of anti-inflammatory and pro-inflammatory biomarkers, respectively IL10 and TNFα genes, increased significantly [38]. On the other hand, IL1β and IL6 (pro-inflammatory) remained at the same levels compared with the control diet group, demonstrating a heterogeneous effect of this type of diet on different cytokines [38].

A significant limitation for the understanding of the real effects of diet-induced CLGI are confounding factors such as the variable quality of fat among the different commercially available diets for animal experiments. It appears that not only the duration of the exposure to an HFD is important, but also its composition. Benoit et al. [41] hypothesized that the difference in fat quality among diets could influence the effects observed in the scientific literature. They tested diets including a regular chow, low-fat diet (cLFD; 8% fat), a semisynthetic low-fat diet (sLFD; 12% fat), and a semisynthetic HFD (sHFD; 40% fat). Differences observed among experimental groups were related to the origin of the fat component, but not the amount of fat per se. Interestingly, for several of the physiological features evaluated, the two LFDs yielded apparently contradictory results. The insulin levels in plasma, for instance, were significantly higher in the sLFD animals, while no difference was evident between regular cLFD or sHFD groups. Similarly, MCP-1 expression in the

epididymis WAT significantly increased only in the 40% fat, sHFD treatment. Pro-inflammatory IL-6 expression was increased only in animals receiving the sLFD, high-lighting how heterogeneous the dietary stimulation of a low-grade inflammation response may be with diets of different quality and composition [41].

Reporting similar findings on the effects of macrophages in adipose tissue, some recent studies have demonstrated the role of macrophage infiltration in the hypothalamus. As stated above, the hypothalamus is a fundamental actor in appetite control, and its proper function is therefore required to maintain energy homeostasis [104]. Remarkably excessive macronutrient intake induces the infiltration of macrophages to the hypothalamic core, which is involved in sensitivity to peripheral levels of glucose and metabolism signals such as leptin, insulin, and free fatty acids (FFA) [105]. Lainez et al. [5] demonstrated that an HFD doubled macrophage infiltration to the hypothalamus of obese male mice compared with controls in regular diet. A second study examined the production of cytokines in the hypothalamic arcuate nucleus, and the overexpression of pro-inflammatory cytokines was demonstrated to be related to a loss of glucose homeostasis coordination in a male mouse model of inflammation (LysM) [24]. In contrast, a transcriptomic approach was used to study the abnormal immune responses of the hypothalamus and demonstrated that inflammation was not associated with HFD consumption. Based on a 4-8-weeks animal experiment including wild type, TLR4 knockout, and CD14 knockout animals, no significant difference in inflammation transcripts was observed among animals of different genotypes receiving an HFD [4]. Both the TLR4 and CD14 receptors are part of the innate immune system, participating in PRRs recognition. This is important because TLR4 and CD14 cooperate in the pro-inflammatory response to exogenous stress factors such as LPS, as described below [106].

5.2. Diet-induced gut microbiota remodeling and CLGI: A Mechanism of Metabolic Endotoxemia

The gut microbiota is an important functional unit established in the gastrointestinal system (GIS) that has coevolved to participate in the regulation of host homeostasis, in addition to its direct role in digestion [107]. The colonization of the GIS by microbiota begins at birth, but its composition is constantly remodeled throughout life according to the host's genetic profile and environmental conditions (*e.g.* diet, smoking) [108]. The gut microbiome comprises a vast community of trillions of microorganisms, the most numerous of which are ensembles of both gram-negative and gram-positive bacteria, and which includes a relatively minor component of fungal species [109]. The structure of gut bacterial communities comprises two main phyla: Bacteroidetes (mostly gram-negative) and Firmicutes (mostly gram-positive), and the proportion of last increases with age [110,111]. Humans and mice have a broadly similar Firmicutes/Bacteroidetes (F/B) ratio, with a pre-dominance of Bacteroidetes over Firmicutes in healthy individuals at adulthood [112]. The prerequisite for a healthy microbiota is an adequately diverse and sufficiently dense microbial community. The intestinal bacterial community underlies important events in both the initiation and progression of CLGI as a result of unbalanced diet [33].

Diet is a major environmental factor in remodeling of the gut microbiome [113] (Table 4). This much is apparent in comparative metagenomic studies, where a lower overall microbial diversity is observed in mice undergoing DIO protocols [114]. Several papers have described a shift in the F/B ratio in mice under HFD, with prominent Bacteroidetes cell death leading to a predominance of Firmicutes taxa [115,116]. Dysbiosis is linked to CLGI owing to the resultant increased permeability of the mucosal barrier in the gut to endotoxins (*e.g.* LPS), promoting a state of metabolic endotoxemia [115]. Diet-induced gut permeability results from the activation of mast cells and tight junction disruption, both associated with the production of tryptase and cytokines' cascade activation [117]. Once gut epithelial permeability is increased, LPS may enter the bloodstream via both diffusion and chylomicrons, inducing a state of metabolic dysfunction mediated by TLR-4, RAGE, and CD14 receptor activation [118]. The causative link between circulating LPS and obesity has been illustrated by the remarkable CLGI in the hypothalamic region and concurrent, intensive local macrophage infiltration [24]. It is worth remembering that

LPS is a gram-negative, cell wall glycolipid. Therefore, beyond the decrease in LPS producing groups in obese mice, such observations raise the possibility that the F/B ratio may not directly explain endotoxemia in obesity and CLGI. Magne et al. [119] proposed that, besides the overall reduction of Bacteroidetes groups in obese subjects, other gram-negative taxa such as the Proteobacteria and Verrucomicrobia phylum remain important producers of LPS.

Table 4 Studies of murine gut microbiota and CLGI.

CLGI Trigger	Target organ	Time of exposure (weeks)	CLGI Assessment Biomarkers	Strain/ Sex	Reference
LPS	Hypothalamus	12	Iba1, TH	Sprague-Dawley/ Males	[59]
	Hypothalamus	1	IRS1, AKT, JNK	Wistar/ Males	[58]
	Liver	4	p38 MAPK, MPO, TNF-α, MCP-1, IL-6	ApoE KO, C57BL/6J/ Males	[52]
	Plasma	8	TNF- α, TNF- β, MCP-1, IL-6	ApoE KO/ Male	[120]
DSS	Colon, feces, plasma	1	Lipocalin-2	C57BL/6/ Males ; IL-10 KO/ Females	[56]

A considerable body of work has addressed the effects of HFD in reshaping the gut microbiome and in metabolic endotoxemia. Cani and colleagues [115] were the first to evidence LPS of gut microbial origin as a trigger of metabolic impairment. Accordingly, obese mice and lean controls presented different gut microbiota compositions and associated inflammation and metabolic dysregulation. The consumption over 4 weeks of an HFD by C57BL/6 male mice (12-weeks-old) doubled the circulating levels of LPS, and a concomitant increase in TNFα, IL1, IL6, and PAI1 levels was observed in the liver, visceral and subcutaneous fat, and muscles. A 4-week follow-up study on 12-week-old C57BL6/J mice fed an HFD also described a 2-fold increase in circulating levels of LPS (from 3 to 6 U/mL) compared with animals fed a regular, nutritionally balanced diet [121]. Some years later, a comparative analysis between germ-free mice and conventional pathogen-free mice pointed to clear evidence of the gut microbiota's contribution to obesity and

inflammation triggers. In this scenario, no metabolic dysfunction was observed in germ-free mice fed an HFD for 16 weeks, while TNFα expression increased (concomitantly with the development of obese and diabetic phenotypes) in the conventional animals receiving the same HFD [122]. Later, a more comprehensive study of the effects of different diets on the gut microbiota was published. Serino et al. [57] compared the consumption of a classical HFD and an HFD enriched with fiber (galactooligosaccharides – HFD-GOS) during 12 weeks in C57BL/6 male mice. Animals receiving the conventional HFD presented an in-version of the F/B ratio, while those in receipt of the fiber-supplemented HFD-GOS retained an abundance of 90% for Bacteroidetes. The lower F/B ratio signature in the former was associated with higher circulating levels of LPS than the HFD-GOS group. In agreement with the increased circulating levels of LPS, plasma levels of IL-6, NF-kB and PAI-1 were also significantly higher in the HFD animals compared with the HFD-GOS group. Finally, the diabetic metabolic profile which developed in the HFD group was accompanied by increased paracellular permeability of the ileum, caecum, and colon, while a protective effect was observed with GOS supplementation [57].

Other consequences for gut homeostasis have been observed in DIO experiments in mice. Food fermentation by the gut flora plays a fundamental role in production of metabolites like short-chain fatty acids (SCFAs). Propionate, butyrate, and acetate are important SCFAs that play anti-inflammatory and immunoregulatory roles in the gut [123]. Butyrate is an important SCFA, originating from the fermentation of fibers, and a major source of energy for the microbial community in the gut. At the host level, butyrate acts as the epigenetic activator of gluconeogenesis, thus playing a role in energy metabolism in several cell types (e.g. hepatocytes, adipocytes), but mainly by influencing enterocyte energy homeostasis and epithelial integrity [123,124]. One effect of an HFD in mice is the diminution of butyrate-producing species (*i.e.* Ruminococcaceae and Lachnospiraceacae families) [125]. The negative effects of increased intestinal permeability are enhanced by the HFD's effect on pro-inflammatory cascade triggers which actively promote cytokine expression (TNFα, interleukin IL1β, IL6, interferon γ (IFNγ), further disrupt tight junctions, and modify mucus composition at the surface of the intestinal epithelium. These factors combine to promote mucosal hyper-sensitization, inflammation, and concomitant villous atrophy [126]. IL-1β, for instance, was demonstrated to be a key molecule in the in vivo permeability control of gut epithelial

cells. In C57BL/6 mice, an increase in IL-1β has been associated with NF-κB activation provoking an inflammatory cascade that in turn resulted in the overexpression of enterocyte myosin light-chain kinase (MLCK), at both the mRNA and protein levels [127]. In addition, an unbalanced diet may promote cytoskeletal cell modifications and epithelial cell apoptosis. Microtubule-actin cross-linking factor-7 (ACF7), for instance, participates in cytoskeleton dynamics and plays an important role in epithelial recovery. A study of HFD-fed ACF7 knockout mice revealed a disrupted intestinal homeostasis and a higher apoptotic level in the gut compared with wild-type mice fed the same diet [128]. Modifications of MLCK and ACF7, together with decreases in occludin, ZO-1, and claudin protein content in tight-junctions, support the theory that cell structure damage is related to epithelial impairment resulting from consumption of an HFD [129].

Considering the relevance of LPS to CI triggers, a cornerstone of the investigation of CLGI is the use of subclinical doses of LPS to mimic metabolic endotoxemia in a murine model [130,131]. In this way, LPS is used as a model molecule for the experimental initiation of systemic CLGI. The effects of administering subclinical doses of endotoxin in murine models have been examined in studies of the impacts of chronic and low-grade inflammation in obese phenotypes, including neuroinflammation and appetite control. The hypothalamus takes part in regulating food intake and body weight. In an investigation of the induction of hypothalamic CLGI, male Wistar rats were periodically injected with subclinical doses of LPS (100 μg/kg) via intraperitoneal injection. Animals chronically ex-posed to LPS (6 doses over 24 hours) became resistant to the hypophagic effect (reduction in feeding behavior) commonly observed as a result of exposure to LPS. These animals presented a 2-fold increase in hypothalamic phosphorylated c-Jun N-terminal kinase (JNK) levels compared with controls on saline injections [58]. JNK is a cell stress signaling marker regulating cell survival, but in the context of obesity and hypothalamic dysfunction it is involved in insulin receptor substrates (IRS) and recruitment of Protein Kinase B (AKT) and insulin-dependent translocation of forkhead box protein O1 (FoxO1) [132]. Chronic exposure to LPS was also shown to affect the phosphorylation of AKT, to block IRS1 and impair the translocation of FoxO1 in hypothalamic GT1-7 mouse cells [58]. In Sprague-Dawley male rats, LPS administration was found to affect the brain via

microglia hypertrophy, and ionized calcium-binding adapter 1 (Iba1) was reported to be overexpressed in immunostaining assay of brain tissue [59].

In addition to these findings, subclinical doses of LPS have been shown to affect the liver and adipose tissue. In male, ApoE knockout C57BL/6J mice, the simultaneous administration of super-low doses of LPS with administration of an HFD resulted in the development of nonalcoholic fatty liver disease (NAFLD) steatohepatitis, followed by intense leukocyte infiltration and sustained expression of p38 mitogen-activated protein kinase (MAPK) [52], a molecule involved in the production of inflammatory mediators such as TNFα and cyclo-oxygenase 2 (COX-2). Hepatocyte apoptosis was also associated with local cellular oxidative stress. Myeloperoxidase, an indicator of ROS production, was 3 times greater after 4 weeks of LPS exposure, and was accompanied by an increase in hepatic expression of pro-inflammatory biomarkers IL6, MCP1, and TNFα [52].

Research aimed at elucidating inflammatory patterns in the murine gut can therefore rely upon measures of the cytokines TNFα, IL6, IL1, NFkB, and IL1β levels in animals receiving fat-rich diets, together with temporal increase of systemic LPS and modified F/B ratios. Investigations which analyze these patterns may prove to be powerful predictive tools of CLGI. More recently, another useful metabolic inflammation biomarker has received attention in studies of intestinal microbial dysfunction mediation. Lipocalin-2 (LCN2) is a glycoprotein secreted by several cell types, but was initially identified in activated neutrophils [133]. LCN2 is readily detected in serum, feces, and adipose tissue in the context of inflammation dysfunction. In the gut, the main sources of LCN2 are myeloid and intestinal epithelial cells – the same cells which are affected by the mucosal barrier dysfunction and increased permeability of the gut epithelium previously described. The responsiveness of LCN2 in the gastrointestinal tract was first demonstrated in colitis-induced models. Colitis has a close relationship with dysfunctional microbiota and permeability of the intestinal epithelium. Murine models of colitis have been adapted to relatively mild protocols in order to study the effect of low-grade endotoxemia on LCN2 expression. Chassaing et al. [56] used 8 days of subclinical doses of dextran sulfate sodium (DSS), an epithelial disruption promoting agent, to study the induction of intestinal CLGI in C57BL/6 mice. Low doses of DSS (0.25 and 0.5%) produced an increase in IL-1β mRNA, as well as significant ulceration of colonic epithelium observed by histopathology. Interestingly, while a dose of 0.25%

DSS induced an increase in LCN2 levels in colon samples as well as in feces, no difference was observed in serum samples, but significant from 0.5% DSS injections. From the clinical point of view, the authors suggested that fecal LCN2 could be a sensitive, non-invasive biomarker of CLGI, and one that also has a close relationship with intestinal dysfunction [56].

6 Perspectives and conclusion

Based on the data presented in this review, the involvement of diet in the induction and progression of CLGI has been clearly demonstrated in murine models. Since multiple factors which contribute to CLGI initiation probably occur simultaneously (*e.g.* higher AGE concentration in the circulation, endotoxemia), a better understanding of the interaction of inflammation biomarkers in different organs and tissues would help to elucidate key biomarkers of CLGI, as well as identify the most susceptible among them, pinpointing the potential physiological implications. The murine models described in this review have shed significant light on CLGI, particularly the importance of local (tissue level) measurements of CLGI biomarkers. The use of murine models is also helping to illuminate CLGI crosstalk among different organs due to the ease of sample collection, preparation and analysis compared with other animal models or clinical studies. Indeed, significant advances have been made in the attribution of the physiological effects of CLGI, and the identification of potential biomarkers induced by target compounds such as dAGEs and dietary lipids in these models. They have enabled the study of direct effects of key dietary influences on animal physiology, but some limitations on the translational use of future biomarkers in clinical applications between murine models and humans may arise (*e.g.* CRP). In the future, the current use of qualitative or semiquantitative techniques for CLGI biomarker analysis should give way to more extensive and specific analytical techniques, such as proteomics, transcriptomics and metabolomics, that could drive research on both screening and quantification of CLGI biomarkers in the whole organism.

From the nutritional perspective, strategies for the prevention of CLGI are required to reduce the impacts of several metabolic diseases, as well as to promote healthy aging. A balanced diet is often recommended to maintain good health [134], and evidence is also emerging from murine models that CLGI may be attenuated

through the use of natural products, hinting at the possibility that dietary intervention may have the potential to limit initiation and/or progression of CLGI. Indeed, the use of probiotics or extracts of certain berries has been reported to ameliorate diet-induced CLGI in murine models under HFD [135–137], though these studies require confirmation in clinical studies in humans.

Lastly, current research on diet-induced CLGI has highlighted the utility of simultaneously examining several different inflammation biomarkers. Ongoing research has confirmed the involvement of several cytokines and other inflammation biomarkers in both the initiation and progression of CLGI, but their use for the prediction, and/or determination of CLGI still lacks consensus. We remain some way from defining a clinical diagnostic test for CLGI, but future CLGI treatment may target important receptors such as TLR4 and RAGE for the prevention of CLGI initiation, and diagnostics may rely upon the recent evolution of non-invasive biomarkers (*e.g.* Lipocalin-2). With respect to the prospection of CLGI biomarkers, candidates should be systematically investigated to fill gaps in the whole-organism picture of inflammatory responses in different organs and tissues. From the diagnostics perspective, biomarker research should integrate current knowledge on the use of multiple biomarkers able to predict CLGI more robustly.

The overconsumption of AGEs (especially dCML) and obesogenic foods leads to several physiological effects which contribute to the onset of CLGI, and their study has contributed greatly to our understanding. Several different classes of biomarkers have been reported as important, but the levels of cytokines such as TNFα and IL6, as well as chemokines such as MCP1 and adhesion molecules (*e.g.* VCAM1), are repeatedly cited as potential biomarkers in CLGI research in murine models. But progress in this field can be only made with more robust analytical protocols. Particular attention should be paid to the quality and homogeneity of the dietary regimes employed, the simultaneous analysis of multiple organs under the same dietary protocol, and establishing both normal and pathological levels of key biomarkers already identified. Metabolomics studies which include multiple CLGI biomarkers have potential in this regard, and offer the possibility of defining clusters or panels of biomarkers capable of specifically targeting this subtle, multilayered and complex inflammatory process.

Author Contributions: M.T.N.S.L. wrote the article, elaborated tables, and figures. M.H. re-viewed the article and assisted with English corrections. P.M.A. critically reviewed the “Diet-induced gut microbiota remodeling and CLGI” topic. C.D.O. critically reviewed and took part in article structure. F.J.T. proposed the review topic and elaboration of the article, taking part in the article conception, structure, and critical review.

Funding: This work was funded by Agence Nationale de la Recherche (ANR), grant number ANR-19-CE34-0013.

7 References

1. Minihane, A. M.; Vinoy, S.; Russell, W. R.; Baka, A.; Roche, H. M.; Tuohy, K. M.; Teeling, J. L.; Blaak, E. E.; Fenech, M.; Vauzour, D.; McArdle, H. J.; Kremer, B. H. A.; Sterkman, L.; Vafeiadou, K.; Benedetti, M. M.; Williams, C. M.; Calder, P. C. Low-Grade Inflammation, Diet Composition and Health: Current Research Evidence and Its Translation. *Br J Nutr* **2015**, *114* (7), 999–1012. https://doi.org/10.1017/S0007114515002093.
2. Jandeleit-Dahm, K.; Cooper, M. E. The Role of AGEs in Cardiovascular Disease. *Curr Pharm Des* **2008**, *14* (10), 979–986. https://doi.org/10.2174/138161208784139684.
3. Teissier, T.; Boulanger, E. The Receptor for Advanced Glycation End-Products (RAGE) Is an Important Pattern Recognition Receptor (PRR) for Inflammaging. *Biogerontology* **2019**, *20* (3), 279–301. https://doi.org/10.1007/s10522-019-09808-3.
4. Dalby, M. J.; Aviello, G.; Ross, A. W.; Walker, A. W.; Barrett, P.; Morgan, P. J. Diet Induced Obesity Is Independent of Metabolic Endotoxemia and TLR4 Signalling, but Markedly Increases Hypothalamic Expression of the Acute Phase Protein, SerpinA3N. *Scientific Reports* **2018**, *8* (1), 15648. https://doi.org/10.1038/s41598-018-33928-4.
5. Lainez, N. M.; Jonak, C. R.; Nair, M. G.; Ethell, I. M.; Wilson, E. H.; Carson, M. J.; Coss, D. Diet-Induced Obesity Elicits Macrophage Infiltration and Reduction in Spine Density in the Hypothalami of Male but Not Female Mice. *Front. Immunol.* **2018**, *9*. https://doi.org/10.3389/fimmu.2018.01992.
6. Cani, P. D.; Delzenne, N. M. The Role of the Gut Microbiota in Energy Metabolism and Metabolic Disease. *Curr Pharm Design* **2009**, *15* (13), 1546–1558. https://doi.org/10.2174/138161209788168164.
7. Calder, P. C.; Ahluwalia, N.; Albers, R.; Bosco, N.; Bourdet-Sicard, R.; Haller, D.; Holgate, S. T.; Jönsson, L. S.; Latulippe, M. E.; Marcos, A.; Moreines, J.; M'Rini, C.; Müller, M.; Pawelec, G.; Neerven, R. J. J. van; Watzl, B.; Zhao, J. A Consideration of Biomarkers to Be Used for Evaluation of Inflammation in Human Nutritional Studies. *Brit J Nutr* **2013**, *109* (S1), S1–S34. https://doi.org/10.1017/S0007114512005119.
8. Calder, P. C.; Ahluwalia, N.; Brouns, F.; Buetler, T.; Clement, K.; Cunningham, K.; Esposito, K.; Jönsson, L. S.; Kolb, H.; Lansink, M.; Marcos, A.; Margioris, A.; Matusheski, N.; Nordmann, H.; O'Brien, J.; Pugliese, G.; Rizkalla, S.; Schalkwijk, C.; Tuomilehto, J.; Wärnberg, J.; Watzl, B.; Winklhofer-Roob, B. M. Dietary Factors and Low-Grade Inflammation in Relation to Overweight and Obesity. *Brit J Nutr* **2011**, *106 Suppl 3*, S5-78. https://doi.org/10.1017/S0007114511005460.
9. Calder, P. C.; Bosco, N.; Bourdet-Sicard, R.; Capuron, L.; Delzenne, N.; Doré, J.; Franceschi, C.; Lehtinen, M. J.; Recker, T.; Salvioli, S.; Visioli, F. Health Relevance of the Modification of Low Grade Inflammation in Ageing (Inflammageing) and the Role of Nutrition. *Ageing Res Rev* **2017**, *40*, 95–119. https://doi.org/10.1016/j.arr.2017.09.001.
10. Yu, H. P.; Chaudry, I. H.; Choudhry, M. A.; Hsing, C.-H.; Liu, F.-C.; Xia, Z. Inflammatory Response to Traumatic Injury: Clinical and Animal Researches in Inflammation. *Mediat Inflamm* **2015**, *2015*, e729637. https://doi.org/10.1155/2015/729637.
11. Ward, P. A. Acute and Chronic Inflammation. In *Fundamentals of Inflammation*; Serhan, C. N., Gilroy, D. W., Ward, P. A., Eds.; Cambridge University Press: Cambridge, 2010; pp 1–16. https://doi.org/10.1017/CBO9781139195737.002.
12. Lawrence, T.; Gilroy, D. W. Chronic Inflammation: A Failure of Resolution? *Int J Exp Pathol* **2007**, *88* (2), 85–94. https://doi.org/10.1111/j.1365-2613.2006.00507.x.
13. Pereira, S. S.; Alvarez-Leite, J. I. Low-Grade Inflammation, Obesity, and Diabetes. *Curr Obes Rep* **2014**, *3* (4), 422–431. https://doi.org/10.1007/s13679-014-0124-9.
14. Pietrzyk, L.; Torres, A.; Maciejewski, R.; Torres, K. Obesity and Obese-Related Chronic Low-Grade Inflammation in Promotion of Colorectal Cancer Development. *Asian Pac J Cancer Prev* **2015**, *16* (10), 4161–4168. https://doi.org/10.7314/apjcp.2015.16.10.4161.
15. Schett, G.; Neurath, M. F. Resolution of Chronic Inflammatory Disease: Universal and Tissue-Specific Concepts. *Nat Comm* **2018**, *9* (1), 3261. https://doi.org/10.1038/s41467-018-05800-6.
16. Ferrucci, L.; Fabbri, E. Inflammageing: Chronic Inflammation in Ageing, Cardiovascular Disease, and Frailty. *Nat Rev Cardiol* **2018**, *15* (9), 505–522. https://doi.org/10.1038/s41569-018-0064-2.
17. Stevens, J. R. Neuropathology of Schizophrenia. *Arch Gen Psychiat* **1982**, *39* (10), 1131–1139. https://doi.org/10.1001/archpsyc.1982.04290100011003.
18. Galea, P.; D'amato, B.; Goel, K. M. Ocular Complications in Juvenile Chronic Arthritis (JCA). *Scott Med J* **1985**, *30* (3), 164–167. https://doi.org/10.1177/003693308503000308.

19. Coelho, M.; Oliveira, T.; Fernandes, R. Biochemistry of Adipose Tissue: An Endocrine Organ. *Arch Med Sci* **2013**, *9* (2), 191–200. https://doi.org/10.5114/aoms.2013.33181.
20. Hotamisligil, G. S.; Shargill, N. S.; Spiegelman, B. M. Adipose Expression of Tumor Necrosis Factor-Alpha: Direct Role in Obesity-Linked Insulin Resistance. *Science* **1993**, *259* (5091), 87–91. https://doi.org/10.1126/science.7678183.
21. Fain, J. N.; Madan, A. K.; Hiler, M. L.; Cheema, P.; Bahouth, S. W. Comparison of the Release of Adipokines by Adipose Tissue, Adipose Tissue Matrix, and Adipocytes from Visceral and Subcutaneous Abdominal Adipose Tissues of Obese Humans. *Endocrinology* **2004**, *145* (5), 2273–2282. https://doi.org/10.1210/en.2003-1336.
22. Vohl, M. C.; Sladek, R.; Robitaille, J.; Gurd, S.; Marceau, P.; Richard, D.; Hudson, T. J.; Tchernof, A. A Survey of Genes Differentially Expressed in Subcutaneous and Visceral Adipose Tissue in Men*. *Obes Res* **2004**, *12* (8), 1217–1222. https://doi.org/10.1038/oby.2004.153.
23. Timper, K.; Brüning, J. C. Hypothalamic Circuits Regulating Appetite and Energy Homeostasis: Pathways to Obesity. *Dis Model Mech* **2017**, *10* (6), 679–689. https://doi.org/10.1242/dmm.026609.
24. Lee, C. H.; Kim, H. J.; Lee, Y.-S.; Kang, G. M.; Lim, H. S.; Lee, S.; Song, D. K.; Kwon, O.; Hwang, I.; Son, M.; Byun, K.; Sung, Y. H.; Kim, S.; Kim, J. B.; Choi, E. Y.; Kim, Y.-B.; Kim, K.; Kweon, M.-N.; Sohn, J.-W.; Kim, M.-S. Hypothalamic Macrophage Inducible Nitric Oxide Synthase Mediates Obesity-Associated Hypothalamic Inflammation. *Cell Rep* **2018**, *25* (4), 934-946.e5. https://doi.org/10.1016/j.celrep.2018.09.070.
25. Thaler, J. P.; Yi, C.-X.; Schur, E. A.; Guyenet, S. J.; Hwang, B. H.; Dietrich, M. O.; Zhao, X.; Sarruf, D. A.; Izgur, V.; Maravilla, K. R.; Nguyen, H. T.; Fischer, J. D.; Matsen, M. E.; Wisse, B. E.; Morton, G. J.; Horvath, T. L.; Baskin, D. G.; Tschöp, M. H.; Schwartz, M. W. Obesity Is Associated with Hypothalamic Injury in Rodents and Humans. *J Clin Invest* **2012**, *122* (1), 153–162. https://doi.org/10.1172/JCI59660.
26. Bektas, A.; Schurman, S. H.; Sen, R.; Ferrucci, L. Human T Cell Immunosenescence and Inflammation in Aging. *J Leukocyte Biol* **2017**, *102* (4), 977–988. https://doi.org/10.1189/jlb.3RI0716-335R.
27. Tahir, S.; Fukushima, Y.; Sakamoto, K.; Sato, K.; Fujita, H.; Inoue, J.; Uede, T.; Hamazaki, Y.; Hattori, M.; Minato, N. A CD153+CD4+ T Follicular Cell Population with Cell-Senescence Features Plays a Crucial Role in Lupus Pathogenesis via Osteopontin Production. *J Immunol* **2015**, *194* (12), 5725–5735. https://doi.org/10.4049/jimmunol.1500319.
28. Fukushima, Y.; Minato, N.; Hattori, M. The Impact of Senescence-Associated T Cells on Immunosenescence and Age-Related Disorders. *Inflamm Regen* **2018**, *38*. https://doi.org/10.1186/s41232-018-0082-9.
29. Murphy, E. A.; Velazquez, K. T.; Herbert, K. M. Influence of High-Fat-Diet on Gut Microbiota: A Driving Force for Chronic Disease Risk. *Curr Opin Clin Nutr Metab Care* **2015**, *18* (5), 515–520. https://doi.org/10.1097/MCO.0000000000000209.
30. Wolters, M.; Ahrens, J.; Romaní-Pérez, M.; Watkins, C.; Sanz, Y.; Benítez-Páez, A.; Stanton, C.; Günther, K. Dietary Fat, the Gut Microbiota, and Metabolic Health - A Systematic Review Conducted within the MyNewGut Project. *Clin Nutr* **2019**, *38* (6), 2504–2520. https://doi.org/10.1016/j.clnu.2018.12.024.
31. Margioris, A. N.; Dermitzaki, E.; Venihaki, M.; Tsatsanis, C. 4 - Chronic Low-Grade Inflammation. In *Diet, Immunity and Inflammation*; Calder, P. C., Yaqoob, P., Eds.; Woodhead Publishing Series in Food Science, Technology and Nutrition; Woodhead Publishing, 2013; pp 105–120. https://doi.org/10.1533/9780857095749.1.105.
32. Giuliani, A.; Prattichizzo, F.; Micolucci, L.; Ceriello, A.; Procopio, A. D.; Rippo, M. R. Mitochondrial (Dys) Function in Inflammaging: Do MitomiRs Influence the Energetic, Oxidative, and Inflammatory Status of Senescent Cells? *Mediat Inflamm* **2017**, *2017*. https://doi.org/10.1155/2017/2309034.
33. Chassaing, B.; Gewirtz, A. T. Gut Microbiota, Low-Grade Inflammation, and Metabolic Syndrome. *Toxicol Pathol* **2014**, *42* (1), 49–53. https://doi.org/10.1177/0192623313508481.
34. Bordoni, A.; Danesi, F.; Dardevet, D.; Dupont, D.; Fernandez, A. S.; Gille, D.; Nunes Dos Santos, C.; Pinto, P.; Re, R.; Rémond, D.; Shahar, D. R.; Vergères, G. Dairy Products and Inflammation: A Review of the Clinical Evidence. *Crit Rev Food Sci Nutr* **2017**, *57* (12), 2497–2525. https://doi.org/10.1080/10408398.2014.967385.

35. Ridker, P. M. Clinical Application of C-Reactive Protein for Cardiovascular Disease Detection and Prevention. *Circulation* **2003**, *107* (3), 363–369. https://doi.org/10.1161/01.CIR.0000053730.47739.3C.
36. Erbaş, O.; Akseki, H. S.; Aktuğ, H.; Taşkıran, D. Low-Grade Chronic Inflammation Induces Behavioral Stereotypy in Rats. *Metab Brain Dis* **2015**, *30* (3), 739–746. https://doi.org/10.1007/s11011-014-9630-4.
37. van der Heijden, R. A.; Sheedfar, F.; Morrison, M. C.; Hommelberg, P. P.; Kor, D.; Kloosterhuis, N. J.; Gruben, N.; Youssef, S. A.; de Bruin, A.; Hofker, M. H.; Kleemann, R.; Koonen, D. P.; Heeringa, P. High-Fat Diet Induced Obesity Primes Inflammation in Adipose Tissue Prior to Liver in C57BL/6j Mice. *Aging (Albany NY)* **2015**, *7* (4), 256–267.
38. Power Guerra, N.; Müller, L.; Pilz, K.; Glatzel, A.; Jenderny, D.; Janowitz, D.; Vollmar, B.; Kuhla, A. Dietary-Induced Low-Grade Inflammation in the Liver. *Biomedicines* **2020**, *8* (12). https://doi.org/10.3390/biomedicines8120587.
39. Mastrocola, R.; Collotta, D.; Gaudioso, G.; Le Berre, M.; Cento, A. S.; Ferreira Alves, G.; Chiazza, F.; Verta, R.; Bertocchi, I.; Manig, F.; Hellwig, M.; Fava, F.; Cifani, C.; Aragno, M.; Henle, T.; Joshi, L.; Tuohy, K.; Collino, M. Effects of Exogenous Dietary Advanced Glycation End Products on the Cross-Talk Mechanisms Linking Microbiota to Metabolic Inflammation. *Nutrients* **2020**, *12* (9), 2497. https://doi.org/10.3390/nu12092497.
40. Matafome, P.; Santos-Silva, D.; Crisóstomo, J.; Rodrigues, T.; Rodrigues, L.; Sena, C. M.; Pereira, P.; Seiça, R. Methylglyoxal Causes Structural and Functional Alterations in Adipose Tissue Independently of Obesity. *Arch Physiol Biochem* **2012**, *118* (2), 58–68. https://doi.org/10.3109/13813455.2012.658065.
41. Benoit, B.; Plaisancié, P.; Awada, M.; Géloën, A.; Estienne, M.; Capel, F.; Malpuech-Brugère, C.; Debard, C.; Pesenti, S.; Morio, B.; Vidal, H.; Rieusset, J.; Michalski, M.-C. High-Fat Diet Action on Adiposity, Inflammation, and Insulin Sensitivity Depends on the Control Low-Fat Diet. *Nutr Res* **2013**, *33* (11), 952–960. https://doi.org/10.1016/j.nutres.2013.07.017.
42. Guo, W. A.; Davidson, B. A.; Ottosen, J.; Ohtake, P. J.; Raghavendran, K.; Mullan, B. A.; Dayton, M. T.; Knight, P. R. Effect of High Advanced Glycation End Product Diet on Pulmonary Inflammatory Response and Pulmonary Function Following Gastric Aspiration. *Shock* **2012**, *38* (6), 677–684. https://doi.org/10.1097/SHK.0b013e318273982e.
43. Teissier, T.; Quersin, V.; Gnemmi, V.; Daroux, M.; Howsam, M.; Delguste, F.; Lemoine, C.; Fradin, C.; Schmidt, A.-M.; Cauffiez, C.; Brousseau, T.; Glowacki, F.; Tessier, F. J.; Boulanger, E.; Frimat, M. Knockout of Receptor for Advanced Glycation End-Products Attenuates Age-Related Renal Lesions. *Aging Cell* **2019**, *18* (2), e12850. https://doi.org/10.1111/acel.12850.
44. Leung, C.; Herath, C. B.; Jia, Z.; Goodwin, M.; Mak, K. Y.; Watt, M. J.; Forbes, J. M.; Angus, P. W. Dietary Glycotoxins Exacerbate Progression of Experimental Fatty Liver Disease. *J Hepatol* **2014**, *60* (4), 832–838. https://doi.org/10.1016/j.jhep.2013.11.033.
45. Tikellis, C.; Thomas, M. C.; Harcourt, B. E.; Coughlan, M. T.; Pete, J.; Bialkowski, K.; Tan, A.; Bierhaus, A.; Cooper, M. E.; Forbes, J. M. Cardiac Inflammation Associated with a Western Diet Is Mediated via Activation of RAGE by AGEs. *Am J Physiol Endocrinol Metab* **2008**, *295* (2), E323–E330. https://doi.org/10.1152/ajpendo.00024.2008.
46. Kim, K. A.; Gu, W.; Lee, I.-A.; Joh, E.-H.; Kim, D.-H. High Fat Diet-Induced Gut Microbiota Exacerbates Inflammation and Obesity in Mice via the TLR4 Signaling Pathway. *PLoS One* **2012**, *7* (10), e47713. https://doi.org/10.1371/journal.pone.0047713.
47. Tikellis, C.; Pickering, R. J.; Tsorotes, D.; Huet, O.; Cooper, M. E.; Jandeleit-Dahm, K.; Thomas, M. C. Dicarbonyl Stress in the Absence of Hyperglycemia Increases Endothelial Inflammation and Atherogenesis Similar to That Observed in Diabetes. *Diabetes* **2014**, *63* (11), 3915–3925. https://doi.org/10.2337/db13-0932.
48. Sowndhar Rajan, B.; Manivasagam, S.; Dhanusu, S.; Chandrasekar, N.; Krishna, K.; Kalaiarasu, L. P.; Babu, A. A.; Vellaichamy, E. Diet with High Content of Advanced Glycation End Products Induces Systemic Inflammation and Weight Gain in Experimental Mice: Protective Role of Curcumin and Gallic Acid. *Food Chem Toxicol* **2018**, *114*, 237–245. https://doi.org/10.1016/j.fct.2018.02.016.
49. Grossin, N.; Auger, F.; Niquet-Leridon, C.; Durieux, N.; Montaigne, D.; Schmidt, A. M.; Susen, S.; Jacolot, P.; Beuscart, J.-B.; Tessier, F. J.; Boulanger, E. Dietary CML-Enriched Protein Induces Functional Arterial Aging in a RAGE-Dependent Manner in Mice. *Mol Nutr Food Res* **2015**, *59* (5), 927–938. https://doi.org/10.1002/mnfr.201400643.

50. Cai, W.; He, J. C.; Zhu, L.; Chen, X.; Wallenstein, S.; Striker, G. E.; Vlassara, H. Reduced Oxidant Stress and Extended Lifespan in Mice Exposed to a Low Glycotoxin Diet. *Am J Pathol* **2007**, *170* (6), 1893–1902. https://doi.org/10.2353/ajpath.2007.061281.
51. Chatzigeorgiou, A.; Kandaraki, E.; Piperi, C.; Livadas, S.; Papavassiliou, A. G.; Koutsilieris, M.; Papalois, A.; Diamanti-Kandarakis, E. Dietary Glycotoxins Affect Scavenger Receptor Expression and the Hormonal Profile of Female Rats. *J Endocrinol* **2013**, *218* (3), 331–337. https://doi.org/10.1530/JOE-13-0175.
52. Guo, H.; Diao, N.; Yuan, R.; Chen, K.; Geng, S.; Li, M.; Li, L. Subclinical-Dose Endotoxin Sustains Low-Grade Inflammation and Exacerbates Steatohepatitis in High-Fat Diet–Fed Mice. *J Immunol* **2016**, *196* (5), 2300–2308. https://doi.org/10.4049/jimmunol.1500130.
53. Shangari, N.; Depeint, F.; Furrer, R.; Bruce, W. R.; Popovic, M.; Zheng, F.; O'Brien, P. J. A Thermolyzed Diet Increases Oxidative Stress, Plasma α-Aldehydes and Colonic Inflammation in the Rat. *Chem-Biol Interact* **2007**, *169* (2), 100–109. https://doi.org/10.1016/j.cbi.2007.05.009.
54. Feng, J. X.; Hou, F. F.; Liang, M.; Wang, G. B.; Zhang, X.; Li, H. Y.; Xie, D.; Tian, J. W.; Liu, Z. Q. Restricted Intake of Dietary Advanced Glycation End Products Retards Renal Progression in the Remnant Kidney Model. *Kidney Int* **2007**, *71* (9), 901–911. https://doi.org/10.1038/sj.ki.5002162.
55. Thornton, K.; Merhi, Z.; Jindal, S.; Goldsammler, M.; Charron, M. J.; Buyuk, E. Dietary Advanced Glycation End Products (AGEs) Could Alter Ovarian Function in Mice. *Mol Cell Endocrinol* **2020**, *510*, 110826. https://doi.org/10.1016/j.mce.2020.110826.
56. Chassaing, B.; Srinivasan, G.; Delgado, M. A.; Young, A. N.; Gewirtz, A. T.; Vijay-Kumar, M. Fecal Lipocalin 2, a Sensitive and Broadly Dynamic Non-Invasive Biomarker for Intestinal Inflammation. *PLOS ONE* **2012**, *7* (9), e44328. https://doi.org/10.1371/journal.pone.0044328.
57. Serino, M.; Luche, E.; Gres, S.; Baylac, A.; Bergé, M.; Cenac, C.; Waget, A.; Klopp, P.; Iacovoni, J.; Klopp, C.; Mariette, J.; Bouchez, O.; Lluch, J.; Ouarné, F.; Monsan, P.; Valet, P.; Roques, C.; Amar, J.; Bouloumié, A.; Théodorou, V.; Burcelin, R. Metabolic Adaptation to a High-Fat Diet Is Associated with a Change in the Gut Microbiota. *Gut* **2012**, *61* (4), 543–553. https://doi.org/10.1136/gutjnl-2011-301012.
58. Rorato, R.; Borges, B. de C.; Uchoa, E. T.; Antunes-Rodrigues, J.; Elias, C. F.; Elias, L. L. K. LPS-Induced Low-Grade Inflammation Increases Hypothalamic JNK Expression and Causes Central Insulin Resistance Irrespective of Body Weight Changes. *Int J Mol Sci* **2017**, *18* (7). https://doi.org/10.3390/ijms18071431.
59. Li, H.; Song, S.; Wang, Y.; Huang, C.; Zhang, F.; Liu, J.; Hong, J.-S. Low-Grade Inflammation Aggravates Rotenone Neurotoxicity and Disrupts Circadian Clock Gene Expression in Rats. *Neurotox Res* **2019**, *35* (2), 421–431. https://doi.org/10.1007/s12640-018-9968-1.
60. Zhu, Y.; Lan, F.; Wei, J.; Chong, B.; Chen, P.; Huynh, L.; Wong, N.; Liu, Y. Influence of Dietary Advanced Glycation End Products on Wound Healing in Nondiabetic Mice. *J Food Sci* **2011**, *76* (1), T5–T10. https://doi.org/10.1111/j.1750-3841.2010.01889.x.
61. Huang, C.-F.; Chiu, S.-Y.; Huang, H.-W.; Cheng, B.-H.; Pan, H.-M.; Huang, W.-L.; Chang, H.-H.; Liao, C.-C.; Jiang, S.-T.; Su, Y.-C. A Reporter Mouse for Non-Invasive Detection of Toll-like Receptor Ligands Induced Acute Phase Responses. *Sci Rep* **2019**, *9* (1), 19065. https://doi.org/10.1038/s41598-019-55281-w.
62. Takahashi, M. Glycation of Proteins. In *Glycoscience: Biology and Medicine*; Taniguchi, N., Endo, T., Hart, G. W., Seeberger, P. H., Wong, C.-H., Eds.; Springer Japan: Tokyo, 2015; pp 1339–1345. https://doi.org/10.1007/978-4-431-54841-6_182.
63. Rahbar, S. The Discovery of Glycated Hemoglobin: A Major Event in the Study of Nonenzymatic Chemistry in Biological Systems. *Ann NY Acad Sci* **2005**, *1043* (1), 9–19. https://doi.org/10.1196/annals.1333.002.
64. Brás, I. C.; König, A.; Outeiro, T. F. Glycation in Huntington's Disease: A Possible Modifier and Target for Intervention. *J Huntington's Disease* **2019**, *8* (3), 245–256. https://doi.org/10.3233/JHD-190366.
65. Chaudhuri, J.; Bains, Y.; Guha, S.; Kahn, A.; Hall, D.; Bose, N.; Gugliucci, A.; Kapahi, P. The Role of Advanced Glycation End Products in Aging and Metabolic Diseases: Bridging Association and Causality. *Cell Metab* **2018**, *28* (3), 337–352. https://doi.org/10.1016/j.cmet.2018.08.014.
66. Lin, L.; Park, S.; Lakatta, E. G. RAGE Signaling in Inflammation and Arterial Aging. *Front Biosci* **2009**, *14*, 1403–1413.

67. Kim, C.-S.; Park, S.; Kim, J. The Role of Glycation in the Pathogenesis of Aging and Its Prevention through Herbal Products and Physical Exercise. *J Exerc Nutr Biochem* **2017**, *21* (3), 55–61. https://doi.org/10.20463/jenb.2017.0027.
68. López-Otín, C.; Blasco, M. A.; Partridge, L.; Serrano, M.; Kroemer, G. The Hallmarks of Aging. *Cell* **2013**, *153* (6), 1194–1217. https://doi.org/10.1016/j.cell.2013.05.039.
69. Uribarri, J.; Cai, W.; Sandu, O.; Peppa, M.; Goldberg, T.; Vlassara, H. Diet-Derived Advanced Glycation End Products Are Major Contributors to the Body's AGE Pool and Induce Inflammation in Healthy Subjects. *Ann N Y Acad Sci* **2005**, *1043*, 461–466. https://doi.org/10.1196/annals.1333.052.
70. Bekedam, E. K.; Schols, H. A.; van Boekel, M. A. J. S.; Smit, G. High Molecular Weight Melanoidins from Coffee Brew. *J Agric Food Chem* **2006**, *54* (20), 7658–7666. https://doi.org/10.1021/jf0615449.
71. Hellwig, M.; Henle, T. Baking, Ageing, Diabetes: A Short History of the Maillard Reaction. *Angew Chem Int Ed Engl* **2014**, *53* (39), 10316–10329. https://doi.org/10.1002/anie.201308808.
72. Nguyen, H. T.; Fels-Klerx, H. J. van der; Boekel, M. A. J. S. van. N ϵ-(Carboxymethyl)Lysine: A Review on Analytical Methods, Formation, and Occurrence in Processed Food, and Health Impact. *Food Rev Int* **2014**, *30* (1), 36–52. https://doi.org/10.1080/87559129.2013.853774.
73. Tessier, F. J.; Birlouez-Aragon, I. Health Effects of Dietary Maillard Reaction Products: The Results of ICARE and Other Studies. *Amino Acids* **2012**, *42* (4), 1119–1131. https://doi.org/10.1007/s00726-010-0776-z.
74. van Dongen, K. C. W.; Linkens, A. M. A.; Wetzels, S. M. W.; Wouters, K.; Vanmierlo, T.; van de Waarenburg, M. P. H.; Scheijen, J. L. J. M.; de Vos, W. M.; Belzer, C.; Schalkwijk, C. G. Dietary Advanced Glycation Endproducts (AGEs) Increase Their Concentration in Plasma and Tissues, Result in Inflammation and Modulate Gut Microbial Composition in Mice; Evidence for Reversibility. *Food Res Int* **2021**, *147*, 110547. https://doi.org/10.1016/j.foodres.2021.110547.
75. Snelson, M.; Tan, S. M.; Clarke, R. E.; de Pasquale, C.; Thallas-Bonke, V.; Nguyen, T.-V.; Penfold, S. A.; Harcourt, B. E.; Sourris, K. C.; Lindblom, R. S.; Ziemann, M.; Steer, D.; El-Osta, A.; Davies, M. J.; Donnellan, L.; Deo, P.; Kellow, N. J.; Cooper, M. E.; Woodruff, T. M.; Mackay, C. R.; Forbes, J. M.; Coughlan, M. T. Processed Foods Drive Intestinal Barrier Permeability and Microvascular Diseases. *Sci Adv* **2021**, *7* (14), eabe4841. https://doi.org/10.1126/sciadv.abe4841.
76. Qu, W.; Yuan, X.; Zhao, J.; Zhang, Y.; Hu, J.; Wang, J.; Li, J. Dietary Advanced Glycation End Products Modify Gut Microbial Composition and Partially Increase Colon Permeability in Rats. *Molecular Nutrition & Food Research* **2017**, *61* (10), 1700118. https://doi.org/10.1002/mnfr.201700118.
77. Seiquer, I.; Rubio, L. A.; Peinado, M. J.; Delgado-Andrade, C.; Navarro, M. P. Maillard Reaction Products Modulate Gut Microbiota Composition in Adolescents. *Mol Nutr Food Res* **2014**, *58* (7), 1552–1560. https://doi.org/10.1002/mnfr.201300847.
78. Delgado-Andrade, C.; Pastoriza de la Cueva, S.; Peinado, M. J.; Rufián-Henares, J. Á.; Navarro, M. P.; Rubio, L. A. Modifications in Bacterial Groups and Short Chain Fatty Acid Production in the Gut of Healthy Adult Rats after Long-Term Consumption of Dietary Maillard Reaction Products. *Food Res Int* **2017**, *100*, 134–142. https://doi.org/10.1016/j.foodres.2017.06.067.
79. Patel, R.; Baker, S. S.; Liu, W.; Desai, S.; Alkhouri, R.; Kozielski, R.; Mastrandrea, L.; Sarfraz, A.; Cai, W.; Vlassara, H.; Patel, M. S.; Baker, R. D.; Zhu, L. Effect of Dietary Advanced Glycation End Products on Mouse Liver. *PLoS One* **2012**, *7* (4). https://doi.org/10.1371/journal.pone.0035143.
80. Harcourt, B. E.; Sourris, K. C.; Coughlan, M. T.; Walker, K. Z.; Dougherty, S. L.; Andrikopoulos, S.; Morley, A. L.; Thallas-Bonke, V.; Chand, V.; Penfold, S. A.; de Courten, M. P. J.; Thomas, M. C.; Kingwell, B. A.; Bierhaus, A.; Cooper, M. E.; Courten, B. de; Forbes, J. M. Targeted Reduction of Advanced Glycation Improves Renal Function in Obesity. *Kidney Int* **2011**, *80* (2), 190–198. https://doi.org/10.1038/ki.2011.57.
81. Lin, R. Y.; Choudhury, R. P.; Cai, W.; Lu, M.; Fallon, J. T.; Fisher, E. A.; Vlassara, H. Dietary Glycotoxins Promote Diabetic Atherosclerosis in Apolipoprotein E-Deficient Mice. *Atherosclerosis* **2003**, *168* (2), 213–220. https://doi.org/10.1016/S0021-9150(03)00050-9.
82. Peppa, M.; Brem, H.; Ehrlich, P.; Zhang, J.-G.; Cai, W.; Li, Z.; Croitoru, A.; Thung, S.; Vlassara, H. Adverse Effects of Dietary Glycotoxins on Wound Healing in Genetically

Diabetic Mice. *Diabetes* **2003**, *52* (11), 2805–2813. https://doi.org/10.2337/diabetes.52.11.2805.
83. Alexiou, P.; Chatzopoulou, M.; Pegklidou, K.; Demopoulos, V. J. RAGE: A Multi-Ligand Receptor Unveiling Novel Insights in Health and Disease. *Curr Med Chem* **2010**, *17* (21), 2232–2252. https://doi.org/10.2174/092986710791331086.
84. Boulanger, E.; Grossin, N.; Wautier, M.-P.; Taamma, R.; Wautier, J.-L. Mesothelial RAGE Activation by AGEs Enhances VEGF Release and Potentiates Capillary Tube Formation. *Kidney Int* **2007**, *71* (2), 126–133. https://doi.org/10.1038/sj.ki.5002016.
85. Toprak, C.; Yigitaslan, S. Alagebrium and Complications of Diabetes Mellitus. *Eurasian J Med* **2019**, *51* (3), 285–292. https://doi.org/10.5152/eurasianjmed.2019.18434.
86. Goldsammler, M.; Merhi, Z.; Thornton, K.; Charron, M. J.; Buyuk, E. Ovarian Rage Expression Changes with Follicular Development and Superovulation. *Fertil Steril* **2018**, *110* (4), e122. https://doi.org/10.1016/j.fertnstert.2018.07.366.
87. Tessier, F. J.; Niquet-Léridon, C.; Jacolot, P.; Jouquand, C.; Genin, M.; Schmidt, A.-M.; Grossin, N.; Boulanger, E. Quantitative Assessment of Organ Distribution of Dietary Protein-Bound 13 C-Labeled Nε -Carboxymethyllysine after a Chronic Oral Exposure in Mice. *Mol Nutr Food Res* **2016**, *60* (11), 2446–2456. https://doi.org/10.1002/mnfr.201600140.
88. Oczypok, E. A.; Perkins, T. N.; Oury, T. D. All the “RAGE” in Lung Disease: The Receptor for Advanced Glycation Endproducts (RAGE) Is a Major Mediator of Pulmonary Inflammatory Responses. *Paediatr Respir Rev* **2017**, *23*, 40–49. https://doi.org/10.1016/j.prrv.2017.03.012.
89. Sanders, K. A.; Delker, D. A.; Huecksteadt, T.; Beck, E.; Wuren, T.; Chen, Y.; Zhang, Y.; Hazel, M. W.; Hoidal, J. R. RAGE Is a Critical Mediator of Pulmonary Oxidative Stress, Alveolar Macrophage Activation and Emphysema in Response to Cigarette Smoke. *Sci Rep* **2019**, *9* (1), 231. https://doi.org/10.1038/s41598-018-36163-z.
90. van Putte, L.; De Schrijver, S.; Moortgat, P. The Effects of Advanced Glycation End Products (AGEs) on Dermal Wound Healing and Scar Formation: A Systematic Review. *Scars Burn Heal* **2016**, *2*. https://doi.org/10.1177/2059513116676828.
91. Ellulu, M. S.; Patimah, I.; Khaza’ai, H.; Rahmat, A.; Abed, Y. Obesity and Inflammation: The Linking Mechanism and the Complications. *Arch Med Sci* **2017**, *13* (4), 851–863. https://doi.org/10.5114/aoms.2016.58928.
92. Kim, J.; Nam, J.-H. Insight into the Relationship between Obesity-Induced Low-Level Chronic Inflammation and COVID-19 Infection. *Int J Obesity* **2020**, *44* (7), 1541–1542. https://doi.org/10.1038/s41366-020-0602-y.
93. Gregor, M. F.; Hotamisligil, G. S. Inflammatory Mechanisms in Obesity. *Ann. Rev Immuno.* **2011**, *29* (1), 415–445. https://doi.org/10.1146/annurev-immunol-031210-101322.
94. Castro, A. M.; Macedo-de la Concha, L. E.; Pantoja-Meléndez, C. A. Low-Grade Inflammation and Its Relation to Obesity and Chronic Degenerative Diseases. *Revista Médica del Hospital General de México* **2017**, *80* (2), 101–105. https://doi.org/10.1016/j.hgmx.2016.06.011.
95. Wang, J.; Chen, W.-D.; Wang, Y.-D. The Relationship Between Gut Microbiota and Inflammatory Diseases: The Role of Macrophages. *Front Microbiol* **2020**, *11*. https://doi.org/10.3389/fmicb.2020.01065.
96. Wang, Y.; Qi, W.; Song, G.; Pang, S.; Peng, Z.; Li, Y.; Wang, P. High-Fructose Diet Increases Inflammatory Cytokines and Alters Gut Microbiota Composition in Rats. *Med Inflamm* **2020**, *2020*, e6672636. https://doi.org/10.1155/2020/6672636.
97. Powell-Wiley, T. M.; Poirier, P.; Burke, L. E.; Després, J. P.; Gordon-Larsen, P.; Lavie, C. J.; Lear, Sc. A.; Ndumele, C. E.; Neeland, I. J.; Sanders, P.; St-Onge, M. P. Obesity and Cardiovascular Disease: A Scientific Statement From the American Heart Association. *Circulation **2021***, 143:e984–e1010. https://doi.org/10.1161/CIR.0000000000000973.
98. Weinstock, A.; Moura, S.H.; Moore, K.J.; Schmidt, A.M.; Fisher, E.A. Leukocyte Heterogeneity in Adipose Tissue, Including in Obesity. *Circ Res* **2020**, *126* (11), 1590–1612. https://doi.org/10.1161/CIRCRESAHA.120.316203.
99. Eguchi, A.; Feldstein, A. E. Adipocyte Cell Death, Fatty Liver Disease and Associated Metabolic Disorders. *Dig Dis* **2014**, *32* (5), 579–585. https://doi.org/10.1159/000360509.
100. Cinti, S.; Mitchell, G.; Barbatelli, G.; Murano, I.; Ceresi, E.; Faloia, E.; Wang, S.; Fortier, M.; Greenberg, A. S.; Obin, M. S. Adipocyte Death Defines Macrophage Localization and Function in Adipose Tissue of Obese Mice and Humans. *J Lipid Res* **2005**, *46* (11), 2347–2355. https://doi.org/10.1194/jlr.M500294-JLR200.

101. Weisberg, S. P.; McCann, D.; Desai, M.; Rosenbaum, M.; Leibel, R. L.; Ferrante, A. W. Obesity Is Associated with Macrophage Accumulation in Adipose Tissue. *J Clin Invest* **2003**, *112* (12), 1796–1808. https://doi.org/10.1172/JCI19246.
102. Öhman, M. K.; Wright, A. P.; Wickenheiser, K. J.; Luo, W.; Russo, H. M.; Eitzman, D. T. Mcp-1 Deficiency Protects Against Visceral Fat-Induced Atherosclerosis. *Arterioscler Thromb Vasc Biol* **2010**, *30* (6), 1151–1158. https://doi.org/10.1161/ATVBAHA.110.205914.
103. Subramanian, V.; Ferrante, Jr., A. W. Obesity, Inflammation, and Macrophages. In *Nestlé Nutrition Institute Workshop Series: Pediatric Program*; Kalhan, S. C., Prentice, A. M., Yajnik, C. S., Eds.; KARGER: *Basel*, **2009**, 63, 151–162. https://doi.org/10.1159/000209979.
104. Ahima, R. S.; Antwi, D. A. Brain Regulation of Appetite and Satiety. *Endocrinol Metab Clin North Am* **2008**, *37* (4), 811–823. https://doi.org/10.1016/j.ecl.2008.08.005.
105. Stern, J. H.; Rutkowski, J. M.; Scherer, P. E. Adiponectin, Leptin, and Fatty Acids in the Maintenance of Metabolic Homeostasis Through Adipose Tissue Crosstalk. *Cell Metab* **2016**, *23* (5), 770–784. https://doi.org/10.1016/j.cmet.2016.04.011.
106. Arroyo-Espliguero, R.; Avanzas, P.; Jeffery, S.; Kaski, J. C. CD14 and Toll-like Receptor 4: A Link between Infection and Acute Coronary Events? *Heart* **2004**, *90* (9), 983–988. https://doi.org/10.1136/hrt.2002.001297.
107. Takiishi, T.; Fenero, C. I. M.; Câmara, N. O. S. Intestinal Barrier and Gut Microbiota: Shaping Our Immune Responses throughout Life. *Tissue Barriers* **2017**, *5* (4). https://doi.org/10.1080/21688370.2017.1373208.
108. Putignani, L.; Del Chierico, F.; Petrucca, A.; Vernocchi, P.; Dallapiccola, B. The Human Gut Microbiota: A Dynamic Interplay with the Host from Birth to Senescence Settled during Childhood. *Pediatr Res* **2014**, *76* (1), 2–10. https://doi.org/10.1038/pr.2014.49.
109. Chin, V. K.; Yong, V. C.; Chong, P. P.; Amin Nordin, S.; Basir, R.; Abdullah, M. Mycobiome in the Gut: A Multiperspective Review. *Med Inflamm* **2020**, *2020*, e9560684. https://doi.org/10.1155/2020/9560684.
110. Mariat, D.; Firmesse, O.; Levenez, F.; Guimarăes, V.; Sokol, H.; Doré, J.; Corthier, G.; Furet, J.-P. The Firmicutes/Bacteroidetes Ratio of the Human Microbiota Changes with Age. *BMC Microbiol* **2009**, *9* (1), 123. https://doi.org/10.1186/1471-2180-9-123.
111. Flint, H. J.; Duncan, S. H.; Scott, K. P.; Louis, P. Links between Diet, Gut Microbiota Composition and Gut Metabolism. *P Nutr Soc* **2015**, *74* (1), 13–22. https://doi.org/10.1017/S0029665114001463.
112. Nguyen, T.L.A.; Vieira-Silva, S.; Liston, A.; Raes, J. How Informative Is the Mouse for Human Gut Microbiota Research? *Dis Model Mech* **2015**, *8* (1), 1–16. https://doi.org/10.1242/dmm.017400.
113. Vital, M.; Howe, A. C.; Tiedje, J. M. Revealing the Bacterial Butyrate Synthesis Pathways by Analyzing (Meta)Genomic Data. *mBio* **2014**, *5* (2). https://doi.org/10.1128/mBio.00889-14.
114. Turnbaugh, P. J.; Ley, R. E.; Mahowald, M. A.; Magrini, V.; Mardis, E. R.; Gordon, J. I. An Obesity-Associated Gut Microbiome with Increased Capacity for Energy Harvest. *Nature* **2006**, *444* (7122), 1027–1031. https://doi.org/10.1038/nature05414.
115. Cani, P. D.; Bibiloni, R.; Knauf, C.; Waget, A.; Neyrinck, A. M.; Delzenne, N. M.; Burcelin, R. Changes in Gut Microbiota Control Metabolic Endotoxemia-Induced Inflammation in High-Fat Diet–Induced Obesity and Diabetes in Mice. *Diabetes* **2008**, *57* (6), 1470–1481. https://doi.org/10.2337/db07-1403.
116. Singh, R.P.; Halaka, D.A.; Hayouka, Z.; Tirosh, O. High-Fat Diet Induced Alteration of Mice Microbiota and the Functional Ability to Utilize Fructooligosaccharide for Ethanol Production. *Front Cell Infect Microbiol* **2020**, *10*. https://doi.org/10.3389/fcimb.2020.00376.
117. Moreira, A. P. B.; Texeira, T. F. S.; Ferreira, A. B.; Peluzio, M. do C. G.; Alfenas, R. de C. G. Influence of a High-Fat Diet on Gut Microbiota, Intestinal Permeability and Metabolic Endotoxaemia. *Brit J Nutr* **2012**, *108* (5), 801–809. https://doi.org/10.1017/S0007114512001213.
118. Wang, L.; Wu, J.; Guo, X.; Huang, X.; Huang, Q. RAGE Plays a Role in LPS-Induced NF-KB Activation and Endothelial Hyperpermeability. *Sensors (Basel)* **2017**, *17* (4). https://doi.org/10.3390/s17040722.
119. Magne, F.; Gotteland, M.; Gauthier, L.; Zazueta, A.; Pesoa, S.; Navarrete, P.; Balamurugan, R. The Firmicutes/Bacteroidetes Ratio: A Relevant Marker of Gut Dysbiosis in Obese Patients? *Nutrients* **2020**, *12* (5). https://doi.org/10.3390/nu12051474.

120. Geng, S.; Chen, K.; Yuan, R.; Peng, L.; Maitra, U.; Diao, N.; Chen, C.; Zhang, Y.; Hu, Y.; Qi, C.-F.; Pierce, S.; Ling, W.; Xiong, H.; Li, L. The Persistence of Low-Grade Inflammatory Monocytes Contributes to Aggravated Atherosclerosis. *Nature Comm* **2016**, *7* (1), 13436. https://doi.org/10.1038/ncomms13436.
121. Amar, J.; Burcelin, R.; Ruidavets, J. B.; Cani, P. D.; Fauvel, J.; Alessi, M. C.; Chamontin, B.; Ferriéres, J. Energy Intake Is Associated with Endotoxemia in Apparently Healthy Men. *Am J Clin Nutr* **2008**, *87* (5), 1219–1223. https://doi.org/10.1093/ajcn/87.5.1219.
122. Ding, S.; Chi, M. M.; Scull, B. P.; Rigby, R.; Schwerbrock, N. M. J.; Magness, S.; Jobin, C.; Lund, P. K. High-Fat Diet: Bacteria Interactions Promote Intestinal Inflammation Which Precedes and Correlates with Obesity and Insulin Resistance in Mouse. *PLOS ONE* **2010**, *5* (8), e12191. https://doi.org/10.1371/journal.pone.0012191.
123. Chakraborti, C. K. New-Found Link between Microbiota and Obesity. *World J Gastrointest Pathophysiol* **2015**, *6* (4), 110–119. https://doi.org/10.4291/wjgp.v6.i4.110.
124. Bridgeman, S.C.; Northrop, W.; Melton, P. E.; Ellison, G. C.; Newsholme, P.; Mamotte, C. D. S. Butyrate Generated by Gut Microbiota and Its Therapeutic Role in Metabolic Syndrome. *Pharm Res* **2020**, *160*, 105174. https://doi.org/10.1016/j.phrs.2020.105174.
125. Daniel, H.; Gholami, A. M.; Berry, D.; Desmarchelier, C.; Hahne, H.; Loh, G.; Mondot, S.; Lepage, P.; Rothballer, M.; Walker, A.; Böhm, C.; Wenning, M.; Wagner, M.; Blaut, M.; Schmitt-Kopplin, P.; Kuster, B.; Haller, D.; Clavel, T. High-Fat Diet Alters Gut Microbiota Physiology in Mice. *ISME J* **2014**, *8* (2), 295–308. https://doi.org/10.1038/ismej.2013.155.
126. Rohr, M. W.; Narasimhulu, C. A.; Rudeski-Rohr, T. A.; Parthasarathy, S. Negative Effects of a High-Fat Diet on Intestinal Permeability: A Review. *Adv Nutr* **2020**, *11* (1), 77–91. https://doi.org/10.1093/advances/nmz061.
127. Al-Sadi, R.; Guo, S.; Dokladny, K.; Smith, M. A.; Ye, D.; Kaza, A.; Watterson, D. M.; Ma, T. Y. Mechanism of Interleukin-1β Induced-Increase in Mouse Intestinal Permeability In Vivo. *J Interferon Cytokine Res* **2012**, *32* (10), 474–484. https://doi.org/10.1089/jir.2012.0031.
128. Shi, C.; Li, H.; Qu, X.; Huang, L.; Kong, C.; Qin, H.; Sun, Z.; Yan, X. High Fat Diet Exacerbates Intestinal Barrier Dysfunction and Changes Gut Microbiota in Intestinal-Specific ACF7 Knockout Mice. *Biom Pharm* **2019**, *110*, 537–545. https://doi.org/10.1016/j.biopha.2018.11.100.
129. Oliveira, R. B.; Canuto, L. P.; Collares-Buzato, C. B. Intestinal Luminal Content from High-Fat-Fed Prediabetic Mice Changes Epithelial Barrier Function in Vitro. *Life Sci* **2019**, *216*, 10–21. https://doi.org/10.1016/j.lfs.2018.11.012.
130. Willenberg, I.; Rund, K.; Rong, S.; Shushakova, N.; Gueler, F.; Schebb, N. H. Characterization of Changes in Plasma and Tissue Oxylipin Levels in LPS and CLP Induced Murine Sepsis. *Inflamm Res* **2016**, *65* (2), 133–142. https://doi.org/10.1007/s00011-015-0897-7.
131. Maitra, U.; Deng, H.; Glaros, T.; Baker, B.; Capelluto, D. G. S.; Li, Z.; Li, L. Molecular Mechanisms Responsible for the Selective and Low-Grade Induction of Proinflammatory Mediators in Murine Macrophages by Lipopolysaccharide. *J Immunol* **2012**, *189* (2), 1014–1023. https://doi.org/10.4049/jimmunol.1200857.
132. Solinas, G.; Becattini, B. JNK at the Crossroad of Obesity, Insulin Resistance, and Cell Stress Response. *Mol Metab* **2016**, *6* (2), 174–184. https://doi.org/10.1016/j.molmet.2016.12.001.
133. Moschen, A. R.; Adolph, T. E.; Gerner, R. R.; Wieser, V.; Tilg, H. Lipocalin-2: A Master Mediator of Intestinal and Metabolic Inflammation. *Trends Endocrinol Metab* **2017**, *28* (5), 388–397. https://doi.org/10.1016/j.tem.2017.01.003.
134. Castillo, M. D. del; Iriondo-DeHond, A.; Iriondo-DeHond, M.; Gonzalez, I.; Medrano, A.; Filip, R.; Uribarri, J. Healthy Eating Recommendations: Good for Reducing Dietary Contribution to the Body's Advanced Glycation/Lipoxidation End Products Pool? *Nutr Res Rev* **2021**, *34* (1), 48–63. https://doi.org/10.1017/S0954422420000141.
135. Joung, H.; Chu, J.; Kim, B.-K.; Choi, I.-S.; Kim, W.; Park, T.-S. Probiotics Ameliorate Chronic Low-Grade Inflammation and Fat Accumulation with Gut Microbiota Composition Change in Diet-Induced Obese Mice Models. *Appl Microbiol Biotechnol* **2021**, *105* (3), 1203–1213. https://doi.org/10.1007/s00253-020-11060-6.
136. Cunha, C.A.; Lira, F.S.; Rosa Neto, J.C.; Pimentel, G.D.; Souza, G.I.H.; da Silva, C.M.G.; de Souza, C.T.; Ribeiro, E.B.; Sawaya, A. C.H.F.; Oller do Nascimento, C.M.; Rodrigues, B.; de Oliveira Carvalho, P.; Oyama, L.M. Green Tea Extract Supplementation Induces the Lipolytic Pathway, Attenuates Obesity, and Reduces Low-Grade Inflammation in Mice Fed a High-Fat Diet. *Med inflamm* 2013, 635470. https://doi.org/10.1155/2013/635470.

137. Heyman-Lindén, L.; Kotowska, D.; Sand, E.; Bjursell, M.; Plaza, M.; Turner, C.; Holm, C.; Fåk, F.; Berger, K. Lingonberries Alter the Gut Microbiota and Prevent Low-Grade Inflammation in High-Fat Diet Fed Mice. *Food Nutr Res* **2016**, *60* (1), 29993. https://doi.org/10.3402/fnr.v60.29993.

CHAPTER 4

Plasma levels of free N^{ε}-carboxymethyllysine (CML) after different oral doses of CML in rats and after the intake of different breakfasts in humans. Postprandial plasma level of sRAGE in humans

Cynthia Helou[1], Matheus Thomaz Nogueira Silva Lima[2], Céline Niquet-Leridon[3], Philippe Jacolot[3], Eric Boulanger[2], Florian Delguste[2], Axel Guilbaud[2], Michael Genin[4], Pauline M. Anton[3], Carine Delayre-Orthez[3], Tatiana Papazian[1], Michael Howsam[2] and Frédéric J Tessier[2,*]

1 Saint Joseph University of Beirut, Faculty of Pharmacy, Department of Nutrition, Beirut, Lebanon; cynthia.helou@usj.edu.lb (C.H.); tatiana.wahanian@usj.edu.lb (T.P.)

2 University Lille, Inserm, CHU Lille, Institut Pasteur de Lille, U1167—RID—AGE—Facteurs de Risque et Déterminants Moléculaires des Maladies Liées au Vieillissement, F-59000 Lille, France; matheustho-maz.nogueirasilvalima@univ-lille.fr (M.T.N.S.L.); eric.boulanger@univ-lille.fr (E.B.); florian.delguste@gmail.com (F.D.); axel.guilbaud@gmail.com (A.G.); michael.howsam@univ-lille.fr (M.H.) ; frederic.tessier@univ-lille.fr (F.J.T.)

3 Institut Polytechnique UniLaSalle, Université d'Artois, ULR 7519, Equipe PETALES, F-60026 Beauvais, France; celine.leridon@unilasalle.fr (C.N.-L.); philipe.jacolot@unilasalle.fr (P.J.); pauline.anton@unilasalle.fr (P.M.A.); carine.delayre@unilasalle.fr (C.D.-O.)

4 Univ. Lille, CHU Lille, ULR 2694 - METRICS : Évaluation des technologies de santé et des pratiques médicales, F-59000 Lille, France ; michael.genin@univ-lille.fr (M.G.)

* Correspondence: frederic.tessier@univ-lille.fr; Tel.: 33 (0)3 20 62 35 61

This review article has been published in Nutrients (MDPI):

Helou C, Nogueira Silva Lima MT, Niquet-Leridon C, Jacolot P, Boulanger E, Delguste F, Guilbaud A, Genin M, Anton PM, Delayre-Orthez C, Papazian T, Howsam M, Tessier FJ. Plasma Levels of Free Nε-Carboxymethyllysine (CML) after Different Oral Doses of CML in Rats and after the Intake of Different Breakfasts in Humans: Postprandial Plasma Level of sRAGE in Humans. Nutrients. 2022 Apr 30;14(9):1890. doi: 10.3390/nu14091890. PMID: 35565855; PMCID: PMC9101122.

ABSTRACT

N-carboxymethyl-lysine (CML) and other dietary advanced glycation end-products (AGEs) are chemically modified amino acids with potential toxicological effects putatively related to their affinity with the receptor for AGEs (RAGE). The goal of this study was to determine the postprandial kinetics of CML in both rodents and humans and, in the latter, to evaluate their relationship with the soluble RAGE isoforms (sRAGE). Four gavage solutions containing different forms of CML were given to rats and blood collected over 8h. Three different breakfasts containing dietary CML (dCML) were administered to 20 healthy volunteers and blood was collected over 2h. Concentrations of CML, CEL and lysine were quantified in plasma and in human meals by LC-MS/MS, and sRAGE was determined in human plasma by ELISA. The results showed that dCML did not affect the concentrations of circulating protein-bound CML and that only free CML increased in plasma, with a postprandial peak at 90 to 120 min. In humans, the postprandial plasmatic sRAGE concentration decreased in a manner independent of the dAGE content of the breakfasts. This study confirms reports of the inverse postprandial relationship between plasmatic free CML and sRAGE, though this requires further investigation for causality to be established.

Keywords: glycation, Maillard reaction, carboxymethyllysine, carboxyethyllysine, lysine, sRAGE

1 Introduction

Chemical reactions occur between the constituents of foods during domestic and industrial processing, as well as during storage. While these reactions can have beneficial effects on the aroma, taste, and appearance of foods, they are also responsible for the degradation of some nutrients [1].

When proteins are involved, one of the main chemical reactions responsible for modifying the side chain of some amino acids is the Maillard reaction, also referred to as “glycation”. This reaction leads to the covalent attachment of reducing sugars and other carbonyl and dicarbonyl compounds to some reactive amino acids such as lysine and arginine [2].

Advanced glycation end-products in the diet (dAGEs) are among the heterogeneous group of Maillard reaction products (MRPs) formed by chemical rearrangements which follow the initial binding of the sugar moiety to amino acids, some of which result in organoleptic improvements of food while others are widely studied for their potential negative impacts on health [2,3]. Most dAGEs found in foodstuffs are non-physiological amino acids that cannot be used as sources of amino acids for protein anabolism in vivo. In addition to this reduction

of dietary amino acid availability and, more generally, to the impairment of the nutritional quality of heated proteins, the metabolic transit and the potential toxicological effects of dAGEs have been subjects of concern for more than 4 decades [4,5]. N-carboxymethyl-lysine (CML) was the first dAGE identified in food, human tissues, and urine [5]. The precise rate of its absorption into the bloodstream, the subsequent distribution and clearance of dietary CML (dCML) from different foods remain ill-defined; however, despite several recent studies of its bioavailability and postprandial kinetics. dCML is largely studied not only because it is considered a good model for the metabolic transit and biological effects of dAGEs, but also because of its relatively high abundance in foods. Different food groups have been analyzed to estimate their contribution to dCML intake, and it has been reported that bakery products are among its major sources [3,6].

Using an in vitro model of human intestinal absorption, it has been found that dAGEs are absorbed in their dipeptide form, presumably via the intestinal peptide co-transporter PepT1 [7]. After intracellular hydrolysis of peptide bonds, free glycated amino acids such as dCML were reportedly released into the in vitro equivalent to the systemic circulation.

This observation agrees with our preliminary data on the postprandial changes in plasma CML concentrations in rats. After an oral intake of food rich in dCML, free CML increased quickly in plasma, whereas protein-bound CML remained unaffected by the dCML intake [8].

Here, we build upon this earlier study and contribute to the understanding of the postprandial kinetics of dCML in both rodents and humans. We measured the changes in plasma CML in rats after receiving four different forms of dCML and in healthy human volunteers after receiving three different breakfasts. In addition, in the human plasma samples, we also measured the changes in soluble RAGE (sRAGE) concentrations, the Receptor for Advanced Glycation End-products being widely considered to be that with which AGEs principally interact.

2 Materials and methods

2.1. Chemicals and materials

Ultra-pure HPLC water was from VWR (Fontenay-sous-Bois, France), HPLC gradient grade acetonitrile, nonafluoropentanoic acid (NFPA) 97%, hydrochloric acid (HCl) 37%, sodium borohydride (NaBH4), boric acid (H_3BO_3) and sodium hydroxide (NaOH), trichlo-roacetic acid (TCA), lysine (Lys), bovine serum albumin (BSA fraction V), glyoxylic acid and sodium cyanoborohydride ($NaBH_3CN$) were all obtained from Sigma–Aldrich (Saint-Quentin-Fallavier, France). The labeled internal standard ($^{15}N_2$)-Lys was purchased from CortecNet (Voisins-le-Bretonneux, France), while CML, (D2)-CML, (D4)-CML, CEL, and (D4)-CEL were all from Polypeptide Group Laboratories (Strasbourg, France). A 0.1 M NaBH4 solution was made up of a 0.2 M borate buffer comprised of (H_3BO_3) and NaOH (pH = 9.5).

2.2. Preparation of the CML-enriched BSA (CML-BSA)

CML-enriched bovine serum albumin (CML-BSA) was prepared as previously described [9]. Briefly, BSA faction V was incubated with glyoxylic acid (60 mM) in phosphate buffer (200 mM, pH 7.4) at 37 °C for 20 h. After 2 h of incubation, NaBH3CN (450 mM) was added to the solution. After incubation, the preparation was dialyzed at 4 °C against phosphate buffer (200 mM, pH 7.4). The dialyzed preparation was lyophilized, and the dried powder was stored in an air-tight container at −20 °C until analysis and utilization in the animal study. The CML-BSA contained 78.1 ± 4.0 mg CML/g BSA.

2.3. Single oral dose studies of free CML, Free (D2)-CML, CML-BSA, and free CML + BSA in rats

One hundred and twenty male Wistar rats (200–224 g–8 weeks old) from Harlan L-boratories (Ganat, France) were housed in stainless steel cages under controlled temperature (21 ± 1 °C) and a 12 h light-dark cycle. During the first week (adaptation period), all rats received A04 pellets (Safe, Augy, France) and water ad libitum. At the end of the adaptation period, rats were divided into four groups of 30. The first group received a single oral dose of free CML solution (410 µg/rat; 1.48 mg/kg BW); the second a dose of free D2-CML solution (520 µg/rat; 1.78 mg/kg BW); the third a dose of CML-BSA solution (415 µg/rat; 1.43 mg/kg BW); and the last group received a dose of the free CML + BSA solution mix (491 µg/rat; 1.60 mg/kg BW). Six rats per group were sacrificed 0, 1, 2, 5, and 8 h after gavage, and blood (2 mL/animal) was collected. At the given time point, rats were anesthetized with an intraperitoneal injection of a mixture of ketamine and xylazine (50% v/v), 100 mg/mL) diluted in saline at a dose of 1 mL/kg. This experiment was conducted at the animal house unit of the Institut Polytechnique LaSalle Beauvais (LaSalle facilities agreement number C60-200-001,) and received prior approval from both the local animal protocol review committee (CEEA n°116) and the French Ministry of Education (MENESR, n°03530.V02).

2.4. Human intervention study

2.4.1. Study design and participants

In this longitudinal crossover study, twenty healthy individuals received three test meals with a 7-day washout period in-between. The test meals were breakfasts inspired by Mediterranean and Westernized diets and included a regular and a grilled version of the latter. For practical reasons, all participants received the breakfasts in the same order, and participants were also kept ignorant of the meals' contents until consumption.

Participants were recruited according to the following inclusion criteria: age between 18 and 30 years, a body mass index (BMI) between 20 and 25 kg/m2, a waist circumference below 80 cm for women and 94 cm for men, a systolic blood pressure ≤ 130 mm Hg and diastolic blood pressure ≤ 85 mm Hg, and normal fasting plasma glucose, triglycerides and cholesterol levels. Subjects were considered ineligible if they suffered from a chronic disease (*e.g.,* type 1 or 2 diabetes, cancer,

cardiovascular disease), were smokers, used medication regularly, reported more than 4 h of physical activity per week, had bariatric surgery, or, for female participants, were pregnant or breastfeeding.

During the screening visit, anthropometric measurements (weight, height, waist circumference, body fat composition) and blood pressure were recorded. A medical history questionnaire, as well as a food frequency questionnaire and a 24-h dietary recall, were completed by the research team during a face-to-face interview. Prior to enrollment, all selected participants gave written, informed consent. The protocol of this study was approved by the ethical committee of Saint-Joseph University of Beirut, Lebanon (FPH58/2017).

2.4.2. Study protocol

Throughout the study period, participants were instructed not to consume fried, grilled, or roasted foods and to refrain from intense physical activity and alcohol consumption. On the evenings before the test days, they were requested to consume their dinner no later than 20h00, though water intake was permitted until midnight. Subjects arrived on the test days with minimal physical effort. A blood sample was drawn at baseline (0 min) to assess the fasting levels of the studied biochemical markers. Then, the participants had 15 min to consume the test meals. Three other blood samples were then taken at 45, 90, and 120 min following the first bite from the test meals.

2.4.3. Test Meals

The three meals assessed during this study had similar caloric values but differed in macronutrient content. Methods corresponding to the analysis of caloric content, fat, carbohydrates, protein, ash, moisture, minerals, and vitamins in each tested breakfast are properly indicated in Supplemental Table S1. The Mediterranean-inspired breakfast (MB) consisted of 65 g whole wheat pita bread (Moulin d'Or, Beirut, Lebanon) with 57 g feta cheese (Dodoni, Greece) and 16 g black olives purchased from a local supermarket. The Western-inspired breakfast (WB) consisted of 57 g of Emmental cheese (Zott, Mertingen, Germany) with turkey ham (Reinert, Versmold, Germany) sandwiched in 79 g of soft white bread (Moulin d'Or, Lebanon). The third meal, the Grilled Western-inspired Break-fast (GWB), was identical to the WB in composition, the difference between WB and GWB being that

the sandwich was grilled for 4 min using a household grill (Russel Hobbs, 1960 W, Sulzbach, Germany). Identical quantities of water (180 mL), cucumbers (80 g), cherry tomatoes (50 g), and apples (130 g) were provided with all three breakfasts. Detailed nutrient compositions are presented in Table 1.

Table 1 Characteristics of the three breakfasts.

	Unit	MB	WB	GWB	*p*-Value		
					MB × WB	MB × GWB	WB × GWB
Fat content	% (g/100 g)	3.8 ± 0.4	2.3 ± 0.2	2.7 ± 0.3	<0.001	<0.001	<0.001
Calories from fat	kcal/100 g	34 ± 3.4	21 ± 2.1	24 ± 2.4	<0.001	<0.001	0.002
Saturated fatty acids	% of total fatty acids	52.9 ± 5.2	57.5 ± 5.7	56.5 ± 5.7	0.029	0.108	0.836
Monounsaturated fatty acids	% of total fatty acids	36.1 ± 3.6	32.6 ± 3.3	33.2 ± 3.3	0.005	0.025	0.843
Polyunsaturated fatty acids	% of total fatty acids	10.2 ± 0.1	9.2 ± 0.9	9.6 ± 1.0	<0.001	0.047	0.244
Trans fat	% (g/100 g)	0.80 ± 0.08	0.7 ± 0.07	0.7 ± 0.07	<0.001	<0.001	>0.999
Carbohydrates (including sugars and fibers)	% (g/100 g)	18.3 ± 1.8	15.0 ± 1.5	16.5 ± 1.6	<0.001	0.003	0.015
Total sugars	% (g/100 g)	3.0 ± 0.3	2.3 ± 0.2	2.8 ± 0.3	<0.001	0.059	<0.001
Total dietary fibers	% (g/100 g)	2.6 ± 0.3	2.2 ± 0.2	2.1 ± 0.2	<0.001	<0.001	0.385
Crude fibers	% (g/100 g)	1.4 ± 0.1	1.1 ± 0.1	0.9 ± 0.1	<0.001	<0.001	<0.001
Protein (N × 6.25)	% (g/100 g)	4.1 ± 0.4	6.1 ± 0.6	6.0 ± 0.6	<0.001	<0.001	0.829
Total breakfast ingested (n = 20)	g	389.1 ± 9.1	437.1 ± 6.1	413.6 ± 5.5	<0.001	<0.001	<0.001
Total CML	mg/100 g	0.52 ± 0.02	0.46 ± 0.01	0.66 ± 0.01	<0.001	<0.001	<0.001
	mg/breakfast	2.02 ± 0.05	2.03 ± 0.03	2.73 ± 0.04	0.720	<0.001	<0.001
Total CEL	mg/100 g	0.47 ± 0.01	0.38 ± 0.01	0.82 ± 0.02	<0.001	<0.001	<0.001
	mg/breakfast	1.83 ± 0.05	1.66 ± 0.03	3.39 ± 0.05	<0.001	<0.001	<0.001
Total lysine	mg/100 g	472 ± 7	547 ± 1	681 ± 37	<0.001	<0.001	<0.001
	mg/breakfast	1836 ± 43	2391 ± 33	2817 ± 46	<0.001	<0.001	<0.001
Ash content	% (g/100 g)	1.10 ± 0.01	0.70 ± 0.01	1.00 ± 0.01	<0.001	<0.001	<0.001
Moisture content	% (g/100 g)	72.7 ± 7.2	75.9 ± 7.6	73.8 ± 7.4	0.365	0.886	0.644
Caloric value	kcal/100 g	124 ± 12	105 ± 10	114 ± 11	<0.001	0.021	0.042
Iron	mg/kg	31.2 ± 3.1	31.5 ± 3.1	40.6 ± 4.1	0.960	<0.001	<0.001
Sodium	g/kg	2.3 ± 0.2	2.0 ± 0.2	1.9 ± 0.2	<0.001	<0.001	0.262
Calcium	% (g/100 g)	0.10 ± 0.01	0.09 ± 0.01	0.07 ± 0.01	0.007	<0.001	<0.001
Vitamin C	mg/100 g	2.2 ± 0.2	1.5 ± 0.1	0.9 ± 0.1	<0.001	<0.001	<0.001
Vitamin E	µg/100 g	385 ± 38	127 ± 12	96 ± 9	<0.001	<0.001	<0.001

CEL: carboxyethyllysine; CML: N^{ε}-carboxymethyllysine; GWB: Grilled Western-inspired Break-fast; MB: Mediterranean-inspired breakfast; WB: Western-inspired breakfast. Data represent mean ± SD. Statistical significance among mean values was evaluated within each line, and reported p values were calculated considering α = 0.05. Standard methods are indicated in the Supplemental Table S1.

2.5. CML quantification in plasma from rats

Total and protein-bound CML were analyzed in plasma samples from rats, both fractions undergoing a reduction step prior to acid hydrolysis. After centrifugation, 25 µL of plasma were placed in a pyrex tube with 100 µL ultra-pure water and 500 µL NaBH4 0.1 M for 2 h at ambient temperature. For total CML analysis, 625 µL of 12 M HCl were added, and the mixture was incubated for 20 h at 110 °C in an oven. For protein-bound CML analysis, a protein precipitation step after reduction was first performed by adding 2 mL of TCA 200 g/L. After centrifugation (2 000× g 10 min), the supernatant was removed. Then, 500 µL HCl 6 M was added, and the tube was incubated for 20 h at 110 °C. An aliquot of each hydrolysate (200 µL) was reduced to dryness in a Speedvac concentrator (ThermoFisher Scientific, Courtaboeuf, France) and stored at −80 °C until analysis.

Liquid chromatography with tandem mass spectrometry (LC-MS/MS) analyses of plasma samples from rats were carried out on a TSQ Quantum Ultra (ThermoFisher) with a Heated Electrospray Ionization (HESI) probe coupled to an Accela HPLC system (ThermoFisher). The chromatographic separation was performed on a Hypercarb column (100 × 2.1 mm, 5 µm, ThermoFisher) with a guard column of the same phase. The column was maintained at 10 °C, and the injection volume was 20 µL. The elution was performed with aqueous 20 mM NFPA solution (solvent A) and acetonitrile (solvent B) at a flow rate of 200 µL/min with the following gradient: percentage of B: 0–10 min, 0–15%; 10–15 min, 15–20%; 15–18 min, 20–50%; 18–22 min, 50%; 22–23, 50–0%; 23–28 min, 100%.

The tandem MS analyses measured the following specific transitions (in elution or-der): m/z 147.0 → 130.0 and m/z 149.0 → 131.0 for lysine and its isotope, respectively; m/z 205.0 → 130.0, 207.0 → 130.0 and m/z 209.0 → 134.0 for CML and its D2 and D4 isotopes, respectively; m/z 219.0 → 130.0 and m/z 223.0 → 134.0 for CEL and its isotope, respectively. Quantification of all compounds utilized the ratio between the peak areas of the analyte: peak area of its isotope (internal standard) and comparison with 7-point calibration curves.

Free CML concentration was obtained by subtracting the protein-bound CML concentration from the total CML concentration.

2.6. CML Quantification in the 3 Human Breakfasts and Human Plasma

The LC-MS/MS analyses were performed on a Vantage instrument with an HESI source (ThermoFisher). A Hypercarb column (100 × 2.1 mm, 5µm; ThermoFisher) with a guard column (10 × 2.1 mm, 5 µm, same phase) was used for chromatographic separation (column temperature 10 °C). Binary mobile phase flow rate was 200 µL/min (A–aqueous 10 mM NFPA, B–acetonitrile; percentage of B: 0–9 min, 0–25%; 9–11 min, 25–60%; 11–13 min, 60%; 13.1–21 min, 0%). The tandem MS analyses measured the same transitions as above (though without D4-CML), and quantification of all compounds utilized the analyte: isotope (internal standard) ratios and comparison with 9-point calibration curves.

A well-mixed, representative aliquot of each breakfast was lyophilized, and three subsamples of each were analyzed by LC-MS/MS. The ca. 150 mg sub-samples were resuspended in 100 µL Ultra-pure HPLC water, to which 500 µL of 0.1 M $NaBH_4$ was added (2 h at ambient temperature) to reduce the samples and prevent de novo production of CML during subsequent acid hydrolysis. Then, 600 µL of 12 M HCl was added, and the sample was hydrolyzed for 21 h at 110 °C. An aliquot (200 µL) was reduced to dryness in a Speedvac concentrator and stored at −80 °C until analysis.

Plasma samples were first subjected to a protein precipitation procedure: 50 µL of plasma was vortexed with 25 µL of aqueous 10% TCA and proteins were left to precipitate on ice for 30 min. Samples were centrifuged at 21,000× g, 4 °C for 10 min, and 30 µL of the supernatant (representing nearly all that could be taken and containing the “free” CML), was aspirated and reduced to dryness in a Speedvac, as above. Because the main objective of our study was to follow the metabolic fate of dCML, and because its impact on protein-bound CML is non-existent, it was decided to study only plasmatic-free CML in the human intervention study.

Immediately before analysis, the breakfast samples were thawed and diluted 20× with aqueous 12.5 mM NFPA containing (D2)-CML and (D4)-CEL, and a further 10× serial dilution with NFPA and (15N2)-Lys was prepared for the quantification of this amino acid. Plasma samples were thawed and resolubilized in 30 µL of 12.5 mM NFPA containing (D2)-CML, (D4)-CEL, and (15N2)-Lys. The preparation and analysis of samples were randomized to avoid any bias from interday variations in instrument performance.

2.7. sRAGE quantification in human plasma

Soluble RAGE (sRAGE) was quantified in duplicate 50 µL aliquots of human plasma for each time point from all individuals by ELISA (Quantikine DRG00, R & D Systems, Oxford, UK), following the manufacturer's instructions. This ELISA was able to detect 2 isoforms of sRAGE: the endogenous secretory (esRAGE) and the cleaved (cRAGE) isoforms. Ninety-six-well plates were read on a Fluorostar Omega plate reader (BNG Lab-tech, Champigny sur Marne, France), and samples were randomized among the different plates. In fact, calibration curves' gradients among the plates varied by less than 10%, while results for samples quantified on several plates were within 1% (data not shown).

2.8. Statistical analyses

Differences in free CML levels and their iAUC in rat samples, and in free CML and CEL, free lysine, and sRAGE levels and their iAUC in human plasma samples, as well as differences in nutritional composition among the different meals presented in Table 1, were all analyzed using ANOVA followed by Tukey's post hoc test for pairwise comparisons. iAUC values were calculated using the trapezoidal rule after baseline correction. Gender differences were evaluated by the student's two-tailed t-test. The correlations between the different parameters were evaluated using Pearson's correlation coefficient. All data are presented as means +/− Standard Deviation (SD). Statistical analysis was performed using GraphPad Prism 9.0 (San Diego, CA, USA) or Minitab 19 using $\alpha = 0.05$ as a threshold value for statistical significance.

3 Results

3.1. Kinetics of free and protein-bound cml in rat plasma after gavage with four different forms of cml

The four gavage solutions contained similar quantities of CML, and rats received 410 to 520 µg CML, corresponding to 1.43 to 1.78 mg of CML per kg of body weight, in a single oral dose. As a comparison, the maximum human exposure to dCML is estimated at 1.1 mg/kg BW/day [10]. The only difference between the four gavages was the form of CML in the solutions. The animals received either free CML, a free deuterated isotope of CML ((D2)-CML), bovine serum albumin-bound CML (CML-BSA), or a mix of free CML and BSA (CML + BSA).

The mean fasting plasma concentrations of free and protein-bound CML before gavage were 437 ± 283 (n = 18) and 391 ± 93 (n = 18) nM, respectively (Figure 1A,C,D). This corresponds to what we had previously observed in male rats of identical age and genotype [8].

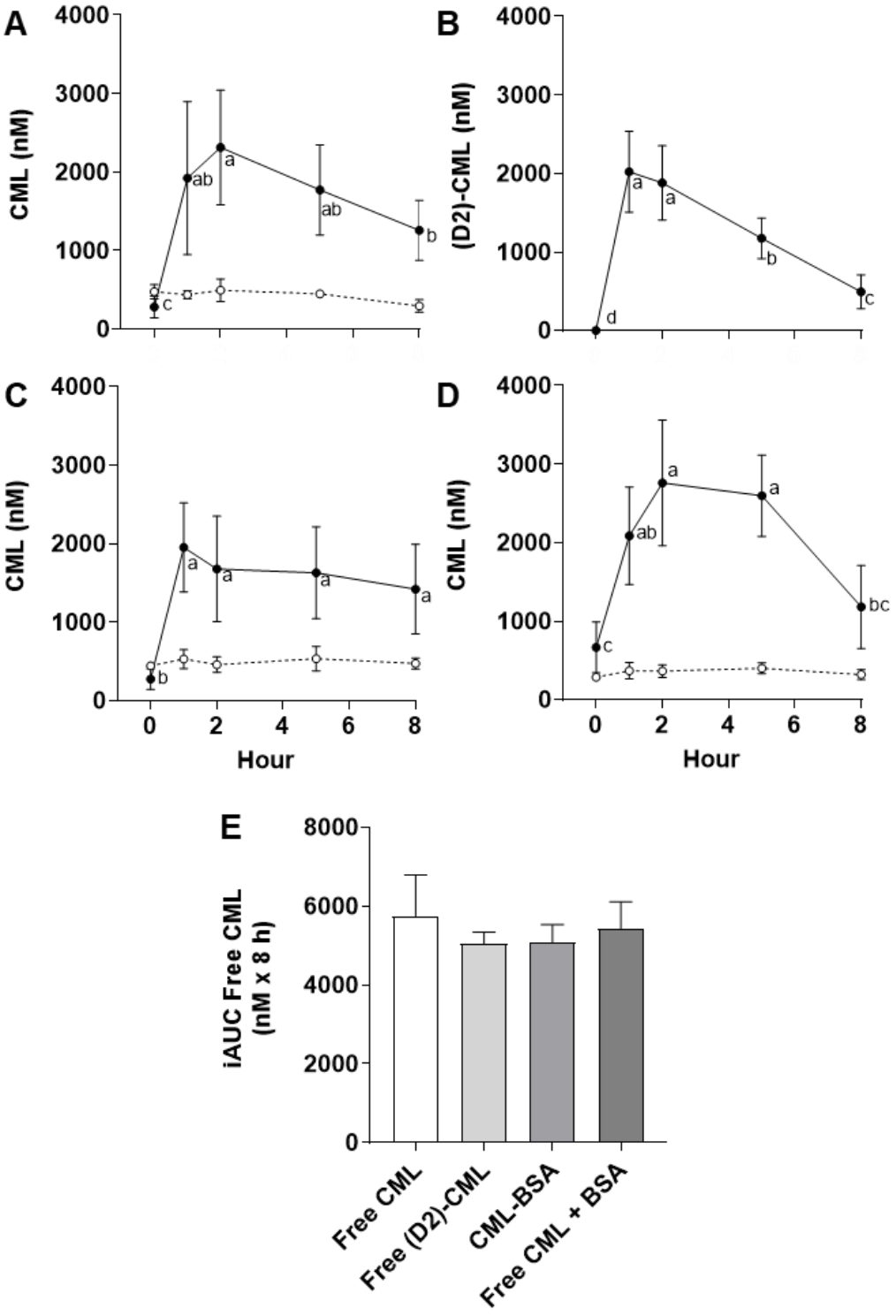

Figure 1 Kinetics of free (●) and protein-bound CML (○) in rats performed over 8 h after a single oral dose of **(A)** free CML, **(B)** free (D2)-CML, **(C)** protein-bound CML (CML-BSA), and **(D)** free CML mixed with BSA (CML + BSA). Charts shows mean ± SD values of CML concentration over time. Different letters denote statistical differences among different time points within free CML measures, taking $p < 0.05$ to be significant. **(E)** shows iAUCFree CML 0–8 h for (A–D). Bars represent mean ± SD values. No statistical significance was observed ($p < 0.05$).

After free CML was administered, its plasma concentration increased to a maximum of 2316 ± 732 nM after 2 h, then decreased slowly to 1259 ± 384 nM at the end of the experiment (8 h) (Figure 1A). Since a linear elimination of free CML was observed from 2 to 8 h, it can be postulated that the rate of decrease in plasma CML concentration depends solely upon a rate constant (slope) and follows a zero-order kinetic model. Using the calculated linear equation, [plasma free CML] = −176 t + 2664, (R2 = 0.999), it can be estimated that it would take approximately 15 h to return to the fasting concentration of free CML in plasma. In addition, the time required to eliminate 50% of the maximal free CML concentration is estimated to be 7 h (t1/2 = 2316/(2 × 176)). The protein-bound concentration of CML in plasma of free-CML challenged rats remained stable throughout the experiment (431 ± 110 nM) (Figure 1A). This observation confirms that the systemic concentration of protein-bound CML is not affected by a single oral intake of free CML.

A dose of free (D2)-CML was compared with the gavage of free native CML above to verify the specificity of plasma-free CML measurements. Free CML in plasma has a dual origin: exogenous from the digestion of dietary glycated proteins and endogenous from the catabolism of in vivo glycated proteins. The use of an isotope of CML as a source of dCML, combined with quantification by LC-MS/MS, is the most accurate way to follow the metabolic transit of this glycation product and avoids potential confusion with endogenous sources of free CML. The postprandial kinetics of free (D2)-CML in plasma are shown in Figure 1B, and it can be seen that the same pattern was observed with free native CML (Figure 1A). The concentration of free (D2)-CML increased as steeply as free native CML, also reached a maximum at 2 h, and its elimination also followed the same trend as that for free native CML. The linear equation of free (D2)-CML elimination, [plasma free (D2)-CML] = −233 t + 2362, (R2 = 0.999), also shows a similar rate constant to that calculated for the elimination of free native CML. Using this last equation, we estimate a total elimination of free (D2)-CML at 10 h post-gavage and a t1/2 of 5 h.

Overall, then, the postprandial kinetics of free (D2)-CML overlap almost perfectly with free native CML, the two approaches differing only in their baseline and maximal plasma concentrations (Figure 1A,B).

After a single oral dose of protein-bound CML (CML-BSA), the postprandial concentration of free CML in plasma (Figure 1C) followed a different pattern than that observed with free CML and free (D2)-CML. After a marked increase during the

first hour, the plasma concentrations of free CML remained relatively high for the duration of the experiment. Clearance of this protein-bound dCML appeared to be much slower when com-pared to the elimination of free CML or free (D2)-CML. The mean protein-bound CML concentration measured in plasma was again stable over the experimental period (490 ± 105 nM) and apparently not influenced by the gavage of CML-BSA (Figure 1C).

Lastly, a fourth form of dCML was tested (Figure 1D). In this case, free CML was mixed with non-glycated BSA, and the protein in this formulation affected the kinetics of free CML transfer into the circulation. Figure 1D shows a unique kinetic profile compared with the other three (Figure 1A–C). Notably, after consumption of the CML + BSA mix, plasma-free CML increased rapidly from 0 to 2 h, reached a plateau from 2 to 5 h, and then decreased more rapidly from 5 to 8 h than any of the other doses tested (slope = −472). The mean concentrations of protein-bound CML in plasma at baseline and after feeding with the mix were similar to each other (348 ± 80 nM) and also to those measured in the other groups of animals.

There was no significant difference among the four forms of dCML gavage for the postprandial Incremental Area Under the Curve (iAUC0–8 h) plasmatic free CML response (Figure 1E), despite the different kinetic profiles observed.

3.2. Comparative interventional study

3.2.1. Composition of the three breakfasts

The mean caloric contents of the three breakfast meals were not significantly different ($p = 0.912$). MB, WB, and GWB provided 482.5 ± 50.2, 458.9 ± 28.6, and 471.5 ± 34.7 kcal/meal, respectively. However, the three meals differed in macronutrient content, as presented in Table 1. Total CML and CEL concentrations were only significantly higher in the GWB compared to the 2 other breakfasts (0.66 ± 0.01 and 0.82 ± 0.02 mg/100 g of the meal, respectively) ($p < 0.05$). When adjusted to the mean total intake of breakfast, volunteers received an average of 2.02 ± 0.05, 2.03 ± 0.03 and 2.73 ± 0.04 mg CML, and 1.83 ± 0.05, 1.66 ± 0.03, and 3.39 ± 0.05 mg CEL, from the MB, WB, and GWB respectively. For CML, it corresponded to dietary exposure of 0.03 to 0.04 mg of CML per kg of body weight. The total intake of dietary lysine was dependent on the protein quality and quantity of each breakfast. Thus, the total quantity of lysine varied from 1836 ± 43 mg/meal in the MB to 2817 ± 46 mg/meal in the GWB.

3.2.2. Free CML, CEL, free lysine, and sRAGE at baseline in human plasma

The design of the interventional study included the collection of fasting blood samples on 3 consecutive weeks, with a 7-day washout period in between, in which free CML, CEL, and lysine were quantified by LC-MS/MS, and sRAGE by ELISA. In Figure 2 A, D, G, J, the data presented at time 0 of the three kinetic studies represent these fasting concentrations. Their comparisons provide information on the variation of the concentration of each adduct over the 3 weeks, independent of the breakfast tested since the measurements were pre-prandial.

The fasting free CML concentrations in plasma did not significantly differ from one week to another ($p = 0.424$), and a mean concentration and standard error of 61.6 ± 3.0 nM ($n = 60$) were calculated (Figure 2A). When the fasting free CEL data of the 3 time points were combined ($n = 60$), the mean plasma concentration was 59.0 ± 2.2 nM (Figure 2D). However, unlike CML, a significant difference was observed between the 3 fasting blood samples ($p < 0.001$). Free lysine values were not significantly different ($p = 0.288$) among the 3 “time 0” samples which had a mean concentration of 218.6 ± 6.0 nM ($n = 60$) (Figure 2G). Nor were there any differences in sRAGE concentrations among the 3 time points, and the mean concentration was 1259.8 ± 46.6 pg/mL ($n = 60$) (Figure 2J).

The distribution of the sRAGE concentration among the 20 healthy volunteers is presented in Figure 3. This figure shows not only that sRAGE ranged from 711 to 2010 pg/mL but also, and perhaps more importantly, that each individual had an almost constant fasting concentration of sRAGE over the 3-week experiment. In other words, people in the lowest (710–969 pg/mL) or highest (1308–2010 pg/mL) tertiles of fasting sRAGE concentrations consistently presented in their respective tertile, regardless of the date of blood collection. This trend was not observed for any of the other 3 adducts quantified in this study. The inter-week relative standard deviation of the mean for each individual (or intraindividual variation for fasting sRAGE) was relatively low (3 to 19%) compared with those for free CML, CEL, and lysine (3–66%, 8–52%, and 2–28%, respectively).

Among the 4 adducts measured in the plasma of the 20 volunteers before breakfast, only free CEL and free lysine were found at higher mean concentrations in male compared with female volunteers (Figure 2 F, I).

The Pearson’s correlation coefficients among pairs of the four plasma adducts at their fasting concentrations were calculated (data not shown), and only

fasting free CML showed a significant positive correlation with fasting free CEL (r = 0.556, p < 0.001).

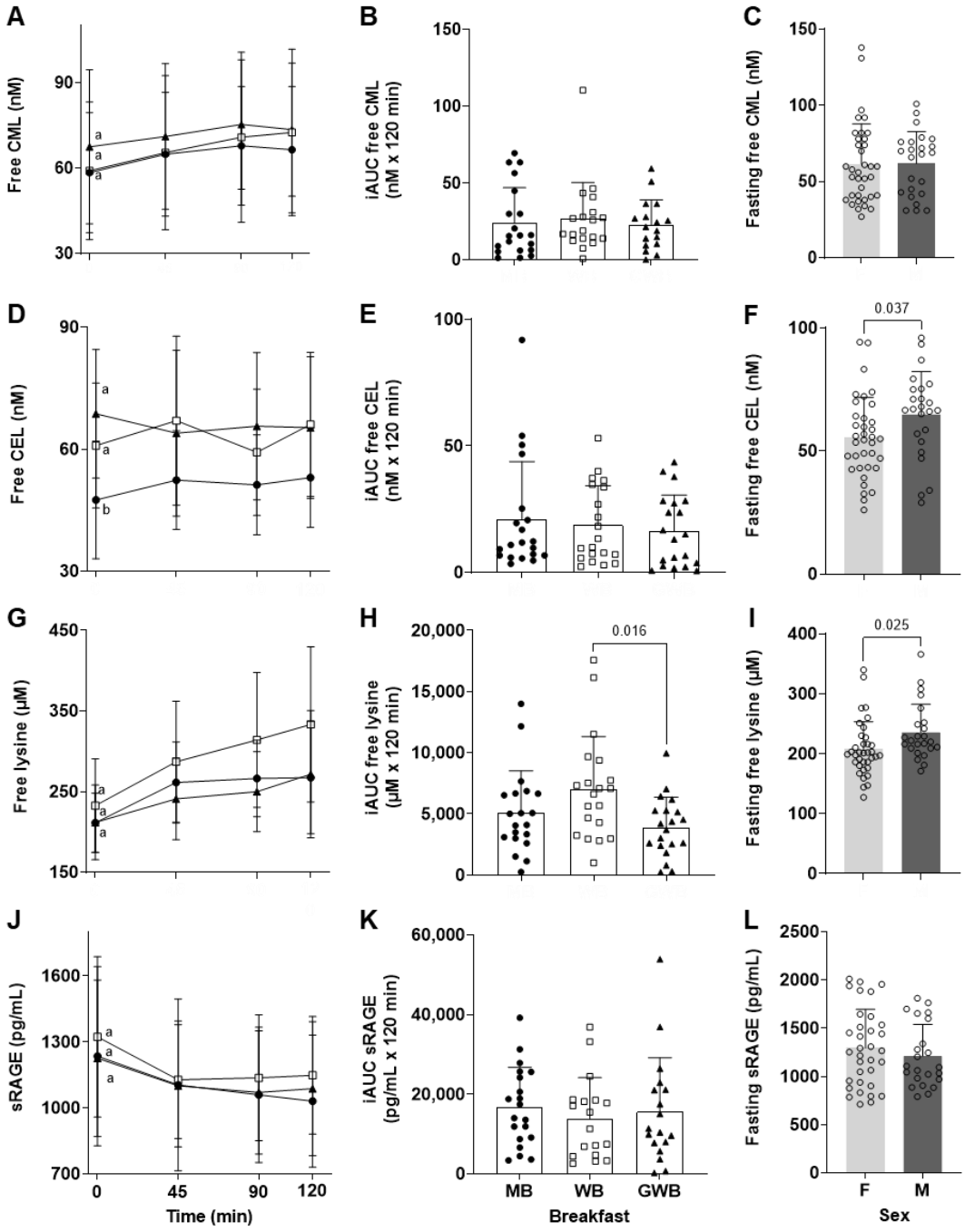

Figure 2 Circulating levels of free AGEs, free lysine, and sRAGE in human plasma. Kinetics of (A) free CML, (D) free CEL, (G) free lysine; and (J) sRAGE were compiled from four plasma samples 0 min (fasting), 45, 90, and 120 min after intake of the MB (●), WB (□), and GWB (▲) breakfasts. Letters denote statistical similarity among the different fasting measures prior to breakfast consumption (p < 0.05). The iAUC0–120 min of each breakfast is shown for (B) free CML, (E) free CEL, (H) free lysine; and (K) sRAGE levels. Gender effects for fasting (C) free CML, (F) free CEL, (I) free lysine; and (L) sRAGE levels are shown for the pool of female (F) and male (M) volunteers over the 3 interventions (n = 60). For both the iAUC0–120 min and gender analyses, statistically significant differences are indicated with significant p values at the level α = 0.05. Data represent mean ± SD.

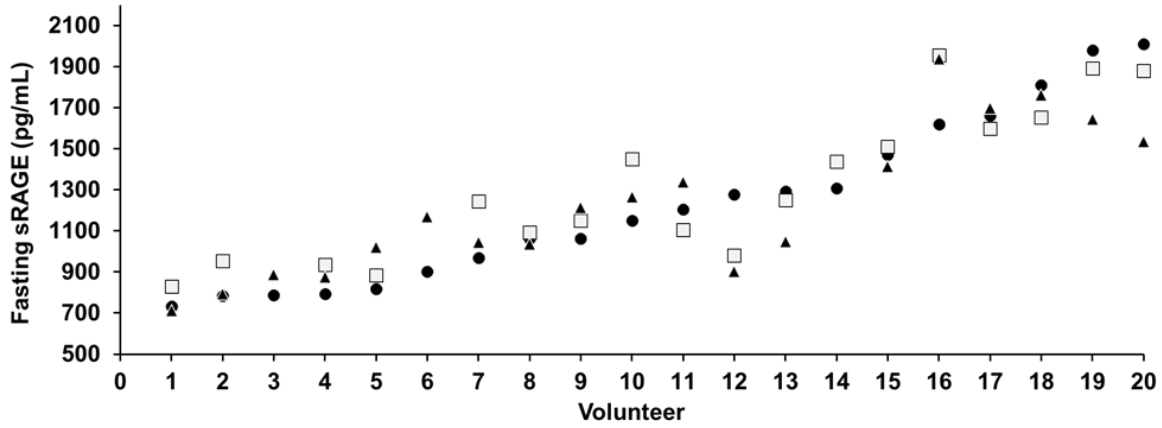

Figure 3 Distribution of fasting plasma sRAGE levels among the 20 volunteers prior to the 3 different interventions (● time 0, □ +7 days, ▲ +14 days).

4 Discussion

This study is the first, to our knowledge, to evaluate the fasting and postprandial concentration of free CML in both rats and humans using robust and validated LC-MS/MS analytical methods. The description of the kinetics of free CML and related adducts in blood after a single ingestion of different forms of well-controlled doses of dCML casts some much-needed light upon their systemic bioavailability and elimination.

Rodent assays for studying human digestion of glycated proteins are common, but their limitations are well known. Hence, we also aimed to compare rat and human fasting concentrations of free CML in plasma, in addition to its postprandial concentrations.

The fasting plasma concentrations of free CML in rats were 7 times higher than we observed in humans (437 ± 283 vs. 62 ± 3 nM, respectively), a magnitude very similar to that found in the literature. One of our previous rat studies reported a fasting plasma CML concentration of 588 nM [8], and two independent human studies measured 78 (66–99) and 74 ± 6 nM [12,13]. Although the present study does not permit the identification of the origin of this difference in baseline plasmatic free CML concentrations, we can offer two hypotheses. First, although all previously conducted studies have shown no relationship between dCML intake and fasting plasma free CML [8,12], it may be that the much higher, lifelong exposure to dCML of laboratory rats compared with humans could permanently increase their baseline plasma concentration of free CML. The dCML accumulated in certain organs may

be partly released during fasting and affect the baseline level of free CML in the circulation [14]. We calculate that with a daily intake of 20 g of standard chow, rats weighing 250 g are exposed to approximately 1450 µgCML/kg/day [15] compared to only 83 µgCML/kg/day in adult humans [3]. The second hypothesis involves the turnover of proteins in mammals. Free CML found in blood derives not only from the digestion of dietary glycated proteins (and absorption of dCML) but also from the in vivo catabolism of glycated proteins. The faster protein turnover in rats compared with humans [16], despite the similar level of CML measured in proteins in the two species [17], may explain the higher baseline plasma-free CML concentration in rats.

In addition to free CML, protein-bound CML was also quantified in the plasma of rats in receipt of different forms of dCML. This revealed plasmatic protein-bound CML at similar concentrations to free CML in fasting animals (391 ± 93 vs. 437 ± 283 nM, respectively). It also showed that the concentration of protein-bound CML varied little between animals and, more importantly, did not change significantly after an oral exposure to dCML in whatever form it was administrated (free or protein-bound). Our previous rat study [8] and clinical intervention [18], as well as the recent CODAM study [12], also concluded that dCML has no impact on the concentration of protein-bound CML in the circulation and that the latter very likely derives only from in vivo glycation of circulating proteins.

The plasma kinetics of free CML after four different single oral doses of dCML in rats, or after three different breakfast meals in humans, revealed comparable but slightly different patterns of absorption and elimination. Firstly, a comparison of the kinetics after gavage with native free dCML or its isotope indicated that a single, high dose of native dCML is sufficiently accurate to assess uptake and elimination of dCML in rats. Under the experimental conditions described, it appeared that the post-gavage kinetics of plasmatic free CML were unaffected by endogenous sources of free CML. We concluded that changes in plasmatic free CML relative to the fasting concentration were due solely to the exogenous dose of CML (*i.e.,* dCML) in the gavage.

Paul-André Finot, a pioneer in the study of the metabolic transit of chemically modified amino acids, highlighted the difference in the absorption of free and protein-bound glycation products [19]. Our comparative animal study revealed, in line with Finot's observations, that the absorption of dCML followed different kinetic

profiles depending on the form of CML ingested (as free or protein-bound CML or CML administered with a protein). On the other hand, the total absorption of dCML was not affected by the form in which it was administered (non-significant difference of iAUC among the four conditions tested). The different kinetics of plasmatic free CML may reflect a slower release of dCML when it is ingested in protein-bound form (CML-BSA) and hint at a competition for the transport of dCML with other amino acids from the gut to the circulation (free CML + BSA). Such animal tests and food model systems are useful for understanding the metabolic transit of dCML. Still, it is important to remember that this approach uses much higher doses than those to which humans are generally exposed.

The second part of the current study aimed to observe the postprandial plasma-free CML response after the intake of three classic breakfasts: a Mediterranean-inspired break-fast (MB), a Western-inspired breakfast (WB), and a Grilled Western-inspired Breakfast (GWB). According to the chemical analysis of the three meals, the intake of dCML ranged from 2.02 ± 0.05 to 2.73 ± 0.04 mg/meal (MB and GWB, respectively). These levels of dietary exposure accord with the daily exposure calculated in our previous intervention study (2.2 ± 0.9 and 5.4 ± 2.3 mg/day for a “steam” and a “standard” French diet) [3] and with that estimated in other epidemiological and clinical studies (2.1 to 4.2 mg/day [12]; 2.6 to 4.9 mg/day [20]). The range of CML exposures, as well as the absolute exposures in both our intervention study and other human studies, are very much lower than those tested in animal studies (including ours).

When exposure to dCML is expressed in proportion to body weight, the twenty healthy volunteers received between 31 ± 1 and 42 ± 1µg CML/kg BW in one or other of the 3 different breakfasts. In contrast, we tested an average of 1570 ± 150µg CML/kg BW in rats receiving a single oral gavage. Despite this large difference in exposure, the kinetics of postprandial absorption of free CML in humans appeared to be similar to that observed in rats (*i.e.,* a postprandial peak of plasmatic free CML at 90 to 120 min). As expected, the differences in dCML exposure among the 3 breakfasts were too small to yield any significant difference in the iAUCfreeCML 0–120 min of the free CML concentration in plasma. Our previous nutritional intervention trial (ICARE clinical study) [18], as well as the more recent cross-sectional CODAM study [12], also report only a weak or non-significant direct relationship between dCML and free CML in fasting plasma or urine. The

relatively low dose of dCML in a regular meal offers a likely explanation of the weakness of the association between ingested dCML and free CML in plasma (plasmatic free CML increased by at most 17% from baseline in our study) and may mean that significant relationships between intake and circulating concentrations of CML are observed only after controlling for several factors pertinent to an individual's metabolism. This appears to be the baseline case, fasting levels of plasmatic free CML: the CODAM study reported a significant association between dCML and fasting plasmatic free CML only after controlling for age, sex, glucose metabolism, and waist circumference. This finding would indirectly support our current and previous observations that recent dCML intake affects postprandial plasmatic free CML but not baseline, fasting free CML levels [8].

Much less research exists on CEL, even though this AGE is also present in food at a level close to CML. The 3 breakfasts studied here contained 1.66 ± 0.03 to 3.39 ± 0.05 mg of dCEL/meal compared to 2.02 ± 0.05 to 2.73 ± 0.04 mg of dCML/meal. Despite the fact that the study volunteers were exposed to dCEL, no postprandial increase of free CEL was observed whatever the breakfast tested. This absence of a postprandial increase in circulating free CEL agrees with recent observations by Perkins et al. in healthy, obese adults [13]. As seen for free CML, the mean fasting free CEL concentrations were comparable: 59.1 ± 10.6 nM among the 20 healthy adults in the current study and 55 ± 5 nM among the 10 healthy obese adults studied by Perkins et al. [13].

The only difference in the chemical structures of CML and CEL is an extra methyl group in CEL. To our knowledge, no significant difference in absorption of these two AGEs by intestinal cells has been described, so the most reasonable hypothesis for this difference in postprandial kinetics is a different metabolic transit of these dAGEs [7]. It is worth mentioning that fasting-free CML was positively correlated with fasting-free CEL in our human study. Could this indicate a common endogenous origin of the basal level of these 2 free AGEs? In this case, could they be two circulating biomarkers of carbonyl stress? This theory remains to be investigated.

For the first time, to our knowledge, we report that fasting-free CEL was at a lower concentration in women (though confirmation of this observation in a larger cohort is required). This gender difference was also observed for fasting free lysine but not for fasting free CML. Even though significant differences in most circulating

free amino acids between men and women were reported many years ago, no clear biological explanation has yet been given [21].

The effects of the Maillard reaction on the nutritional quality of food proteins have been widely studied, the loss of lysine being a major concern for nutritionists. This essential amino acid is one of the main targets of glycation, and its transformation into CML, CEL, and other AGEs results in chemically modified lysine, which is unavailable for protein anabolism after ingestion (also known as “blocked lysine”). Animal experiments [22] and clinical studies [23] conducted with exaggeratedly glycated proteins (>50% blocked lysine) have reported reduced postprandial plasma-free lysine responses. However, when normally processed foods are compared in a clinical study, such as pasteurized and ultrahigh temperature processed milk, no significant difference is observed in postprandial plasma lysine concentrations [24]. Our clinical study was not designed to compare 3 breakfasts with an equal quantity of proteins (and hence lysine) (Table 1), and any comparison of the postprandial plasmatic free lysine kinetics must be made with this in mind (Figure 2 G, H). Nevertheless, the WB and GWB contained similar amounts of intact lysine, yet the latter exhibited lower postprandial free lysine concentrations ($p = 0.016$). While our study was not designed specifically to address this question, this result suggests that when the sandwich (bread, cheese, and ham) was toasted for 4 min, the heat treatment of the protein may have reduced lysine uptake. A decreased protein digestibility has been described for thermally processed foods tested in in vitro digestive model systems, but is not consistently found in clinical studies [5].

In addition to the nutritional issue of the assimilation of the essential amino acid lysine, the main reason for measuring free lysine in the plasma of our healthy volunteers was to compare the kinetic trends between the uptake of free lysine and its glycated derivatives CML and CEL and confirm that they were indeed similar.

The putative deleterious effects of dCML and other dAGEs are often justified by their affinity for the cell-membrane RAGE receptor and the consequent activation of pro-inflammatory and pro-oxidative pathways. While some studies have reported that protein-bound CML is unable to bind RAGE and induce a pro-inflammatory response [25], others suggest that this type of glycated protein is an important ligand for RAGE, while free CML is not [26]. The binding of protein-bound CML and other glycated proteins to RAGE and the subsequent activation of RAGE signaling and its

associated pathological consequences are nevertheless widely accepted as a key biological mechanism by which dAGEs may affect health. Other studies have not only confirmed that free CML and CEL do not bind to RAGE, but also report that protein-bound CML is only a weak ligand compared to protein-bound MG-H1 (Methylglyoxal-derived hydroimidazolone 1) [27]. Considering that free AGEs (i.e., modified amino acids of low molecular weight) are unlikely to be RAGE ligands, it is difficult to understand how they can be involved in RAGE signaling after intestinal absorption. The discovery of soluble isoforms of RAGE (sRAGE including es- and c-RAGE) complexified the study of the so called AGE-RAGE axis [28] but also offered hope for therapy against glycation-related pathologies. It is considered (perhaps simplistically) that sRAGE may act as a decoy receptor for AGEs and thus prevent or reduce the activation of inflammatory and oxidative pathways.

With all this in mind, the current clinical study aimed to evaluate the change in plasma sRAGE after the intake of 3 different breakfasts containing different amounts of CML and CEL. Prior to administration, fasting sRAGE was at an average concentration of 1260 ± 373 pg/mL with no difference between males and females. This absence of a gender difference has already been observed in cohorts of different ages [29–31]. Notably, each participant had a unique and remarkably constant level of sRAGE in the blood samples collected over the 3 weeks of the study. Clinical data on the association between fasting sRAGE and serum concentrations of protein-bound AGEs are discordant and scarce, however. Yamagishi et al. found a positive association among 184 non-diabetic Japanese subjects [31], while De Courten et al. reported a moderate negative association among 20 non-diabetic, overweight Australian subjects [20]. Our current clinical study tested the as-sociation between sRAGE and free CML and CEL levels at baseline and up to 2 h post-prandial, and no correlation was found.

Temporal fluctuations of sRAGE in humans remain poorly understood. Synthesizing the limited data available is further complicated by the fact that they derive from type 1 or 2 diabetic patients, from obese and healthy subjects [11,13,32]. Despite the heterogeneity of these populations, a common trend of daily circulating sRAGE is nevertheless evident, with its production higher following an overnight fast [32] and decreasing after breakfast [11,13]. The current study confirms that plasma sRAGE concentrations decreased after breakfast, while we additionally observed here that this was independent of the dAGE contents of the meals. As described in

type 1 diabetic patients by Miranda et al., no statistically significant inverse correlation was found between sRAGE and free CML or CEL among the healthy participants in our study. Among the free AGEs measured by Miranda et al., only the overnight decrease in free MG-H1 was associated with the concurrent increase in sRAGE levels. Among other things, the authors suggested that the higher affinity for RAGE of MG-H1 compared to CML and CEL could be the reason for this only inverse correlation. However, we were unable to find a study demonstrating that a free AGE could bind to RAGE (either soluble or membrane-bound), and an elimination of MG-H1 and other free AGEs by a mechanism of sequestration by sRAGE has yet to be demonstrated.

The inverse fluctuation of circulating sRAGE and free AGEs observed here, and the more or less significant inverse correlations observed by the pioneering study of Miranda et al. are far from proof that sRAGE traps circulating free AGEs and eliminates them. Since no control group without breakfast intake was included in our clinical study, the direct effect of food intake on circulating sRAGE concentration remains to be proven. This also applies to the association of sRAGE and free AGEs following an overnight fast [32].

In conclusion, research on the time-dependent modulation of sRAGE and the metabolic transit of dAGEs and other MRPs merits further investigation. While we have shed a little more light on the relationship between free AGEs and sRAGE in plasma with this study, the biological mechanisms by which dietary and other environmental factors affect their circulating concentrations require further elucidation.

Author Contributions: Animal study, P.M.A., C.N.-L., P.J., C.D.-O., and F.J.T.; human study, C.H., T.P., M.H., A.G., F.D., and F.J.T.; data analysis and interpretation, M.T.N.S.L., C.N.-L., P.J., M.G., M.H., and F.J.T.; resources and funding acquisition, C.H., E.B. and F.J.T.; original draft preparation, C.H., M.T.N.S.L., C.N.-L., P.M.A., M.H., and F.J.T.; reviewing and editing, C.H., M.T.N.S.L., M.H., and F.J.T. C.H. and M.T.N.S.L. are co-first authors who contributed equally to the publication. All authors have read and agreed to the published version of the manuscript.

Funding: This work was partly funded by the French Agence Nationale de la Recherche (ANR), grant number ANR-19-CE34-0013.

Institutional Review Board Statement: The animal experiment was conducted at the animal house unit of the Institut Polytechnique LaSalle Beauvais, France (LaSalle facilities agreement number C60-200-001,) and received prior approval from both the local animal protocol review committee (CEEA n°116) and the French Ministry of Education (MENESR, n°03530.V02). The human study was conducted according to the guidelines of the Declaration of Helsinki, and approved by the Ethics Committee of Saint-Joseph University of Beirut, Lebanon (FPH58/2017).

Informed Consent Statement: Informed consent was obtained from all subjects involved in the human study.

Conflicts of Interest: The authors declare no conflict of interest.

5 References

1. Tessier, F.J.; Niquet, C. The metabolic, nutritional and toxicological consequences of ingested dietary Maillard reaction products: A literature review. *J. Soc. Biol.* **2007**, *201*, 199–207. https://doi.org/10.1051/jbio:2007025.
2. Delgado-Andrade, C.; Fogliano, V. Dietary Advanced Glycosylation End-Products (DAGEs) and Melanoidins Formed through the Maillard Reaction: Physiological Consequences of Their Intake. *Annu. Rev. Food Sci. Technol.* **2018**, *9*, 271–291. https://doi.org/10.1146/annurev-food-030117-012441.
3. Tessier, F.J.; Birlouez-Aragon, I. Health Effects of Dietary Maillard Reaction Products: The Results of ICARE and Other Studies. *Amino Acids* **2012**, *42*, 1119–1131. https://doi.org/10.1007/s00726-010-0776-z.
4. Finot, P.-A.; Bujard, E.; Mottu, F.; Mauron, J. Availability of the True Schiff's Bases of Lysine. Chemical Evaluation of the Schiff's Base between Lysine and Lactose in Milk. In *Protein Crosslinking*; Springer: Berlin/Heidelberg, Germany, 1977; pp. 343–365.
5. Tessier, F.J.; Boulanger, E.; Howsam, M. Metabolic Transit of Dietary Advanced Glycation End-Products-the Case of NƐ-Carboxymethyllysine. *Glycoconj. J.* **2021**, *38*, 311–317.
6. Scheijen, J.L.J.M.; Clevers, E.; Engelen, L.; Dagnelie, P.C.; Brouns, F.; Stehouwer, C.D.A.; Schalkwijk, C.G. Analysis of Advanced Glycation Endproducts in Selected Food Items by Ultra-Performance Liquid Chromatography Tandem Mass Spectrometry: Presentation of a Dietary AGE Database. *Food Chem.* **2016**, *190*, 1145–1150. https://doi.org/10.1016/j.foodchem.2015.06.049.
7. Hellwig, M.; Geissler, S.; Matthes, R.; Peto, A.; Silow, C.; Brandsch, M.; Henle, T. Transport of Free and Peptide-Bound Glycated Amino Acids: Synthesis, Transepithelial Flux at Caco-2 Cell Monolayers, and Interaction with Apical Membrane Transport Proteins. *ChemBioChem* **2011**, *12*, 1270–1279.
8. Alamir, I.; Niquet-Leridon, C.; Jacolot, P.; Rodriguez, C.; Orosco, M.; Anton, P.M.; Tessier, F.J. Digestibility of Extruded Proteins and Metabolic Transit of N ε-Carboxymethyllysine in Rats. *Amino Acids* **2013**, *44*, 1441–1449.
9. Faist, V.; Müller, C.; Drusch, S.; Erbersdobler, H.F. Selective Fortification of Lysinoalanine, Fructoselysine and N Epsilon-Carboxymethyllysine in Casein Model Systems. *Nahrung* **2001**, *45*, 218–221. https://doi.org/10.1002/1521-3803(20010601)45:3<218::AID-FOOD218>3.0.CO;2-Q.
10. Grossin, N.; Auger, F.; Niquet-Leridon, C.; Durieux, N.; Montaigne, D.; Schmidt, A.M.; Susen, S.; Jacolot, P.; Beuscart, J.-B.; Tessier, F.J.; et al. Dietary CML-Enriched Protein Induces Functional Arterial Aging in a RAGE-Dependent Manner in Mice. *Mol. Nutr. Food Res.* **2015**, *59*, 927–938. https://doi.org/10.1002/mnfr.201400643.
11. Fotheringham, A.K.; Bagger, J.I.; Borg, D.J.; McCarthy, D.A.; Holst, J.J.; Vilsbøll, T.; Knop, F.K.; Forbes, J.M. Circulating Levels of the Soluble Receptor for AGE (SRAGE) during Escalating Oral Glucose Dosages and Corresponding Isoglycaemic Iv Glucose Infusions in Individuals with and without Type 2 Diabetes. *Nutrients* **2020**, *12*, 2928.
12. Scheijen, J.L.J.M.; Hanssen, N.M.J.; Greevenbroek, M.M. van; Kallen, C.J.V. der; Feskens, E.J.M.; Stehouwer, C.D.A.; Schalkwijk, C.G. Dietary Intake of Advanced Glycation Endproducts Is Associated with Higher Levels of Advanced Glycation Endproducts in Plasma and Urine: The CODAM Study. *Clin. Nutr.* **2018**, *37*, 919–925. https://doi.org/10.1016/j.clnu.2017.03.019.
13. Perkins, R.K.; Miranda, E.R.; Karstoft, K.; Beisswenger, P.J.; Solomon, T.P.; Haus, J.M. Experimental Hyperglycemia Alters Circulating Concentrations and Renal Clearance of Oxidative and Advanced Glycation End Products in Healthy Obese Humans. *Nutrients* **2019**, *11*, 532.
14. Tessier, F.J.; Niquet-Léridon, C.; Jacolot, P.; Jouquand, C.; Genin, M.; Schmidt, A.-M.; Grossin, N.; Boulanger, E. Quantitative Assessment of Organ Distribution of Dietary Protein-Bound 13 C-Labeled Nε -Carboxymethyllysine after a Chronic Oral Exposure in Mice. *Mol. Nutr. Food Res.* **2016**, *60*, 2446–2456. https://doi.org/10.1002/mnfr.201600140.
15. Guilbaud, A.; Howsam, M.; Niquet-Léridon, C.; Jacolot, P.; Boulanger, E.; Tessier, F. Dietary Exposure to Maillard Reaction Products Is an Important Confounding Factor When Murine Models of Diet Induced Obesity Are Compared with Unmatched Control Groups; IMARS Highlights 2019; 14,1, 5–7.
16. Swovick, K.; Firsanov, D.; Welle, K.A.; Hryhorenko, J.R.; Wise, J.P.; George, C.; Sformo, T.L.; Seluanov, A.; Gorbunova, V.; Ghaemmaghami, S. Interspecies Differences in

Proteome Turnover Kinetics Are Correlated with Life Spans and Energetic Demands. *Mol. Cell. Proteom.* **2021**, *20*, 100041.
17. Thornalley, P.J.; Battah, S.; Ahmed, N.; Karachalias, N.; Agalou, S.; Babaei-Jadidi, R.; Dawnay, A. Quantitative Screening of Advanced Glycation Endproducts in Cellular and Extracellular Proteins by Tandem Mass Spectrometry. *Biochem. J.* **2003**, *375*, 581–592.
18. Birlouez-Aragon, I.; Saavedra, G.; Tessier, F.J.; Galinier, A.; Ait-Ameur, L.; Lacoste, F.; Niamba, C.-N.; Alt, N.; Somoza, V.; Lecerf, J.-M. A Diet Based on High-Heat-Treated Foods Promotes Risk Factors for Diabetes Mellitus and Cardiovascular Diseases. *Am. J. Clin. Nutr.* **2010**, *91*, 1220–1226. https://doi.org/10.3945/ajcn.2009.28737.
19. Finot, P.-A. The Absorption and Metabolism of Modified Amino Acids in Processed Foods. *J. AOAC Int.* **2005**, *88*, 894–903.
20. De Courten, B.; De Courten, M.P.; Soldatos, G.; Dougherty, S.L.; Straznicky, N.; Schlaich, M.; Sourris, K.C.; Chand, V.; Scheijen, J.L.; Kingwell, B.A. Diet Low in Advanced Glycation End Products Increases Insulin Sensitivity in Healthy Overweight Individuals: A Double-Blind, Randomized, Crossover Trial. *Am. J. Clin. Nutr.* **2016**, *103*, 1426–1433.
21. Armstrong, M.D.; Stave, U. A Study of Plasma Free Amino Acid Levels. II. Normal Values for Children and Adults. *Metabolism* **1973**, *22*, 561–569.
22. Rérat, A.; Calmes, R.; Vaissade, P.; Finot, P.-A. Nutritional and Metabolic Consequences of the Early Maillard Reaction of Heat Treated Milk in the Pig. *Eur. J. Nutr.* **2002**, *41*, 1–11. https://doi.org/10.1007/s003940200000.
23. Nyakayiru, J.; van Lieshout, G.A.A.; Trommelen, J.; van Kranenburg, J.; Verdijk, L.B.; Bragt, M.C.E.; van Loon, L.J.C. The Glycation Level of Milk Protein Strongly Modulates Post-Prandial Lysine Availability in Humans. *Br. J. Nutr.* **2019**, *123*, 545–552. https://doi.org/10.1017/S0007114519002927.
24. Lacroix, M.; Bon, C.; Bos, C.; Léonil, J.; Benamouzig, R.; Luengo, C.; Fauquant, J.; Tomé, D.; Gaudichon, C. Ultra High Temperature Treatment, but Not Pasteurization, Affects the Postprandial Kinetics of Milk Proteins in Humans. *J. Nutr.* **2008**, *138*, 2342–2347. https://doi.org/10.3945/jn.108.096990.
25. Buetler, T.M.; Leclerc, E.; Baumeyer, A.; Latado, H.; Newell, J.; Adolfsson, O.; Parisod, V.; Richoz, J.; Maurer, S.; Foata, F. Nε-Carboxymethyllysine-Modified Proteins Are Unable to Bind to RAGE and Activate an Inflammatory Response. *Mol. Nutr. Food Res.* **2008**, *52*, 370–378.
26. Kislinger, T.; Fu, C.; Huber, B.; Qu, W.; Taguchi, A.; Yan, S.D.; Hofmann, M.; Yan, S.F.; Pischetsrieder, M.; Stern, D.; et al. N ε-(Carboxymethyl)Lysine Adducts of Proteins Are Ligands for Receptor for Advanced Glycation End Products That Activate Cell Signaling Pathways and Modulate Gene Expression. *J. Biol. Chem.* **1999**, *274*, 31740–31749. https://doi.org/10.1074/jbc.274.44.31740.
27. Xue, J.; Ray, R.; Singer, D.; Böhme, D.; Burz, D.S.; Rai, V.; Hoffmann, R.; Shekhtman, A. The Receptor for Advanced Glycation End Products (RAGE) Specifically Recognizes Methylglyoxal-Derived AGEs. *Biochemistry* **2014**, *53*, 3327–3335.
28. Dubois, C.; Fradin, C.; Boulanger, É. Axe AGE-RAGE: Conséquences Physiopathologiques et Inflammaging. *Médecine Mal. Métaboliques* **2019**, *13*, 595–601.
29. Davis, K.E.; Prasad, C.; Vijayagopal, P.; Juma, S.; Imrhan, V. Serum Soluble Receptor for Advanced Glycation End Products Correlates Inversely with Measures of Adiposity in Young Adults. *Nutr. Res.* **2014**, *34*, 478–485.
30. Scavello, F.; Zeni, F.; Tedesco, C.C.; Mensà, E.; Veglia, F.; Procopio, A.D.; Bonfigli, A.R.; Olivieri, F.; Raucci, A. Modulation of Soluble Receptor for Advanced Glycation End-Products (RAGE) Isoforms and Their Ligands in Healthy Aging. *Aging* **2019**, *11*, 1648.
31. Yamagishi, S.; Adachi, H.; Nakamura, K.; Matsui, T.; Jinnouchi, Y.; Takenaka, K.; Takeuchi, M.; Enomoto, M.; Furuki, K.; Hino, A. Positive Association between Serum Levels of Advanced Glycation End Products and the Soluble Form of Receptor for Advanced Glycation End Products in Nondiabetic Subjects. *Metabolism* **2006**, *55*, 1227–1231.
32. Miranda, E.R.; Fuller, K.N.Z.; Perkins, R.K.; Beisswenger, P.J.; Farabi, S.S.; Quinn, L.; Haus, J.M. Divergent Changes in Plasma AGEs and SRAGE Isoforms Following an Overnight Fast in T1DM. *Nutrients* **2019**, *11*, 386. https://doi.org/10.3390/nu11020386.

CHAPTER 5

Glycated bovine serum albumin for use in feeding trials with animal models – in vitro methodology and characterization of a glycated substrate for modifying feed pellets

MT Nogueira Silva Lima[1], M Howsam[1], C Delayre-Orthez[2], P Jacolot[2], S Jaisson[3], J Criquet[4], M Billamboz[1,5], A Ghinet[1,5], C Fradin[1], E Boulanger[1], F Bray[6], S Flament[6], C Rolando[6], P Gillery[3], C Niquet-Léridon[2], FJ Tessier[1]

U1167—RID—AGE—Facteurs de Risque et Déterminants Moléculaires des Maladies Liées au Vieillissement, Institut Pasteur de Lille, University Lille, Inserm, CHU Lille, F-59000 Lille, France; [2]Institut Polytechnique UniLaSalle, Université d'Artois, ULR 7519, 60000 Beauvais, France; [3]University of Reims Champagne-Ardenne, Laboratory of Biochemistry and Molecular Biology, CNRS/URCA UMR 7369 MEDyC, Faculté de Médecine, 51095 Reims, France; University Hospital of Reims, Laboratory of Biochemistry-Pharmacology-Toxicology, 51092 Reims, France [4] Univ. Lille, Laboratory of Advanced Spectroscopy for Interactions, Reactivity and Environment, CNRS, UMR 8516 – LASIRE, Lille F-59000, France; [5]Junia, Health and Environment, Laboratory of Sustainable Chemistry and Health, 59000 Lille, France; [6]Miniaturization for Synthesis, Analysis & Proteomics, UAR 3290, CNRS, University of Lille, 59655 Villeneuve d'Ascq Cedex, France.

This review article has been published in Food Chemistry:

Nogueira Silva Lima, MT, M Howsam, C Delayre-Orthez, P Jacolot, S Jaisson, J Criquet, M Billamboz, et al. "Glycated Bovine Serum Albumin for Use in Feeding Trials with Animal Models – In Vitro Methodology and Characterization of a Glycated Substrate for Modifying Feed Pellets". *Food Chemistry* 428 (1º de dezembro de 2023): 136815.

ABSTRACT

This study investigated different methods to produce N^{ε}-carboxymethyl-lysine (CML)-enriched bovine serum albumin (BSA) as alternatives to the classical approach using glyoxylic acid (GA) and sodium cyanoborohydride ($NaBH_3CN$) which results in toxic hydrogen cyanide (HCN). The reaction of GA (6 mmol/L**)** and $NaBH_3CN$ (21 mmol/L**)** to produce CML remained the most effective with CML yields of 24-35%, followed by 13-24% using 300 mmol/L glyoxal (GO). GA promoted specific modification of lysine to CML, and fewer structural modifications of the BSA molecule compared with GO, as evidenced by fluorescence and proteomic analyses. GO promoted greater arginine modification compared with GA (76 vs 23%). Despite structural changes to BSA with GO, murine fecal clearance of CML was similar to literature values. Hence, BSA glycation with 300 mmol/L glyoxal is a suitable alternative to GA and $NaBH_3CN$ for generating CML-enriched protein free of HCN, but a CML-only fortification model remains to be described.

Keywords: carboxymethyllysine; glycation; BSA; glyoxal

1 Introduction

Advanced Glycation End-Products (AGEs) are a heterogeneous group of compounds resulting from the non-enzymatic condensation between reducing sugars and amino groups, primarily lysine and arginine moieties [1]. The *in vivo* glycation of proteins is part of normal metabolism, but pathological implications, as well as molecular aging, have also been associated with it [2]. In addition to the putative health effects of endogenously formed AGEs, their presence in food is a matter of concern. In industrial or household cooking processes, the development of appealing aromas, flavors, and colors goes hand-in-hand with the formation of dietary AGEs (dAGEs) [3]. It is well-documented that thermally-processed foods are a key dietary source of these neo-formed compounds. Endogenous AGEs and dAGEs are thought to exert their pro-inflammatory effect at least in part through binding with the Receptor for Advanced Glycation End-products (RAGE) [4].

In rodents, studies of increased exposure to glycated proteins in food have employed protocols including heating of food (*e.g.* autoclaving, baking) [5], supplementing food with free AGEs [6], or administering a diet enriched in protein-bound AGEs (*e.g.* casein, bovine serum albumin) [7]. Given the heterogeneous nature of dAGEs resulting from these different methods, it is difficult to decipher the effect of a single compound and the precise implications of dAGEs for health remain elusive. This is partly because the different protocols are intended to address different research questions. In animal experiments, heating food has the advantage of representing a process similar to industrial processing or household cooking and enables the study of a representative cocktail of dAGEs. However, the disadvantage is that certain micronutrients are degraded, potentially biasing the effects of dAGEs [8]. Conversely, the addition of free AGEs to food has enabled the study of specific glycation products, but this approach does not represent the main route of exposure to dAGEs as they exist primarily in the protein-bound form in food. Lastly, administering diets supplemented with synthetic, well-characterized, protein-bound dAGEs enables the study of a predominant dAGE and reduces nutritional confounders associated with the heating of foods. However, the synthesis of protein-bound dAGEs often lacks an extensive assessment of the precise modifications of glycated proteins.

Protein-bound N^{ε}-carboxymethyl-lysine (CML) is the most studied dAGE due to its chemical stability and abundance in food [9]. Dietary CML (dCML) has been

shown to accumulate in organs such as the gut and kidneys [10]. Peptides including lysine moieties modified into CML exhibited 7-times greater affinity for RAGE compared with non-glycated fragments [11]. Protein-bound dCML is formed preferentially compared with free CML in thermally processed foods [5], making the specific effects of protein-bound dCML on health a *bona fide* research objective.

Many strategies have been used to synthesize protein-bound CML. While no CML-exclusive synthesis method has been described the most selective approach, to our knowledge, uses glyoxylic acid and sodium cyanoborohydride ($NaBH_3CN$) for the generation of dCML in proteins including casein, ovalbumin, or albumin [12,13]. Classic reductive amination of glyoxylic acid in the presence of $NaBH_3CN$ has been reported to convert 16%-44% of the lysine moieties into CML [12,14]. Despite the high CML yields of this approach, the toxic hydrogen cyanide (HCN) gas produced is potentially harmful to laboratory personnel and an inherent contaminant of animal food preparations. Chemically safer alternative methods have been proposed using sodium borohydride ($NaBH_4$), sodium triacetoxyborohydride ($NaBH(OAc)_3$) reducing agents, and ribose- or glyoxal-driven reactions [12,13,15]. These methods do not result in the production of HCN, but they may be expensive or require inflammable or toxic solvents (*e.g.* dichloroethane).

Here we present a broad, comparative characterization of classical and alternative methods of converting lysine into CML, investigating other glycation hotspots such as arginine residues as well as more complex forms of glycation products as crosslinks. This work presents, for the first time, not only an alternative to the use of $NaBH_3CN$, but also an effective way of producing CML without the nutritional loss associated with heat treatment. Our goal here was to compare the efficiency of different reducing agents and carbonyl compounds for dCML fortification of bovine serum albumin (BSA) using an extensive suite of quantitative and qualitative analytical methods. We employed isotope-dilution, high-performance liquid chromatography coupled with tandem mass spectrometric detection (HPLC-MS/MS), western-blot, fluorescence, and proteomic analyses, using matrix-assisted laser desorption ionization with tandem time-of-flight MS (MALDI-TOF/TOF) and nanoLC with tandem, high-resolution MS (LC-HRMS/MS), to provide an extensive characterization of the possible modifications of BSA promoted by different carbonyl compounds. We further studied the efficiency of the incorporation of protein-bound

dCML into mouse feed pellets, their stability over different storage periods, and finally the clearance of dCML in mouse feces.

2 Material and methods

2.1. Chemicals and reagents

Bovine serum albumin (BSA) Fraction V was from Euromedex (Souffelweyersheim, France) and ribose from TCI Chemicals (Zwijndrecht, Belgium). Ammonium formate (>99%) and **u**ltra-pure HPLC water were from VWR (Fontenay-sous-Bois, France), sodium triacetoxyborohydride ($NaBH(OAc)_3$) from ACROS Organics (Geel, Belgium), Nonafluoropentanoic acid (NFPA) 97%, formic acid (>95%), acetonitrile (ACN), $NaBH_3CN$, glyoxylic acid and glyoxal (40% w/v), hydrochloric acid (HCl) 37%, sodium borohydride ($NaBH_4$)**,** boric acid (H_3BO_3), sodium hydroxide (NaOH), lysine (Lys) and arginine (Arg), as well as all chemicals for proteomics assays were obtained from Sigma–Aldrich (Saint-Quentin-Fallavier, France). Furosine (Fur), Fur-d_4, CML, and CML-d_2 were from Polypeptide Group Laboratories (Strasbourg, France)**.** Labeled lysine (Lys-$^{15}N_2$) was from CortecNet (Voisins-le-Bretonneux, France) and Arg-^{13}C from Carl Roth (Karlsruhe, Germany).

2.2. N^{ε}-carboxymethyl-lysine synthesis in different BSA model systems

We compared three approaches for preparing CML-fortified BSA, all representative of common practice in the literature, and present the molar ratios in Table 1 [12]. The first examined the efficiency of the reducing agents $NaBH_4$, $NaBH(OAc)_3$, and $NaBH_3CN$ in combination with glyoxylic acid (GA-A to GA-F): BSA and glyoxylic acid were allowed to react for 2h at 37°C to form imine precursors before addition of the reducing agents. A second approach employed glyoxal at 40% w/v and ribose (R-A to R-GO-B), while a third employed glyoxal only (GO-A to GO-E). Reactions GA-A to -F and R-A to R-GO-B, were prepared in a phosphate buffer (0.2 M, pH 8.0) and incubated for 16h at 37°C; reactions GO-A to -E were incubated for 4 days at 37°C under sterile conditions. All samples were then dialyzed for 24h (4°C) using a Spectra/Por 4 MWCO 10-14 kDa membrane (Spectrum Chemicals) with two water bath changes (1:23 v:v), before western-blot and LC-MS/MS analysis. Having thus identified the two best approaches for forming protein-bound CML in BSA, three replicates of GA-E (GA-E.1, 2 and 3) and GO-E (GO-E.1, 2 and 3) were prepared and characterized using western-blot, LC-MS/MS, fluorescence

spectroscopy and proteomic analyses to assess inter-day variability of these reactions (Table 1).

Table 1 Model systems for the production of protein-bound CML by modification of BSA (Lys - lysine; GA - glyoxylic acid; GO - glyoxal).

Sample	Molar ratio	Final concentration (mmol/L)						
		Lys	GA	GO	Ribose	$NaBH_4$	$NaBH(OAc)_3$	$NaBH_3CN$
Native BSA (Control)	-	175						
GA-A	1 (Lys) : 1.2 (GA) : 4.9 ($NaBH_4$)	5	6			22		
GA-B	1 (Lys) : 2.4 (GA) : 3.0 ($NaBH(OAc)_3$)	3	7				9	
GA-C	1 (Lys) : 2.4 (GA) : 9.8 ($NaBH(OAc)_3$)	3	7				30	
GA-D	1 (Lys) : 0.5 (GA) : 4.9 ($NaBH_3CN$)	5	3					21
GA-E	1 (Lys) : 1.2 (GA) : 4.9 ($NaBH_3CN$)	5	6					21
GA-F	1 (Lys) : 2.4 (GA) : 9.8 ($NaBH_3CN$)	5	12					42
R-A	1 (Lys) : 1.5 (R)	175			300			
R-B	1 (Lys) : 3.0 (R)	175			600			
R-GO-A	1 (Lys) : 0.1 (GO) : 1.5 (R)	175		20	300			
R-GO-B	1 (Lys) : 0.2 (GO) : 3.0 (R)	175		40	600			
GO-A	1 (Lys) : 0.1 (GO)	175		20				
GO-B	1 (Lys) : 0.2 (GO)	175		40				
GO-C	1 (Lys) : 0.6 (GO)	175		100				
GO-D	1 (Lys) :1.2 (GO)	175		200				
GO-E	1 (Lys) :1.8 (GO)	175		300				
GA-E.1*								
GA-E.2*	1 (Lys) : 1.2 (GA) : 4.9 ($NaBH_3CN$)	5	6					21
GA-E.3*								
GO-E.1**								
GO-E.2**	1 (Lys) :1.8 (GO)	175		300				
GO-E.3**								

Inter-day replicates of (*) GA-E reactions, and (**) GO-E reactions.

2.3. Western blot analysis of native and glycated BSA

Protein concentration was determined by the Pierce™ BCA Protein Assay Kit (ThermoFisher, Courtaboeuf, France). A total of 200 ng of protein was separated in 8% Bis-Tris (ThermoFisher) gels. Nonspecific binding sites were blocked for 1h at 20°C with 3% milk in tris-buffered saline added to 0.05% Tween 20 (TBS-T); PVDF membranes (BioRad, France) were incubated overnight at 4°C with rabbit polyclonal anti-CML primary antibody (Abcam 27684, 1/5000, Cambridge, England), followed by TBS-T washing and incubation for 2h with anti-rabbit, alkaline phosphatase-

conjugated secondary antibody (Abcam 97048, 1/5000). Membrane revelation was performed with 1-Step™ NBT/BCIP (ThermoFisher).

2.4. Fluorescence spectroscopy of native and glycated BSA solutions

Fluorescence spectra and intensity were measured in the native BSA and the triplicate reactions of GA-E (GA-E.1 to 3) and GO-E (GO-E.1 to 3) (Table 1) using a Cary Eclipse Fluorescence Spectrometer (Agilent, Les Ulis, France) in solutions at concentrations of 1 mg/mL, at pH 8.0.

2.5. Mass spectrometry characterization of native and glycated BSA

2.5.1. LC-MS/MS quantification of lysine, arginine, and CML after acid hydrolysis

Analyses of native and glycated BSA (all reactions) were performed in triplicate using positive electrospray ionization (ESI+) on a Quattro Premier XE triple-quadrupole mass spectrometer (Waters, Saint-Quentin-en-Yvelines, France) using a Hypercarb column (100 × 2.1 mm, 5 µm; same phase guard column 10 × 2.1 mm, 5 µm; column at 10°C; ThermoFisher). The binary mobile phase was aqueous 12.5 mmol/L NFPA (solvent A) and ACN (solvent B) with the gradient pumped at 200 µL/min over 23 mins as follows: %B: 0–10 mins, 0–22.5%; 10–15 mins, 60%; 15–23 mins, 0%.

Five hundred microliter aliquots of each BSA preparation were lyophilized, and samples reduced for 2h at room temperature with 500 µL 1M $NaBH_4$ in sodium borate buffer (pH 9.2). Five hundred microliters of 12M HCl were added, and samples hydrolyzed at 110°C for 21 h. Aliquots of 100 µL hydrolysate were concentrated in a Speed-Vac (ThermoFisher) and re-solubilized in 1 mL aqueous 12.5 mmol/L NFPA. Samples were filtered (0.45 µm) before preparing x10 dilutions with 12.5 mmol/L aqueous NFPA solutions of Lys-$^{15}N_2$ and Arg-^{13}C (10 µg/mL) for analysis of Lys and Arg, x200 dilutions with CML-d_2 (0.2 µg/mL) in NFPA for the analysis of CML.

The current study is part of a larger, ongoing collaborative project. An in-house reference material (lyophilized infant milk formula) was included in each analytical batch in both LC-MS/MS laboratories (*viz.* the UMR 1167 and ULR 7519 partners (Section 2.6.2.): briefly, one *ca.*50 mg sample of lyophilized milk powder was reduced with $NaBH_4$ prior to hydrolysis in 6M HCl (110°C for 21h). This

reference material is analyzed frequently, and results for all compounds were consistently within one standard deviation of the mean values obtained at both sites (Data not shown).

2.5.2. Proteomic analyses

Proteomic analyses were performed on the native BSA and the triplicate reactions of GA-E (GA-E.1 to 3) and GO-E (GO-E.1 to 3) (Table 1). Matrix-assisted laser desorption/ionization with tandem time-of-flight spectrometric detection (Sciex 4800+ MALDI-TOF/TOF, Sciex, Framingham, MA, USA) [16] was used to determine the molecular weight of the native and glycated BSA (GA-E and GO-E).

The native BSA and triplicate GA-E and GO-E glycated BSA samples were then subjected to protein digestion (100 µg) performed with an eFASP method (enhanced Filter Aided Sample Preparation) [17,18] using chymotrypsin at a protein:enzyme ratio of 1:50 (w/w). After digestion, the peptide concentration was determined with Denovix 11 + (DS-11+, Denovix, Wilmington, USA), and the concentration was adjusted to 1 µg/µL by dilution with ultrapure water containing 0.1% formic acid (Sigma-Aldrich). NanoLC-MS/MS was performed on an Orbitrap Q Exactive plus mass spectrometer via a U3000 RSLC Microfluidic HPLC System (ThermoFisher Scientific, Massachusetts, USA) (Helle et al 2018). One microliter of the peptide mixture at a concentration of 1 µg/µL was injected with solvent A (5% acetonitrile and 0.1% formic acid v/v) for 3 min at a flow rate of 10 µl/min on an Acclaim PepMap100 C18 pre-column (5 µm, 300 µm i.d. × 5 mm). The peptides were separated on a C18 Acclaim PepMap100 C18 reversed phase column (3 µm, 75 mm i.d. × 500 mm), using a linear gradient (5-40%) of solution B (75% acetonitrile and 0.1% formic acid) at a rate of 250 nL.min-1. The column was washed with 100% solution B for 5 minutes and then re-equilibrated with solvent A. The column and pre-column were maintained at 40°C. The analysis duration was 185mins. The LC runs were acquired in positive ion mode with MS scans from m/z 350-1,500 in the Orbitrap at a resolution of 70,000 at m/z 400. The automatic gain was set at $1e10^6$. Sequential MS/MS scans were acquired at 35,000 resolution at m/z 400 in the high-energy collision/dissociation cell for the 15 most-intense ions detected by full-MS survey scans. Automatic gain control was set at $5e10^5$, and the collision energy was 28 eV. Dynamic exclusion was set at 90s and ions with 1 and more than 8 charges were excluded.

Proteomics data were processed with PEAKS X+ (Bioinformatics software, Waterloo, Canada) against a homemade database containing BSA sequences (Swissprot accession number, P02769). Precursor ion mass tolerance was 10 ppm and fragment ion mass tolerance 0.05 Da. Three missed cleavages were allowed. Cysteine carbamidomethylation (C) (+57.02 Da) was set as a fixed modification. Deamidation (NQ) (+0.98 Da), Oxidation or Hydroxylation (MRYPNKD) (+15.99 Da), Carboxymethyl (KR) (+58.005 Da), Glyoxal-derived hydroimidazolones (R) (+39.994 Da), N^{ε}-acetyl-lysine (K) (+42.010 Da), N^{ε}-formyl-lysine (K) (+27.994 Da) were selected as variable modifications. Six variable PTMs (post-translational modifications) were allowed per peptide. PEAKS PTM and SPIDER algorithms were run with similar parameters to search for 313 PTMs, and peptide mutations and homology. The false detection rate (FDR) was set to 1%, and minimal ion intensity for modification was set to 2%.

Raw files from eFASP were analyzed using Mass Spec Studio v 2.1.2.3107 [19]**.** Thus, GOLA (2S)-amino-6-(2-((5S)-amino-5-carboxypentylamino)acetamido)hexanoic acid hydrochloride salt (+39.994 Da), GODIC (2S)-2-amino-6-[[2-[[(4S)-4-amino-4-carboxybutyl]amino]-1,4-dihydroimidazol-5-ylidene]amino]hexanoic acid (+21.984 Da) and GOLD (6-{1-[(5S)-5-ammonio-6-oxido-6-oxohexyl]imidazolium-3-yl}norleucinate) lysine – lysine crosslink (+34.992 Da) were selected as variable modifications**, and c**arbamidomethyl cysteine and methionine oxidation were set as a dynamic modifications. Trypsin was selected as an enzyme with 3 missed cleavages. The error of MS and MS/MS precursors was set to 10 ppm, while the minimum charge of peptides was 3 and the maximum 8. Peptide cross-links with a score higher than 18 were considered for further analysis. The percentages presented correspond to the proportion, relative to the control BSA, of a given modification on a specific peptide modified by the GA or GO reactions. These percentages were calculated for each of the triplicate proteomics analyses, enabling an average value to be calculated for a given modification of a given peptide [16]. The MS proteomics data have been deposited on the ProteomeXchange Consortium (http://proteomecentral.proteomexchange.org) via the PRIDE partner repository with the data set identifier PXD041212.

2.6. Stability of rodent feed pellets enriched with native or glycated BSA

Rodent feed pellets (A04) were prepared by SAFE Custom Diets (Augy, France) and enriched with native or glycated BSA (GO) by extrusion. A total of 7.5 $g/kg_{pellets}$ of glycated BSA was incorporated into pellets to give a dCML diet with 200 $\mu g_{CML}/g_{pellets}$. Similarly, 7.5 $g/kg_{pellets}$ of non-glycated, native BSA was incorporated into pellets as a control diet (STD). A 50 kg batch of the STD diet and a 40 kg batch of the dCML diet were prepared. Each preparation was divided into vacuum-sealed plastic bags containing 10 kg each, submitted to gamma radiation (25 kGy), then stored at 20°C for up to 80 days. Individual bags were opened for use approximately every 20 days and the assays described below were performed.

2.6.1. Quantitation of total protein content

Total protein in feed pellets was determined in triplicate using the Dumas method in a LECO FP528 nitrogen analyzer (Garges les Gonesse, France). One hundred milligrams of powdered pellets were analyzed according to AOAC method 990.03 (AOAC, 1995). The classical nitrogen-to-protein conversion factor of 6.25 was used to calculate protein content.

2.6.2. LC-MS/MS quantification of lysine, CML, and furosine after acid hydrolysis

Triplicate analyses of feed pellets were performed in ESI+ mode on a TSQ Quantum Ultra MS/MS (ThermoFisher) using a Raptor PolarX column (100 x 2.1 mm, 2.7 µm; same-phase guard column 5 x 2.1 mm, 2.7 µm; column at 40°C; Restek, Lisses, France). The binary mobile phase, pumped at 500 µL/min over 13 mins, consisted of 10% 200 mmol/L ammonium formate in ACN (solvent A**)** and aqueous 0.5% formic acid (solvent B), with the following gradient: %B: 0–3.5 min, 12%; 3.5–8 min, 12–70%; 8–13 min, 12%.

Thirty-milligram sub-samples of crushed, homogenized pellets were accurately weighed, and samples were either reduced with $NaBH_4$ prior to hydrolysis (quantification of Lys and CML) or hydrolyzed in 6M HCl without prior reduction (110°C for 21h - quantification of Fur). The analysis procedure was similar

to that described in section 2.5.1., except re-solubilization and dilutions were in aqueous 0.01 M HCl (x20 for Lys, x2 for CML, x10 for Fur).

2.7. Total CML quantification in mouse feces

Mouse feces from animals fed with either the STD or dCML diets were collected from two independent cages housing three animals each. A total of 3 g of feces were collected (weekly collections from the same cages over 3 weeks), and the results presented here represent the averaged CML concentrations in feces over this period. The LC-MS/MS analyses of mouse feces were performed in triplicate (500 mg subsamples) (section 2.5.1). The animals from which feces were collected were not sacrificed at this stage since they were part of another study (Project approval number: 23208-2019120215543800 v4; they were later euthanized by intraperitoneal injection of ketamine (150 mg/kg) and xylazine (10 mg/kg) followed by cervical dislocation for collection of biological fluids and organs).

2.8. Statistical analyses

Data are represented as means ± standard deviation. One way ANOVA test followed by Tukey's posthoc test was performed for multiple comparisons (BSA-GA *vs.* Native BSA (control) *vs.* BSA-GO) of the significance of differences between the control group and the other samples. Analyses were performed using GraphPad Prism 9.0 (San Diego, CA, USA) at $\alpha = 0.05$.

3 Results and discussion

3.1. Quantification of CML, lysine, and arginine in BSA model systems using glyoxylic acid or ribose with or without glyoxal

We explored different approaches to establish an efficient method for CML fortification of BSA which avoided heating or the use of $NaBH_3CN$. In a first set of experiments, five reactions (GA-A to -F) with equimolar quantities of lysine were incubated with different molar ratios of GA and $NaBH_4$, $NaBH(OAc)_3$, or $NaBH_3CN$ (Table 1). The formation of CML ranged between 13.0 ±1.3 and 235.0 ±23.5 µmol/g BSA, corresponding to a minimum of 1% of lysine transformed into CML using $NaBH(OAc)_3$ (GA-B and -C), and a maximum of 24% of CML using $NaBH_3CN$ (GA-E) (Table 2). No linear increase in CML yield was observed with increasing molar

ratios of glyoxylic acid and $NaBH_3CN$ to lysine (GA-F), but increasing GA and $NaBH_3CN$ resulted in a higher loss of lysine, indicating that modifications other than CML took place under these more reactive conditions. The CML yields (%) are presented in Table 2 with corresponding percentage losses of lysine.

Table 2 CML yield (% lysine converted) and lysine loss (%) in native BSA and in BSA glycated with glyoxylic acid (GA) using reductive amination with $NaBH_4$, $NaBH(OAc)_3$, or $NaBH_3CN$, or from BSA glycated with ribose (R) +/- glyoxal (GO; see also Table 1).

Sample	CML Yield		Lysine loss
	µmol/g BSA	% of lysine converted into CML	% of initial lysine
Native BSA (Control)	0.5 ± 0.05	0.05 ± 0.005	0
GA-A	29.0 ± 2.9	3.0 ± 0.3	3.0 ± 0.3
GA-B	13.0 ± 1.3	1.0 ± 0.1	1.0 ± 0.1
GA-C	13.0 ± 1.3	1.0 ± 0.1	1.0 ± 0.1
GA-D	104.0 ± 10.4	11.0 ± 1.1	12.0 ± 1.2
GA-E	235.0 ± 23.5	24.0 ± 2.4	24.0 ± 2.4
GA-F	182.0 ± 18.2	20.0 ± 2.0	29.0 ± 2.9
R-A	19.0 ± 2.3	2.1 ± 0.2	37.5 ± 2.0
R-B	15.5 ± 1.0	1.7 ± 0.1	58.5 ± 5.0
R-GO-A	20.2 ± 2.5	2.2 ± 0.2	41.2 ± 2.7
R-GO-B	32.0 ± 3.2	3.5 ± 0.1	51.7 ± 5.0

Different boron hydrides have been extensively used as reducing agents in the synthesis of protein-bound CML. Overall, we observed that $NaBH_4$ (GA-A) and $NaBH(OAc)_3$ (GA-B and -C) were relatively ineffective compared with $NaBH_3CN$ (GA-D to -F). Others have reported that $NaBH_4$ is a less selective reagent, requiring a pre-incubation phase for imine formation [20], while $NaBH(OAc)_3$ has a limited reduction activity due to the stereo effect of the three acetoxy groups [21]. As anticipated, $NaBH_3CN$ proved to be the most effective reducing agent due to the preferential reduction of iminium ions formed under oxidative conditions at physiological pH [22]. The CML yields presented here were similar to other studies using comparable synthetic routes. The study of Ikeda et al. (1996), working on CML-BSA fortification via reductive amination of a BSA-GA system, reported 16% of lysine was converted to CML. In another protein model (casein), lysine modification to CML was shown to be 38-55% using $NaBH_3CN$ [12,13].

To examine whether other carbonyl compounds could improve CML yield, we tested the synergy of ribose with glyoxal. Ribose has an unstable cyclic form,

rendering it a more reactive sugar compared with hexoses [23], which could favor the glycation of proteins [24]. Here, reactions including ribose (R-A and R-B, R-GO-A and R-GO-B; Table 1) exhibited no real increase in CML production over the BSA-GA system, reaching a maximum of 3.5% lysine transformation to CML. However, high percentage losses of lysine were observed (38%-59%), suggesting the transformation of lysine residues into glycation products other than CML (Table 2). In line with the CML yields observed after 16h of reaction between BSA and ribose, the glycation of BSA by ribose alone was shown to produce 0.1 and 10.3% of CML after 5h and 170h incubation at 37°C, respectively [24].

3.2. Quantification of CML, lysine, and arginine in a new BSA model system using only glyoxal

We then examined a glycation system using glyoxal as the only carbonyl compound (GO-A to -E, Table 1). Under these conditions, CML was formed proportionally with the glyoxal concentration: 0.5, 1, 4, 9 & 13% of lysine modification with 20, 40, 100, 200, and 300 mmol/L of glyoxal, respectively (Figures 1a and 1b). Exceeding 300 mmol/L of glyoxal did not generate more CML (data not shown). Nevertheless, the increase in glyoxal concentrations promoted a concomitant loss of lysine (3, 6, 10, 22, and 31%), accompanied by the emergence of high-molecular-weight BSA complexes visible on western blot membranes (Figure 1b). The glycation process likely changed the intrinsic characteristics of BSA. This phenomenon has been demonstrated recently in a BSA-glucose model where glycation-induced conformational changes were reported, such as the loss of the secondary α-helix structures of BSA [25]. In addition, glyoxal is a well-known protein crosslinking agent, resulting in the formation of GOLD, GOLA, and GODIC [15,26], which may explain the occurrence of a higher proportion of high molecular weight (>130 kDa) protein with increasing glyoxal concentrations (Figure 1b). We discuss this in more detail later in this text.

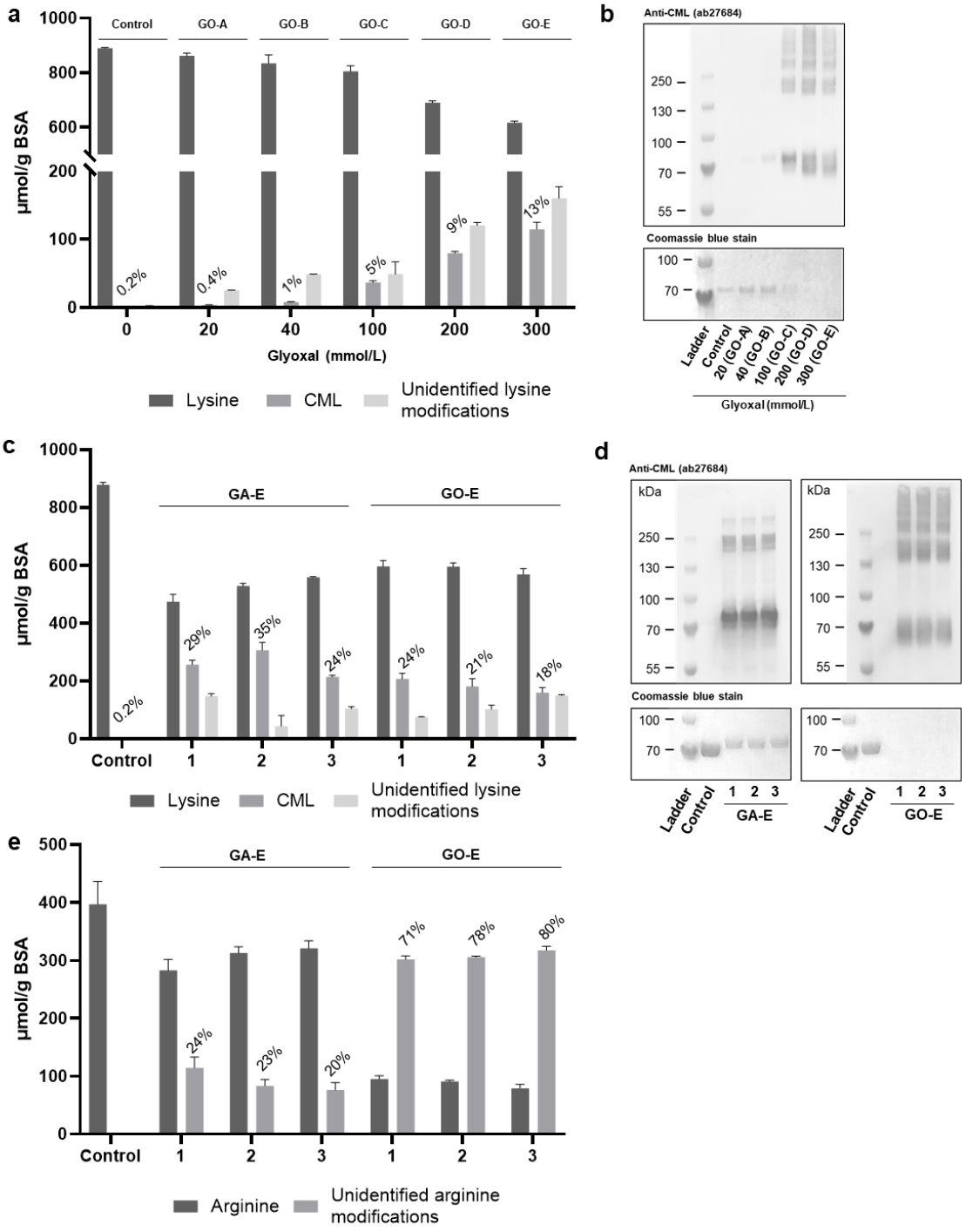

Figure 1 CML formation after incubating BSA with glyoxylic acid (GA) or glyoxal (GO). **(a)** LC-MS/MS quantification of lysine, CML, and the estimation of lysine modifications other than CML in samples GO-A to -E. Percent notations indicate the proportions of lysine residues converted to CML in GA- and GO-BSA glycation systems relative to native BSA. **(b**) Protein-bound CML detection on a western blot with increasing concentrations of glyoxal. Respective Coomassie blue staining of the acrylamide gel in GO-A to -E samples. **(c)** LC-MS/MS quantification of lysine, CML, and the estimation of lysine modifications other than CML within GA-E triplicates (GA-E.1, GA-E.2, GA-E.3) and GO-E triplicates (GO-E.1, GO-E.2, GO-E.3). Percent notations indicate the number of lysine residues converted to CML relative to native BSA. **(d)** Protein-bound CML detection on a western blot on GA-E and GO-E replicates, together with their respective Coomassie blue staining on acrylamide gel. **(e)** LC-MS/MS quantification of arginine and its modifications on GA-E and GO-E

replicates. Percent notations indicate the number of arginine residues converted to unknown arginine modifications, again relative to native BSA.

Although serum albumins (bovine or human) have a higher proportion of lysine than arginine, glyoxal would preferentially promote limited protein modifications of arginine rather than lysine residues [27]. While other amino acids such as tryptophan, histidine and cysteine are also susceptible to modification with glyoxylic acid and glyoxal [28], and modifications of cysteine were observed in our proteomics analyses (data not shown), the focus of our study was the more significant modifications of lysine and arginine residues of our BSA protein. In a recent investigation by Henning et al. (2022), less than 4% of the lysine in a BSA-GO (18 mmol/L) model system was converted to CML, while almost 10% of the total arginine residues were converted into N^{ω}-carboxymethyl-arginine (CMA) [29]. From our experience, a gradual loss of Coomassie blue staining was noticed with the increase in glyoxal concentration (Figures 1b and 1d). This protein staining occurs through the interaction of the dye with basic (lysine, arginine, and histidine) and hydrophobic moieties (phenylalanine and tryptophan), and arginine has been indicated as a primary interaction site with Coomassie anionic species [30]. Hence, the high arginine loss in GO-E samples (>70%, Figure 1e) may have resulted in reduced Coomassie blue staining (Figures 1b and 1d). In addition, it is important to highlight that the overall electrostatic affinity is reduced when glycation takes place. The conversion of lysine, a basic amino acid, into CML which includes an acidic carboxylate, may also have reduced the extent of Coomassie blue staining in both GA-E and GO-E samples.

3.3. Fluorescent characterization of native and glycated BSA

While CML is not fluorescent, other AGEs such as argpyrimidine, HA-triosidine, pentosidine, and vesperlysine [1]. The excitation and emission wavelength ranges for fluorescent AGEs are around 320-380 nm and 380-440 nm, respectively. Measuring fluorescence at their classical wavelengths is an easy and inexpensive way to estimate the formation of AGEs other than CML during the

protein-bound CML fortification, and additionally provides an indication of the specificity of the chemical reaction.

We determined the fluorescence spectra in GA-E and GO-E samples, then compared their fluorescence using 340 nm and 425 nm as excitation and emission wavelengths, respectively (Figure 2). Greatest fluorescence intensity was observed in the GO-E samples, indicating extensive formation of fluorescent glycation adducts or crosslinks under these conditions. A 15-fold difference in fluorescence intensity was observed between the GA-modified BSA and the GO-modified BSA (p<0.0001; Figure 2b). None of the fluorescent AGEs listed above are known to be formed from glyoxylic acid or glyoxal alone, however, and their formation pathways have been shown to involve reducing sugars with at least 3-carbons [31]. The fluorescent adducts or crosslinks formed in our BSA-GA or BSA-GO systems therefore remain to be elucidated.

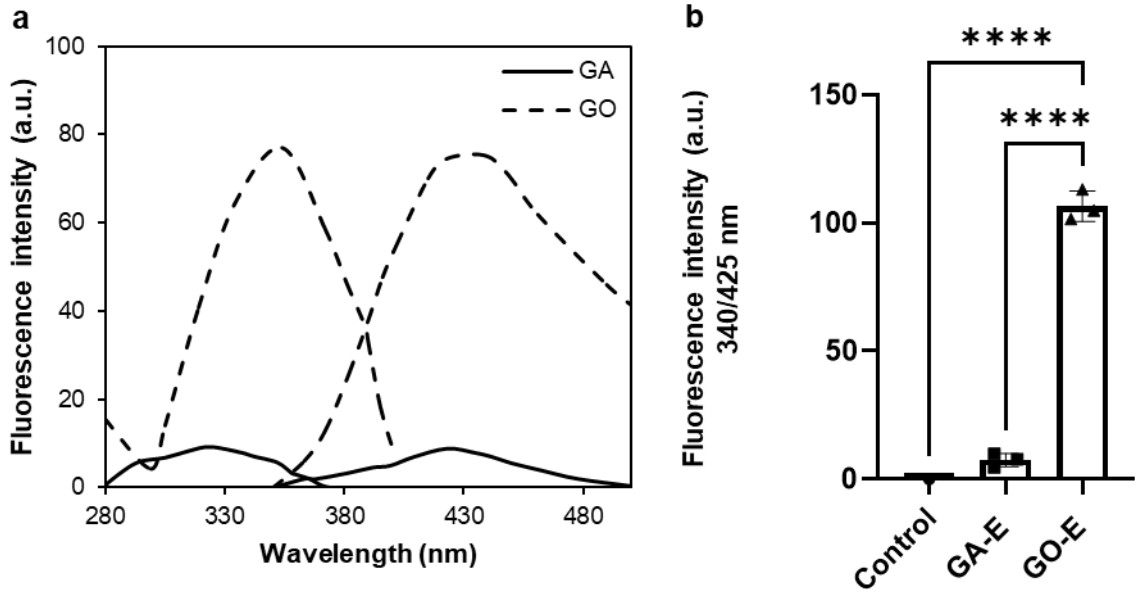

Figure 2 (a) Excitation and emission spectra of glyoxylic acid-modified BSA (GA-E samples) and glyoxal-modified BSA (GO-E samples) and **(b)** fluorescence intensity of native BSA (control), GA-E and GO-E samples at pH 8. Fluorescence excitation was set to 340 nm for the emission spectra, and emission to 425 nm for the excitation spectra. Control versus GA groups: p= 0.4305. Bars represent fluorescence intensity means ± SD of the GA-E (GA-E.1 to 3) and GO-E triplicates (GO-E.1 to 3). **** p≤0.0001.

3.4. Proteomic characterization of native and glycated BSA

In an attempt to identify the modifications promoted by the glycation of BSA, we further compared the triplicate GA-E (GA-E.1 to 3) and GO-E reactions (GO-E.1 to 3 –Table 1) using proteomic approaches. To overcome the decrease in digestion yield by trypsin following the creation of CML and CMA, which remove the basic sites recognized by this enzyme [32], we performed a chymotrypsin digestion which is not hampered by this change as it cleaves the protein after large, hydrophobic amino acids. The CML incidence (%) was calculated relative to non-glycated, native BSA. The average CML yield from the BSA-GA system was 29 ±6%, while the CML yield from the BSA-GO incubations was similar at 21 ±3% (Figure 1c). Both the CML yields and shifts in electrophoretic migration of the protein were relatively reproducible among the triplicates (Figures 1c and 1d).

The native BSA protein contains 59 lysine residues, of which 52 exhibited modifications in both native and glycated BSA (Supplemental material). Differences in the incidence of lysine modifications between native BSA and the GA- or GO-glycated BSA were statistically significant for only 34 of these residues ($p<0.05$, Figure 3a). Among these, GA promoted a higher incidence of CML in residues commonly glycated by both reagents. This was observed for 17 lysine residues where the intensity of modifications promoted by GA was significantly higher compared with GO ($p<0.05$). Six further residues were exclusively modified in the GA-E samples (K155, K183, K204, K211, K235, K495). These observations suggest a greater chemical efficacy of the glycation of lysine residues to CML by GA compared with GO, while the glycation of lysine residues only accessible to GA might explain the slightly higher CML yield we observed in our BSA-GA system. Some of the modified residues in Figure 3a accord with previous studies on the glycation of BSA by fructose. Hinton & Ames (2006) identified nine lysine residues particularly susceptible to glycation with fructose (K28, K36, K151, K180, K399, K437, K495, K523, K548), eight of which feature among the residues in Figure 3a, suggesting that glycation of lysine to CML occurs preferentially at these specific sites on the BSA protein.

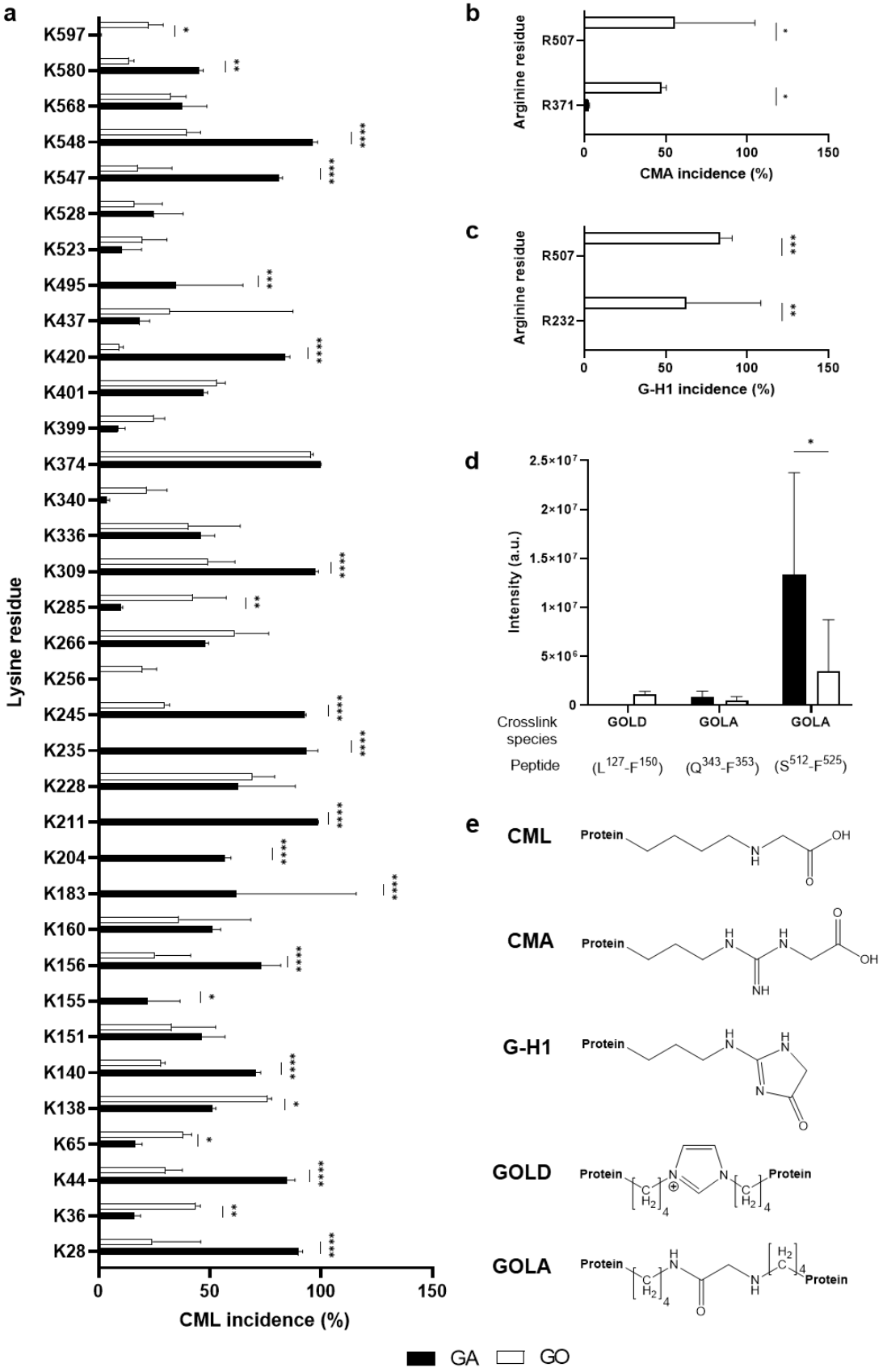

Figure 3 Proteomic analysis of glyoxylic acid (GA) and glyoxal (GO) modified BSA. Only the residues that were significantly modified relative to the original amino acid in non-glycated, native BSA have their p value indicated. **(a)** Average CML incidence (%) in GA- and GO-modified BSA molecules.

Average CMA **(b)** and G-H1 **(c)** incidence (%) in GA- and GO-modified BSA. **(d)** Identification of potential crosslink sites on GA- and GO-modified BSA. Bars represent mean ± SD values (n=3). **(e)** Chemical structures of the main glycation products identified by proteomic analyses. *p≤0.05; **p≤0.01; ***p≤0.001; ****p≤0.0001 for comparisons between the control (non-glycated, native BSA), GA-BSA, and GO-BSA. Bars corresponding to non-glycated BSA are all equal to zero.

A significant incidence of arginine modifications was only observed with glyoxal. A small proportion of arginine residues R371 and R507 were converted into CMA (Figure 3b), but the main glycation adduct of this amino acid was G-H1, which exceeded 80% of the R232 and R507 residues in the GO-E samples (Figure 3c). The incidence of glycation modifications of residues R232, R371, and R507 did not completely explain the average 76% arginine loss we observed in our BSA-GO system, involving a total of 23 arginine residues (Figure 1e). This implies that low-incidence modifications may affect these residues, but that their detection was limited by the sensitivity of our proteomics method.

MALDI-TOF analysis comparing native BSA, GA- and GO-modified BSA revealed a molecular weight change from 66,762 Da (native BSA) to 68,043 Da (GA-E samples) and 68,830 Da (GO-E samples), a difference of 1281 Da and 2068 Da, respectively. The percentage incidence of CML on the lysine residues in Figure 3a enabled an estimate of CML-related increases in the molecular weight of glycated BSA, and showed increases of 1033 Da (GA) and 608 Da (GO). Hence, the CML-related increment in mass (Da) accounted for 80% of the total mass gain in the GA-E samples, but only 30% of the mass gain in the GO-E samples. As expected, then, the increases in molecular weight observed by MALDI-TOF were not explained by the formation of CML alone, but were likely also due to the formation of other glycation adducts and crosslinks. These results are also in line with evidence of a greater diversity of glycation products in GO-E samples seen in the western blot (Figure 1b and 1d) and fluorescence assays (Figure 2).

We detected signals for high molecular weight molecules by both western blot (Figure 1b and 1d) and MALDI-TOF (data not shown) which we hypothesize result from the formation of BSA dimers and trimers associated with glycation crosslinking. The GO-E samples exhibited a significant incidence of the lysine-lysine crosslink GOLD (LSHK^{130}DDSPDLPK^{138}LK^{140}PDPNTLCDEF) between two identical peptides from two different BSA molecules which was not detected in either the native BSA nor the GA-E samples (Figure 3d). This may explain the higher proportion of high molecular weight (>130 kDa) bands clearly observed in western-

blot membranes of these samples (Figures 1b and 1d). Both GA- and GO-BSA exhibited signals for the lysine-lysine, glyoxal-derived cross-link GOLA (QEAK^{346}DAFLGSF and AEDK^{336}DVCK^{340}NY, SALTPDETYVPK^{523}AF and DEK^{528}LF), but this was significant only in the GA-E samples. The low incidence of these crosslinks accords with the literature, where the formation of GOLD, GOLA (two lysine-lysine crosslinks), or GODIC (a lysine-arginine crosslink) are described as being of minor quantitative importance [29]. The low signal intensity from the depleted fractions in such crosslinks observed here could be improved by a pre-concentration of BSA dimers and trimers prior to proteomic analysis.

3.5. Stability of rodent feed pellets enriched with native or GO-glycated BSA

The work described so far was intended to provide a more complete understanding of precisely which glycation products would be added to rodent feed pellets enriched with glycated BSA. The experimental design involved long-term exposure to high dCML, and so CML and furosine (an acid-hydrolysis derivative of the Amadori product fructose-lysine) were rigorously quantified by LC-MS/MS; we were also curious as to the stability of our BSA-enriched pellets over time. Both STD and dCML diets were respectively supplemented with equal amounts of non-glycated, native BSA and glyoxal-glycated BSA (equivalent to GO-E samples). The inclusion of native or GO-modified protein was performed in batches by SAFE Diets and both were stored at 20°C in 10 kg bags. The concentrations of lysine, total protein, furosine and CML of the initial batches are presented in Figure 4, which also illustrates their stability over time.

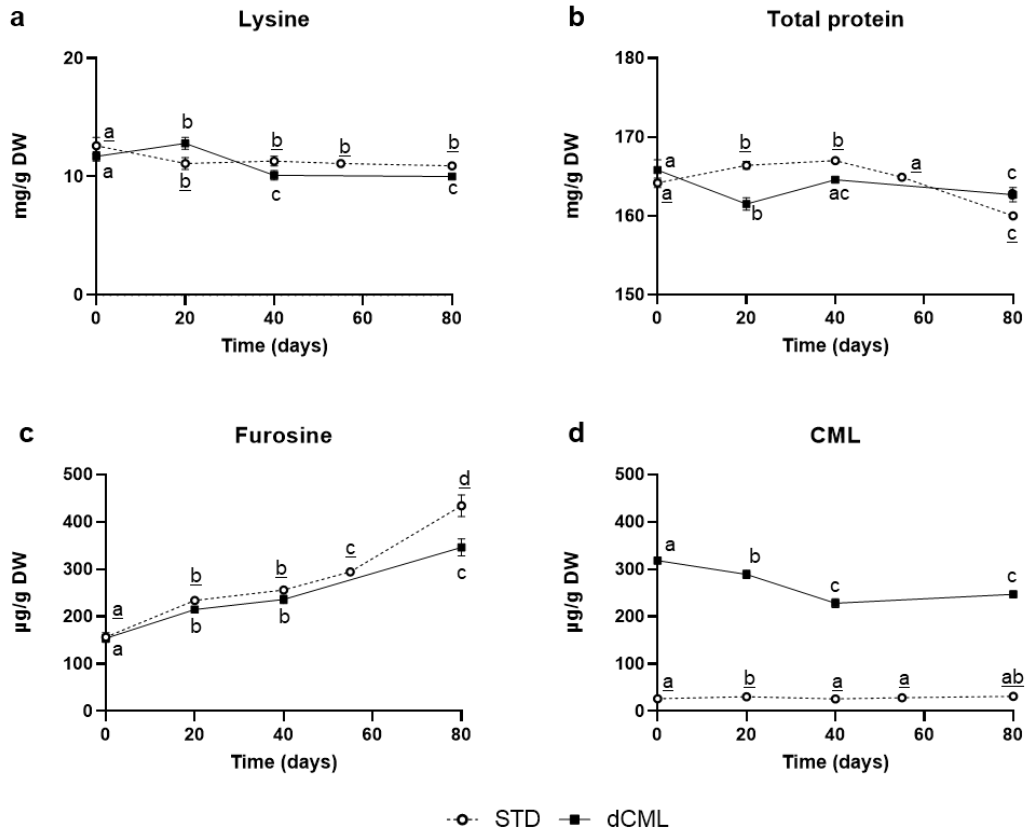

Figure 4 Temporal LC-MS/MS quantification of **(a)** lysine, **(b)** total protein, **(c)** furosine, and **(d)** CML in extruded mouse food pellets enriched with native BSA (STD) or GO-BSA to mimic a CML-rich diet (dCML), over 80 days of storage at 20 °C. Values are expressed as a function of the dry weight (DW) of rodent food. Different letters represent significant difference within diets. Underlined letters correspond to comparisons within STD diet, while non-underlined letters show comparisons within dCML at α=0.05.

The STD and dCML diets did not differ in initial concentrations of lysine, total protein or furosine levels (p>0.05) (Figure 4a - c). The dCML diet contained 270.5 ±40.6 µg CML/g DryWeight of food, approximately 10-fold more CML than the STD diet (26.3 ±0.9 µg CML/g DryWeight of food) (Figure 4d). The different diets were fed to mice during 80 days of experiments and the stability of lysine, total protein, furosine, and CML was assessed by analyzing a sample at the opening of each 10 kg bag. While small fluctuations in these concentrations were expected due to the relatively small sample size taken from each bag, the overall stability of the lysine and total protein contents was good (Figures 4a and 4b).

While there was no difference in initial furosine levels between the two diets, concentrations rose significantly in both diets over the 80 days of storage (p<0.05; this effect was also verified in other batches, data not shown). Furosine is a product formed during acid hydrolysis of Amadori products, and is a widely used surrogate

measure of fructose-lysine [34]. We observed an increase in furosine with storage time which we hypothesize results from the presence of reactive sugars in the raw material used for rodent food preparation. This increase was not affected by the type of BSA used to fortify the feed pellets (either native or glycated), and the formation of fructose-lysine during the storage of common foods is widely described. For example, an increase in furosine of up to 37% has been reported in infant formulas stored at 25°C [35]. To our knowledge, our results present for the first time the evolution of an early glycation product in animal feed pellets stored at 20°C.

The stability of CML in rodent food over 80 days at 20°C is shown in Figure 4d. The STD diet, supplemented with native BSA, showed small but nonetheless significant reduction in dCML contents over time (p<0.05). The dCML diet, supplemented with GO-glycated BSA, exhibited a decrease in CML over time from 40 days in stock (p<0.05). Very few studies have assessed the stability of CML in foods during cooking or storage. This may be linked to the widely held belief that AGEs are, by definition, chemically stable molecules with low reactivity that simply accumulate over time. However, we have already observed a degradation of CML during prolonged cooking of meats (unpublished data), and Cheng et al. (2014) have also shown a decrease in CML over time in cookies heated from 180 to 230°C. But the decrease in dCML content we observed was after long-term storage of the feed pellets at room temperature, and the time/temperature combination is thus totally different from the observation by Cheng et al. (2014). And since we observe an increase in fructose-lysine during storage, it is possible that at least part of the CML is lost to the formation of N-ε-carboxymethyl-N-ε-(1-deoxyfructosyl)-l-lysine (CMFL), which has been recently described in model systems [37]. This newly reported glycation product confirms the reactivity of the secondary amino group of CML, and we have already observed the formation of N-ε-di-carboxymethyl-l-lysine in model systems (unpublished data), but CMFL is the first heterogeneous, multiple glycation to be described. Future analyses of rodent pellets will include CMFL, but with regard to the current study we are not aware of any reports of chemical instability of CML during storage and, while the decrease is small, its apparent instability in fortified rodent chow requires further consideration.

3.6. dCML excretion in mouse feces

Mice fed with the STD diet had an average dCML intake approximately 10-fold less than animals on the dCML diet. The daily exposure to dCML was estimated to be 2.1 mg CML/kg body weight in the STD group and 23 mg CML/kg in the dCML group. We confirmed that CML fecal excretion was proportional to this disparity in CML concentrations between the 2 diets. The average CML concentration in fresh feces of the STD and dCML groups was 35.00 ±2.64 μg CML/g_{feces} in the STD group, and 299.67 ±14.74 μg CML/g_{feces}, respectively (p<0.05). When CML excretion was expressed as a percentage of ingested CML, we found a small but significant difference between groups corresponding to 26% (STD) and 33% (dCML), or roughly 1/3 of the ingested CML (p=0.02). Overall, CML fecal excretion was found to be proportional to the daily dietary intake. Others have reported similar results in mice, rats, and humans. A study which quantified the fecal elimination of CML by adult rats reported an excretion of about 37% among animals that consumed extruded proteins [38]. Our results are also in line with a previous study in humans exposed to a low- or high-CML diet (22.5-31.7% CML excretion) [39]. The excretion of CML is reported to be associated with clearance into urine as well as feces, partial retention in organs and tissues, as well as partial metabolism, essentially by colonic microbiota [10,40]. However, a complete picture of all the mechanisms that govern dCML accumulation, metabolism, and excretion remains to be elucidated.

4 Conclusions

In summary, we have shown that an efficient and reproducible synthesis of protein-bound CML can be achieved with the use of glyoxal in a BSA model system. The reaction of glyoxylic acid and $NaBH_3CN$ to produce CML remains the most effective method with respect to the CML yields, resulting in fewer structural modifications of the BSA molecule compared with glyoxal. We recognize that the glyoxal concentrations used here may seem extreme, but it was necessary to minimize the volume of reactions to be dialyzed for the large-scale production of protein-bound CML. Although no food models perfectly mimic the glycation of BSA, and none of the reactions herein can be described as representative of glycation as it may occur during industrial or domestic food preparation, we aimed to add glycated BSA to animal feed pellets in a way that minimized alterations to the food

matrix. The fecal excretion of CML in animals on the dCML diet, produced from extruded pellets fortified with glyoxal-modified BSA, was very similar to literature values for CML excretion in both animals and humans. This suggests that, despite the highly artificial conditions associated with our manufacture of a synthetic dCML diet, CML absorption/excretion dynamics in our murine model remained similar to those reported elsewhere.

Although using glyoxylic acid with $NaBH_3CN$ induced more specific glycation of the BSA's lysine residues, the results of our comparative study underline that even this method does not generate CML alone. Acid hydrolysis followed by isotope-dilution LC-MS/MS allowed us to precisely determine the concentrations of CML, lysine and arginine. A limitation of this approach is of course that it was not possible to quantify other AGEs more or less sensitive to acid hydrolysis such as CMA and G-H1, but our proteomic analyses, using a milder enzymatic hydrolysis, enabled us to reveal the presence of these AGEs. Lysine-lysine dimers GOLD and GOLA occurred at only a low frequency, indicating a low probability of formation of these AGEs even under the very intensive conditions of *in vitro* glycation, but which was also close to the limits of sensitivity for our analytical technique. It may be that further characterization of these samples, notably the number and type of crosslinks, will raise further research questions, but this study nevertheless adds significant knowledge to facilitate the production of glycated proteins for the study of dietary AGEs.

Declaration of interests: Authors declare no conflict of interest.

Ethical approval: All experiments carried out in animals were in accordance with the French ethical laws. Project approval number: 23208-2019120215543800 v4.

Acknowledgments: This study was funded by the French Agence Nationale de la Recherche (ANR-19-CE34-0013 ExoAGEing). The authors thank S. Balasanyants for preliminary bibliographical research.

5 References

1. Perrone, A.; Giovino, A.; Benny, J.; Martinelli, F. Advanced Glycation End Products (AGEs): Biochemistry, Signaling, Analytical Methods, and Epigenetic Effects. *Oxidative Medicine and Cellular Longevity* **2020**, *2020*, 1–18, doi:10.1155/2020/3818196.
2. Briceno Noriega, D.; Zenker, H.E.; Croes, C.-A.; Ewaz, A.; Ruinemans-Koerts, J.; Savelkoul, H.F.J.; van Neerven, R.J.J.; Teodorowicz, M. Receptor Mediated Effects of Advanced Glycation End Products (AGEs) on Innate and Adaptative Immunity: Relevance for Food Allergy. *Nutrients* **2022**, *14*, 371, doi:10.3390/nu14020371.
3. Lund, M.N.; Ray, C.A. Control of Maillard Reactions in Foods: Strategies and Chemical Mechanisms. *J. Agric. Food Chem.* **2017**, *65*, 4537–4552, doi:10.1021/acs.jafc.7b00882.
4. Nogueira Silva Lima, M.T.; Howsam, M.; Anton, P.M.; Delayre-Orthez, C.; Tessier, F.J. Effect of Advanced Glycation End-Products and Excessive Calorie Intake on Diet-Induced Chronic Low-Grade Inflammation Biomarkers in Murine Models. *Nutrients* **2021**, *13*, 3091, doi:10.3390/nu13093091.
5. van Dongen, K.C.W.; Linkens, A.M.A.; Wetzels, S.M.W.; Wouters, K.; Vanmierlo, T.; van de Waarenburg, M.P.H.; Scheijen, J.L.J.M.; de Vos, W.M.; Belzer, C.; Schalkwijk, C.G. Dietary Advanced Glycation Endproducts (AGEs) Increase Their Concentration in Plasma and Tissues, Result in Inflammation and Modulate Gut Microbial Composition in Mice; Evidence for Reversibility. *Food Research International* **2021**, *147*, 110547, doi:10.1016/j.foodres.2021.110547.
6. Helou, C.; Nogueira Silva Lima, M.T.; Niquet-Leridon, C.; Jacolot, P.; Boulanger, E.; Delguste, F.; Guilbaud, A.; Genin, M.; Anton, P.M.; Delayre-Orthez, C.; et al. Plasma Levels of Free Nε-Carboxymethyllysine (CML) after Different Oral Doses of CML in Rats and after the Intake of Different Breakfasts in Humans: Postprandial Plasma Level of SRAGE in Humans. *Nutrients* **2022**, *14*, 1890, doi:10.3390/nu14091890.
7. Grossin, N.; Auger, F.; Niquet-Leridon, C.; Durieux, N.; Montaigne, D.; Schmidt, A.M.; Susen, S.; Jacolot, P.; Beuscart, J.-B.; Tessier, F.J.; et al. Dietary CML-Enriched Protein Induces Functional Arterial Aging in a RAGE-Dependent Manner in Mice. *Mol Nutr Food Res* **2015**, *59*, 927–938, doi:10.1002/mnfr.201400643.
8. Luevano-Contreras, C.; Chapman-Novakofski, K. Dietary Advanced Glycation End Products and Aging. *Nutrients* **2010**, *2*, 1247–1265, doi:10.3390/nu2121247.
9. Scheijen, J.L.; Clevers, E.; Engelen, L.; Dagnelie, P.C.; Brouns, F.; Stehouwer, C.D.; Schalkwijk, C.G. Analysis of Advanced Glycation Endproducts in Selected Food Items by Ultra-Performance Liquid Chromatography Tandem Mass Spectrometry: Presentation of a Dietary AGE Database. *Food chemistry* **2016**, *190*, 1145–1150.
10. Tessier, F.J.; Niquet-Léridon, C.; Jacolot, P.; Jouquand, C.; Genin, M.; Schmidt, A.-M.; Grossin, N.; Boulanger, E. Quantitative Assessment of Organ Distribution of Dietary Protein-Bound 13 C-Labeled Nε -Carboxymethyllysine after a Chronic Oral Exposure in Mice. *Mol Nutr Food Res* **2016**, *60*, 2446–2456, doi:10.1002/mnfr.201600140.
11. Xue, J.; Rai, V.; Frolov, S.; Singer, D.; Chabierski, S.; Xie, J.; Reverdatto, S.; Burz, D.S.; Schmidt, A.M.; Hoffman, R.; et al. Advanced Glycation End Product (AGE) Recognition by the Receptor for AGEs (RAGE). *Structure* **2011**, *19*, 722–732, doi:10.1016/j.str.2011.02.013.
12. Andersen, J.M.; Hjelmgaard, T.; Dragsted, L.O.; Nielsen, J. Convenient Synthesis of Nε-(Carboxymethyl)Lysine, a Key Advanced Glycation Endproduct Biomarker. *Synlett* **2012**, *2012*, 531–534, doi:10.1055/s-0031-1290348.
13. Faist, V.; Müller, C.; Drusch, S.; Erbersdobler, H.F. Selective Fortification of Lysinoalanine, Fructoselysine and Nε-Carboxymethyllysine in Casein Model Systems. *Nahrung* **2001**, *45*, 218–221, doi:10.1002/1521-3803(20010601)45:3<218::AID-FOOD218>3.0.CO;2-Q.
14. Ikeda, K.; Higashi, T.; Sano, H.; Jinnouchi, Y.; Yoshida, M.; Araki, T.; Ueda, S.; Horiuchi, S. *N* ε -(Carboxymethyl)Lysine Protein Adduct Is a Major Immunological Epitope in Proteins Modified with Advanced Glycation End Products of the Maillard Reaction. *Biochemistry* **1996**, *35*, 8075–8083, doi:10.1021/bi9530550.
15. Glomb, M.A.; Pfahler, C. Amides Are Novel Protein Modifications Formed by Physiological Sugars. *Journal of Biological Chemistry* **2001**, *276*, 41638–41647, doi:10.1074/jbc.M103557200.
16. Pien, N.; Bray, F.; Gheysens, T.; Tytgat, L.; Rolando, C.; Mantovani, D.; Dubruel, P.; Vlierberghe, S.V. Proteomics as a Tool to Gain next Level Insights into Photo-Crosslinkable

Biopolymer Modifications. *Bioactive Materials* **2022**, *17*, 204–220, doi:10.1016/j.bioactmat.2022.01.023.
17. Erde, J.; Loo, R.R.O.; Loo, J.A. Enhanced FASP (EFASP) to Increase Proteome Coverage and Sample Recovery for Quantitative Proteomic Experiments. *J. Proteome Res.* **2014**, *13*, 1885–1895, doi:10.1021/pr4010019.
18. Helle, S.; Bray, F.; Verbeke, J.; Devassine, S.; Courseaux, A.; Facon, M.; Tokarski, C.; Rolando, C.; Szydlowski, N. Proteome Analysis of Potato Starch Reveals the Presence of New Starch Metabolic Proteins as Well as Multiple Protease Inhibitors. *Frontiers in Plant Science* **2018**, *9*.
19. Sarpe, V.; Rafiei, A.; Hepburn, M.; Ostan, N.; Schryvers, A.B.; Schriemer, D.C. High Sensitivity Crosslink Detection Coupled With Integrative Structure Modeling in the Mass Spec Studio. *Mol Cell Proteomics* **2016**, *15*, 3071–3080, doi:10.1074/mcp.O116.058685.
20. Ranu, B.C.; Majee, A.; Sarkar, A. One-Pot Reductive Amination of Conjugated Aldehydes and Ketones with Silica Gel and Zinc Borohydride. *J. Org. Chem.* **1998**, *63*, 370–373, doi:10.1021/jo971117h.
21. Abdel-Magid, A.F.; Carson, K.G.; Harris, B.D.; Maryanoff, C.A.; Shah, R.D. Reductive Amination of Aldehydes and Ketones with Sodium Triacetoxyborohydride. Studies on Direct and Indirect Reductive Amination Procedures1. *J. Org. Chem.* **1996**, *61*, 3849–3862, doi:10.1021/jo960057x.
22. Borch, R.F.; Bernstein, M.D.; Durst, H.D. Cyanohydridoborate Anion as a Selective Reducing Agent. *J. Am. Chem. Soc.* **1971**, *93*, 2897–2904, doi:10.1021/ja00741a013.
23. Wei, Y.; Han, C.S.; Zhou, J.; Liu, Y.; Chen, L.; He, R.Q. D-Ribose in Glycation and Protein Aggregation. *Biochim Biophys Acta* **2012**, *1820*, 488–494, doi:10.1016/j.bbagen.2012.01.005.
24. Glomb, M.A.; Monnier, V.M. Mechanism of Protein Modification by Glyoxal and Glycolaldehyde, Reactive Intermediates of the Maillard Reaction (∗). *Journal of Biological Chemistry* **1995**, *270*, 10017–10026, doi:10.1074/jbc.270.17.10017.
25. Peng, J.; Wen, W.; Liang, G.; Huang, W.; Qiu, Z.; Wang, Q.; Xiao, G. Camellia Oleifera Shells Polyphenols Inhibit Advanced Glycation End-Products (AGEs) Formation and AGEs-Induced Inflammatory Response in RAW264.7 Macrophages. *Industrial Crops and Products* **2023**, *197*, 116589, doi:10.1016/j.indcrop.2023.116589.
26. Lopez-Clavijo, A.F.; Duque-Daza, C.A.; Soulby, A.; Canelon, I.R.; Barrow, M.; O'Connor, P.B. Unexpected Crosslinking and Diglycation as Advanced Glycation End-Products from Glyoxal. *J. Am. Soc. Mass Spectrom.* **2014**, *25*, 2125–2133, doi:10.1007/s13361-014-0996-7.
27. Henning, C.; Glomb, M.A. Pathways of the Maillard Reaction under Physiological Conditions. *Glycoconj J* **2016**, *33*, 499–512, doi:10.1007/s10719-016-9694-y.
28. Herraiz, T.; Peña, A.; Mateo, H.; Herraiz, M.; Salgado, A. Formation, Characterization, and Occurrence of β-Carboline Alkaloids Derived from α-Dicarbonyl Compounds and l-Tryptophan. *Journal of Agricultural and Food Chemistry* **2022**, *70*, 9143–9153.
29. Henning, C.; Stübner, C.; Arabi, S.H.; Reichenwallner, J.; Hinderberger, D.; Fiedler, R.; Girndt, M.; Di Sanzo, S.; Ori, A.; Glomb, M.A. Glycation Alters the Fatty Acid Binding Capacity of Human Serum Albumin. *J. Agric. Food Chem.* **2022**, *70*, 3033–3046, doi:10.1021/acs.jafc.1c07218.
30. Georgiou, C.D.; Grintzalis, K.; Zervoudakis, G.; Papapostolou, I. Mechanism of Coomassie Brilliant Blue G-250 Binding to Proteins: A Hydrophobic Assay for Nanogram Quantities of Proteins. *Anal Bioanal Chem* **2008**, *391*, 391–403, doi:10.1007/s00216-008-1996-x.
31. Tessier, F.J.; Monnier, V.M.; Sayre, L.M.; Kornfield, J.A. Triosidines: Novel Maillard Reaction Products and Cross-Links from the Reaction of Triose Sugars with Lysine and Arginine Residues. *Biochemical Journal* **2003**, *369*, 705–719, doi:10.1042/bj20020668.
32. Lapolla, A.; Fedele, D.; Reitano, R.; Aricò, N.C.; Seraglia, R.; Traldi, P.; Marotta, E.; Tonani, R. Enzymatic Digestion and Mass Spectrometry in the Study of Advanced Glycation End Products/Peptides. *J. Am. Soc. Mass Spectrom.* **2004**, *15*, 496–509, doi:10.1016/j.jasms.2003.11.014.
33. Hinton, D.J.S.; Ames, J.M. Site Specificity of Glycation and Carboxymethylation of Bovine Serum Albumin by Fructose. *Amino Acids* **2006**, *30*, 425–434, doi:10.1007/s00726-006-0269-2.

34. Erbersdobler, H.F.; Somoza, V. Forty Years of Furosine - Forty Years of Using Maillard Reaction Products as Indicators of the Nutritional Quality of Foods. *Mol Nutr Food Res* **2007**, *51*, 423–430, doi:10.1002/mnfr.200600154.
35. Bosch, L.; Alegrı´a, A.; Farré, R.; Clemente, G. Effect of Storage Conditions on Furosine Formation in Milk–Cereal Based Baby Foods. *Food Chemistry* **2008**, *107*, 1681–1686, doi:10.1016/j.foodchem.2007.09.051.
36. Cheng, L.; Jin, C.; Zhang, Y. Investigation of Variations in the Acrylamide and N(ε) -(Carboxymethyl) Lysine Contents in Cookies during Baking. *J Food Sci* **2014**, *79*, T1030-1038, doi:10.1111/1750-3841.12450.
37. Hellwig, M.; Nitschke, J.; Henle, T. Glycation of N-ε-Carboxymethyllysine. *Eur Food Res Technol* **2022**, *248*, 825–837, doi:10.1007/s00217-021-03931-7.
38. Alamir, I.; Niquet-Leridon, C.; Jacolot, P.; Rodriguez, C.; Orosco, M.; Anton, P.M.; Tessier, F.J. Digestibility of Extruded Proteins and Metabolic Transit of Nε-Carboxymethyllysine in Rats. *Amino Acids* **2013**, *44*, 1441–1449, doi:10.1007/s00726-012-1427-3.
39. Delgado-Andrade, C.; Tessier, F.J.; Niquet-Leridon, C.; Seiquer, I.; Pilar Navarro, M. Study of the Urinary and Faecal Excretion of Nε-Carboxymethyllysine in Young Human Volunteers. *Amino Acids* **2012**, *43*, 595–602, doi:10.1007/s00726-011-1107-8.
40. Hellwig, M.; Auerbach, C.; Müller, N.; Samuel, P.; Kammann, S.; Beer, F.; Gunzer, F.; Henle, T. Metabolization of the Advanced Glycation End Product N-ε-Carboxymethyllysine (CML) by Different Probiotic E. Coli Strains. *J Agric Food Chem* **2019**, *67*, 1963–1972, doi:10.1021/acs.jafc.8b06748.

CHAPTER 6

Effects of early-life and chronic exposure to dietary AGEs on local and systemic inflammatory and oxidative stress biomarkers

This chapter presents the primary findings associated with the animal experiments conducted in this doctoral project. The data presented here have not been published, and ongoing analysis of several organs and biological samples is still underway. Therefore, the interpretations provided below are preliminary and subject to revision in light of future results.

ABSTRACT

Among the various factors that contribute to the onset of chronic inflammation, diet is suggested to play a role in triggering inflammation, oxidative stress, senescence, and the modulation of the gut microbiota. These changes may have implications from early life onwards. Advanced Glycation End-Products (AGEs), a class of neoformed compounds generated during the thermal processing of foods, are widely present in “Westernized diets”. The accumulation of dietary AGEs in various organs is believed to contribute to the initiation of Chronic Low-Grade Inflammation (CLGI), the induction of glycoxidative stress, and the modulation of the gut microbiota. Carboxymethyl-lysine (CML) is a well-known AGE used as a benchmark biomarker of protein glycation. Whether the interaction between glycation products such as CML and the Receptor for Advanced Glycation End-Products (RAGE) takes part in establishing CLGI and is involved in glycoxidative stress and immunosenescence has been widely studied. However, it remains unclear whether an early and/or lifelong exposure to dietary AGEs participates in the installation of CLGI favoring inflammaging, and whether these potential changes are reversible or permanent. We aimed to investigate the physiological changes in Wild-Type (WT) and RAGE KO mice fed since the perinatal period with a standard diet (STD - 20.8 ± 5.1 $\mu g_{dCML}/g_{food}$) or a dCML-enriched diet (255.2 ± 44.5 $\mu g_{dCML}/g_{food}$) during 35 or 70 weeks. Further, we aimed to investigate whether a diet-switch (dCML → STD) at an early age (6 weeks) would contribute to a reversion of the putative deleterious effects of dCML. We confirmed the RAGE-independent accumulation of free CML in the kidneys, ileum, and colon after 35 and 70 weeks of dietary intervention. Diet switching diminished tissue dCML levels to concentrations comparable with the STD diet. The dCML diet had no obvious effect on endogenous glycation, inflammation oxidative stress, and senescence parameters. The relative expression of *TNFα*, *VCAM1*, *IL6*, and *P16* genes were all upregulated in an age-dependent manner, most notably in the kidneys of WT animals. Such increases were less remarkable in RAGE KO mice. In addition, RAGE knockout seemed to have a role in the downregulation of *EZH2*, which may indicate a possible involvement of RAGE in renal cell epigenetic control. Overall, the chronic consumption of dCML led to increased levels of free CML in tissues, but no real increments in inflammaging-related parameters, while RAGE knockout appeared to be protective and reduced age-related inflammation. Ongoing research will examine biomarkers of immunosenescence and the composition of the intestinal microbiota. This will help in understanding the impact of dCML on the immune system and its potential implications for the gut-brain axis.

Key-words: glycation, carboxymethyl-lysine, lysine, RAGE, inflammaging, senescence, oxidative stress

1 Introduction

Human life expectancy has increased over recent decades [1], and has been associated with medical progress and the implementation of public policies (*e.g.* nutritional information, encouraging physical activity) to encourage healthy lifestyles [2]. Despite rapid advancements in medical care, the growing population of elderly individuals may lead to an elevated occurrence of age-related diseases and a decline in quality of life [3]. Aging is a multifactorial process under the influence of intrinsic (*e.g.* individual genome, metabolism), and environmental (*e.g.* diet, smoking) factors [4]. The presence of persistent Chronic Low-Grade Inflammation (CLGI) throughout a person's lifespan, coupled with increased oxidative stress processes, are thought to play a fundamental role in the development of age-related changes in physiological function, commonly collectively referred to as "Inflammaging" [5,6]. However, the precise mechanisms, and in particular how they may interfere with metabolic dysfunctions and play a role in chronic pathologies and immunosenescence, remain to be fully elucidated [7,8].

Diet is increasingly acknowledged as an important environmental factor that plays a role in the onset of chronic dysfunctions, and which can therefore contribute to a gradual decline in overall well-being. Nutritional imbalance is a well-known risk factor for the development of diabetes, cardiovascular diseases, or obesity, to cite only three of the main health concerns among Westernized populations [9]. Diet may not only influence an adult's quality of life but is considered to have a major influence on health from very early in life, including the intrauterine period [10,11] Parental eating behavior was demonstrated to reprogram children's epigenome, having permanent neurobiological effects that increased susceptibility to diabetes and obesity [12,13]. These findings suggest that this period of life may be regarded as an opportunity window for genomic, metabolic, immunological, and gut microbiota reprogramming [12,14,15]. They build upon the concept of early-life defining adaptability to environmental stimuli and have especial relevance with respect the maturation of the brain-gut-microbiota axis [16,17].

The harmful effects of diet are discussed in the context of excessive calorie consumption in an imbalanced diet, but the presence of food contaminants such as pesticides and neoformed compounds is also receiving attention [18]. A part of these neoformed compounds is a group of chemically diverse molecules, called Advanced Glycation End-Products (AGEs), which originate from the reaction between amino

acids and reactive sugars [19]. Lysine moieties are major glycation targets leading to the formation of diverse AGEs such as N^{ε}-carboxymethyl-lysine (CML), a stable biomarker of endogenous and exogenous glycation [20]. Glycation, as it may also be named, happens both under physiological conditions (endogenous glycation) and food processing and storage conditions (exogenous glycation) [21].

Protein-bound glycation products, including protein-bound CML, are the predominant form of glycation found in foods and were suggested to have strong binding affinity to the Receptor for Advanced Glycation End-Products (RAGE) [22,23]. RAGE is a transmembrane receptor with multiple ligands that is involved in cellular survival responses [24]. However, a significant concern related to the intake of AGEs is the quantity acquired through dietary sources. Several food products such as breads, cookies, and milk (including infant formulas) have elevated levels of CML, for example. The estimated levels of CML in bread were 1.29 mg_{CML}/100 g_{food}, in cereals 2.55 mg_{CML}/100 g_{food}, and 0.13 mg_{CML}/100 g_{food} in fruits and vegetables [25]. RAGE, which plays a role in downstream inflammation activation, partially mediates the impact of AGEs on CLGI, oxidative stress activation, and subsequent acceleration of the aging process [26]. Furthermore, studies have shown that the accumulation of dietary CML (dCML) in the kidneys or aorta can induce local inflammation and contribute to tissue dysfunction [27,28]. Although no consensus may exist in the academic community on the precise mechanisms promoting physiological dysfunctions, circulatory and tissue accumulation of dietary AGEs in the body are considered potential activating factors of inflammation, oxidative stress, immunosenescence, and cellular aging [29].

With the main concepts and the recent scientific discoveries in mind, it is hypothesized that exposure to dCML (in early life and/or lifelong) takes part in the installation of CLGI and pro-oxidative status in a mechanism mediated by the AGE-RAGE axis. Meanwhile, we believed that the absence of RAGE in genetically modified knockout mice would play a protective role in this dietary context. In addition, the consumption of dCML was hypothesized to promote dCML tissue accumulation, increase oxidative stress, and remodel gut microbiota. On the reversibility of the effects of the exposure to dCML, we hypothesized that an early-life diet switch to a lower level of dCML could contribute to the attenuation or reversibility of the possible long-term deleterious effects. To resolve this question, molecular markers on inflammation, oxidative stress, immunosenescence, the

analysis of gut microbiota, as well as the accumulation of free and protein-bound glycation products have been investigated on multiple samples from 6, 35, and 70 weeks old Wild-Type (WT) and RAGE KO C57BL/6 mice on control diets or enriched in dCML.

2 Materials and methods

2.1. *In vivo* experiments

2.1.1. Animals

Mice were housed in stainless steel cages under a controlled temperature (20 °C) and 12 h light-dark cycles in compliance with current legislation and recommendations. They had free access to food and water throughout the study. The health status of the animals was constantly verified, and the weight was measured weekly (from the 15 weeks old). Animals were housed and experiments carried out at the EOPS1 Animal Facility, University of Lille (France), according to local ethical procedures and the approval of protocol APAFIS 23208-2019120215543800 v4 (ANR ExoAgeing Project). Animal care, handling, and experimentation all complied with the current EU guidelines for the use of laboratory animals. Inbred Wild-Type (WT) mice were used as a reference for a “regular” aging response, and RAGE-deficient mice (RAGE KO lineage engineered at the University of Heidelberg, Germany [30]) were used as a potentially less-susceptible strain to CLGI and inflammaging. Animals used in these experiments were generated from the crossing of heterozygous founder animals (1st Generation - F1). From the resulting offspring, only homozygous animals were selected, either for the presence or absence of RAGE, ensuring a common genetic background. Littermates were then crossed (2nd generation - F2) to generate the offspring used in early-life and lifelong dietary experiments. A total of six reproduction series were required to achieve the desired number of animals.

2.1.2. Diet

To test the effects of dCML consumption, two diets (low and high levels of dCML) were prepared by modifying the base rodent regimes (SAFE A03 and SAFE A04; SAFE Diets, Augy, France). The A03 diet was provided during breeding and maternal feeding periods since it is higher in proteins and fats; on the other hand, A04 was better for the growing phase and during adult life. In our experiments, A03 diets were provided throughout the reproduction period to parents (males and females) and up to offspring weaning, while A04 diets were provided from weaning onwards (Figure 1). Both A03 and A04 were enriched with the addition of glycated or non-glycated bovine serum albumin (BSA). A complete description of the synthesis of glycation of BSA with glyoxal is described in CHAPTER 5 of this thesis.

Types of diets:

i. **Standard Diet (STD)** | A03 or A04 enriched with non-glycated BSA

ii. **dCML Diet (dCML)** | A03 or A04 enriched with dCML-BSA

The average amount (± SD) of dCML in the STD diet was measured to be 20.8±5.0 $\mu g_{dCML}/g\ DW_{food}$, and in the dCML-enriched diet it was 255.2±44.0 $\mu g_{dCML}/g\ DW_{food}$. The proportion of BSA added to the feed pellets, glycated or not, was adjusted so there was no difference in protein content between the diets. Nutritional quality (lysine and total protein levels), as well as CML and furosine amounts, were measured across the different batches to verify the homogeneity in feed pellet preparation (data presented in CHAPTER 4). Food and water were provided *ad libitum* throughout the whole experiment. Food intake was estimated among adult animals (50-70 weeks old) during one week of surveillance.

2.1.3. Experimental design

The experimental design, including the different treatments, is graphically represented in Figure 1. For testing the lifelong effects of dCML exposure, WT animals were divided into two groups fed either STD or dCML diets (Figure 1). Similarly, RAGE KO mice were separated into two groups with an STD group, and a dCML group (Figure 1). To test whether the reversibility of the effects of dCML resulting from an early life consumption would be possible, a third group of WT animals was created where a diet switch took place at 6 weeks of life, changing from the dCML to the STD diet (Figure 1). Animals were randomly allocated into the different diet treatments presented in Table 1.

Table 1 The effective number of animals attributed to each treatment.

		Sample size					
		6 weeks		**35 weeks**		**70 weeks**	
Diet	**Genotype**	Female	Male	Female	Male	Female	Male
STD	WT	4	4	8	12	8	14
dCML	WT	2	2	10	3	9	8
Switch	WT	-	-	10	3	7	7
STD	RAGE KO	3	4	11	7	12	6
dCML	RAGE KO	2	2	5	7	12	9

2.1.4. Collection of tissues and fluids

Sacrifices proceeded after the injection of ketamine/xylazine (150 mg/kg:10 mg/kg) followed by cervical dislocation. After 6, 35, and 70 weeks of dietary intervention animals were sacrificed and the kidneys, ileum, colon, skin, and plasma were collected to evaluate inflammatory and aging parameters. The relationship between the collected organs and analyses conducted are presented in Table 2. For the switch group, animals were sacrificed, and organs were collected at the end of 35, and 70 weeks of diet. Lung samples were only collected from 70-week-old animals. Collected samples were immediately preserved in liquid nitrogen and stored at -80°C until analysis. Samples of spleen and caecum were collected, under the same conditions described above, for the assessment of immunosenescence parameters and gut microbial diversity (Table 2). However, data acquisition was not completed at the time of submission of the thesis.

Table 2 Biomarker panel for the evaluation of CLGI and its crosstalking factors in the murine model under dAGE exposure.

Parameter	Target	Biomarker	Technique
Glycation	Kidneys ileum, colon, skin, serum	Free and protein-bound CML	LC/MS-MS
Inflammation	Kidneys ileum, colon, lungs	*IL-6, TNFα, VCAM-1, RAGE, P16, GLβ1, SIRT1, PGC1α, GLO1*	RT-qPCR
Oxidative stress	Plasma	MDA, protein carbonylation, Myeloperoxidase, *SOD1/2*	ELISA, RT-qPCR
Cell signaling	Kidneys	RAGE, AKT, mTOR	Western blot
Immune profile of CD4+ cells and immunoscence	Spleen	TBox21, GATA 3, FOXp3, RORγT SIRT1, P16	RT-qPCR
Microbiota	Caecum	Firmicutes, bacteroidetes, verrucomibrobia, total microbiota	RT-qPCR, Metagenomics

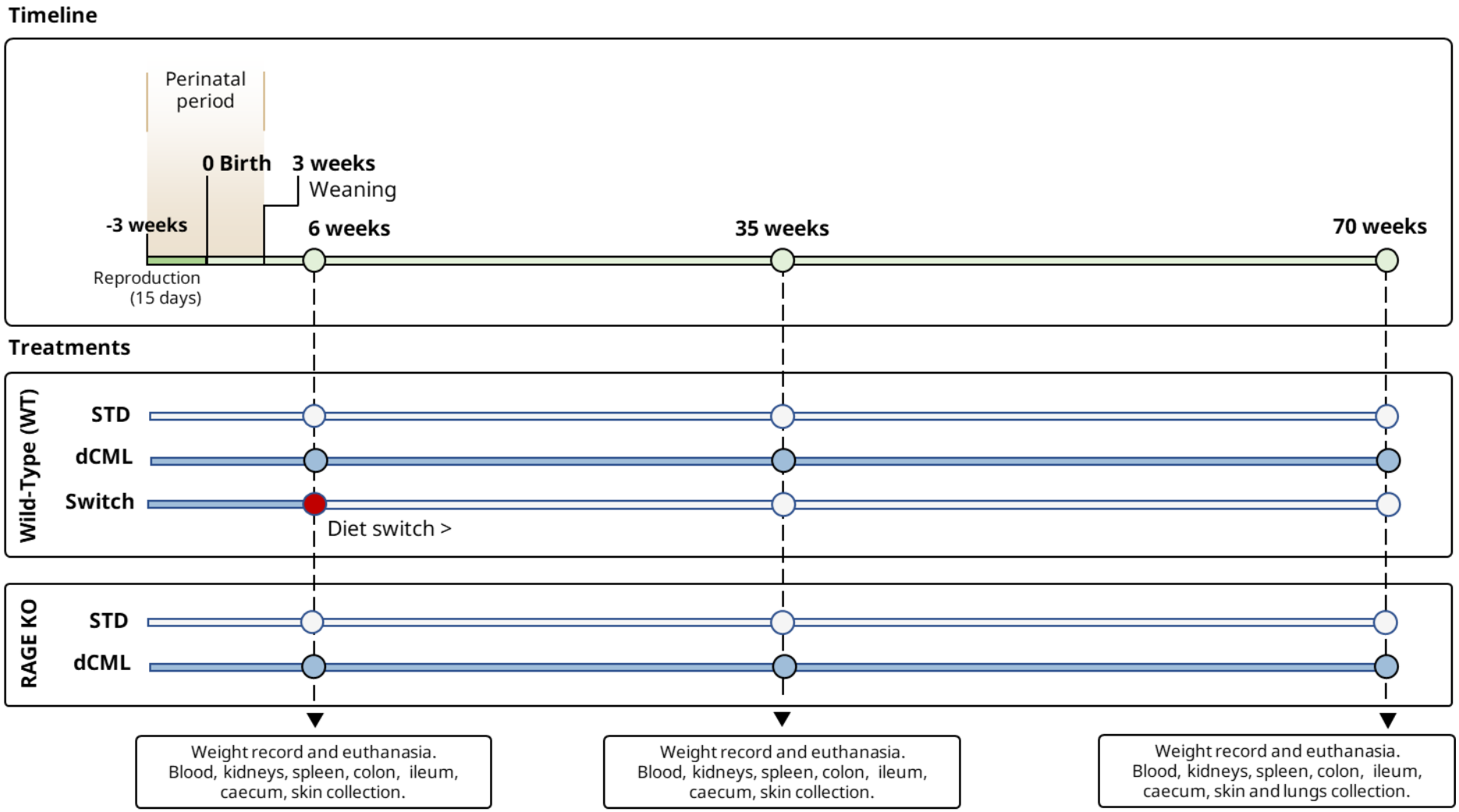

Figure 1 Schematic representation of the experimental design for the ANR ExoAGEing project.

2.2. Quantification of free and protein-bound CML

2.2.1. Chemical and reagents

All reagents used were analytical grade. Ultra-pure HPLC water and Ammonium formate (>99%) were from VWR (Fontenay-sous-Bois, France). Acetonitrile (ACN), boric acid (H_3BO_3), formic acid (>95%), hydrochloric acid (HCl) 37%, sodium hydroxide (NaOH), trichloroacetic acid (TCA), nonafluoropentanoic acid (NFPA) 97% and lysine (Lys), were all obtained from Sigma–Aldrich (Saint-Quentin-Fallavier, France. The CML and CML-d_2 standards were from Iris Biotech (Marktredwitz, Germany). Labeled Lys-d8 and Lys-$^{15}N_2$ were from CDN Isotopes (Toronto, Canada) and CortecNet (Voisins-le-Bretonneux, France), respectively.

2.2.2. Quantification of free and protein-bound CML by mass spectrometry methods

Free CML was measured in all samples, while protein-bound CML was measured in plasma, kidneys, and skin.

2.2.2.1. Sample preparation for the quantification of free and protein-bound CML in plasma

Free CML was determined by direct measurement in the supernatant after precipitating protein in the sample. Lysine was measured simultaneously with CML in the protein fractions. Quantification of CML and lysine was by isotope dilution using liquid chromatography with tandem mass spectrometry detection (LC-MS/MS) in all cases.

Plasma was isolated from the blood sample by centrifuge (15 000g for 5mins at 4°C) and 30µL plasma was transferred to a 2mL, screw-top polypropylene (PP) tube to which 30µL of 20% TCA was added. This was mixed with a vortex mixer and then left on ice for 30mins before centrifuging at 20 000g for 5mins at 4°C. The supernatant was aspirated (40µL for all samples) and evaporated to dryness in a Speed-vac apparatus (Thermo). Just before analysis, the dried supernatant was resolubilized in the HPLC mobile phase with CML-d_2 internal standard.

The protein pellet remaining in the 2mL PP tube after the supernatant was removed was then reduced with 600µL of 0.1M NaBH4 for 2h at room temperature. At the end of this time, 600µL of 12M HCl was added, and the sample hydrolyzed at 110°C for 18h, after which the tubes were centrifuged once more (15 000g, 5mins

at 4°C) before 1mL of supernatant was aspirated and evaporated to dryness under nitrogen. One milliliter of water was added, and the sample again evaporated to dryness in order to remove as much residual HCl as possible, before the sample was resolubilized in the HPLC mobile phase with CML-d_2 internal standard, centrifuged (15 000g, 5min at 4°C), then filtered into HPLC vials (Uptidisc PTFE, 0.45µm).

2.2.2.2. Sample preparation for the quantification of free CML in kidneys, skin, colon, and ileum and protein-bound CML in kidneys and skin

Free CML was determined by direct measurement in the supernatant after precipitating protein in all samples. Twenty-five to eighty milligrams of tissue were homogenized in a bead mill (FastPrep24, FischerSci) with 800µL ultrapure water (4x 40s cycles at 6m/s). The tube was centrifuged (15 000g, 5 mins at 4°C) and 200µL of supernatant was transferred to a 2mL, screw-top PP tube. Fifty microliters of TCA (50%) were added, mixed with a vortex mixer, then the tube was left on ice for 30mins before centrifuging at 20 000g for 5min at 4°C. The supernatant was aspirated (180µL for all samples) and evaporated to dryness in a Speed-vac. Just before analysis, the dried supernatant was resolubilized in the HPLC mobile phase with CML-d_2 and lysine-d_8 / lysine-$^{15}N_2$ internal standards.

For samples of kidney and skin, 600µL of 0.1M $NaBH_4$ was added to the protein pellet remaining in the 2mL PP tube, and the tube was left for 2h at room temperature. Then 600µL of 12M HCl was added and the sample hydrolyzed at 110°C for 18h. Tubes were centrifuged once more (15 000g, 5 mins at 4°C) before 1mL of supernatant was aspirated and evaporated to dryness under nitrogen. One milliliter of water was added and the sample again evaporated to dryness to remove as much residual HCl as possible, before the sample was resolubilized in the HPLC mobile phase with CML-d2 and lysine-d8 / lysine-15N2 internal standards, centrifuged (15 000g, 5mins at 4°C), then filtered into HPLC vials (Uptidisc PTFE, 0,45µm).

2.2.2.3. Quantification of CML in kidneys, skin, colon, ileum, and plasma by LC-MS/MS

This study is the result of a collaborative project in which two laboratories shared the analysis of CML in plasma and organs, hence the two different analytical methods described below.

Samples of plasma, kidneys, and skin were separated on a BEH HILIC column (50 x 2.1mm, 1.7µm; Waters, France) maintained at 30°C, with positive-mode ionization in a heated electrospray (HESI) source. An Ultimate 3000 UPLC (Thermo Fischer) pumped a binary solvent mixture using the following gradient: solvent A (5mM aqueous ammonium formate) and solvent B (0.1 % formic acid in acetonitrile (ACN)) were pumped at 500 µL/min (% B: 0–0.7min, 95%; 0.7–1.0 min, 95–5%; 1.0–2.0min, 5 %; 2.0–3.0, 5–95%; 3.0–4.0, 95%). The following ion transitions were monitored on a TSQ Quantis triple quadrupole MS/MS: m/z 205.1–84.1 and 205.1–130.1 for CML (quantification and confirmation ions, respectively); m/z 207.1–84.1 for CML-d_2 internal standard; m/z 147.1–84.1 and 147.1–130.1 for lysine (quantification and confirmation ions, respectively); m/z 155.2–92.2 for Lysine-d_8 internal standard.

Samples of colon and ileum were injected using an Accela HPLC system (ThermoFisher) onto a Raptor PolarX column maintained at 40 °C (100 x 2.1 mm, 2.7 µm; same-phase guard column 5 x 2.1 mm, 2.7 µm; Restek, France), and the eluant introduced to a TSQ Quantum Ultra MS/MS (ThermoFisher) using HESI+ mode. Solvent A (10% 200 mmol/L ammonium formate in ACN) and Solvent B (0.5 % formic acid) were pumped at 500 µL/min (% B: 0–3.5 min, 12 %; 3.5–8 min, 12–70 %; 8–13 min, 12 %). The following ion transitions were monitored: m/z 205.1–130.1 and 205.1–84.1 for CML (quantification and confirmation ions, respectively); m/z 207.1–130.1 for CML-d_2 internal standard; m/z 147.1–130.1 and 147.1–84.1 for lysine (quantification and confirmation ions, respectively); m/z 149.1–131.1 for Lysine-$^{15}N_2$ internal standard.

2.3. Protein carbonyl derivatives and Malondialdehyde (MDA) analysis

Protein carbonyls and MDA assessment were performed in heparinized plasma samples. Assessments were performed using the Protein Carbonyl Assay kit (Product ref. 10005020) and TBARS Assay kit (Product ref. 10009055) provided by Cayman Chemical Company, respectively. Blood samples were centrifuged at 2000 g for 10 min at 4°C before analysis. Tests were performed according to the manufacturer's instructions. Absorbances were measured at 360-385 nm spectra for protein carbonyl estimation, and at 530-540 nm wavelength for MDA estimations on a 96-well plate reader (SpectroStar Nano, BMG Labtech).

2.4. RT-qPCR

Tissue samples (kidneys, ileum, colon, and lungs) from the different experimental groups described above were preserved in RNA Later and kept in an ultra-freezer (-80°C) for later analysis. Total RNA extraction was performed with TRIzol™ Reagent (Invitrogen) protocol. Reverse transcription was performed with the High-Capacity cDNA RT Kit (Applied Biosystems) from 1 µg of total RNA. After cDNA synthesis, the relative expression of candidate genes was evaluated by real-time PCR using the PowerUp™ SYBR™ Green Master Mix (Applied Biosystems) on QuantStudio 3 System (Applied Biosystems). Primers were designed according to the following parameters: PCR products with lengths between 80-20 nucleotides; primer dissociation temperature of 58-62 °C with a maximum difference of 2°C; CG content between 40 and 60% and oligonucleotide size between 18 and 23 nucleotides. For the analysis of relative expression, cDNA samples were diluted 100x for the quantification of the expression of target genes relative to the endogenous control gene, PPIA, and β-actin. Primer pairs for all analyses of genes are listed in Table 3. Reactions (10 µL final volume), conducted in three technical replicates, contained 2.5 µL of diluted cDNA, 5 µL of SYBR, 0.5 µL of primers mix (5 mM each), and 2 µL of deionized water. Relative expression was assessed using the ΔΔCt method [31]

Table 3 List of genes and primers sequences analyzed by RT-qPCR.

Target gene	Direction	Sequence (5'-3')	Reference
Actin	F	GCTTCTTGGGTATGGAATCCTGT	RID-AGE
	R	CACTGTGTTGGCATAGAGGTCTTTAC	
AGER (RAGE)	F	GCCACTGGAATTGTCGATGAGG	RID-AGE
	R	GCTGTCAGTTCAGAGGCAGGAT	
EZH2	F	TCTGGAGGGAGCTAAGGAGT	[32]
	R	GTCCCTGCTTCTCTGTCACT	
GLβ1	F	GGATGGACAGCCATTCCGAT	RID-AGE
	R	CACATCACGGTCCCCAGAAA	
GLO1	F	CCTGCTATGAAGTTCTCGCTCT	[33]
	R	CTGTCTTCTCGGACTTGTCCTT	
IL-6	F	ACCACGGCCTTCCCTACTTC	[34]
	R	TCCACGATTTCCCAGAGAACA	
p16	F	CCCAACGCCCCGAACT	[35]
	R	GCAGAAGAGCTGCTACGTGAA	
PGC1a	F	TTCGGTCATCCCTGTCAAGC	RID-AGE
	R	CAATGAATAGGGCTGCGTGC	
PPIA	F	GCGTCTCCTTCGAGCTGTTT	RID-AGE
	R	GCGTGTAAAGTCACCACCCT	
SIRT1	F	CGGCTACCGAGGTCCATATAC	[36]
	R	ACAATCTGCCACAGCGTCAT	
SOD1	F	ACTTCGAGCAGAAGGCAAGC	[37]
	R	TTAGAGTGAGGATTAAAATGAGGTC	
SOD2	F	AAGGGAGATGTTACAACTCAGG	[38]
	R	CTCAGGTTTGTCCAGAAAATG	
TNFα	F	GCCACCACGCTCTTCTGTCT	[34]
	R	TGAGGGTCTGGGCCATAGAA	
VCAM1	F	GCACAAAGAAGGCTTTGAAGCA	[39]
	R	GATTTGAGCAATCGTTTTGTATTCAG	

F : forward; R : reverse

2.5. Western blot

Tissue samples (lungs) from the different experimental groups described above were preserved in an ultra-low temperature freezer (-80°C) before protein extraction including membrane-bound proteins with NP-40 buffer. Protein concentration was determined by the Pierce™ BCA Protein Assay Kit (ThermoFisher, Courtaboeuf, France). A total of 20 µg of protein was separated in 8% Bis-Tris (ThermoFisher) gels. Nonspecific binding sites were blocked for 1 h at 20 °C with 5% BSA in tris-buffered saline added to 0.05% Tween 20 (TBS-T); PVDF membranes (BioRad, France) were incubated overnight at 4 °C with total-mTOR (1:5000, #4517, CellSignaling); phospho-mTOR Ser2448 (1:5000, ab109268,

ABCAM); RAGE (1:500, AF1145); actin (1:2000; 4967S, CellSignaling); followed by TBS-T washing and incubation for 2h with horseradish peroxidase (HRP) linked anti-rabbit (1:2500, 7074, CellSignaling) or anti-mouse (1:5000, 7076, CellSignaling) secondary antibodies. Membrane revelation was performed with Cytiva Western Blotting ECL Substrate (Amersham). Analysis of kidneys samples is ongoing, but data acquisition was unfortunately not completed before the submission of the current thesis.

2.6. Data management and statistical analysis

Data was treated with R version 4.2.1 making use of integrated statistical RStatix, GGPubR, and GGPLOT2 packages [40]. Data was primarily evaluated for normal distribution fit using the Shapiro-Wilk test. Non-parametric comparisons proceeded including Wilcoxon Test or Kruskal-Wallis rank test followed by Dunn's multiple comparison test when appropriate. All data were presented as means +/− Standard Error of Mean (SEM) (bar plots), or median + quartiles (box plots). Statistical significance was performed taking into consideration $\alpha = 0.05$ as a threshold.

3 Results and discussion

Dietary glycation products are predominantly found in foods that have undergone industrial or domestic thermal processing. To provide a clearer understanding of the effects of a chronic exposure to dCML, we present here, for the first time, the physiological effects of an early-life (including the intrauterine period) and a long-term exposure to a dCML-enriched diet compared with a control diet (STD). Experiments were conducted on an aging rodent model for a duration of up to 70 weeks. Hence, we studied the functional changes associated with the consumption of dCML in the context of aging and explored the potential connections established between dCML intake, RAGE (the primary cell receptor associated with glycation), and the initiation of inflammatory, oxidative stress responses, and cellular senescence.

Prior to discussing the findings, it is crucial to emphasize that the experiments involved a diverse group of female and male C57BL/6 mice. This approach was adopted to ensure a more comprehensive and representative evaluation of the physiological aspects associated with the different treatments. While it is important to acknowledge that the small sample sizes within each sex/group may limit the interpretation of results, gender-related effects, such as weight variations, are highlighted when relevant. In addition, we are acutely aware that the small number of animals of 6 weeks of age was a limiting factor for this group, and there were large variances within genotypes and diet treatments at this time point. Due to these considerations, data regarding the 6-week-old mice is not presented in this text.

Several organs and biological samples are still being analyzed. The interpretations presented below are therefore preliminary and may be revised in the light of future results.

3.1. Diet quality, and food consumption

Prior to the evaluation of the health effects of a dCML-enriched diet and the consequences of knocking-out RAGE in this dietary context, we assessed the nutritional quality of the food fed to the animals (Table 4). Furthermore, we conducted estimations of food consumption rates and assessed weight variances among the different animal groups (Table 5). These measurements provide valuable insights into the potential effects of the different dietary conditions on food intake

and body weight changes. The diets used in the study were very similar in terms of energy content, ensuring a similar intake of calories, lipids, fibers, and carbohydrates across the different experimental groups (Table 4). This approach aimed to minimize confounding factors related to variations in nutrient composition and focus on the specific effects of dCML intake. Equivalent amounts of non-glycated and glycated BSA were added to the standard (STD) and CML-enriched (dCML) diets. The final addition of protein did not exceed 0.8% of the total amount of protein provided to animals. Total protein (159.4 - 162.4 mg/g DW) and lysine (10.9 - 11.2 mg/g DW) amounts were periodically checked and there was no significant variation (p>0.05) between groups (Table 4). A 13-times difference in dCML concentrations was verified between the STD diet (20.8 ± 5.1 µg/g DW) and dCML-enriched diet (255.2 ± 44.5 µg/g DW) (p<0.001).

Table 4 Diet composition, and CML quantification on the different mouse diet preparations.

	Unit	Diet	
		STD	**dCML**
Calories	kcal/g	3.1 ± 0.3	3.1 ± 0.3
Fatty acids	%	3.1 ± 0.3	3.1 ± 0.3
Fibers	%	3.9 ± 0.3	3.9 ± 0.3
Carbohydrates	%	46.7 ± 4.6	46.7 ± 4.6
Proteins	mg/g DW	162.4 ± 6.0	159.4 ± 8.8
Lysine	mg/g DW	11.2 ± 1.0	10.9 ± 0.9
Total CML	µg/g DW	20.8 ± 5.1	255.2 ± 44.5*

DW: dry weight. Total CML = free and protein-bound CML. * p<0.001. Statistical tests corresponded to comparisons within lines.

We estimated the food intake among the older animals, with an average age of 63 weeks. Food intake data were recorded over a period of one week, allowing us to assess the dietary consumption patterns in mature animals. A lower consumption was evident among RAGE KO mice on the STD diet (p<0.01), but all other groups consumed a very similar amount (Table 5). Hence, CML intake estimations were statistically similar within animals exposed to STD and within animals receiving the dCML diets (Table 5). Glycation of proteins during cooking is associated with the development of appetizing colours and aromas which may induce a preference [41]. Our procedure for producing glycated BSA (CHAPTER 5)

did not have this effect and, at least among the WT animals, we observed no preference for either the STD or d-CML diet.

Table 5 Diet composition, and CML quantification on the different mouse diet preparations.

		WT			RAGE KO	
		STD	**Switch**	**dCML**	**STD**	**dCML**
Food intake	g/day/animal	5.7 ± 1.1	5.2 ± 0.6	5.3 ± 0.7	4.2 ± 0.5*	5.7 ± 0.7
CML Intake	µg/day/animal	119.3 ± 23.6	108.8 ± 14.1	1367.9 ± 190.0**	90.3±9.4	1464.8 ± 198.0**

Food intake: calculated among adult animals (age average 63 weeks). *p<0.01; ** p<0.001. Statistical tests corresponded to multiple comparisons within lines.

3.2. Animal physiology at 35 and 70 weeks of treatment

Throughout the entire experimental procedure, we closely monitored the weight of the animals. Importantly, no significant differences in weight gain rates were observed among the different groups. This suggests that the dCML-enriched diet did not have a notable impact on overall weight changes compared with the STD diet. Weekly weight gains estimated from the 15th week of life were 381-532 mg/week and 366-673 mg/week, for 35-week-old female and male animals, respectively, and 312-391 mg/week and 218-306 mg/week for 70-week-old female and male mice, respectively. Increased mortality or obesity were neither observed nor associated with any of the treatments presented here.

On the day of sacrifice, the animals were weighed, and the corresponding data are presented in Figure 2. At 35 weeks of age, the average weight was estimated to be 31.8 ± 4.6 and 40.2 ± 4.4 g for females and males, respectively, and at 70 weeks of age it was 42.8 ± 3.1 and 46.4 ± 4.4 g, respectively. For both genders, weights were in the physiological range expected for healthy C57BL/6 animals at these ages [42]. Here it is worth highlighting that the knockout of RAGE seemed not to interfere with the physiological traits of these animals, both WT and RAGE animals having a similar weight and food intake.

The weights of the male groups within the 35 and 70-weeks of age categories were comparable. The STD-RAGE KO mice (both female and male) did not present significantly reduced weight associated with the slightly lower food intake mentioned in section 3.1.

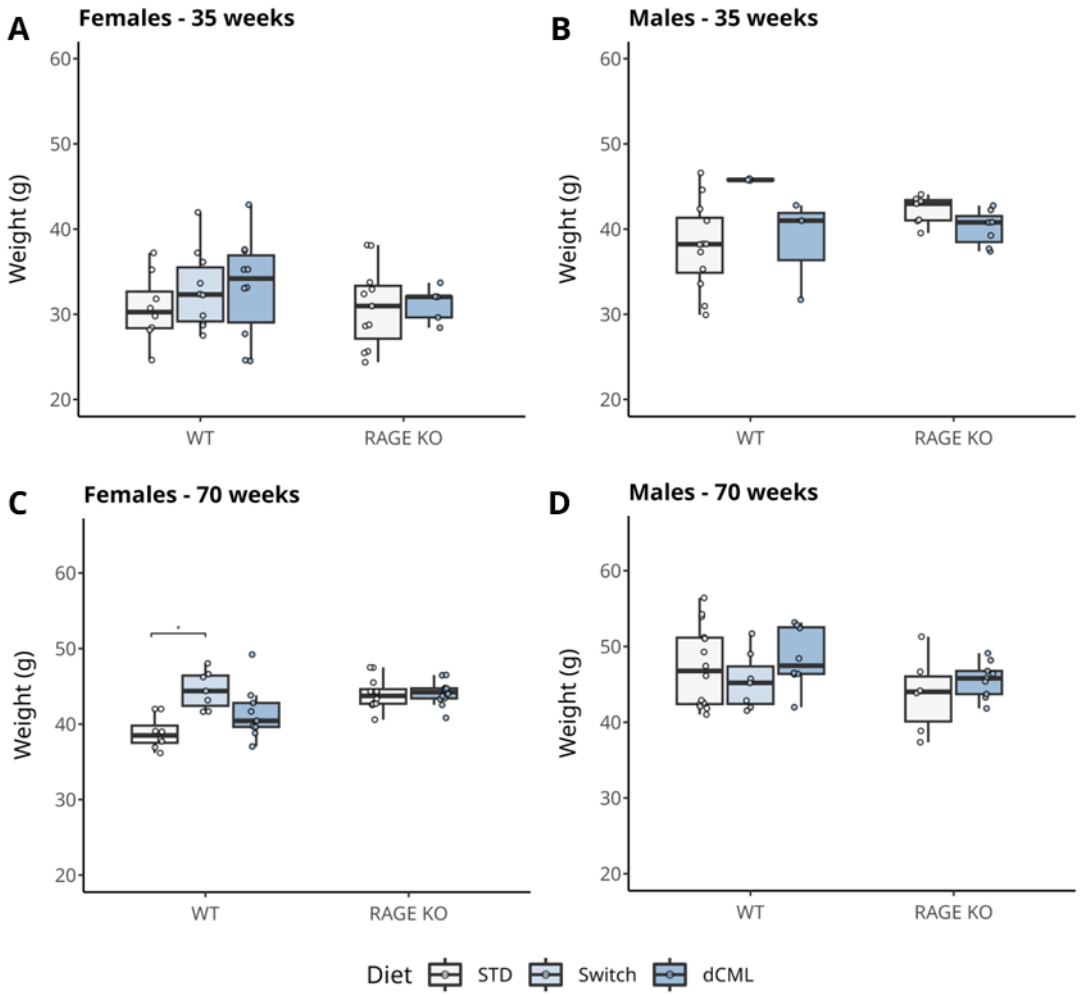

Figure 2 Weight (g) distribution among females and male mice. **(A)** 35-weeks-old females; **(B)** 35-weeks-old males; **(C)** 70-weeks-old females; **(D)** 70-weeks-old males. Center black bars represent medians and whiskers represent lower and upper quartiles. Statistical significance between groups is indicated by (*) taking into account *p≤0.05 resulting from non-parametric analysis (Wilcoxon-test).

3.3. A diet enriched in dCML increases mainly free CML form in multiple organs

In order to investigate the potential contribution of a dCML-enriched diet to the accumulation of CML in various organs, we quantified the levels of both free and protein-bound CML using LC-MS/MS. The organs analyzed included the kidneys, ileum, colon, skin, and serum of animals that were administered either a STD or a dCML diet (Figure 3). CML was found to accumulate in different organs in a diet-dependent manner, mainly in the free form, while CML accumulation occurred independently of RAGE ablation.

Free CML was significantly increased in the digestive and urinary systems, including the kidneys and the colonic and ileum portions of the small intestinal tract of animals that received a dCML-enriched diet (Figure 3A to 3C). Conversely, no change or else a slight, non-significant increase in free CML were observed in skin and serum (Figures 3D and 3E).

In general, free CML levels were found to be consistently lower in the STD diet groups compared with the dCML-diet groups regardless of age. In the kidneys, free CML concentrations varied from 72.3 ± 14.6 pmol/mg of tissue in the STD-diet groups compared with 192.1 ± 50.6 pmol/mg of tissue in the dCML-diet groups (p<0.001) (Figure 3A). In the ileum, an 11-times difference in free CML levels was found between the STD and dCML-diet groups: 5.35 ± 2.9 versus 57.3 ± 29.4 pmol/mg of tissue, respectively (p<0.001) (Figure 3B). A greater difference in free CML concentrations (16-times) between STD-diet groups and dCML-diet groups was found in colon samples: 1.3 ± 1.5 versus 21.4 ± 17.7 pmol/mg of tissue, respectively (p<0.001) (Figure 3C). In skin samples, STD and dCML-diet groups were similar in dermal free CML concentrations at 41.1 ± 4.3 and 48.1 ± 7.8 pmol/mg of tissue, respectively (Figure 3D). Serum free CML amounts varied from 23.5 ± 2.4 pmol/mg of serum in the STD-diet groups to 27.6 ± 3.4 pmol/mg in the dCML-diet groups (Figure 3E). It is important to underline that the animals were not subjected to fasting prior to sacrifice. Therefore, any fluctuations observed in the serum levels of free CML can be attributed to their eating behavior leading up to the time of euthanasia.

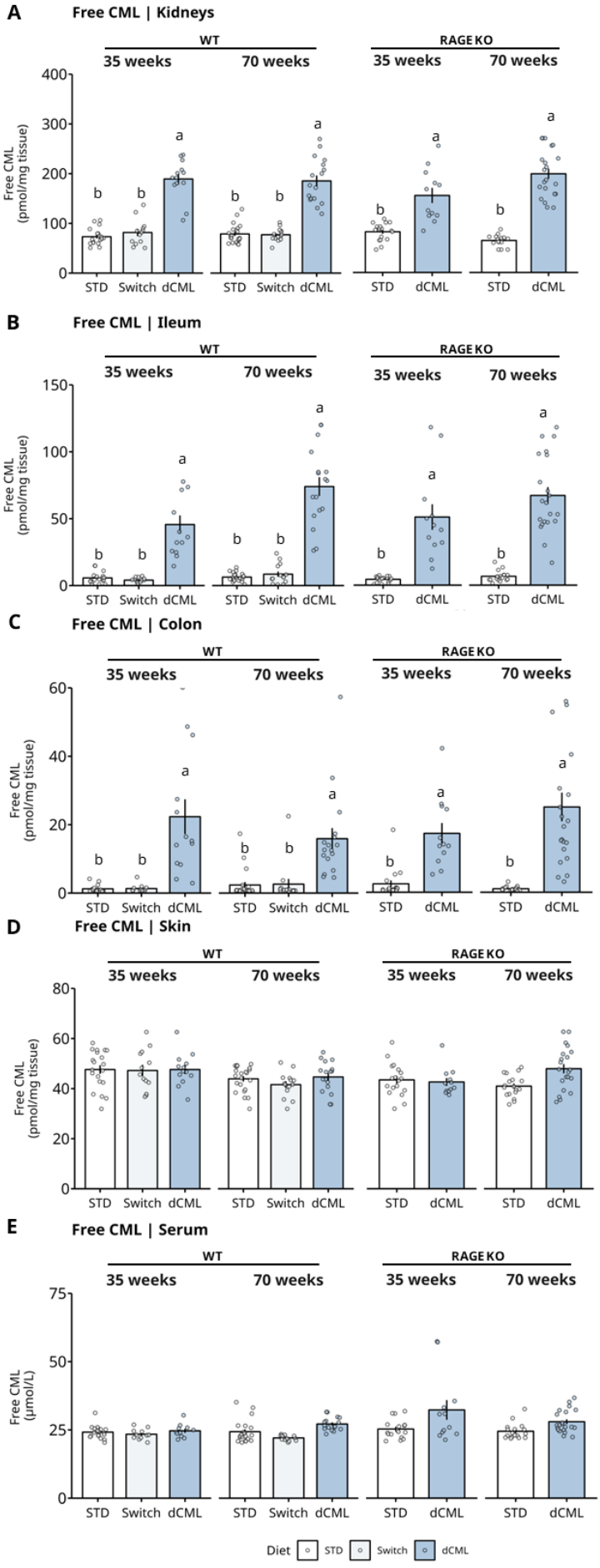
A
Free CML | Kidneys
WT
RAGE KO
35 weeks
70 weeks
Free CML (pmol/mg tissue)
STD
Switch
dCML
B
Free CML | Ileum
C
Free CML | Colon
D
Free CML | Skin
E
Free CML | Serum
Free CML (µmol/L)
Diet

Figure 3 Free CML quantification by LC-MS/MS in **(A)** kidneys, **(B)** ileum, **(C)** colon, **(D)** skin, and **(E)** serum of 35- and 70-week-old C57BL/6 mice (WT and RAGE KO) administered a control (STD), or a dCML-enriched diet (dCML), or which been submitted to a diet switch from dCML to STD diet at 6 weeks of age. Bars represent means ± SEM. Letter indices (Kruskal-Wallis rank test followed by Dunn's posthoc test for multi-comparisons) indicate statistical differences among groups within each organ. α=0.05.

A significantly higher level of protein-bound CML was observed only in the renal tissue of 35-week-old WT animals that received the dCML-enriched diet (Figure 4A). No other significant differences in protein-bound levels were noticed in the other genotype or in other organs. The study from van Dongen et al. (2021) [22] also indicate that a baked chow diet high in dAGEs increases CML, CEL and MH-H1 in kidneys, but mainly in the free form.

Our investigation confirmed the increase in free CML levels associated with the consumption of a dCML-enriched diet compared with a STD diet. Moreover, our findings corroborate previous studies, demonstrating that the accumulation of exogenous dCML occurs independently of RAGE [43]. Greater accumulation of free CML was observed in organs of the digestive-excretory system, the primary interface between environmental toxicants, including dietary neoformed compounds [44]. It has been roughly estimated that around 10% of the pool of ingested dCML is absorbed and accumulated in tissues [45]. The utilization of dietary sources containing isotopic protein-bound ^{13}C-CML has previously demonstrated that exogenous dCML primarily accumulates in the ileum, colon, and kidneys [43]. These findings align with the results presented here, further supporting the notion that these organs are major sites of accumulation for exogenous dCML.

To the best of our knowledge, this is the first study to demonstrate the effects of chronic consumption of a dCML-enriched diet on the skin of an animal model. It is well-accepted that AGEs, including CML, are spontaneously formed and accumulate linearly with age in human skin collagen [46,47]. In murine models, it has been observed that CML accumulation in the skin increases with age but at a non-linear rate [47]. Skin glycation has been extensively explored as an epidermal aging biomarker in the context of diabetic complications [48]. In the current study, it appears that neither the diet nor the age-related low-grade disturbances investigated here led to detectable changes in either free or protein-bound CML

levels in the skin of mice (Figures 3-D & 4B). The primary interest in skin glycation relies on the non-invasive measurement of skin fluorescence related to fluorescent AGEs as a prognostic method for the emergence of chronic diseases [48]. Although CML is not a fluorescent AGE, here we demonstrated by a reliable quantitative method (LC-MS/MS) that it does not accumulate significantly in the skin, neither as a function of dietary exposure to dCML, nor by potential indirect stresses (*e.g.* dicarbonyl stress, oxidative stress) caused by a high-AGE consumption. However, this does not exclude the possible accumulation of dAGEs other than dCML, even though these were not explored in this study.

In the serum, we observed a tendency towards a slight increase in free CML levels in some groups of animals in receipt of the dCML-enriched diet (Figure 3E), but no effect of the diet on the concentration of protein-bound CML in serum proteins. These observations agree the study published by Alamir et al. (2013) [49], and our study presented in CHAPTER 4, which indicate that protein-bound CML is not affected by the level of dietary exposure to CML and that while free CML concentrations increase postprandially, levels return to baseline when serum was sampled from fasted animals. It is important to note that the interpretation of the current observation about free CML levels in serum is limited due to the animals not being subjected to fasting before blood collection and, thus, that food intake was uncontrolled and potentially highly variable among animals immediately before blood sampling.

The recent study on mice from van Dongen et al. (2021) [22] did not observe the same effects of a CML-enriched diet on serum CML as our study. In their study the authors observed not only an increase in free CML in serum (with a 2-fold variation among animals) but also an increase in the protein-bound CML concentration when mice were fed a baked chow diet.

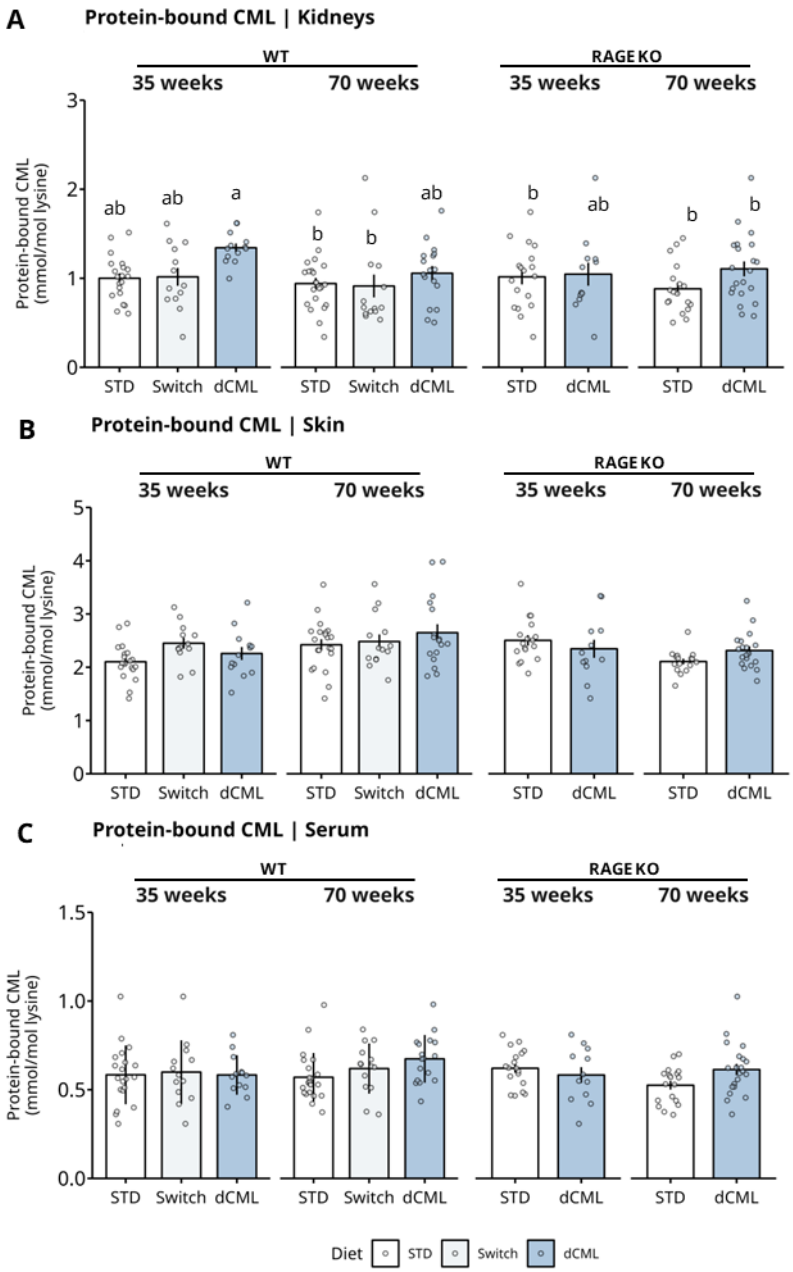

Figure 4 Protein-bound CML quantification by LC-MS/MS in **(A)** kidneys, **(B)** skin, and **(C)** serum of 35- and 70-week-old C57BL/6 mice (WT and RAGE KO) submitted to a control (STD) or a dCML-enriched diet (dCML), or which were submitted to a diet switch from dCML to STD diet at 6 weeks of age. Bars represent means ± SEM. Letter indices (Kruskal-Wallis rank test followed by Dunn's posthoc test for multi-comparisons) indicate statistical differences among groups within each organ. α=0.05..

Although protein-bound CML is the main form of occurrence of CML in foods [22], the absorption of dCML by the intestinal epithelium occurs predominantly through digested free or dipeptide forms [51]. Accordingly, the pool of protein-bound CML in organs or in circulation cannot be exclusively derived from dietary, protein-bond CML. At best we can assume that the increase in protein-bound CML previously observed in some animal studies [27,50,52] results from the indirect effects of dCML ingestion and accumulation, especially by mediating an activation of a glycoxidative stress [53]. In this regard, Grossin et al. (2015) showed, by immunohistochemical staining in the aortic tissue of animals exposed to dCML, that antibodies were selective to protein-bound CML formed from the *de novo* synthesis of proteins, but did not recognize free CML of dietary origin [27]. In this same dietary context, authors demonstrated the repression of *SIRT1* in WT animals that received a diet rich in dCML. SIRT1 is an important NFκβ repressor and, therefore, plays a role in regulating the oxidative stress activation response [54].

In the present study, small but signficant rise in protein-bound CML levels was detected in the kidneys of WT animals at 35 weeks old, as shown in Figure 4A, with similar trend observed at 70 weeks old. Similar findings have been reported in previous studies investigating the effects of both a dCML-enriched diet and a rodent baked-chow on the kidneys of animals [28,50]. Both investigations proposed a potential link between local tissue stress and the observed outcomes in the kidneys of animals consuming a dCML-enriched diet. We further investigated oxidative stress biomarkers in these samples, and findings are presented in section 3.5.

3.4. Diet-switching reverses levels of free CML in kidneys, ileum, and colon

The accumulation of free CML can be reversed by switching to a STD-diet from a dCML diet at an early stage of life (6 weeks). This diet-switching intervention led to significantly lower free CML levels in the kidneys, ileum, and colon of animals at both 35 and 70 weeks of age (Figures 3A, 3B, and 3C). Importantly, the free CML levels in the switched group were comparable to those observed in animals that had been continuously fed the STD diet (p>0.05). As no significant differences were observed in the levels of free CML in the skin and serum following the dietary intervention, it was not possible to infer a reversibility effect on free CML accumulation in these matrices (Figure 3D and 3E).

Our study represents the first exploration of the reversibility of the effects of high dCML consumption, including exposure of the parental line to STD and dCML diets during the breeding period. Taking into consideration the differences in free CML content in the kidneys, ileum, and colon, an early-life diet switch returned free CML levels to concentrations similar to those in the control groups. While there is no consensus regarding the specific cellular compartment where dAGEs may accumulate, we assume that exogenous glycation adducts might be primarily associated with the extracellular matrix. These findings are a positive indicator of the reversibility of potentially deleterious effects that dAGEs may play on human health. To our knowledge, only one study has investigated the possible reversibility of dAGEs accumulation thus far, and it did not specifically explore perinatal exposure. Working exclusively on 9-week-old C57BL/6/OlaHsd female mice, Linkens and colleagues compared some short-term effects of a baked chow diet versus a standard chow diet, and demonstrated the reversibility of the accumulation of CML in serum, liver, and kidneys [22].

3.5. RAGE genetic invalidation corroborates with age-related oxidative stress progression in serum and kidneys

We assayed an oxidative stress phenotype panel including the assessment the serum levels of malondialdehyde (MDA) as a measure of lipid peroxidation and protein oxidation, and the measurement of protein carbonylation (PC) in serum samples. In addition, the relative expression of *SOD1*, *SOD2*, and *GLO1* was evaluated in the kidney since the greatest accumulation of dAGEs has been reported in this organ. There was no significant difference in lipid peroxidation as indicated by MDA levels, nor protein oxidation as measured by PC levels (Figures 5A and 5B) in relation to the different diets, age groups, or genotypes (p>0.05).

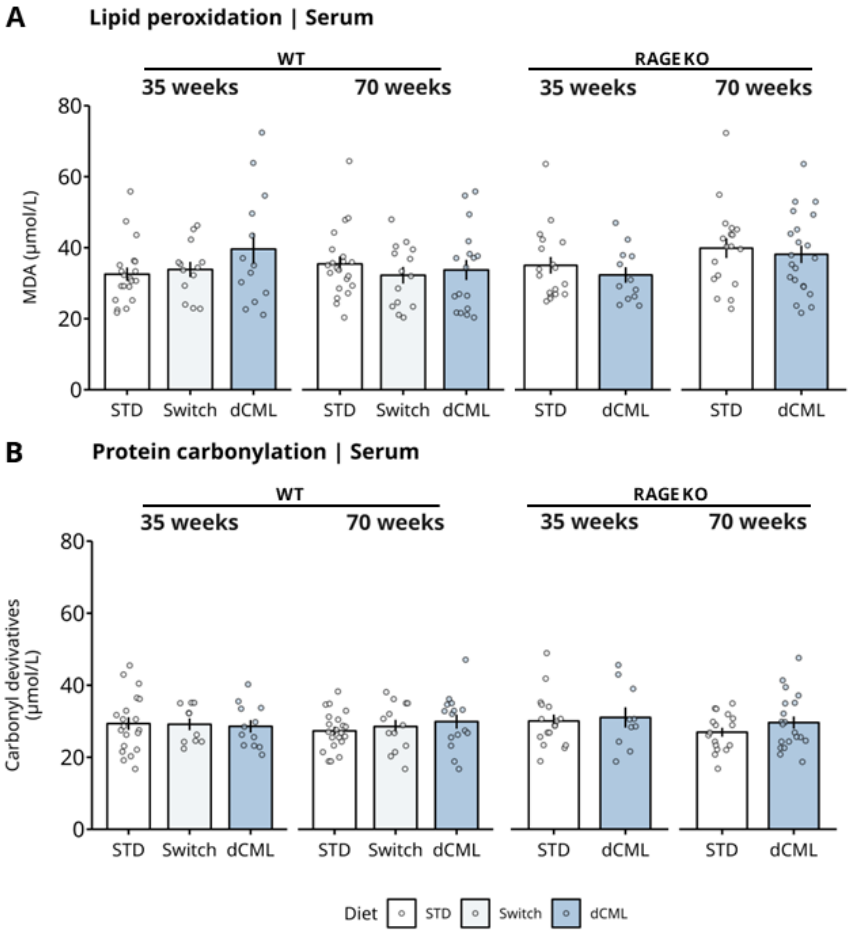

Figure 5 Oxidative stress assessment in serum samples across the different dietary treatments in WT and RAGE KO mice between 35 and 70 weeks. **(A)** Lipid peroxidation assessment measured by MDA levels (µmol/L); **(B)** Protein oxidation assessment measured by protein carbonyl derivatives levels (µmol/L). Bars represent means ± SEM.

No difference in *SOD1* and *SOD2* was observed associated with the different diets (Figures 6A and 6C). The absence of any significant effect of diet allowed us to combine the data by genotype and age for further statistical analysis with larger numbers of mice per group. The data analysis after regrouping the animals by genotype, as presented in Figures 6B and 6D, indicates a modest genotypic effect in the increased expression of the *SOD2* gene in RAGE knockout (KO) mice, whereas no effect of the genotype was observed on the *SOD1* gene expression. No effect of age (35 versus 70 weeks old) was observed on the expression of these genes.

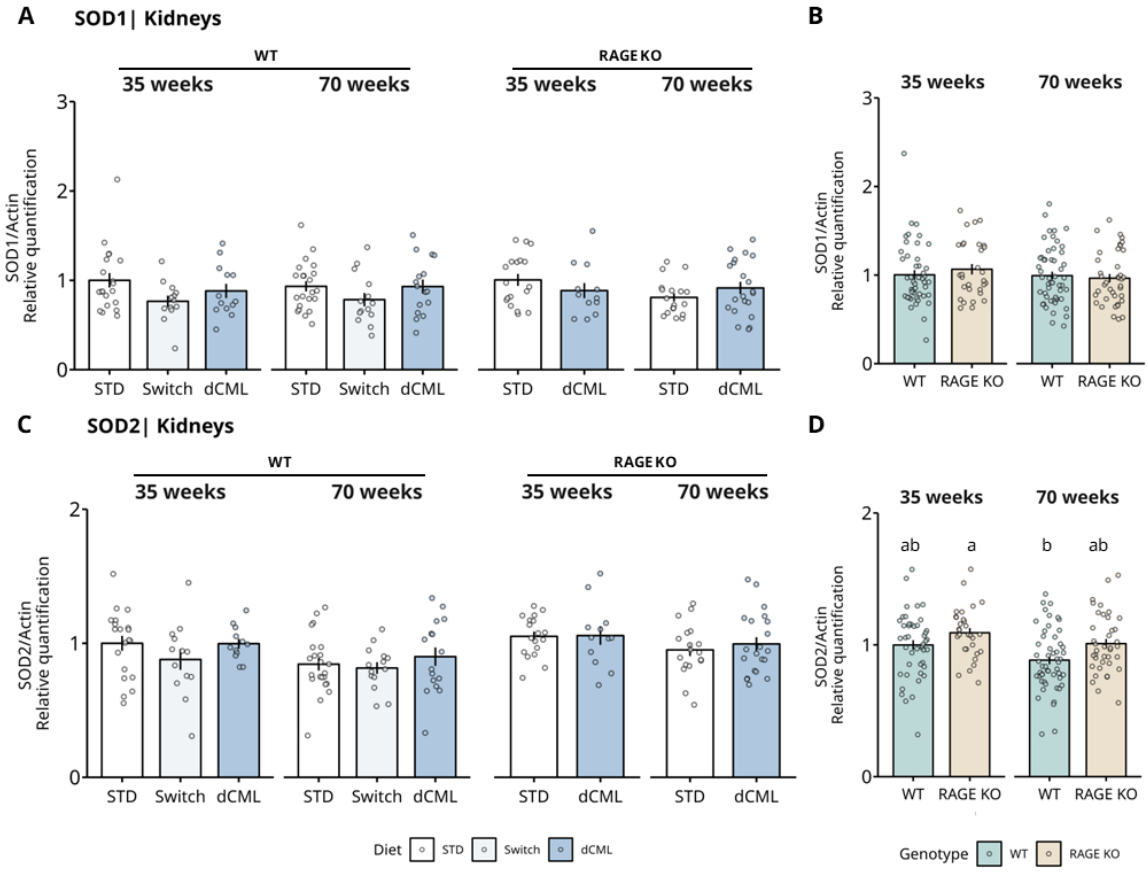

Figure 6 Relative expression of *SOD1* and *SOD2* from RT-qPCR on kidney samples. **(A)** Relative expression of SOD1 across the different dietary treatments administered to WT and RAGE KO mice after 35 and 70 weeks. **(B)** Genotype effect on the relative expression of SOD1. **(C)** Relative expression of SOD2 across the different dietary treatments in WT and RAGE KO mice at 35 and 70 weeks. **(D)** Genotype effect on the relative expression of SOD2. Bars represent means ± SEM. Letter indices (Kruskal-Wallis rank test followed by Dunn's posthoc test for multi-comparisons) indicate statistical differences among groups within each chart. α=0.05. Housekeeping gene: Actin. Reference group: **(A)** and **(C)** WT-STD group; **(B)** and **(D)** WT-35 weeks.

We next assessed whether variation in *GLO1* mRNA expression would result from a dCML-enriched diet (Figures 7A and 7B). Changes in *GLO1* expression as a function of diet were not seen, however a 2-fold increase was observed when comparing RAGE KO with WT animals (Figure 7B).

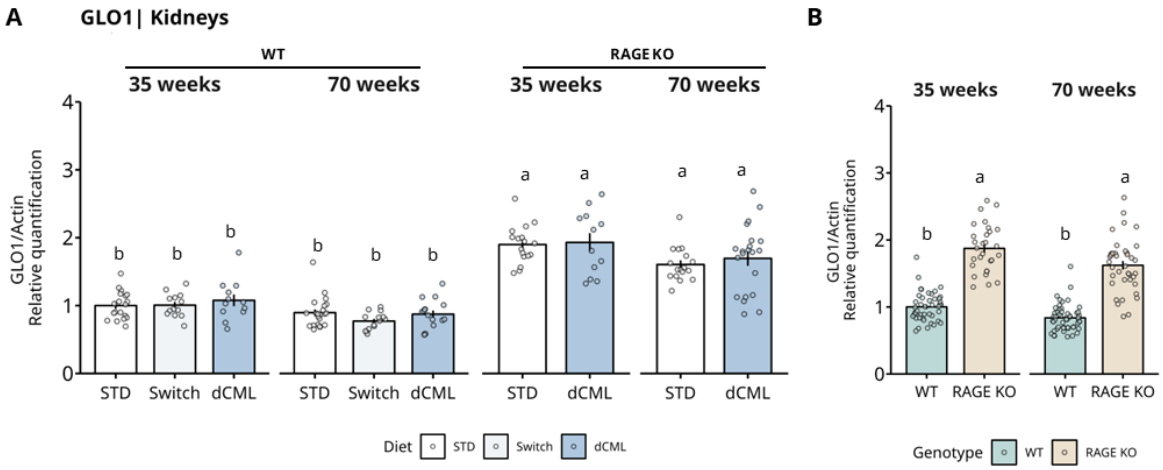

Figure 7 Relative expression of *GLO1* assessed by RT-qPCR on kidney samples. **(A)** Relative expression of GLO1 across the different dietary treatments administered to WT and RAGE KO mice at 35 and 70 weeks. **(B)** Genotype effect on the relative expression of *GLO1*. Bars represent means ± SEM. Letter indices (Kruskal-Wallis rank test followed by Dunn's posthoc test for multi-comparisons) indicate statistical differences among groups within each chart. α=0.05. Housekeeping gene: Actin. Reference group: **(A)** WT-STD group 35 weeks; **(B)** WT-35 weeks.

Protein and lipid oxidation, along with glycation, are interconnected processes associated with pro-oxidative conditions. The promotion of oxidative stress can occur through various mechanisms, such as the autoxidation of glucose, the breakdown of Maillard reaction intermediates, or the interaction between AGE and RAGE [55]. The results obtained from the assessment of lipid peroxidation, protein carbonylation, and the expression of various enzymes provided multiple lines of evidence indicating that the consumption of the dCML diet did not lead to an exacerbated oxidative stress.

Overall, no differences were observed concerning cytoplasmic (*SOD1*) or mitochondrial matrix (*SOD2*) superoxide dismutase, suggesting no direct dysfunction in mitochondrial functionality between 35 and 70 weeks of age in mice. According to our results, only a trend of age-related reduction in *SOD2* expression was observed comparing 35- versus 70-week-old animals. It is well-accepted that decline of mitochondrial functional is associated with age, and hence with increased

age-related oxidative stress [56]. Such a phenomenon was additionally demonstrated to be succeeded by an age-dependent decline of *SOD1* and *SOD2* expression. In the study conducted by Pérez et al. (2018) [57], a comparison of gene expression between mice aged 4 and 24 months revealed a significant decrease associated with the progression of age in the liver. However, extrapolating these data to our results is complicated by the difference in the age of our animals.

In addition, the knockout of the receptor for advanced glycation end products (RAGE KO) resulted in an upregulation of SOD2 mRNA expression compared to wild-type (WT) mice of approximately 90-week-old [28]. Although not statistically significant, a comparison of our results in mice at 35 and 70 weeks old would seem to reflect this same trend.

A *GLO1* gene duplication was discovered as an artifact resulting from the multiple backcrossing procedures used in the generation of the RAGE KO lineage [58]. *GLO1* has been treated as a “vitagene” once associated with decreased oxidative stress and increased lifespan promotion [59]. From our results, we noticed a 2-fold increase in *GLO1* expression in RAGE KO mice compared with WT animals. Besides being a genetic artifact in this lineage, considering the implications of *GLO1* on glycation discussed in the introduction of this thesis, it was important for us to identify possible anti-glycation mechanisms that could compensate for the deleterious effects of dAGEs. Hence, the over-expression of *GLO1* could have been involved in an anti-oxidant response within RAGE KO animals or even take part in the prevention of endogenous glycation (or glycoxidation) that could arise from oxidative stress. However, we observed no significant reduction of oxidative stress in the circulation (Figure 5A and 5B) and kidneys (Figure 6B and 6D) among RAGE KO mice, and also no decrease in the concentration of protein-bound CML in organs or serum (Figure 4).

Finally, it is interesting to note that RAGE activation has been demonstrated to downregulate *GLO1* expression, contributing to increased endogenous formation of methylglyoxal and methylglyoxal-derived AGEs [60]. Knowing this, it would have been interesting to compare the formation of protein-bound CEL and MG-H1 in the serum and organs of WT and RAGE KO mice. For the general interpretation of the results of this animal experiment, it should not be forgotten that the higher expression of *GLO1* observed in the RAGE KO animals could potentially act as a confounding factor.

3.6. Inflammaging is attenuated by RAGE ablation in kidneys, ileum, and colon

To provide further clarity on the potentially pro-inflammatory role of a dCML-enriched diet, we conducted additional assessments of RAGE expression, both at the transcript and translated product levels. In addition, we measured the expression (mRNA) of key cytokines *TNFα* and *IL6*, and the vascular adhesion molecule *VCAM1*, associated with inflammation regulation in the endothelium, as a comprehensive inflammatory profiling panel.

The deleterious effects of dAGEs are thought to be partially mediated by the AGE-RAGE axis. Among the different organs screened in this study (kidneys, ileum, colon, and lungs) a non-significant (p=0.2) trend in increased relative *RAGE* gene expression was only observed in the kidneys of 35-week-old WT animals (Figure 8A). Lung RAGE protein expression, measured only in 70-week-old animals, did not differ significantly across the different diet treatments (Figure 8E). A similar approach is currently being carried out in renal tissue of 35- and 70-week-old animals. However, due to the weak expression of proteins such as RAGE in the kidneys, the analyses were initially optimized using lung samples.

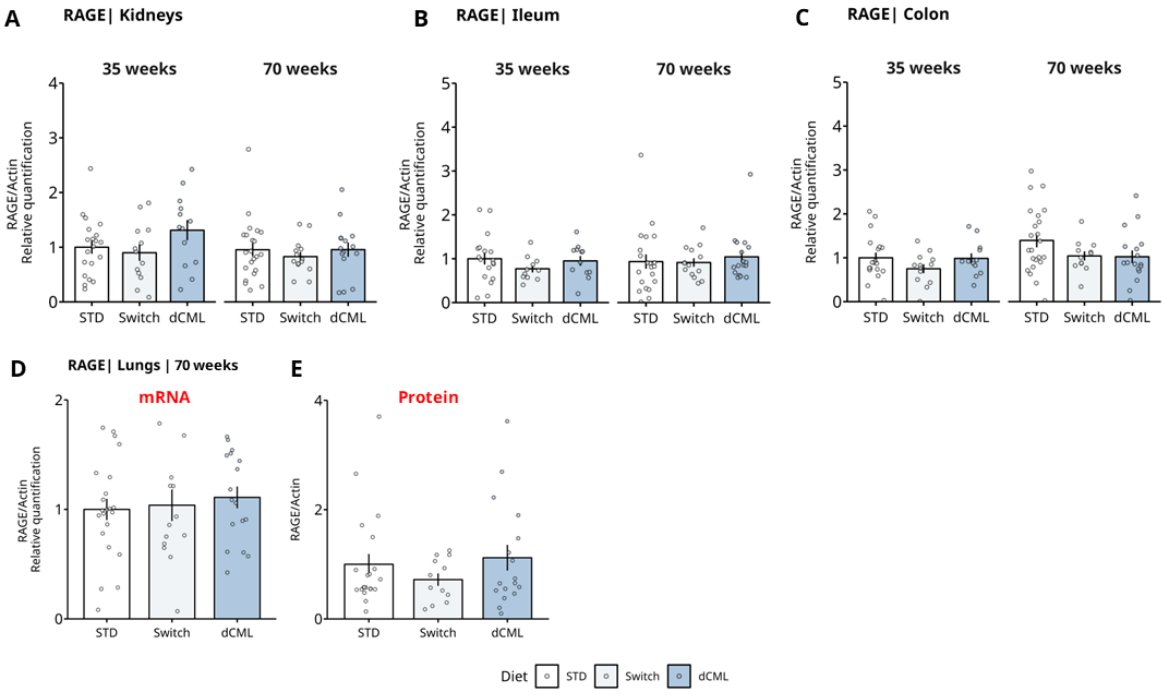

Figure 8 Relative expression of *RAGE* across the different dietary treatments administered to WT and RAGE KO mice between 35- and 70-weeks-old in **(A)** kidneys**, (B)** ileum**, (C)** colon**,** and **(D)** lungs (70-weeks-old animals only)**. (E)** Relative quantification of RAGE protein across the different dietary treatments in 70-week-old WT mice. Bars represent means ± SEM. Housekeeping gene or protein: Actin. Reference group: **(A-C)** WT-STD group 35 weeks; **(D-E)** WT-70 weeks.

The expression of RAGE did not correspond to the accumulation of free CML in any of the organs investigated in this study. Additionally, although non-significant, a trend towards RAGE upregulation was noted in the kidneys of 35-week-old WT animals fed the dCML diet. This coincided with a greater accumulation of protein-bound CML in the kidneys (Figure 4A). Considering the relatively high affinity of protein-bound CML to RAGE [61], and the suggested positive feedback over RAGE expression mediated by NFκβ [62], we hypothesize that a mechanistic relationship between these events may induce an increase in *RAGE* expression in renal tissue under the indirect influence of the dCML diet. In the endothelium of the aorta of 48-week-old mice, a similar pattern was observed, wherein no significant transcriptional variation of RAGE was found to be affected by diet. However, an immunohistochemical analysis revealed a 2-fold change in RAGE protein expression in the aorta of 35-week-old animals after a diet consumption of 200 $\mu g_{CML}/g_{food}$ for 40 weeks [27]. However, it should be noted that this result was not

replicated in the lungs of 70-week-old animals, as confirmed in the present study (Figures 8D and 8E).

An age-related increase in pro-inflammatory biomarkers *TNFα* and *VCAM1* (Figure 9) was more evident among WT mice (although non-statistically significant) compared with RAGE KO mice. A similar pattern was previously described in a comparison of the kidneys of 20-month-old WT and RAGE KO animals to those of 3-month-old animals [28]. These biomarkers, *TNFα* and *VCAM1*, have been shown to be upregulated in older mice compared with younger animals in various fluids and tissues, including serum and the brain [63–65].

RAGE knockout exhibited a hint of a protective effect, with less pronounced age-associated upregulation of both *TNFα* and *VCAM1* genes. The expression of *IL6*, on the other hand, exhibited a time-dependent increase in both genotypes (Figure 10). Noticeable age-related variations of *TNFα*, *VCAM1*, and *IL6* were found mainly in the kidneys, while greater variability was characterized data from the ileum and colon. In the kidneys, we observed an increase in mRNA expression of pro-inflammatory *TNFα* and *VCAM1* by approximately 1.5 to 2-fold in 70-week-old mice compared with 35-week-old mice. In this same organ, *IL6* (an anti-inflammatory cytokine) had a similar expression profile with a ~1.5 to ~2-fold increase in *IL6* expression in 70-week-old compared with 35-week-old animals (Figure 10). However, no effect of diet was observed for any of the inflammatory biomarkers we studied here.

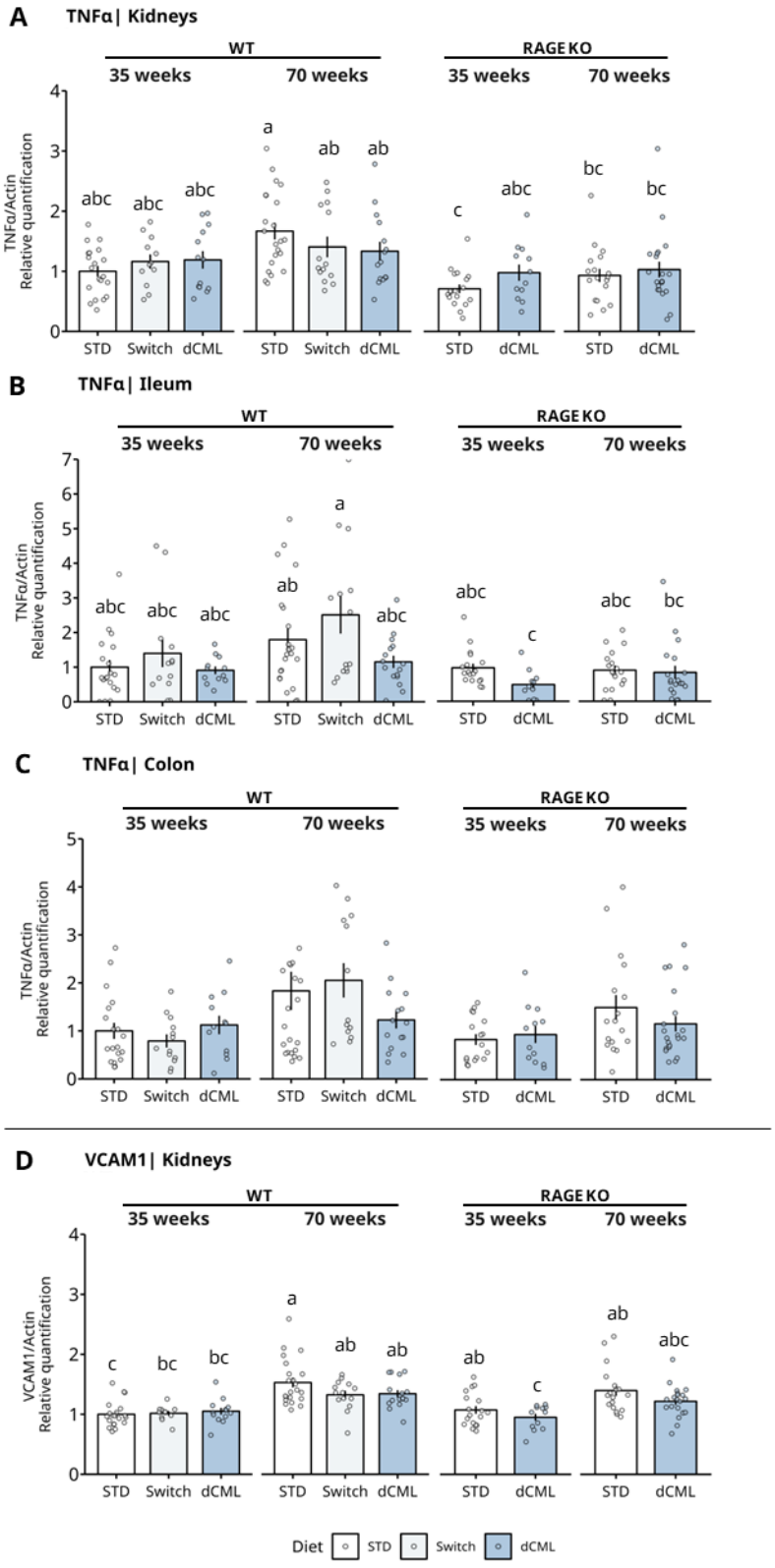

Figure 9 Relative expression of *TNFα* and *VCAM1* from RT-qPCR analysis. Relative expression of TNFα across the different dietary treatments administered to WT and RAGE KO mice for 35 and 70 weeks in **(A)** kidneys, **(B)** ileum, and **(C)** colon. **(D)** Relative expression of VCAM1 across the different dietary treatments in WT and RAGE KO mice at 35 and 70 weeks in the kidneys. Bars represent means ± SEM. Letter indices (Kruskal-Wallis rank test followed by Dunn's posthoc test for multi-comparisons) indicate statistical differences among groups within each organ. α=0.05. Housekeeping gene: Actin. Reference group: WT-STD group 35 weeks.

The pro-inflammatory potential of dAGEs remains a topic of ongoing debate, and recent studies have reported conflicting findings. Mice receiving a diet enriched with dCML at a dose of 200 $\mu g_{dCML}/g_{food}$ for 40-weeks exhibited increased expression of *VCAM1* in the arteriolar tissue [66], but no other organ was analyzed. Further, studies on animals that received an AGE-enriched diet (casein-methylglyoxal - 17.4 $g_{MG\text{-}H1}/kg_{food}$) over 22 weeks had increased levels of Il1β, IL17 and TNFα, while anti-inflammatory agents such as *IL10* and *IL6* were downregulated [67]. In contrast to the 2 previous studies, a recent paper published by van Dongen et al. demonstrated that a baked chow diet high in dAGEs, had a limited pro-inflammatory effect in C57BL/6 female mice. The study measured the levels of six inflammatory biomarkers, including CRP, TNFα, INF, KC/GRO, IL6, and IL10 [22]. Among them, only the systemic level of the anti-inflammatory cytokine *IL10* showed a significant decrease when the mice were fed a baked chow diet and none of the other inflammatory biomarkers were affected by diet. These latest findings are in line with what we observed in our study, namely that the proinflammatory effects of a short- or long-term dietary exposure to AGEs seem extremely limited, at least in the mouse models used.

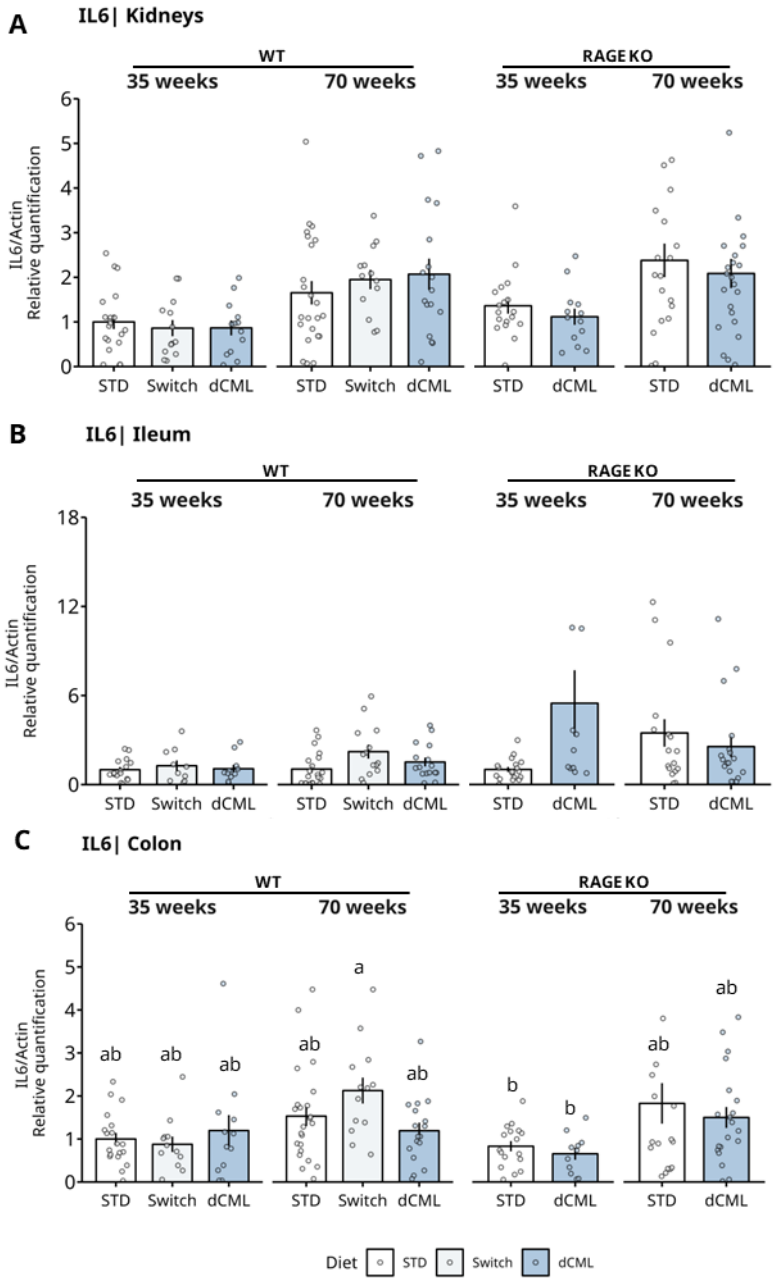

Figure 10 Relative expression of *IL6* RT-qPCR analysis. Relative expression of *IL6* across the different dietary treatments administered to WT and RAGE KO mice at 35- and 70-weeks-old in **(A)** kidneys, **(B)** ileum, and **(C)** colon. Bars represent means ± SEM. Letter indices (Kruskal-Wallis rank test followed by Dunn's posthoc test for multi-comparisons) indicate statistical differences among groups within each organ. α=0.05. Housekeeping gene: Actin. Reference group: WT-STD group 35 weeks.

Teissier et al. (2019) took into consideration that, besides the putative involvement of dCML in the aggravation of nephropathies, age was a preponderant factor in the variations of the biomarkers mentioned above. This age-related factor could be a confounding variable when distinguishing the actual effects of the diet in this context. Additionally, in this same study, the deletion of RAGE appeared to be

strongly associated with the progression of inflammation, including a compensatory mechanism that led to an increase in anti-inflammatory pathways, as indicated by *IL6*. [28].

3.7. RAGE is suggested to play a role in age-related epigenetic control in kidneys

To investigate the mechanisms of epigenomic control associated with a dCML-enriched diet, we quantified the expression of two key epigenetic switchers, *SIRT1* (encoding a deacetylase) and *EZH2* (encoding a methyltransferase). We did not observe an overall effect of the diets on *SIRT1* and *EZH2* mRNA relative expressions (Figures 11A and 11C). This absence of any significant effect of diet allowed us to combine the data by genotype and age for further statistical analysis with larger numbers of mice per group. Figure 11B shows no effect of the genotype or of age on the SIRT1 mRNA relative expression. However, a non-significant lower relative expression of *EZH2* transcripts was detected in RAGE KO animals compared with WT mice at both 35 and 70 weeks (Figure 11D).

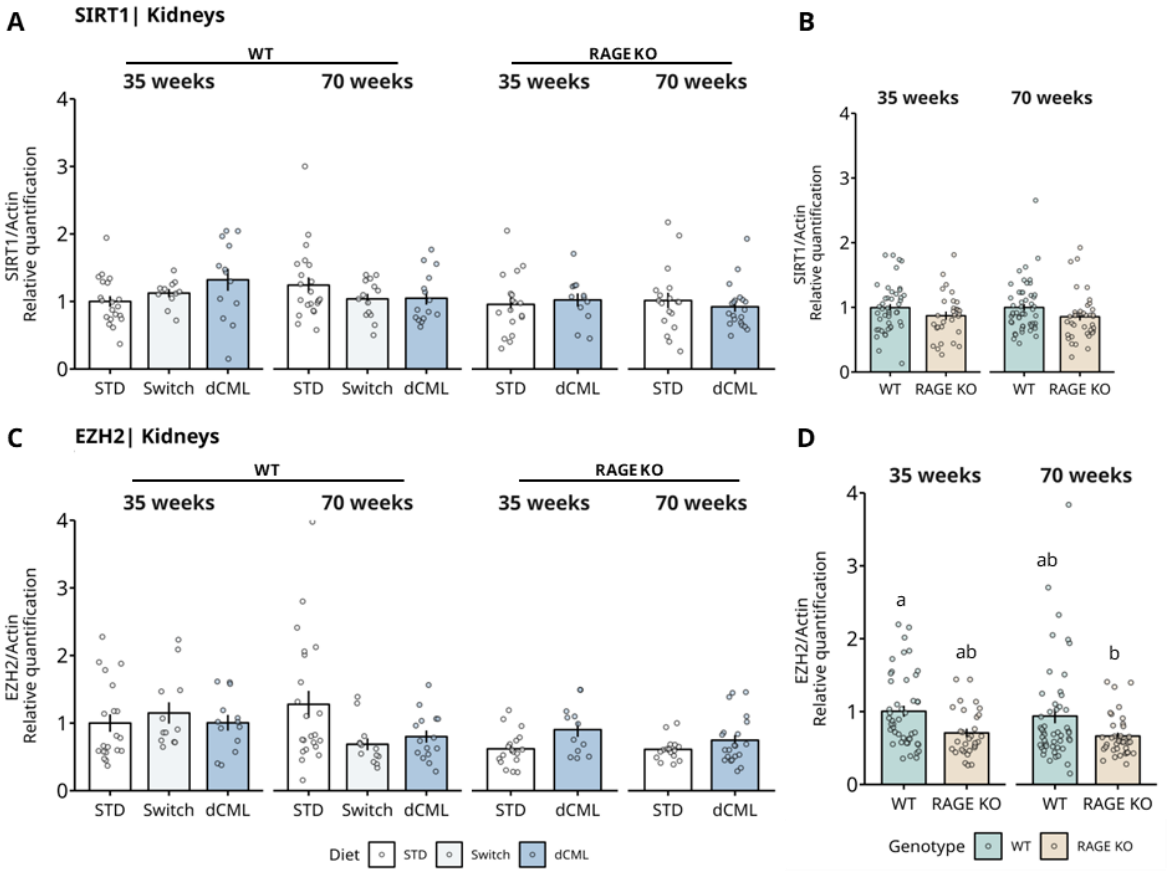

Figure 11 Relative expression of *SIRT1* and *EZH2* from RT-qPCR analysis in kidney samples. **(A)** Relative expression of SIRT1 across the different dietary treatments administered to WT and RAGE KO mice at 35- and 70-weeks-old, and **(B)** cumulative effect in both diets between genotypes. **(C)** Relative expression of *EZH2* across the different dietary treatments administered to WT and RAGE KO mice at 35- and 70-weeks-old, and **(D)** cumulative effect between genotypes**.** Bars represent means ± SEM. Letter indices (Kruskal-Wallis rank test followed by Dunn's posthoc test for multi-comparisons) indicate statistical differences among groups within each chart. α=0.05. Housekeeping gene: Actin. Reference group: **(A-C)** WT-STD group 35 weeks; **(B- D)** WT-35 weeks.

SIRT1 has been reported to be downregulated with age in both humans and mice, and also to be associated with cellular aging/senescence regulation [68,69]. According to the data presented here (Figure 11B), no differences were observed when comparing animals at 35 and 70 weeks. As a class-III histone deacetylase (HDAC), SIRT1 plays a role in epigenetic control, acting through the deacetylation in the nucleus of both histone (H1K26ac, H3K9ac, and H4K16ac) and non-histone targets (AKT/mTOR, FOXO) [70,71]. Such control acts both on the deacetylation of epigenetic hotspots (known to participate in gene deactivation) or by DNA damage control associated with senescence (SIRT1 action over non-histone proteins) [70]. In the context of a dietary influence of high glycated-protein consumption, *SIRT1* has been reported to be downregulated in the aortic wall of 48-week-old WT mice in receipt of a dCML-enriched diet for 40 weeks, compared with mice fed a regular diet [27]. The authors proposed that the suppression of SIRT1 in the aortic endothelium was associated with arterial aging, reporting lower flexibility and higher CML accumulation in this tissue. Others have demonstrated that the activation of the AGE-RAGE axis decreased SIRT1 expression by enhanced ubiquitination and proteasomal degradation of SIRT1 [72]. SIRT1 suppression by AGE consumption has also been shown to be associated with muscular oxidative stress and insulin resistance [73]. Although the precise mechanisms governing the relationship between RAGE and SIRT1 pathways are not fully elucidated, the absence of RAGE-induced NF-κB pathways in RAGE KO mice would reduce aging-related signaling and the expression of SIRT1 by removing the inflammatory responses mediated by RAGE [74].

EZH2, on the other hand, acts only on histone targets, affecting gene silencing by promotion of the trimethylation of H3K27ac [75]. AGEs were demonstrated to reduce H3K27me3 glomerular podocytes (*in vitro*) chronically exposed to AGEs by downregulating EZH2 expression [76]. The modulation of *EZH2* was associated with podocyte injury mediated by the suppression of NIPP1 [32]. Here, although we worked on a pool of renal cells (*i.e.* podocytes, glomeruli), the trend of reduced *EZH2* in RAGE KO animals was also evident in our results and may be associated with the protective effect of RAGE ablation postulated previously.

3.8. Is cell senescence increased by a diet high in dCML?

Real-time RT-PCR demonstrated that there was little or no effect of the dietary treatments on the renal expression of cell senescence markers *P16*, *GLβ1*, and *PGC1α* (Figure 12). Within the WT animal group, there was a noticeable trend for an increase in *P16* expression with age (significant among mice fed the STD diet). No similar effect was observed among RAGE KO animals, underlining the influence of RAGE knock out on *P16* expression. No distinguishable changes were detected in the relative expression profile of *GLβ1* or mitochondrial *PGC1α*, neither related to diet nor to genotype.

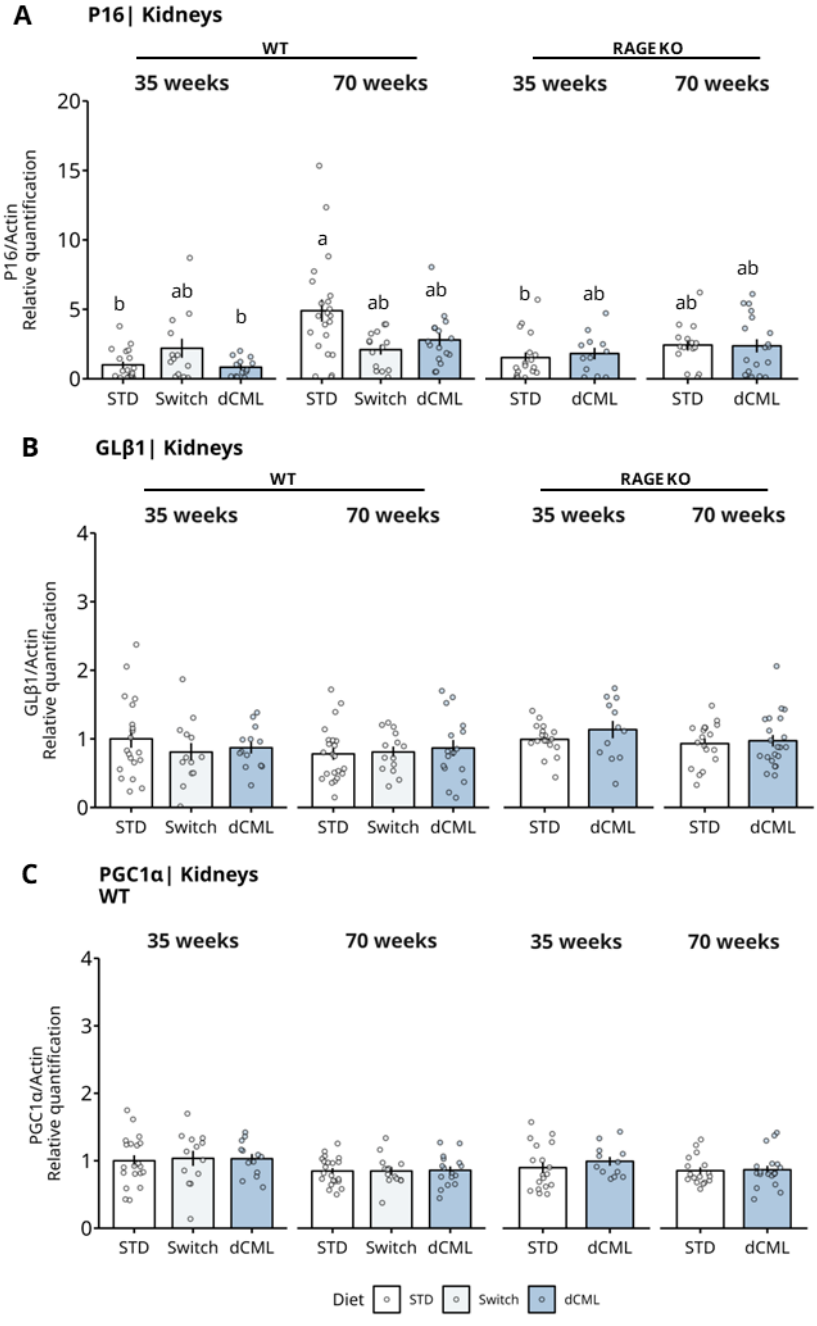

Figure 12 Relative expression of *P16*, *GLβ1*, and *PGC1α* from RT-qPCR analysis in kidney samples. Relative expression of *P16* across the different dietary treatments administered to WT and RAGE KO mice at 35 and 70 weeks **(A)**. Relative expression of *GLβ1* across the different dietary treatments administered to WT and RAGE KO mice at 35 and 70 weeks **(B)** Relative expression of *PGC1α* across the different dietary treatments in WT and RAGE KO mice at 35 and 70 weeks **(C)**. Bars represent means ± SEM. Letter indices (Kruskal-Wallis rank test followed by Dunn's posthoc test for multi-comparisons) indicate statistical differences among groups within each chart. α=0.05. Housekeeping gene: Actin. Reference group: WT-STD group 35 weeks.

Increased *P16* expression is related to cell cycle arrest and senescence progression. In this context, senescent cells show increased expression of *P16* as well as other senescent phenotype molecules such as *GLβ1* [77]. The rise of a senescent phenotype has as its main function the activation of downstream survival pathways [78]. *P16* has been implicated in cellular senescence and is associated with the activation of inflammation. Therefore, the lower expression of *P16* in the RAGE KO group may contribute to a decrease in macrophage recruitment and subsequent inflammatory response [79]. We speculate here that comparable mechanisms likely contributed to a lesser progression of inflammatory markers in RAGE KO animals, as illustrated in Figure 12.

The transcriptional co-activator *PGC1α* is an important regulator of mitochondrial homeostasis, especially in coordinating energy expenditure and biogenesis [80]. *PGC1α* expression is notably increased in tissues with high energy expenditure such as muscles, kidneys and the heart [80]. In the kidneys, *PGC1α* dysregulation has been associated with the development of diabetes and fibrosis [81]. Despite the high occurrence of mitochondria in the renal matrix, we observe no evidence of an increase or decrease of *PGC1α* in this organ. Corroborating with these results, we observed that WT and RAGE KO animals presented similar activation of the mTOR protein pathways in the lungs (Figure 13). As no evidence for exacerbated and ongoing oxidative stress, nor for the emergence of renal diseases was observed, we expected that these pathways would remain unchanged.

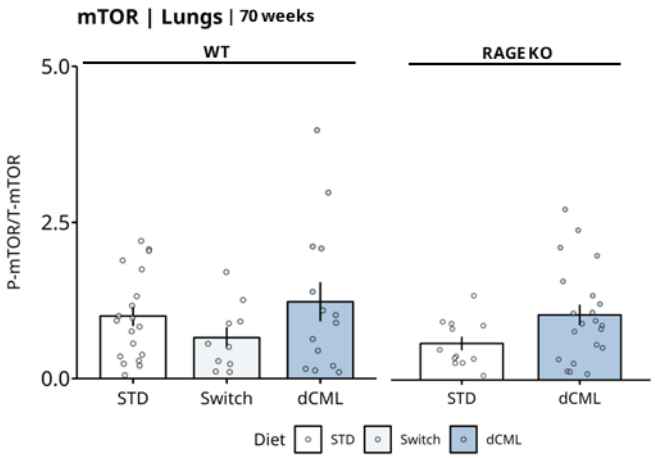

Figure 13 Protein quantification (western blot) of phosphorylated (P-mTOR) and total mTOR (T-mTOR) normalized to actin protein expression. P-mTOR/T-mTOR ratio across the different dietary treatments administered to WT and RAGE KO mice at 35 and 70 weeks. Housekeeping protein: Actin. Reference group: WT-STD group.

mTOR pathways are involved with monitoring of energy expenditure and cell growth. In the lungs, the activation mediated by the phosphorylation of the mTOR complex has been demonstrated to lead to cell senescence and emphysema [82], while in the kidneys it was demonstrated to be involved in glomerular hypertrophy [83]. Recent studies on rat vascular smooth muscle cells cell culture (VSMC) [84] as well as podocytes [85], demonstrated that the *in vitro* exposure of these cells to AGEs impaired the mTOR pathway, suppressing autophagy by upregulating P-mTOR. However, no effects on this metabolic pathway were detected in our study. We thus suggest that a high dietary exposure to dCML does not result in mTOR activation, at least in the lungs. Ongoing investigations will examine the behavior of mTOR phosphorylation in the kidneys.

4 Conclusions

Taken together, our findings suggest that although free-CML accumulates in target organs such as the kidneys, ileum, and colon, it does not appear to have a significant impact on overall health. It is worth noting that such effects were not observed either in the short term (35 weeks), nor in long term (up to 70 weeks of chronic exposure to dCML). Together with previous studies [41,192, 209], and with reference to results presented in CHAPTER 4, our study sheds light on concerns that short-term or life-long exposure to dCML does not prominently influence endogenous glycation, inflammation, oxidative stress, and senescence parameters in a rodent model.

We have demonstrated here for the first time that an early dietary change (dCML → STD) resulted in a return to baseline dCML accumulation in vital organs of the excretory and digestive systems, even in animals exposed to dCML during gestation. In addition, intrauterine exposure to a diet rich in CML did not seem to have any influence on the physiological traits observed in the offspring.

Finally, the expression levels of *TNFα*, *VCAM1*, *IL6*, and *P16* genes were upregulated in an age-dependent manner, particularly noticeable in the kidneys of WT animals. These increases were smaller in RAGE KO mice. Moreover, the ablation of RAGE appears to contribute to the downregulation of *EZH2*, indicating a potential involvement of RAGE in the epigenetic control of renal cells. It appears that RAGE is directly associated to age-related pro-inflammatory effects, and we observed no effect of the consumption of AGEs. This observation sheds further light on the involvement of RAGE in processes related to inflammaging.

We recognize that our study has a limitation in terms of sample sizes. An important limitation was the small number of animals, especially among the 6-week-old group. The small sample sizes reduced our capacity to interpret the results at this time point and warrants further investigation with a larger number of animals per group to better define the physiological effects of dietary AGEs at this age.

As an integrated project, we made use of different analytical approaches (*i.e.* LC-MS/MS, RT-qPCR, western blot), to identify the effects of a diet enriched in AGEs across a wide panel of biomarkers at the local and systemic levels. Given the results presented here on the accumulation of free CML in the colon and ileum, and taking into consideration the published literature, metagenomic analysis of the caecum microbiota is ongoing to study the effect of dCML consumption on the gut

bacterial biodiversity (variation on bacterial genus level, and the determination of Firmicutes/Bacteroidetes ratio). In addition to this, ileum samples will be further explored concerning the expression of genes associated with intestinal tight junctions (*e.g.* occludin, claudin).

Furthermore, it remains to be explored if some of the biomarkers, mostly presented here on the transcript level, vary at the protein level. Hence, ongoing western blot analysis on kidney samples (including animals of 6, 35, and 70 weeks of age from all treatments) may help to elucidate if there is indeed a translational control on the expression of target proteins (*e.g.* RAGE, mTOR, AKT). Finally, to further address immunosenescence, a panel of genes (*e.g. GATA3, FOXp3, BOX21, SIRT1, P16*) is being evaluated in the spleen to define if there is an involvement with dCML enriched diet and immune cell functional decline.

5 References

1. WHO GHE: Life Expectancy and Healthy Life Expectancy Available online: https://www.who.int/data/gho/data/themes/mortality-and-global-health-estimates/ghe-life-expectancy-and-healthy-life-expectancy (accessed on 31 May 2023).
2. Miladinov, G. Socioeconomic Development and Life Expectancy Relationship: Evidence from the EU Accession Candidate Countries. *Genus* **2020**, *76*, 2, doi:10.1186/s41118-019-0071-0.
3. Galor, O. The Demographic Transition: Causes and Consequences. *Cliometrica (Berl)* **2012**, *6*, 1–28, doi:10.1007/s11698-011-0062-7.
4. Melzer, D.; Pilling, L.C.; Ferrucci, L. The Genetics of Human Ageing. *Nat Rev Genet* **2020**, *21*, 88–101, doi:10.1038/s41576-019-0183-6.
5. Sanada, F.; Taniyama, Y.; Muratsu, J.; Otsu, R.; Shimizu, H.; Rakugi, H.; Morishita, R. Source of Chronic Inflammation in Aging. *Front Cardiovasc Med* **2018**, *5*, 12, doi:10.3389/fcvm.2018.00012.
6. Zuo, L.; Prather, E.R.; Stetskiv, M.; Garrison, D.E.; Meade, J.R.; Peace, T.I.; Zhou, T. Inflammaging and Oxidative Stress in Human Diseases: From Molecular Mechanisms to Novel Treatments. *Int J Mol Sci* **2019**, *20*, 4472, doi:10.3390/ijms20184472.
7. Carrasco, E.; Gómez de las Heras, M.M.; Gabandé-Rodríguez, E.; Desdín-Micó, G.; Aranda, J.F.; Mittelbrunn, M. The Role of T Cells in Age-Related Diseases. *Nat Rev Immunol* **2022**, *22*, 97–111, doi:10.1038/s41577-021-00557-4.
8. Zamboni, M.; Nori, N.; Brunelli, A.; Zoico, E. How Does Adipose Tissue Contribute to Inflammageing? *Experimental Gerontology* **2021**, *143*, 111162, doi:10.1016/j.exger.2020.111162.
9. Kopp, W. How Western Diet And Lifestyle Drive The Pandemic Of Obesity And Civilization Diseases. *Diabetes Metab Syndr Obes* **2019**, *12*, 2221–2236, doi:10.2147/DMSO.S216791.
10. Dawson, S.L.; Mohebbi, M.; Craig, J.M.; Dawson, P.; Clarke, G.; Tang, M.L.; Jacka, F.N. Targeting the Perinatal Diet to Modulate the Gut Microbiota Increases Dietary Variety and Prebiotic and Probiotic Food Intakes: Results from a Randomised Controlled Trial. *Public Health Nutrition* **2021**, *24*, 1129–1141, doi:10.1017/S1368980020003511.
11. Dunkerton, S.; Aiken, C. Impact of the Intrauterine Environment on Future Reproductive and Metabolic Health. *The Obstetrician & Gynaecologist* **2022**, *24*, 93–100, doi:10.1111/tog.12797.
12. Bodden, C.; Hannan, A.J.; Reichelt, A.C. Diet-Induced Modification of the Sperm Epigenome Programs Metabolism and Behavior. *Trends in Endocrinology & Metabolism* **2020**, *31*, 131–149, doi:10.1016/j.tem.2019.10.005.
13. Chen, Q.; Yan, W.; Duan, E. Epigenetic Inheritance of Acquired Traits through Sperm RNAs and Sperm RNA Modifications. *Nat Rev Genet* **2016**, *17*, 733–743, doi:10.1038/nrg.2016.106.
14. Fetissov, S.O.; Hökfelt, T. On the Origin of Eating Disorders: Altered Signaling between Gut Microbiota, Adaptive Immunity and the Brain Melanocortin System Regulating Feeding Behavior. *Current Opinion in Pharmacology* **2019**, *48*, 82–91, doi:10.1016/j.coph.2019.07.004.
15. Tamashiro, K.L.K.; Moran, T.H. Perinatal Environment and Its Influences on Metabolic Programming of Offspring. *Physiology & Behavior* **2010**, *100*, 560–566, doi:10.1016/j.physbeh.2010.04.008.
16. Korgan, A.C.; Foxx, C.L.; Hashmi, H.; Sago, S.A.; Stamper, C.E.; Heinze, J.D.; O'Leary, E.; King, J.L.; Perrot, T.S.; Lowry, C.A.; et al. Effects of Paternal High-Fat Diet and Maternal Rearing Environment on the Gut Microbiota and Behavior. *Sci Rep* **2022**, *12*, 10179, doi:10.1038/s41598-022-14095-z.
17. Myles, I.A.; Fontecilla, N.M.; Janelsins, B.M.; Vithayathil, P.J.; Segre, J.A.; Datta, S.K. Parental Dietary Fat Intake Alters Offspring Microbiome and Immunity. *J Immunol* **2013**, *191*, 10.4049/jimmunol.1301057, doi:10.4049/jimmunol.1301057.
18. Margină, D.; Ungurianu, A.; Purdel, C.; Tsoukalas, D.; Sarandi, E.; Thanasoula, M.; Tekos, F.; Mesnage, R.; Kouretas, D.; Tsatsakis, A. Chronic Inflammation in the Context of Everyday Life: Dietary Changes as Mitigating Factors. *Int J Environ Res Public Health* **2020**, *17*, 4135, doi:10.3390/ijerph17114135.

19. Rabbani, N.; Thornalley, P.J. Advanced Glycation End Products in the Pathogenesis of Chronic Kidney Disease. *Kidney International* **2018**, *93*, 803–813, doi:10.1016/j.kint.2017.11.034.
20. Delgado-Andrade, C. Carboxymethyl-Lysine: Thirty Years of Investigation in the Field of AGE Formation. *Food Funct.* **2016**, *7*, 46–57, doi:10.1039/C5FO00918A.
21. van Dongen, K.C.W.; Kappetein, L.; Miro Estruch, I.; Belzer, C.; Beekmann, K.; Rietjens, I.M.C.M. Differences in Kinetics and Dynamics of Endogenous versus Exogenous Advanced Glycation End Products (AGEs) and Their Precursors. *Food and Chemical Toxicology* **2022**, *164*, 112987, doi:10.1016/j.fct.2022.112987.
22. van Dongen, K.C.W.; Linkens, A.M.A.; Wetzels, S.M.W.; Wouters, K.; Vanmierlo, T.; van de Waarenburg, M.P.H.; Scheijen, J.L.J.M.; de Vos, W.M.; Belzer, C.; Schalkwijk, C.G. Dietary Advanced Glycation Endproducts (AGEs) Increase Their Concentration in Plasma and Tissues, Result in Inflammation and Modulate Gut Microbial Composition in Mice; Evidence for Reversibility. *Food Research International* **2021**, *147*, 110547, doi:10.1016/j.foodres.2021.110547.
23. Xue, J.; Ray, R.; Singer, D.; Böhme, D.; Burz, D.S.; Rai, V.; Hoffmann, R.; Shekhtman, A. The Receptor for Advanced Glycation End Products (RAGE) Specifically Recognizes Methylglyoxal-Derived AGEs. *Biochemistry* **2014**, *53*, 3327–3335.
24. Rojas, A.; Schneider, I.; Lindner, C.; Gonzalez, I.; Morales, M.A. The RAGE/Multiligand Axis: A New Actor in Tumor Biology. *Bioscience Reports* **2022**, *42*, BSR20220395.
25. Hull, G.L.J.; Woodside, J.V.; Ames, J.M.; Cuskelly, G.J. Nε-(Carboxymethyl)Lysine Content of Foods Commonly Consumed in a Western Style Diet. *Food Chemistry* **2012**, *131*, 170–174, doi:10.1016/j.foodchem.2011.08.055.
26. Frimat, M.; Teissier, T.; Boulanger, E. Is RAGE the Receptor for Inflammaging? *Aging (Albany NY)* **2019**, *11*, 6620–6621, doi:10.18632/aging.102256.
27. Grossin, N.; Auger, F.; Niquet-Leridon, C.; Durieux, N.; Montaigne, D.; Schmidt, A.M.; Susen, S.; Jacolot, P.; Beuscart, J.-B.; Tessier, F.J.; et al. Dietary CML-Enriched Protein Induces Functional Arterial Aging in a RAGE-Dependent Manner in Mice. *Mol Nutr Food Res* **2015**, *59*, 927–938, doi:10.1002/mnfr.201400643.
28. Teissier, T.; Quersin, V.; Gnemmi, V.; Daroux, M.; Howsam, M.; Delguste, F.; Lemoine, C.; Fradin, C.; Schmidt, A.-M.; Cauffiez, C.; et al. Knockout of Receptor for Advanced Glycation End-Products Attenuates Age-Related Renal Lesions. *Aging Cell* **2019**, *18*, e12850, doi:10.1111/acel.12850.
29. Nogueira Silva Lima, M.T.; Howsam, M.; Anton, P.M.; Delayre-Orthez, C.; Tessier, F.J. Effect of Advanced Glycation End-Products and Excessive Calorie Intake on Diet-Induced Chronic Low-Grade Inflammation Biomarkers in Murine Models. *Nutrients* **2021**, *13*, 3091, doi:10.3390/nu13093091.
30. Constien, R.; Forde, A.; Liliensiek, B.; Gröne, H.J.; Nawroth, P.; Hämmerling, G.; Arnold, B. Characterization of a Novel EGFP Reporter Mouse to Monitor Cre Recombination as Demonstrated by a Tie2 Cre Mouse Line. *Genesis* **2001**, *30*, 36–44, doi:10.1002/gene.1030.
31. Livak, K.J.; Schmittgen, T.D. Analysis of Relative Gene Expression Data Using Real-Time Quantitative PCR and the 2(-Delta Delta C(T)) Method. *Methods* **2001**, *25*, 402–408, doi:10.1006/meth.2001.1262.
32. Liebisch, M.; Wolf, G. AGE-Induced Suppression of EZH2 Mediates Injury of Podocytes by Reducing H3K27me3. *AJN* **2020**, *51*, 676–692, doi:10.1159/000510140.
33. Oh, S.; Rho, N.-K.; Byun, K.-A.; Yang, J.Y.; Sun, H.J.; Jang, M.; Kang, D.; Son, K.H.; Byun, K. Combined Treatment of Monopolar and Bipolar Radiofrequency Increases Skin Elasticity by Decreasing the Accumulation of Advanced Glycated End Products in Aged Animal Skin. *International Journal of Molecular Sciences* **2022**, *23*, 2993, doi:10.3390/ijms23062993.
34. Sathyanesan, M.; Haiar, J.M.; Watt, M.J.; Newton, S.S. Restraint Stress Differentially Regulates Inflammation and Glutamate Receptor Gene Expression in the Hippocampus of C57BL/6 and BALB/c Mice. *Stress* **2017**.
35. Drummond, D.; Baravalle-Einaudi, M.; Lezmi, G.; Vibhushan, S.; Franco-Montoya, M.-L.; Hadchouel, A.; Boczkowski, J.; Delacourt, C. Combined Effects of *in Utero* and Adolescent Tobacco Smoke Exposure on Lung Function in C57Bl/6J Mice. *Environmental Health Perspectives* **2017**, *125*, 392–399, doi:10.1289/EHP54.
36. Niu, B.; He, K.; Li, P.; Gong, J.; Zhu, X.; Ye, S.; Ou, Z.; Ren, G. SIRT1 Upregulation Protects against Liver Injury Induced by a HFD through Inhibiting CD36 and the NF-κB Pathway in

Mouse Kupffer Cells. *Molecular Medicine Reports* **2018**, *18*, 1609–1615, doi:10.3892/mmr.2018.9088.
37. Gagliardi, S.; Ogliari, P.; Davin, A.; Corato, M.; Cova, E.; Abel, K.; Cashman, J.R.; Ceroni, M.; Cereda, C. Flavin-Containing Monooxygenase MRNA Levels Are Up-Regulated in ALS Brain Areas in SOD1-Mutant Mice. *Neurotox Res* **2011**, *20*, 150–158, doi:10.1007/s12640-010-9230-y.
38. Chang, L.-W.; Juang, L.-J.; Wang, B.-S.; Wang, M.-Y.; Tai, H.-M.; Hung, W.-J.; Chen, Y.-J.; Huang, M.-H. Antioxidant and Antityrosinase Activity of Mulberry (Morus Alba L.) Twigs and Root Bark. *Food Chem Toxicol* **2011**, *49*, 785–790, doi:10.1016/j.fct.2010.11.045.
39. Johansson, M.E.; Zhang, X.-Y.; Edfeldt, K.; Lundberg, A.M.; Levin, M.C.; Borén, J.; Li, W.; Yuan, X.-M.; Folkersen, L.; Eriksson, P.; et al. Innate Immune Receptor NOD2 Promotes Vascular Inflammation and Formation of Lipid-Rich Necrotic Cores in Hypercholesterolemic Mice. *European Journal of Immunology* **2014**, *44*, 3081–3092, doi:10.1002/eji.201444755.
40. R Core Team R: The R Project for Statistical Computing Available online: https://www.r-project.org/ (accessed on 30 May 2023).
41. Starowicz, M.; Zieliński, H. How Maillard Reaction Influences Sensorial Properties (Color, Flavor and Texture) of Food Products? *Food Reviews International* **2019**, *35*, 707–725, doi:10.1080/87559129.2019.1600538.
42. The Jackson Laboratory Body Weight Information for Aged C57BL/6J (000664) Available online: https://www.jax.org/jax-mice-and-services/strain-data-sheet-pages/body-weight-chart-aged-b6 (accessed on 16 October 2022).
43. Tessier, F.J.; Niquet-Léridon, C.; Jacolot, P.; Jouquand, C.; Genin, M.; Schmidt, A.-M.; Grossin, N.; Boulanger, E. Quantitative Assessment of Organ Distribution of Dietary Protein-Bound 13C-Labeled Nε-Carboxymethyllysine after a Chronic Oral Exposure in Mice. *Molecular Nutrition & Food Research* **2016**, *60*, 2446–2456, doi:https://doi.org/10.1002/mnfr.201600140.
44. Sarron, E.; Pérot, M.; Barbezier, N.; Delayre-Orthez, C.; Gay-Quéheillard, J.; Anton, P.M. Early Exposure to Food Contaminants Reshapes Maturation of the Human Brain-Gut-Microbiota Axis. *World J Gastroenterol* **2020**, *26*, 3145–3169, doi:10.3748/wjg.v26.i23.3145.
45. Koschinsky, T.; He, C.-J.; Mitsuhashi, T.; Bucala, R.; Liu, C.; Buenting, C.; Heitmann, K.; Vlassara, H. Orally Absorbed Reactive Glycation Products (Glycotoxins): An Environmental Risk Factor in Diabetic Nephropathy. *Medical Sciences* **1997**, 6.
46. Dunn, J.A.; McCance, D.R.; Thorpe, S.R.; Lyons, T.J.; Baynes, J.W. Age-Dependent Accumulation of N Epsilon-(Carboxymethyl)Lysine and N Epsilon-(Carboxymethyl)Hydroxylysine in Human Skin Collagen. *Biochemistry* **1991**, *30*, 1205–1210, doi:10.1021/bi00219a007.
47. Gorisse, L.; Pietrement, C.; Vuiblet, V.; Schmelzer, C.E.H.; Köhler, M.; Duca, L.; Debelle, L.; Fornès, P.; Jaisson, S.; Gillery, P. Protein Carbamylation Is a Hallmark of Aging. *Proc Natl Acad Sci U S A* **2016**, *113*, 1191–1196, doi:10.1073/pnas.1517096113.
48. Fokkens, B.T.; Smit, A.J. Skin Fluorescence as a Clinical Tool for Non-Invasive Assessment of Advanced Glycation and Long-Term Complications of Diabetes. *Glycoconj J* **2016**, *33*, 527–535, doi:10.1007/s10719-016-9683-1.
49. Alamir, I.; Niquet-Leridon, C.; Jacolot, P.; Rodriguez, C.; Orosco, M.; Anton, P.M.; Tessier, F.J. Digestibility of Extruded Proteins and Metabolic Transit of Nε-Carboxymethyllysine in Rats. *Amino Acids* **2013**, *44*, 1441–1449, doi:10.1007/s00726-012-1427-3.
50. van Dongen, K.C.W.; Linkens, A.M.A.; Wetzels, S.M.W.; Wouters, K.; Vanmierlo, T.; van de Waarenburg, M.P.H.; Scheijen, J.L.J.M.; de Vos, W.M.; Belzer, C.; Schalkwijk, C.G. Dietary Advanced Glycation Endproducts (AGEs) Increase Their Concentration in Plasma and Tissues, Result in Inflammation and Modulate Gut Microbial Composition in Mice; Evidence for Reversibility. *Food Research International* **2021**, *147*, 110547, doi:10.1016/j.foodres.2021.110547.
51. Hellwig, M.; Geissler, S.; Matthes, R.; Peto, A.; Silow, C.; Brandsch, M.; Henle, T. Transport of Free and Peptide-Bound Glycated Amino Acids: Synthesis, Transepithelial Flux at Caco-2 Cell Monolayers, and Interaction with Apical Membrane Transport Proteins. *ChemBioChem* **2011**, *12*, 1270–1279.
52. Li, M.; Zeng, M.; He, Z.; Zheng, Z.; Qin, F.; Tao, G.; Zhang, S.; Chen, J. Increased Accumulation of Protein-Bound Nε-(Carboxymethyl)Lysine in Tissues of Healthy Rats after Chronic Oral Nε-(Carboxymethyl)Lysine. *J. Agric. Food Chem.* **2015**, *63*, 1658–1663, doi:10.1021/jf505063t.

53. Boesten, D.M.P.H.J.; Elie, A.G.I.M.; Drittij-Reijnders, M.-J.; den Hartog, G.J.M.; Bast, A. Effect of Nε-Carboxymethyllysine on Oxidative Stress and the Glutathione System in Beta Cells. *Toxicol Rep* **2014**, *1*, 973–980, doi:10.1016/j.toxrep.2014.06.003.
54. Salminen, A.; Kaarniranta, K.; Kauppinen, A. Crosstalk between Oxidative Stress and SIRT1: Impact on the Aging Process. *Int J Mol Sci* **2013**, *14*, 3834–3859, doi:10.3390/ijms14023834.
55. Rabbani, N.; Thornalley, P.J. Glycation Research in Amino Acids: A Place to Call Home. *Amino Acids* **2012**, *42*, 1087–1096, doi:10.1007/s00726-010-0782-1.
56. Chistiakov, D.A.; Sobenin, I.A.; Revin, V.V.; Orekhov, A.N.; Bobryshev, Y.V. Mitochondrial Aging and Age-Related Dysfunction of Mitochondria. *Biomed Res Int* **2014**, *2014*, 238463, doi:10.1155/2014/238463.
57. Pérez, S.; Rius-Pérez, S.; Tormos, A.M.; Finamor, I.; Nebreda, Á.R.; Taléns-Visconti, R.; Sastre, J. Age-Dependent Regulation of Antioxidant Genes by P38α MAPK in the Liver. *Redox Biology* **2018**, *16*, 276–284.
58. Bartling, B.; Zunkel, K.; Al-Robaiy, S.; Dehghani, F.; Simm, A. Gene Doubling Increases Glyoxalase 1 Expression in RAGE Knockout Mice. *Biochimica et Biophysica Acta (BBA) - General Subjects* **2020**, *1864*, 129438, doi:10.1016/j.bbagen.2019.129438.
59. Rabbani, N.; Thornalley, P.J. Dicarbonyls Linked to Damage in the Powerhouse: Glycation of Mitochondrial Proteins and Oxidative Stress. *Biochem Soc Trans* **2008**, *36*, 1045–1050, doi:10.1042/BST0361045.
60. Paul J. Thornalley PROTEIN AND NUCLEOTIDE DAMAGE BY GLYOXAL AND METHYLGLYOXAL IN PHYSIOLOGICAL SYSTEMS - ROLE IN AGEING AND DISEASE. *Drug Metabolism and Drug Interactions* **2008**, *23*, 125–150, doi:10.1515/DMDI.2008.23.1-2.125.
61. Xue, J.; Rai, V.; Frolov, S.; Singer, D.; Chabierski, S.; Xie, J.; Reverdatto, S.; Burz, D.S.; Schmidt, A.M.; Hoffman, R.; et al. Advanced Glycation End Product (AGE) Recognition by the Receptor for AGEs (RAGE). *Structure* **2011**, *19*, 722–732, doi:10.1016/j.str.2011.02.013.
62. Lin, J.-A.; Wu, C.-H.; Lu, C.-C.; Hsia, S.-M.; Yen, G.-C. Glycative Stress from Advanced Glycation End Products (AGEs) and Dicarbonyls: An Emerging Biological Factor in Cancer Onset and Progression. *Molecular Nutrition & Food Research* **2016**, *60*, n/a-n/a, doi:10.1002/mnfr.201500759.
63. Ishikawa, S.; Matsui, Y.; Wachi, S.; Yamaguchi, H.; Harashima, N.; Harada, M. Age-Associated Impairment of Antitumor Immunity in Carcinoma-Bearing Mice and Restoration by Oral Administration of Lentinula Edodes Mycelia Extract. *Cancer Immunol Immunother* **2016**, *65*, 961–972, doi:10.1007/s00262-016-1857-y.
64. Miró, L.; Garcia-Just, A.; Amat, C.; Polo, J.; Moretó, M.; Pérez-Bosque, A. Dietary Animal Plasma Proteins Improve the Intestinal Immune Response in Senescent Mice. *Nutrients* **2017**, *9*, 1346, doi:10.3390/nu9121346.
65. Yousef, H.; Czupalla, C.J.; Lee, D.; Chen, M.B.; Burke, A.N.; Zera, K.A.; Zandstra, J.; Berber, E.; Lehallier, B.; Mathur, V.; et al. Aged Blood Impairs Hippocampal Neural Precursor Activity and Activates Microglia via Brain Endothelial Cell VCAM1. *Nat Med* **2019**, *25*, 988–1000, doi:10.1038/s41591-019-0440-4.
66. Grossin, N.; Auger, F.; Niquet-Leridon, C.; Durieux, N.; Montaigne, D.; Schmidt, A.M.; Susen, S.; Jacolot, P.; Beuscart, J.-B.; Tessier, F.J.; et al. Dietary CML-Enriched Protein Induces Functional Arterial Aging in a RAGE-Dependent Manner in Mice. *Mol Nutr Food Res* **2015**, *59*, 927–938, doi:10.1002/mnfr.201400643.
67. Mastrocola, R.; Collotta, D.; Gaudioso, G.; Le Berre, M.; Cento, A.S.; Ferreira Alves, G.; Chiazza, F.; Verta, R.; Bertocchi, I.; Manig, F.; et al. Effects of Exogenous Dietary Advanced Glycation End Products on the Cross-Talk Mechanisms Linking Microbiota to Metabolic Inflammation. *Nutrients* **2020**, *12*, 2497, doi:10.3390/nu12092497.
68. Gong, H.; Pang, J.; Han, Y.; Dai, Y.; Dai, D.; Cai, J.; Zhang, T.-M. Age-Dependent Tissue Expression Patterns of Sirt1 in Senescence-Accelerated Mice. *Molecular Medicine Reports* **2014**, *10*, 3296–3302, doi:10.3892/mmr.2014.2648.
69. Wang, Z.A.; Hsu, W.; Liu, W.R. Role of SIRT1 in Epigenetics. In *Handbook of Nutrition, Diet, and Epigenetics*; Patel, V.B., Preedy, V.R., Eds.; Springer International Publishing: Cham, 2019; pp. 311–329 ISBN 978-3-319-55530-0.

70. Alves-Fernandes, D.K.; Jasiulionis, M.G. The Role of SIRT1 on DNA Damage Response and Epigenetic Alterations in Cancer. *Int J Mol Sci* **2019**, *20*, 3153, doi:10.3390/ijms20133153.
71. Yang, K.; Dong, W. SIRT1-Related Signaling Pathways and Their Association With Bronchopulmonary Dysplasia. *Frontiers in Medicine* **2021**, *8*.
72. Huang, K.-P.; Chen, C.; Hao, J.; Huang, J.-Y.; Liu, P.-Q.; Huang, H.-Q. AGEs-RAGE System down-Regulates Sirt1 through the Ubiquitin-Proteasome Pathway to Promote FN and TGF-B1 Expression in Male Rat Glomerular Mesangial Cells. *Endocrinology* **2015**, *156*, 268–279, doi:10.1210/en.2014-1381.
73. Cai, W.; Ramdas, M.; Zhu, L.; Chen, X.; Striker, G.E.; Vlassara, H. Oral Advanced Glycation Endproducts (AGEs) Promote Insulin Resistance and Diabetes by Depleting the Antioxidant Defenses AGE Receptor-1 and Sirtuin 1. *Proc Natl Acad Sci U S A* **2012**, *109*, 15888–15893, doi:10.1073/pnas.1205847109.
74. Kauppinen, A.; Suuronen, T.; Ojala, J.; Kaarniranta, K.; Salminen, A. Antagonistic Crosstalk between NF-KB and SIRT1 in the Regulation of Inflammation and Metabolic Disorders. *Cell Signal* **2013**, *25*, 1939–1948, doi:10.1016/j.cellsig.2013.06.007.
75. Gan, L.; Yang, Y.; Li, Q.; Feng, Y.; Liu, T.; Guo, W. Epigenetic Regulation of Cancer Progression by EZH2: From Biological Insights to Therapeutic Potential. *Biomarker Research* **2018**, *6*, 10, doi:10.1186/s40364-018-0122-2.
76. Thieme, K.; Pereira, B.M.V.; da Silva, K.S.; Fabre, N.T.; Catanozi, S.; Passarelli, M.; Correa-Giannella, M.L. Chronic Advanced-Glycation End Products Treatment Induces TXNIP Expression and Epigenetic Changes in Glomerular Podocytes in Vivo and in Vitro. *Life Sciences* **2021**, *270*, 118997, doi:10.1016/j.lfs.2020.118997.
77. Kaarniranta, K.; Kajdanek, J.; Morawiec, J.; Pawlowska, E.; Blasiak, J. PGC-1α Protects RPE Cells of the Aging Retina against Oxidative Stress-Induced Degeneration through the Regulation of Senescence and Mitochondrial Quality Control. The Significance for AMD Pathogenesis. *International Journal of Molecular Sciences* **2018**, *19*, 2317, doi:10.3390/ijms19082317.
78. Hall, B.M.; Balan, V.; Gleiberman, A.S.; Strom, E.; Krasnov, P.; Virtuoso, L.P.; Rydkina, E.; Vujcic, S.; Balan, K.; Gitlin, I.I.; et al. P16(Ink4a) and Senescence-Associated β-Galactosidase Can Be Induced in Macrophages as Part of a Reversible Response to Physiological Stimuli. *Aging (Albany NY)* **2017**, *9*, 1867–1884, doi:10.18632/aging.101268.
79. Liu, J.-Y.; Souroullas, G.P.; Diekman, B.O.; Krishnamurthy, J.; Hall, B.M.; Sorrentino, J.A.; Parker, J.S.; Sessions, G.A.; Gudkov, A.V.; Sharpless, N.E. Cells Exhibiting Strong P16INK4a Promoter Activation in Vivo Display Features of Senescence. *Proceedings of the National Academy of Sciences* **2019**, *116*, 2603–2611, doi:10.1073/pnas.1818313116.
80. Anderson, R.; Prolla, T. PGC-1α in Aging and Anti-Aging Interventions. *Biochim Biophys Acta* **2009**, *1790*, 1059–1066, doi:10.1016/j.bbagen.2009.04.005.
81. Lynch, M.R.; Tran, M.T.; Parikh, S.M. PGC1α in the Kidney. *Am J Physiol Renal Physiol* **2018**, *314*, F1–F8, doi:10.1152/ajprenal.00263.2017.
82. Houssaini, A.; Breau, M.; Kebe, K.; Abid, S.; Marcos, E.; Lipskaia, L.; Rideau, D.; Parpaleix, A.; Huang, J.; Amsellem, V.; et al. MTOR Pathway Activation Drives Lung Cell Senescence and Emphysema. *JCI Insight* **2018**, *3*, doi:10.1172/jci.insight.93203.
83. Kajiwara, M.; Masuda, S. Role of MTOR Inhibitors in Kidney Disease. *Int J Mol Sci* **2016**, *17*, 975, doi:10.3390/ijms17060975.
84. Liu, Y.; Li, J.; Han, Y.; Chen, Y.; Liu, L.; Lang, J.; Yang, C.; Luo, H.; Ning, J. Advanced Glycation End-Products Suppress Autophagy by AMPK/MTOR Signaling Pathway to Promote Vascular Calcification. *Mol Cell Biochem* **2020**, *471*, 91–100, doi:10.1007/s11010-020-03769-9.
85. Zhao, X.; Chen, Y.; Tan, X.; Zhang, L.; Zhang, H.; Li, Z.; Liu, S.; Li, R.; Lin, T.; Liao, R.; et al. Advanced Glycation End-Products Suppress Autophagic Flux in Podocytes by Activating Mammalian Target of Rapamycin and Inhibiting Nuclear Translocation of Transcription Factor EB. *J Pathol* **2018**, *245*, 235–248, doi:10.1002/path.5077.

CHAPTER 7

Final remarks and perspectives

1 Main findings and final remarks

The impact of dietary habits on human health has received significant attention due to the well-documented effects of unbalanced diets on the incidence and development of chronic diseases [1–3]. The rising prevalence of obesity, cancer and cardiovascular diseases in the modern world has coincided with changes in dietary behavior, among other things, and more specifically the consumption of "Westernized diets" [4–6]. These diets consist of processed foods that are high in refined fats, sugars, and proteins, which undergo thermal processing to enhance taste and extend shelf life [7]. Consequently, these processed foods contain a higher amount of neoformed compounds, such as glycation products, compared with less processed food items [8]. As extensively discussed in the introductory part of this thesis, there is a significant debate regarding the involvement of AGEs in the pathophysiology of chronic diseases. These shifts in dietary patterns, sometimes called nutritional transition, have far-reaching implications for the future prevalence of these diseases. This is particularly significant as populations in both developed and developing countries undergo demographic transitions, resulting in an increasing number of older individuals [9].

The above-mentioned factors serve as motivations for research aimed at elucidating the impact of AGEs on health, particularly those associated with chronic pathophysiological processes. Based on the findings derived from this current work, we believe that we can now provide answers to some of the questions (CHAPTER 2) that served as the driving force behind this thesis.

The main goal of this project was to investigate the physiological effects associated with a diet high in dCML, with a specific focus on the activation of oxidative stress, inflammation, and cellular senescence.

First, we aimed to build up knowledge on the postprandial fate of dCML both in rodents and humans. Questions around the kinetics of dCML in rodents and humans were addressed in CHAPTER 4. Our results provide evidence that only the free form of CML increased in plasma in rats and humans. These data also provided novel evidence that the administration of dCML to a rodent model did not lead to endogenous glycation and the formation of protein-bound CML. A peak in postprandial free CML was observed from 90 to 120 min, both in rats and humans,

while the postprandial level of sRAGE was inversely correlated to circulating levels of dCML. sRAGE has been extensively described as a scavenger receptor, being suggested to alleviate the potential harmful effects of circulating AGEs [10]. However, the observed fluctuation between circulating sRAGE and free AGEs in our study does not offer conclusive evidence regarding the ability of sRAGE to effectively trap and eliminate circulating free AGEs. Furthermore, future studies should incorporate a control group (no breakfast consumption) in order to better understand the direct influence of food intake on circulating sRAGE concentration. This would help to establish the direct impact of food consumption on sRAGE levels. Moreover, it is still necessary to demonstrate the fate of such a complex (sRAGE + AGE) and how it behaves in the body.

In CHAPTER 5 we addressed our need to develop an efficient method for producing large quantities of CML without the generation of toxic HCN. We were able to propose and characterize an alternative and reproducible method for synthesizing protein-bound CML on a BSA model system. Our glycated protein model helped to avoid confounding factors sometimes seen in other feeding studies such as the loss of vitamins in diets high in AGEs. While the reaction of glyoxylic acid and $NaBH_3CN$ remains the most efficient method for producing CML in terms of yields, our research demonstrated that this reaction not only generates CML but also other compounds (*i.e.* arginine modifications, and protein crosslinks). Due to the high concentrations of glyoxal utilized in our study, a more extensive and significant formation of other glycation products occurred compared with glyoxylic acid and $NaBH_3CN$ reactions. However, these additional structural changes did not seem to impair the digestion of proteins, as revealed by the analysis of CML in the feces of mice subjected to a dCML-enriched diet. Despite the formation of glycation products other than CML, this neoformed compound has been established as a reliable biomarker for glycation within the food matrix. Furthermore, the extensive exploration of CML in the scientific literature enabled us to compare and extrapolate our results with data generated by other research groups.

Finally, this glycated protein model was used in an animal feeding study. Adverse health effects have been inferred from the consumption of dietary AGEs for many years in the academic literature. We confirmed the RAGE-independent accumulation of free CML in the kidneys, ileum, and colon after 35- and 70-weeks of dietary intervention. A diet switch (dCML → STD) at 6 weeks of life returned the

tissue levels of free CML to concentrations comparable to the STD diet. The dCML diet had no obvious effect on the physiological parameters measured in this study: endogenous glycation, inflammation, oxidative stress, and senescence. This lack of evident effect was observed in both the short- and long-term exposure scenarios.

It is important to emphasize that despite the significantly higher levels of dCML in the modified diet compared with the standard diet (a 13-fold difference), these elevated concentrations did not result in noticeable changes in the many and varied biomarkers examined in this study.

Regarding the dose administered to the animals in this study, the concentration of dCML in the modified diet (approximately 200 mg/kg food) was chosen based on the work by Grossin et al. (2015) [15]. The authors determined that this was the lowest dose at which a harmful effect of dCML was observed in mice. Considering that the daily consumption of dCML in adults is estimated to be around 83 μg_{dCML}/kgBW/day [11], and extrapolating the dose administered in our rodent study to an equivalent human dose (3000 μg_{dCML}/kgBW/day), the approach utilized in this study would correspond to more than 35 times the maximum estimated intake of dCML in the human diet. This obviously presents a challenge in accurately assessing the true health effects of dCML in human subjects.

While the biomarkers and methods employed here are all commonly used and considered standard tools for assessing inflammation, senescence, and oxidative stress in academic research, their sensitivity in detecting subtle effects may be limited. This may have contributed to the large variances across the sample sets we observed. While it may, at first sight, appear evident that increasing the number of animals would be best strategy to reduce such variability, it is worth noting that we included both males and females, which is not common in the literature, and that this study involved over 200 animals. Increasing the number of animals would render this project unfeasible in terms of logistics and budgetary constraints, and it would also make it challenging to comply with the principles of the 3Rs (Replacement, Reduction, and Refinement).

RAGE ablation seems to play an important role in alleviating inflammaging, although it appears not to eliminate the initiation of inflammatory processes. The genesis of such a mechanism might be related to the multiple cellular receptors (*e.g.* TLR4) with redundant functions which also participate in pro-inflammatory responses [12]. Furthermore, we would like to highlight the protective effect of RAGE

knock out we observed, emphasizing the clinical potential of blocking RAGE to mitigate the effects of cellular aging [13]. Unfortunately, the available RAGE KO strains exhibit genetic or behavioral artifacts that need to be taken into consideration when interpreting the results. As already mentioned, the duplication of the *GLO1* gene in the RAGE KO lineage used here may be involved in mitigating glycoxidation-related stress. This possibility warrants further investigation to better understand, for instance, whether this increased expression of *GLO1* is wholly or partly responsible for a compensatory effect against oxidative stress.

Drawing on the wealth of available evidence in the literature on CML, protein-bound CML exhibits a notable affinity for RAGE [14] and has long been regarded as the primary cellular mediator of inflammation and oxidative stress induced by dietary AGEs. But there seems to be no direct association between this affinity, the consumption of glycation products, and deleterious health effects. Indeed, recent studies conducted on both animal models [15–17] and humans [18–22] have indicated that the influence of dietary AGEs on health outcomes, whether observed over a short or long period of time, is not substantial. Regarding animal studies, the wide range of experimental protocols employed enables us to deduce that whether derived from thermally treated diets (*i.e.* autoclaved animal feed), or the incorporation of glycated model proteins, the impact of dAGEs on inflammation, senescence, or oxidation is negligible or undetectable using current preclinical research methodologies. Alternatively, it is possible that the currently used biomarkers may not accurately predict low-level cellular responses, and this potential lack of sensitivity warrants further methodological investigation.

An important finding from our experimental design is that the parental exposure to a diet rich in dCML did not seem to have an influence on the the offspring – or at least, if such an effect exists, it was not detected after a single generation. In this regard, our results suggested that the expression of *EZH2* was modulated in RAGE KO animals. Epigenetic inheritance can be transmitted through intergenerational (F0-F1) or transgenerational (F0-F2) mechanisms [23]. Therefore, the epigenetic control associated to food toxicants like pesticides [24] or AGEs [25], should be investigated across multiple generations. Further studies focusing on AGEs in this context merit investigation.

2 Perspectives

We believe that our work opens new perspectives and possibilities for further research and exploration:

Further studies dedicated to this area are highly valuable, particularly those that are more sensitive and capable of identifying the primary mechanisms involved in the action of dietary AGEs. We contend that a crucial requirement for advancing research in CLGI is the establishment and validation of sensitive biomarkers capable of accurately defining this physiological condition. Firstly, there does not appear to be an equivalence between humans and rodents regarding the expression of biomarkers such as CRP. This biomarker is perhaps the most explored inflammation biomarker in humans, where CRP levels are sensitive to minor inflammatory stimuli. In rodents, on the other hand, peaks in CRP expression are only observed in cases of acute inflammation and appear not to be sensitive to low-grade stimuli [26]. In technical terms the use of RNASeq, for instance, would allow more precise quantification of gene expression levels but also be highly valuable in identifying genetic variants associated with such stress. For example, RAGE demonstrates multiple variants that are expressed in various organs. RNASeq would be capable of indicating the specific forms of the receptor expressed and whether there is any associated transcriptional control or not. Similarly, the use of techniques such as Histology-Guided Mass Spectrometry (HGMS) would allow for the subcellular localization and quantification of dCML and other dietary AGEs, perhaps enabling further insights into any relationship between exogenous and endogenous glycation.

Finally, an important aspect to consider is that, in this study and in most other investigations examining the effects of AGE-enriched diets, analysis is conducted on whole organ homogenates. To further explore this issue, cell-culture approaches involving specific cell types (*e.g.* podocytes, enterocytes) could help identify the effects of exogenous AGEs at the cellular level. Additionally, the use of gene editing techniques such as CRISPR Cas-9 could contribute to the creation of modified cell lines (*e.g.* RAGE knockout) to better elucidate the involvement of receptors like RAGE in cellular aging and differentiation, or the effect of cell exposure to dietary AGEs.

3 References

1. Calder, P.C.; Ahluwalia, N.; Brouns, F.; Buetler, T.; Clement, K.; Cunningham, K.; Esposito, K.; Jönsson, L.S.; Kolb, H.; Lansink, M.; et al. Dietary Factors and Low-Grade Inflammation in Relation to Overweight and Obesity. *Br J Nutr* **2011**, *106 Suppl 3*, S5-78, doi:10.1017/S0007114511005460.
2. Christ, A.; Lauterbach, M.; Latz, E. Western Diet and the Immune System: An Inflammatory Connection. *Immunity* **2019**, *51*, 794–811, doi:10.1016/j.immuni.2019.09.020.
3. Zhu, Q.; Tong, Y.; Wu, T.; Li, J.; Tong, N. Comparison of the Hypoglycemic Effect of Acarbose Monotherapy in Patients With Type 2 Diabetes Mellitus Consuming an Eastern or Western Diet: A Systematic Meta-Analysis. *Clinical Therapeutics* **2013**, *35*, 880–899, doi:10.1016/j.clinthera.2013.03.020.
4. Khan, M.A.B.; Hashim, M.J.; King, J.K.; Govender, R.D.; Mustafa, H.; Al Kaabi, J. Epidemiology of Type 2 Diabetes – Global Burden of Disease and Forecasted Trends. *J Epidemiol Glob Health* **2020**, *10*, 107–111, doi:10.2991/jegh.k.191028.001.
5. Pakhomov, N.; Baugh, J.A. The Role of Diet-Derived Short-Chain Fatty Acids in Regulating Cardiac Pressure Overload. *American Journal of Physiology-Heart and Circulatory Physiology* **2021**, *320*, H475–H486, doi:10.1152/ajpheart.00573.2020.
6. Rakhra, V.; Galappaththy, S.L.; Bulchandani, S.; Cabandugama, P.K. Obesity and the Western Diet: How We Got Here. *Mo Med* **2020**, *117*, 536–538.
7. Crimarco, A.; Landry, M.J.; Gardner, C.D. Ultra-Processed Foods, Weight Gain, and Co-Morbidity Risk. *Curr Obes Rep* **2022**, *11*, 80–92, doi:10.1007/s13679-021-00460-y.
8. Bettiga, A.; Fiorio, F.; Di Marco, F.; Trevisani, F.; Romani, A.; Porrini, E.; Salonia, A.; Montorsi, F.; Vago, R. The Modern Western Diet Rich in Advanced Glycation End-Products (AGEs): An Overview of Its Impact on Obesity and Early Progression of Renal Pathology. *Nutrients* **2019**, *11*, 1748, doi:10.3390/nu11081748.
9. da Silva, J.B.; Rowe, J.W.; Jauregui, J.R. Healthy Aging in the Americas. *Rev Panam Salud Publica* **2021**, *45*, e116, doi:10.26633/RPSP.2021.116.
10. Perrone, A.; Giovino, A.; Benny, J.; Martinelli, F. Advanced Glycation End Products (AGEs): Biochemistry, Signaling, Analytical Methods, and Epigenetic Effects. *Oxidative Medicine and Cellular Longevity* **2020**, *2020*, e3818196, doi:10.1155/2020/3818196.
11. Tessier, F.J.; Birlouez-Aragon, I. Health Effects of Dietary Maillard Reaction Products: The Results of ICARE and Other Studies. *Amino Acids* **2012**, *42*, 1119–1131, doi:10.1007/s00726-010-0776-z.
12. Zhong, H.; Li, X.; Zhou, S.; Jiang, P.; Liu, X.; Ouyang, M.; Nie, Y.; Chen, X.; Zhang, L.; Liu, Y.; et al. Interplay between RAGE and TLR4 Regulates HMGB1-Induced Inflammation by Promoting Cell Surface Expression of RAGE and TLR4. *The Journal of Immunology* **2020**, *205*, 767–775, doi:10.4049/jimmunol.1900860.
13. Singh, H.; Agrawal, D.K. Therapeutic Potential of Targeting the Receptor for Advanced Glycation End Products (RAGE) by Small Molecule Inhibitors. *Drug Development Research* **2022**, *83*, 1257–1269, doi:10.1002/ddr.21971.
14. Xue, J.; Rai, V.; Frolov, S.; Singer, D.; Chabierski, S.; Xie, J.; Reverdatto, S.; Burz, D.S.; Schmidt, A.M.; Hoffman, R.; et al. Advanced Glycation End Product (AGE) Recognition by the Receptor for AGEs (RAGE). *Structure* **2011**, *19*, 722–732, doi:10.1016/j.str.2011.02.013.
15. Grossin, N.; Auger, F.; Niquet-Leridon, C.; Durieux, N.; Montaigne, D.; Schmidt, A.M.; Susen, S.; Jacolot, P.; Beuscart, J.-B.; Tessier, F.J.; et al. Dietary CML-Enriched Protein Induces Functional Arterial Aging in a RAGE-Dependent Manner in Mice. *Mol Nutr Food Res* **2015**, *59*, 927–938, doi:10.1002/mnfr.201400643.
16. Teissier, T.; Quersin, V.; Gnemmi, V.; Daroux, M.; Howsam, M.; Delguste, F.; Lemoine, C.; Fradin, C.; Schmidt, A.-M.; Cauffiez, C.; et al. Knockout of Receptor for Advanced Glycation End-Products Attenuates Age-Related Renal Lesions. *Aging Cell* **2019**, *18*, e12850, doi:10.1111/acel.12850.
17. van Dongen, K.C.W.; Linkens, A.M.A.; Wetzels, S.M.W.; Wouters, K.; Vanmierlo, T.; van de Waarenburg, M.P.H.; Scheijen, J.L.J.M.; de Vos, W.M.; Belzer, C.; Schalkwijk, C.G. Dietary Advanced Glycation Endproducts (AGEs) Increase Their Concentration in Plasma and Tissues, Result in Inflammation and Modulate Gut Microbial Composition in Mice; Evidence

for Reversibility. *Food Research International* **2021**, *147*, 110547, doi:10.1016/j.foodres.2021.110547.

18. Aengevaeren, V.L.; Berge, K.; Mosterd, A.; Velthuis, B.; Lyngbakken, M.N.; Omland, T.; Schalkwijk, C.; Eijsvogels, T.M.H. Advanced Glycation Endproducts and Dicarbonyl Compounds Are Not Associated with Coronary Atherosclerosis Characteristics in Middle-Aged and Older Male Athletes. *European Journal of Preventive Cardiology* **2023**, *30*, zwad125.104, doi:10.1093/eurjpc/zwad125.104.
19. Berge, K.; Aengevaeren, V.L.; Mosterd, A.; Velthuis, B.K.; Lyngbakken, M.N.; Omland, T.; Schalkwijk, C.G.; Eijsvogels, T.M. Plasma Advanced Glycation End Products and Dicarbonyl Compounds Are Not Associated with Coronary Atherosclerosis in Athletes. *Medicine and Science in Sports and Exercise* **2023**, *55*, 1143.
20. Linkens, A.M.; Houben, A.J.; Niessen, P.M.; Wijckmans, N.E.; de Goei, E.E.; Van den Eynde, M.D.; Scheijen, J.L.; van den Waarenburg, M.P.; Mari, A.; Berendschot, T.T.; et al. A 4-Week High-AGE Diet Does Not Impair Glucose Metabolism and Vascular Function in Obese Individuals. *JCI Insight* **2022**, *7*, e156950, doi:10.1172/jci.insight.156950.
21. Linkens, A.M.; Eussen, S.J.; Houben, A.J.; Mari, A.; Dagnelie, P.C.; Stehouwer, C.D.; Schalkwijk, C.G. Habitual Intake of Advanced Glycation Endproducts Is Not Associated with Worse Insulin Sensitivity, Worse Beta Cell Function, or Presence of Prediabetes or Type 2 Diabetes: The Maastricht Study. *Clinical Nutrition* **2023**.
22. Linkens, A.M.A.; Houben, A.J.H.M.; Kroon, A.A.; Schram, M.T.; Berendschot, T.T.J.M.; Webers, C.A.B.; van Greevenbroek, M.; Henry, R.M.A.; de Galan, B.; Stehouwer, C.D.A.; et al. Habitual Intake of Dietary Advanced Glycation End Products Is Not Associated with Generalized Microvascular Function-the Maastricht Study. *Am J Clin Nutr* **2022**, *115*, 444–455, doi:10.1093/ajcn/nqab302.
23. Tuscher, J.J.; Day, J.J. Multigenerational Epigenetic Inheritance: One Step Forward, Two Generations Back. *Neurobiology of Disease* **2019**, *132*, 104591, doi:10.1016/j.nbd.2019.104591.
24. Nicolella, H.D.; de Assis, S. Epigenetic Inheritance: Intergenerational Effects of Pesticides and Other Endocrine Disruptors on Cancer Development. *Int J Mol Sci* **2022**, *23*, 4671, doi:10.3390/ijms23094671.
25. Wu, X.; Shi, X.; Chen, X.; Yin, Z. Advanced Glycation End Products Regulate the Receptor of AGEs Epigenetically. *Front Cell Dev Biol* **2023**, *11*, 1062229, doi:10.3389/fcell.2023.1062229.
26. Huang, C.-F.; Chiu, S.-Y.; Huang, H.-W.; Cheng, B.-H.; Pan, H.-M.; Huang, W.-L.; Chang, H.-H.; Liao, C.-C.; Jiang, S.-T.; Su, Y.-C. A Reporter Mouse for Non-Invasive Detection of Toll-like Receptor Ligands Induced Acute Phase Responses. *Sci Rep* **2019**, *9*, 19065, doi:10.1038/s41598-019-55281-w.

ACADEMIC PRODUCTION

Publications directly related to this thesis

Lima, M. T. N. S., Howsam, M., Tessier, F. J. et al. (2023)**.** Glycated Bovine Serum Albumin for Use in Feeding Trials with Animal Models – In Vitro Methodology and Characterization of a Glycated Substrate for Modifying Feed Pellets. *Food Chemistry*, 136815. https://doi.org/10.1016/j.foodchem.2023.136815.

Helou, C., **Lima, M. T. N. S.**, Niquet-Leridon, C., Jacolot, P., Boulanger, E., Delguste, F., Guilbaud, A., Genin, M., Anton, P. M., Delayre-Orthez, C., Papazian, T., Howsam, M., & Tessier, F. J. (2022). Plasma Levels of Free Nε-Carboxymethyllysine (CML) after Different Oral Doses of CML in Rats and after the Intake of Different Breakfasts in Humans: Postprandial Plasma Level of sRAGE in Humans. *Nutrients*, *14*(9).

Lima, M. T. N. S., Howsam, M., Anton, P. M., Delayre-Orthez, C., & Tessier, F. J. (2021). Effect of Advanced Glycation End-Products and Excessive Calorie Intake on Diet-Induced Chronic Low-Grade Inflammation Biomarkers in Murine Models. *Nutrients*, *13*(9).

Lima, M. T. N. S., Howsam, M., Paul-Constant, C, Takahashi, J. A., Boulanger, E. & Tessier, F. J. (2020). The Effects of Glycosaminoglycans Over RAGE Cell Signaling. IMARS Highlights. 15 (6), 5-16

Other publications

Lima, M. T. N. S., Boulanger, E., Tessier, F. J., & Takahashi, J. A. (2022). Hibiscus, Rooibos, and Yerba Mate for Healthy Aging: A Review on the Attenuation of In Vitro and In Vivo Markers Related to Oxidative Stress, Glycoxidation, and Neurodegeneration. *Foods*, *11*(12).

Congress

Poster - Lima, M. T. N. S., Howsam, M., Tessier, F. J. et al. (2021)**.** *In vitro* fortification of *N*-carboxymethyl-lysine in bovine serum albumin model systems. IMARS14 2021